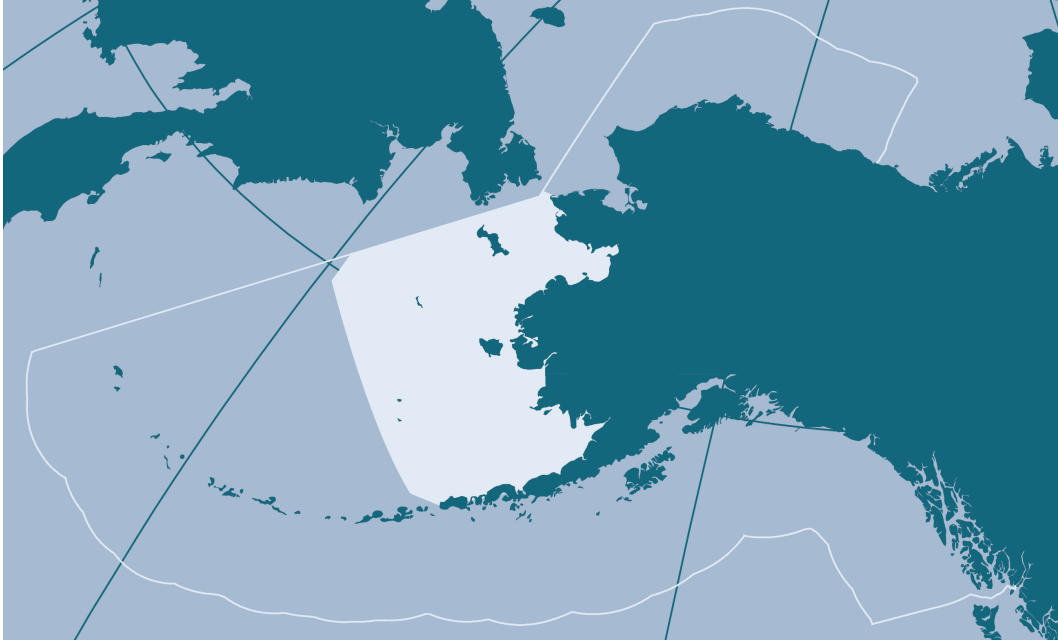# Ecosystem Status Report 2023
EASTERN BERING SEA

Edited by:

Elizabeth Siddon

Auke Bay Laboratories, Alaska Fisheries Science Center, NOAA Fisheries

With contributions from:

Anna Abelman, Grant Adams, Donald M. Anderson, Alexander G. Andrews III, Kerim Aydin, Steve Barbeaux, Cheryl Barnes, Lewis A.K. Barnett, Sonia Batten, Shaun W. Bell, Nick Bond, Emily Bowers, Caroline Brown, Thaddaeus Buser, Matt Callahan, Louisa Castrodale, Patricia Chambers, Patrick Charapata, Daniel Cooper, Bryan Cormack, Jessica Cross, Curry J. Cunningham, Lukas DeFilippo, Andrew Dimond, Lauren Divine, Sherri Dressel, Kathleen Easley, Lisa Eisner, Jack Erickson, Evangeline Fachon, Ed Farley, Thomas Farrugia, Emily Fergusson, Sarah Gaichas, Adrian Gall, Jeanette Gann, Sabrina Garcia, Sulli Gibson, Colleen Harpold, Ron Heintz, Tyler Hennon, Kirstin K. Holsman, Kathrine Howard, Tom Hurst, Jim Ianelli, Timothy Jones, Phil Joy, Robb Kaler, Kelly Kearney, Esther Kennedy, David Kimmel, Geoffrey M. Lang, Scott I. Large, Ben Laurel, Elizabeth Lee, Kathi Lefebvre, Emily Lemagie, Aaron Lestenkof, Jackie Lindsey, W. Christopher Long, Andrew Magel, Jacek Maselko, Sara Miller, Todd Miller, Natalie Monacci, Calvin W. Mordy, James Murphy, Jens M. Nielsen, Trevor Niksik, Clare Ostle, Jim Overland, Johanna Page, Melanie Paquin, Emma Pate, Robert Pickart, Darren Pilcher, Cody Pinger, Bianca Prohaska, Patrick H. Ressler, Felipe Restrepo, Jon Richar, Sean Rohan, Natalie Rouse, Matthew Rustand, Gay Sheffield, Kalei Shotwell, Elizabeth Siddon, Kevin Siwicke, Scott Smeltz, Mason Smith, Brooke Snyder, Adam Spear, Ingrid Spies, Phyllis Stabeno, Raphaela Stimmelmayr, Robert Suryan, Rick Thoman, James Thorson, Rodney Towell, Stacy Vega, Terese Vicente, Vanessa von Biela, Muyin Wang, Jordan Watson, George A. Whitehouse, Kevin Whitworth, Alexis Will, Megan Williams, Ellen M. Yasumiishi, Stephani Zador, and Molly Zaleski

Citing the complete report:
Siddon, E. 2023. Ecosystem Status Report 2023: Eastern Bering Sea, Stock Assessment and Fishery Evaluation Report, North Pacific Fishery Management Council, 1007 West 3rd Ave., Suite 400, Anchorage, Alaska 99501.

Citing the Ecosystem Assessment:
Siddon, E. 2023. Ecosystem Assessment. In: Siddon, E. 2023. Ecosystem Status Report 2023: Eastern Bering Sea, Stock Assessment and Fishery Evaluation Report, North Pacific Fishery Management Council, 1007 West 3rd Ave., Suite 400, Anchorage, Alaska 99501.

Citing an individual section:
Contributor name(s), 2023. Contribution title. In: Siddon, E. 2023. Ecosystem Status Report 2023: Eastern Bering Sea, Stock Assessment and Fishery Evaluation Report, North Pacific Fishery Management Council, 1007 West 3rd Ave., Suite 400, Anchorage, Alaska 99501.

QR code for NOAA Alaska Fisheries Science Center's Ecosystem Status Reports webpage[1].Time series from the report cards are also available [2]

---

[1]https://www.fisheries.noaa.gov/alaska/ecosystems/ecosystem-status-reports-gulf-alaska-bering-sea-and-aleutian-islands

[2]https://apps-afsc.fisheries.noaa.gov/refm/reem/ecoweb/index.php

2023 Contributing Partners

Purpose of the Ecosystem Status Reports

This document is intended to provide the North Pacific Fishery Management Council, including its Scientific and Statistical Committee (SSC) and Advisory Panel (AP), with information on ecosystem status and trends. This information provides context for the SSC's acceptable biological catch (ABC) and overfishing limit (OFL) recommendations, as well as for the Council's final total allowable catch (TAC) determination for groundfish and crab. It follows the same annual schedule and review process as groundfish stock assessments, and is made available to the Council at the annual December meeting when Alaska's federal groundfish harvest recommendations are finalized.
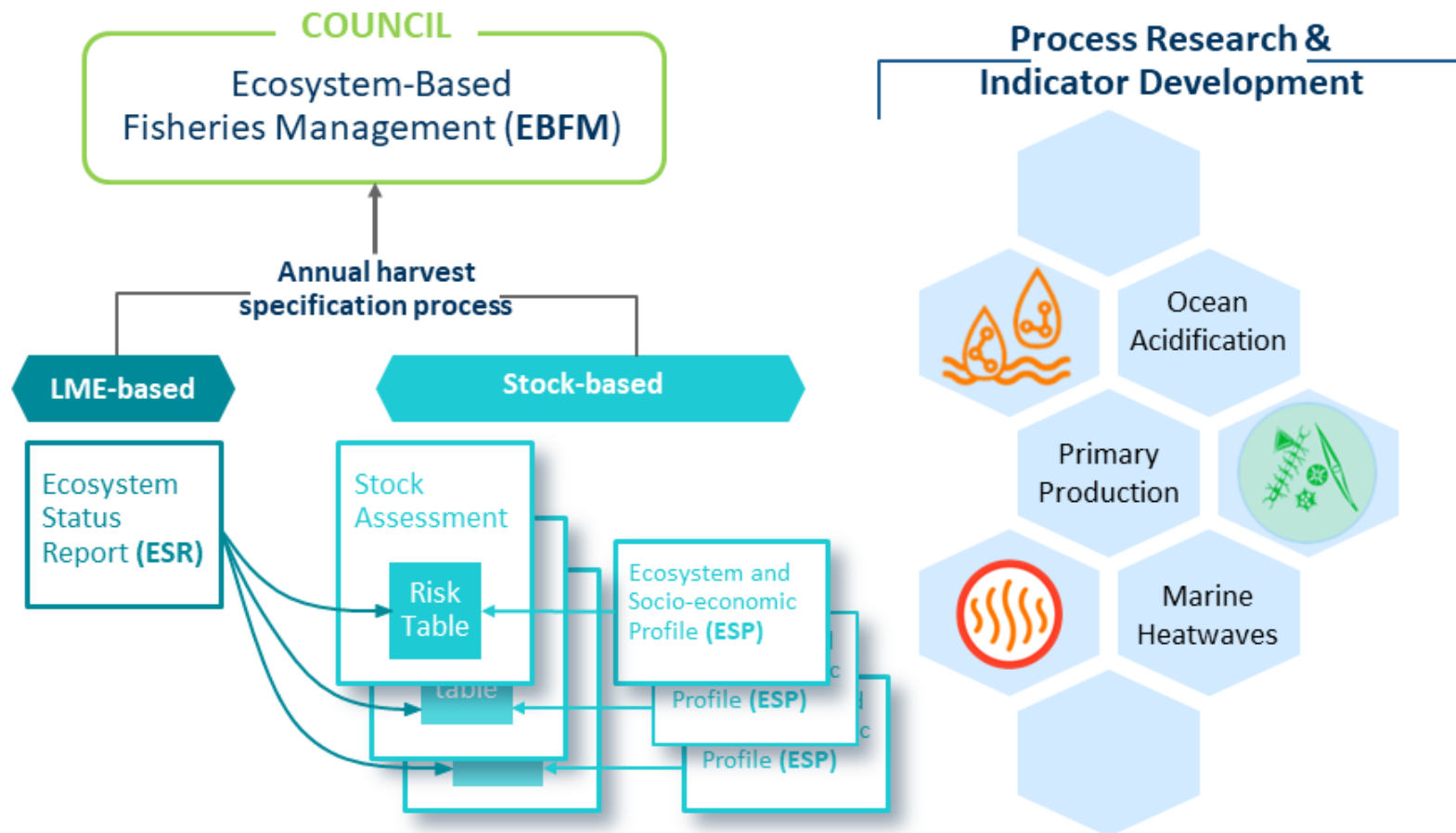
Ecosystem Status Reports (ESRs) include assessments based on ecosystem indicators that reflect the current status and trends of ecosystem components, which range from physical oceanography to biology and human dimensions. Many indicators are based on data collected from NOAA's Alaska Fishery Science Center surveys. All are developed by, and include contributions from, scientists and fishery managers at NOAA, other U.S. federal and state agencies, academic institutions, tribes, nonprofits, and other sources. The ecosystem information in this report will be integrated into the annual harvest recommendations through inclusion in stock assessment-specific risk tables (Dorn and Zador, 2020), presentations to the Groundfish and Crab plan teams in annual September and November meetings, presentations to the Council in their annual October and December meetings, and submission of the final report to the Council in December (see Figure 1).

The SSC is the primary audience for this report, as the final ABCs are determined by the SSC, based on biological and environmental scientific information through the stock assessment and Tier process[3],[4]. TACs may be set lower than the ABCs due to biological and socioeconomic information. Thus, the ESRs are also presented to the AP and Council to provide ecosystem context to inform TAC and as well as other Council decisions. Additional background can be found in the Appendix (p. 223).
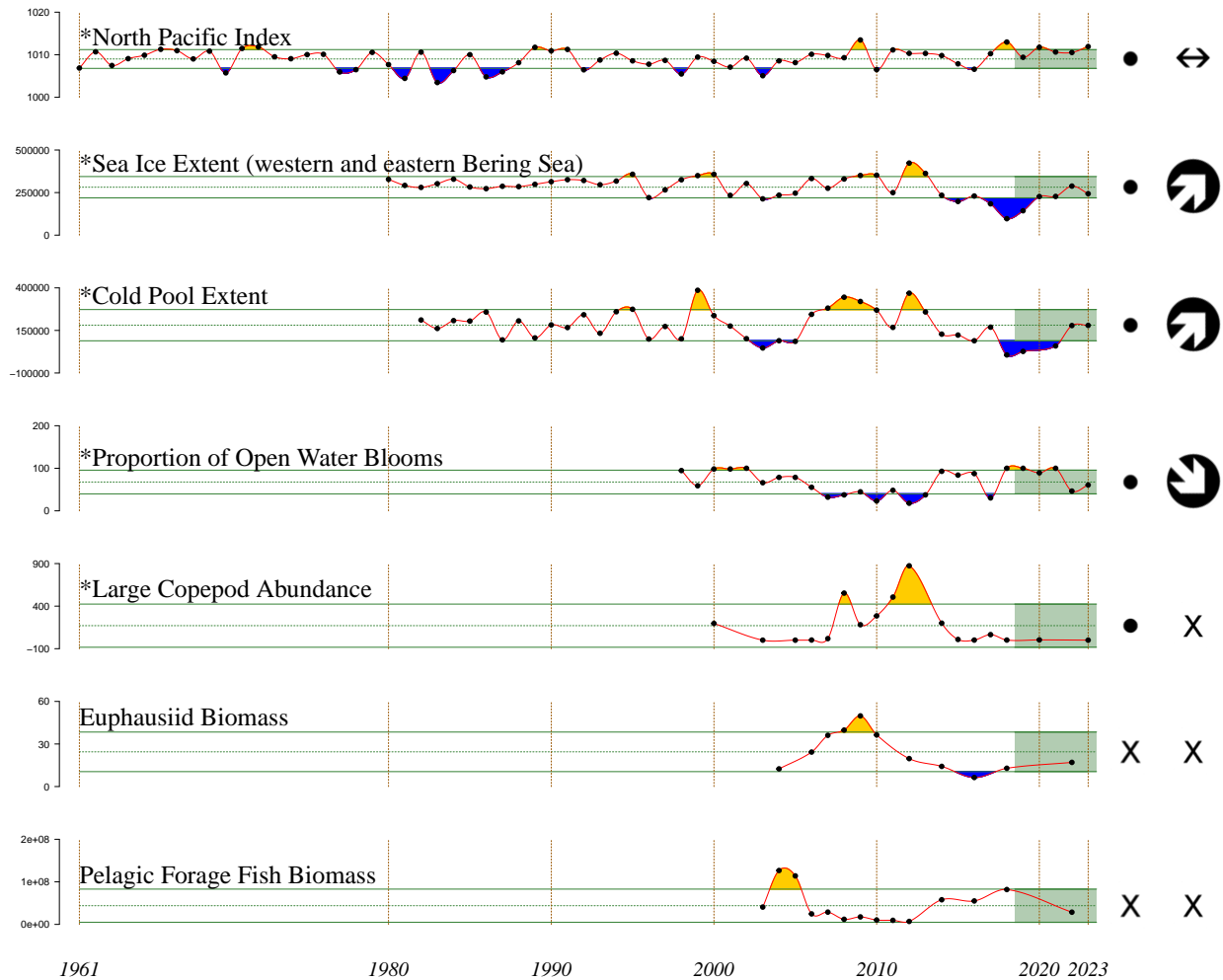
---

[3]https://www.npfmc.org/wp-content/PDFdocuments/fmp/GOA/GOAfmp.pdf
[4]https://www.npfmc.org/wp-content/PDFdocuments/fmp/BSAI/BSAIfmp.pdf

Figure 1: Ecosystem information mapping to support Ecosystem-Based Fisheries Management through Alaska's annual harvest specification process. The 'honeycomb' on the right shows examples of ecosystem indicators that are provided to Ecosystem Status Reports (ESRs) at the Large Marine Ecosystem (LME) scale and/or to Ecosystem and Socioeconomic Profiles (ESPs) at the species-based level.

Eastern Bering Sea 2023 Report Card

*North Pacific Index

*Sea Ice Extent (western and eastern Bering Sea)

*Cold Pool Extent

*Proportion of Open Water Blooms

*Large Copepod Abundance

Euphausiid Biomass

Pelagic Forage Fish Biomass

1961   1980   1990   2000   2010   2020 2023

2019–2023 Mean
- ⊕ 1 s.d. above mean
- ⊖ 1 s.d. below mean
- • within 1 s.d. of mean
- X fewer than 2 data points

2019–2023 Trend
- ↻ increase by 1 s.d. over time window
- ↺ decrease by 1 s.d. over time window
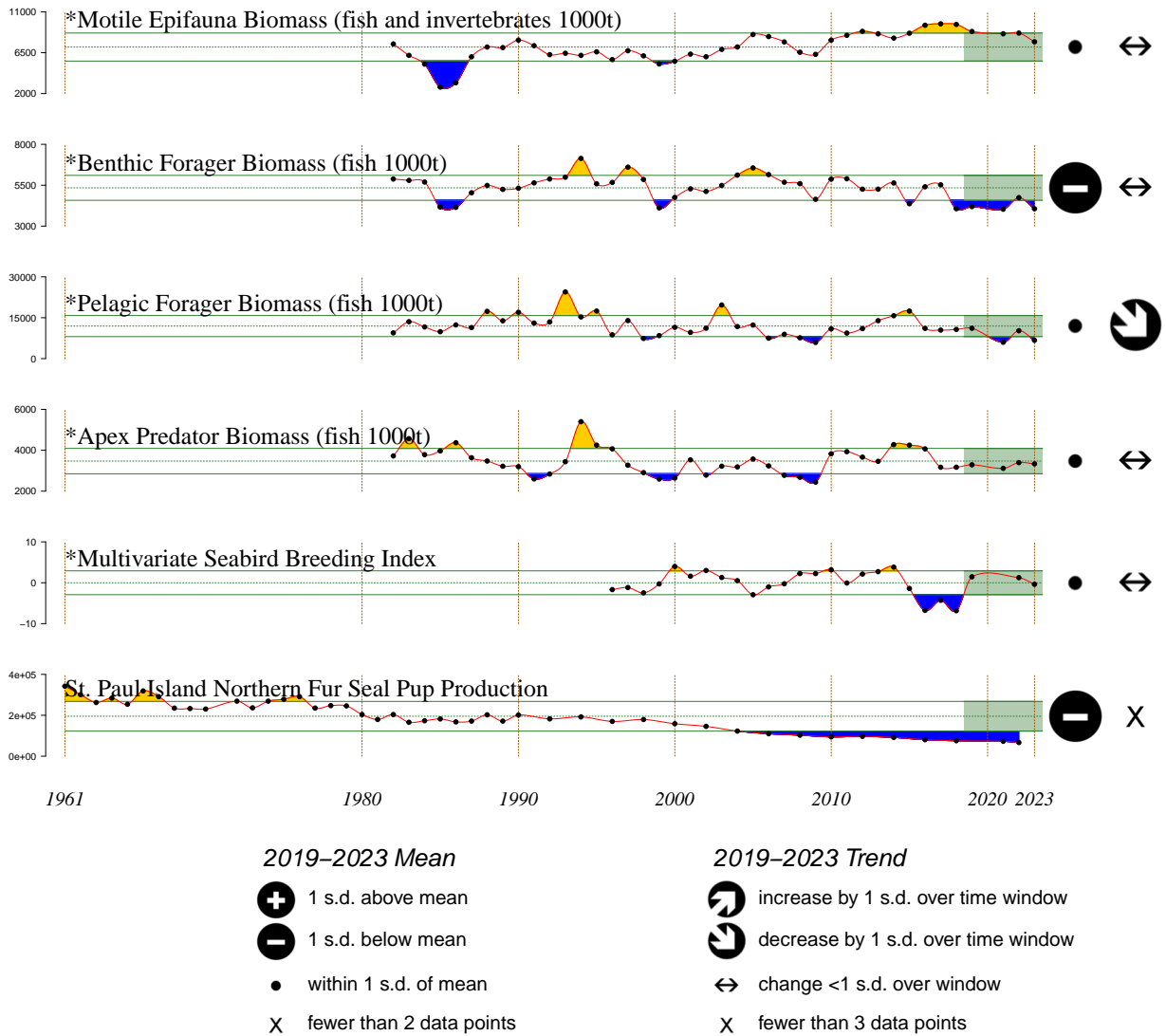- ↔ change <1 s.d. over window
- X fewer than 3 data points

Figure 2: 2023 Eastern Bering Sea report card; see text for indicator descriptions.
*indicates time series updated with 2023 data.

For more information on individual Report Card indicators, please see 'Description of the Report Card indicators' (p. 236). For more information on the methods for plotting the Report Card indicators, please see 'Methods Description for the Report Card Indicators' (p. 240).
* indicates Report Card information updated with 2023 data.

- *The **North Pacific Index (NPI)** effectively represents the state of the Aleutian Low Pressure System. Above average winter (Nov-Mar) NPI values imply a weak Aleutian Low and generally calmer conditions. The NPI was above the average during winter 2022-2023. The systematically above-average state of the NPI (i.e., weak Aleutian Low) is consistent with the overall decline in the PDO during the interval (see Figure 5).

- *The mean **sea-ice extent** across the Bering Sea exhibited no long-term trend 1980–2013 (ice year is defined as 1 August to 31 July; western and eastern). Since 2014, average sea ice extent has generally been near or below the lowest year prior to 2014. The 2023 extent of 243,431 km^2 was about 15% lower than the 2022 average extent and more than 20% below the 1980 to 2013 median. Seasonal sea-ice extent has implications for the cold pool, spring bloom strength and timing, and bottom-up productivity.

- *The areal **extent of the cold pool** in eastern Bering Sea (EBS), as measured during the bottom trawl survey (Jun-Aug; including strata 82 and 90; 1982–2023), increased from the time series minimum in 2018 through 2022. The 2023 extent (179,550 km^2) was similar to 2022 and near the time series average.

- *The **proportion of open water blooms** in the southeastern Bering Sea (SEBS) was about 50% during 2023, which is lower than during the warmer period 2014–2021, but higher than during the cold period 2007–2012.

- *The **abundance of large copepods** (predominantly *Calanus* spp.) as measured during August/September along the 70m isobath over the southern shelf, peaked in 2008 and 2012 during cold years, but has remained below the time series (2000–2023) mean since 2015.

- An acoustic estimate of euphausiid density was **below average** in 2022 (2004–2022), but remained **greater than the lowest** point in the time series that occurred in 2016.

- The biomass of **pelagic forage fish** (i.e., age-0 pollock, age-0 Pacific cod, herring, capelin, and all species of juvenile salmonids) sampled by surface trawl in late-summer (Aug-Sep; 2003–2022) peaked in 2004 and 2005, was below the time series average from 2006–2012, was above average in 2014, 2016, and 2018, but **dropped to just below the long-term mean in 2022**. The trends are dominated by age-0 pollock and juvenile sockeye salmon; in 2022 juvenile sockeye salmon were higher and age-0 pollock were lower.

- *The biomass of **motile epifauna** measured during the standard EBS bottom trawl survey (Jun-Aug; 1982–2023) declined in 2023 from 2022 but remains **above the long term mean**. Collectively, brittle stars, sea stars, and other echinoderms account for more than 50% of the biomass in this guild, and current (2016–2023) mean biomass for all three of these functional groups are above their long term means. Brittle stars alone have accounted for more than 31% of motile epifauna biomass since 1997. They have trended downward since their peak biomass in 2016 but remain above their long-term mean. The current mean biomass index for king crabs, tanner crab, and snow crab are all below their long-term means. Trends in motile epifauna biomass **indicate trends in benthic productivity**, although individual species and/or taxa may reflect varying time scales of productivity.

- *The biomass of **benthic foragers** measured during the standard EBS bottom trawl survey (Jun-Aug; 1982–2023) decreased from 2022 to 2023 and **remain below the time series mean**. The biomass of yellowfin sole decreased 32% from 2022 and remain below their long-term mean. Additionally, the biomass of flathead sole and Alaska plaice both declined. The biomass of northern rock sole increased 6.6% but remain below their long-term mean. Trends in benthic forager biomass are variable over the time series and **indirectly indicate changes in availability of infauna** (i.e., prey of these species).

- *The biomass of **pelagic foragers** measured during the standard EBS bottom trawl survey (Jun-Aug; 1982–2023) decreased 34% from 2022 to 2023 and is **below the long-term mean**. The biomass of the pelagic forager guild was generally stable from 2016 to 2019, but dropped to their second lowest value over the time series (1982–2023) in 2021, and is now at its third lowest value in 2023. The trend in the pelagic forager guild is largely driven by walleye pollock that, on average, account for 68% of the biomass in this guild. In 2023, the index for pollock decreased 25% from 2022. Among species of secondary importance, Pacific herring have decreased 75% from a time series high in 2022, but remain above their long-term mean.

- *The biomass of **apex predators** measured during the standard EBS bottom trawl survey (Jun-Aug; 1982–2023) in 2023 was **nearly equal to their long-term mean**. The trend in the apex predator guild is largely driven by Pacific cod, which had a modest increase from 2022, and arrowtooth flounder, which experienced a decrease from 2022. Trends in apex predator biomass reflect relative **predation pressure on forage fish and crab**.

- *The **multivariate seabird breeding index** indicated that, on the whole, seabird reproductive timing and success at the Pribilof Islands **was about average in 2023**, although there were differences between islands and species that may reflect local-scale processes and/or diversity in foraging strategies. Seabirds had generally better reproductive success on St. George than St. Paul Island. Also, kittiwakes hatched earlier than average on both islands, while murres hatched about a week later than average. Reproductive success and/or early breeding are assumed to be mediated through food supply, therefore above-average values may indicate better than average recruitment of year classes that seabirds feed on (e.g., age-0 pollock), or better than average supply of forage fish that commercially fished species feed on (e.g., capelin eaten by both seabirds and Pacific cod).

- **Northern fur seal pup production** at St. Paul Island in 2022 continued a declining trend since 1998 that may be partially attributed to low pup growth rates.

Ecosystem Assessment

Elizabeth Siddon
Auke Bay Laboratories, Alaska Fisheries Science Center, NOAA Fisheries
Contact: elizabeth.siddon@noaa.gov

Last updated: November 2023

Introduction

The eastern Bering Sea (EBS) transitioned from an ecosystem governed by interannual variability (1982–2000) into one that has experienced multi-year stanzas of warm (2000–2005, 2014–2021) and cold (2007–2013) periods (Baker et al., 2020) of varying durations. At present, the North Pacific is also undergoing a transition from three consecutive years of La Niña conditions to predicted El Niño conditions by early 2024. Since 2021, oceanographic metrics (i.e., sea ice extent, sea surface and bottom temperatures) have cooled to near average based on respective time series. However, biological metrics like zooplankton and fish dynamics have lagged in their expected response to cooler conditions. Therefore, ecologically, the EBS remains in a transitional state in 2023.

Seasonal sea ice and the resulting cold pool extent are defining features over the Bering Sea shelf. The recent warm stanza (2014–2021) included unprecedented low sea ice extents in winters 2017/2018 and 2018/2019 with near nonexistent cold pool extents in summers 2018 and 2019. The lack of thermal barrier resulted in the northward distributional shifts of groundfish stocks (e.g., Thorson et al., 2019; DeFilippo et al., 2023) that potentially impacted the food web dynamics and carrying capacity of the northern Bering Sea (NBS) ecoregion.

The delineation between the southeastern and northern Bering Sea is often considered at 60°N latitude on the basis of the physical and biological distinctions between these ecological systems, existing research and analyses in these areas, and available data and survey designs. This delineation is supported by broad-scale analyses of the physical oceanography and hydrography (Stabeno et al., 2012; Baker et al., 2020) and zoogeography of the region (Sigler et al., 2017). For an in-depth review of distinguishing characteristics between these ecoregions, see Baker (2023).

An assessment of the ecological trends during the recent transitional state (since 2021) and current 2023 status in the eastern and northern Bering Sea ecoregions is provided.

Southeastern Bering Sea

The recent warm stanza (2014–2021) in the EBS was unprecedented in terms of magnitude and duration (Figure 13), and included the near-absence of sea ice in the winters of 2017/2018 and 2018/2019 and subsequent absence of cold pool the following summers. Groundfish and crab stocks shifted their distribution in response to changes in sea ice and cold pool extent (Thorson et al., 2019; DeFilippo et al., 2023). However, since that time stocks have experienced variable responses in their population trends. Stocks that experienced increased reproductive success and recruitment during the warm stanza include the 2018 year class of pollock, the 2014–2019 year classes of sablefish (with juvenile sablefish increasing in the EBS; Goethel et al. (2022)), the 2017 year class of Togiak herring (see p. 115), and 8 years of Bristol Bay sockeye salmon returns (year classes precede returns by 3-5 years; see p. 125). Conversely, stocks that experienced reduced survival and stock declines include several crab stocks (notably snow crab and Bristol Bay red king crab; Figure 97) and multiple Western Alaska Chinook, chum, and coho salmon runs whose marine residency time may include the southeastern Bering Sea (SEBS) ecosystem.

Since 2021, oceanographic metrics of the thermal state of the SEBS shelf, including sea surface temperature (SST; see Figures 16, 18, and 25), bottom temperature (BT; see Figure 25), wintertime sea ice extent and thickness (see Figures 30 and 34), and cold pool extent (Figure 2) have largely returned to near their respective historical baselines through August 2023. While the summer 2023 cold pool pool was of moderate extent and among the largest of the past several years, it was significantly below the large cold pool extents that were common prior to the recent warm stanza.

Seasonally, winter conditions contribute to determining summer oceanographic conditions over the EBS shelf and impact vertical (through water column stratification) and horizontal (through cold pool extent) thermal barriers important for predator/prey dynamics (p. 113). The overall moderate winter conditions in 2022/2023 led to summer conditions that, while variable relative to long-term means, did not show any extreme characteristics. Winter 2022/2023 was on the warmer side while summer 2023 was cooler (Figure 19). Sea-ice dynamics are driven by both temperature and winds. Winter winds (Nov 2022-Mar 2023) were more southerly (Figure 8), which brings warm and moist air from the south and inhibits sea ice advance (Figure 31). This resulted in the sea ice phenology (winter ice advance and spring meltout) to be shifted ∼1 month later than 2021/2022. Sea ice did eventually reach as far south as St. Paul Island in 2023, providing a source of freshwater as ice melted at the ice edge, and reversing a trend of increasing salinity during the recent warm stanza (Figure 23).

Overall, water temperature patterns in 2023 moderated relative to recent years. Winter through spring SSTs (Dec 2022-May 2023) were above the long-term average for the outer and middle domains. However, bottom temperatures (from the ROMS model) were below average over the outer domain all year (Figure 21), resulting in a potentially strongly stratified system. Stratification can impact phytoplankton blooms and the vertical distribution of prey and predators. By summer, both observed (from the NOAA bottom trawl survey) and modeled (from the ROMS) bottom temperatures noted a cold 'tongue' of bottom water along the 50m isobath that contributed to the coldest inner domain temperatures since 2013 (Figure 26).

Wind patterns did not show a consistent directional signal. Winds can impact transport and surface (upper ∼30–40m) drift of early life stages of groundfish (e.g., pollock) and crab species (e.g., snow crab). For example, recruitment of winter-spawning flatfish (e.g., northern rock sole, arrowtooth flounder) is higher when spring winds result in in-shore advection to favorable nursery grounds (Wilderbuer et al.,

2002, 2013). In 2023, spring (Mar-May) winds generally favored off- shelf surface transport while summer (Jun-Aug) 2023 winds favored on-shelf surface transport (Figure 12). These patterns suggest reduced recruitment for winter-spawning flatfish.

Metrics of benthic habitat condition also show mixed signs following the recent warm stanza. There are continued declines in the estimated percentage of habitat disturbance by fishing gear (see p. 201), which is assumed to be beneficial to structural epifauna. The biomass of some structural epifauna (e.g., anemones and sea whips) increased in 2022 and 2023, however sponges have had a steady decline since 2015 (Figure 38). Meanwhile, the catch of structural epifauna in groundfish fisheries had been declining since 2013 but increased slightly in 2021 and 2022 (Figure 114, middle).

Indirect measures of benthic productivity include trends in motile epifauna (e.g., sea stars, brittle stars, crabs), benthic foragers (such as small-mouthed flatfish), and some benthic-associated species. Motile epifauna have declined since the peak in 2017 but remain above the long term mean in 2023 (1982–2023; Figure 2). Some of this decline can be attributed to the rapid increase immediate prior to the 2017/2018– 2018/2019 marine heatwaves, then subsequent collapse of the snow crab stock. Echinoderms, and specifically brittle stars, continue to dominate this group that, while below their peak abundance, still reflect decades of steady increase in abundance and biomass in the ecosystem. Several crab stocks showed biomass declines in 2023 (Figure 97), including Bristol Bay red king crab males (female biomass increased from 2022, but remains below 1SD below the time series average; 1982–2023), St. Matthew Island blue king crab males, snow crab, and Pribilof Islands blue king crab. Tanner crab males and females remain below the time series average, though female biomass increased from 2022 (see p. 166). Trends in benthic foragers indirectly indicate availability of infauna, which are their prey. Trends of several component flatfishes (e.g., yellowfin sole, flathead sole) decreased, and the guild remains below 1 standard deviation (SD) below the time series mean (1982–2023; Figure 2), suggesting that some stocks could be experiencing prey limitations. These coincident trends among small-mouthed flatfish may warrant further attention to identify potential common stressors. Eelpouts have been increasing since 2019 and are just above the time series average while poachers decreased to just below the time series average (1982–2023; Figure 95).

Trends in primary productivity over the SEBS shelf have not tracked synchronously with thermal conditions. With the moderation from the recent heatwave conditions, the expectation is that primary productivity indicators would increase. In contrast, chlorophyll-a biomass has generally been decreasing, with 2023 being among the lowest across sub-regions (see Figures 45 and 24). Also, coccolithophore blooms have been more prominent over the shelf since 2017 with the 2023 index being the highest observed in the time series (1997–2023; p. 83). Coccolithophore blooms are not considered a positive sign of ecosystem productivity as their large blooms are thought to negatively impact foraging success of visual foragers such as pollock and seabirds. The size structure of the phytoplankton community reflects the quantity and quality of primary production as smaller phytoplankton assemblages lead to longer food webs and a less efficient energy transfer. While the observed size structure of phytoplankton was variable during the recent warm stanza, it was average in 2022, which is the most recent available data (Figure 40). Additionally, measures of large diatoms from the continuous plankton recorder (CPR) showing a declining trend 2020–2022 (Figure 50).

The Rapid Zooplankton Assessment in the SEBS in spring 2023 noted a moderate abundance of small copepods, but low abundance and low lipid content of large copepods and euphausiids. In spring, sea ice and cooler temperatures over the shelf reduced zooplankton abundances and limited the development of the zooplankton community. In fall, the moderate abundance of small copepods continued, and while the abundance of large copepods and euphausiids remained low, abundances increased from south to

north (see p. 90). This spatial pattern reflects more favorable conditions in the north; cold pool extent is one of the most important factors that correlates to the presence of *Calanus* spp. (Eisner et al., 2018; Kimmel et al., 2018). As large, lipid-rich copepods are linked to better overwinter survival of age-0 pollock, the low availability of large copepod prey in 2022 (Figure 50) may result in reduced overwinter survival and recruitment of pollock to age-3 in 2025 (see p. 159). The abundance of jellyfish over the SEBS shelf was average in 2023 (Figure 61, top), representing no significant change in competitive pressure for planktivorous predators.

Trends in forage fish abundance were also mixed in 2023. For example, capelin and eulachon were at near all-time lows while Pacific herring has been above average for the last several years. As the numerically dominant forage fish in the EBS, age-0 pollock are an important component of available forage over the SEBS shelf to piscivorous predators such as Pacific cod, pollock, seabirds, and marine mammals. In 2023, age-0 pollock showed continued declines in several metrics of condition (i.e., length/weight residuals, energy density residuals, and %lipid) (see p. 109), indicating that predators may have experienced some prey limitations. The extent of any negative impact may be influenced by whether predators could access alternate prey.

Some species, such as herring and salmon, experienced strong year classes during the recent warm stanza that have buoyed their adult biomasses. Togiak herring biomass has been increasing as a result of strong 2016 and 2017 year classes (see p. 115). Bristol Bay sockeye salmon remained abundant in 2023, continuing a 9-year pattern of high returns (see p. 125). These consistent high returns represent extended foraging pressure on their prey, such as euphausiids. It is not currently known whether this has created competitive pressure on other species that feed on similar prey. Interestingly, juvenile salmon condition in 2022, measured by energy density anomalies, was negative for pink, chum, sockeye, and Chinook salmon in the SEBS, consistent with lower energy stores and a reduced capacity for overwinter survival (Figure 70). This represents a departure from recent trends and may indicate lower future returns for sockeye salmon.

Groundfish condition, as measured by length-weight residuals of fish collected during the SEBS bottom trawl survey, was poor for pollock and arrowtooth flounder in 2023, indicating these species may have experienced some prey limitations. Condition of several species (e.g., Pacific cod, northern rock sole, yellowfin sole, flathead sole, Alaska plaice) showed slight increases in condition from 2021 to 2022 followed by declines from 2022 to 2023. Juvenile (100–250mm) and adult (>250mm) pollock condition has declined since 2021 and 2019, respectively, with adult pollock condition this year being second-lowest in the time series (1999–2023) (Figure 78). Additionally, pollock condition as inferred from the mean biomass anomaly in the commercial fishery was the lowest that has been recorded. Through 2022, continued favorable top-down conditions existed for juvenile groundfish survival due to predator release as a result of the declining biomass of groundfish (see p. 150).

The impacts of marine heatwave induced increases in thermal experience and metabolic demand, and declines in growth potential, are borne out in bioenergetic-based metrics that integrate thermal experience, prey quantity and quality, and metabolic demands (see p. 143). Available metrics for age-0, juvenile, and adult pollock allow finer-scale tracking of the impacts of temperature and prey conditions across life stages. The %lipid and energy density of age-0 pollock underwent a step-change to lower values in the recent warm stanza beginning in 2014 and have remained low through 2023 (Figures 63 and 64), indicating potential declines in prey availability or a switch to less energetically valuable species. For adult pollock, prey limitation is indicated by multiple consumption indices (see p. 143). The cumulative effects of the multi-year warm stanza, in terms of thermal experience, metabolic demand, and prey availability, are evident in the 2023 adult pollock fish condition (Figure 78).

Seabirds are indicators of secondary productivity and shifts in prey availability that may similarly affect commercial fish populations. Trends in seabird reproductive success were mixed on the Pribilof Islands in 2023, with higher reproductive success for both fish-eating and plankton-eating species on St. George Island than on St. Paul Island (Figures 98 and 99). Species that experienced recent population losses (least auklets and common murres) do not appear to be rebounding to historic numbers. On St. Paul Island common and thick-billed murres had very low egg abundance early in the season, therefore no subsistence harvest took place in 2023. Community observations throughout the summer reported eventually seeing "a lot" of murre eggs, though murres seemed to experience nest failure later in the summer. Overall, reproductive success was mixed across species, but generally higher for species on St. George Island. This may indicate differences in local availability of zooplankton and small schooling forage fish in feeding areas utilized by seabirds of each island. No major seabird die-off events were observed in 2023 (Figure 101).

Metrics of stability in the fish community (for species regularly caught in the SEBS bottom trawl survey) indicate overall stability and resilience, although there are anomalous peaks in individual species (e.g., capelin, sablefish). Trends in mean lifespan (Figure 102) show little year-to-year variability and give no indication of shifts between short-lived and longer-lived species. The mean length of the fish community remained above the time series mean in 2023 (1982–2023; Figure 103) while the biomass index for pollock was below average, corroborating declines in fish condition (Figure 78). The stability of the groundfish community also remained above the time series mean in 2023 (Figure 104).

We track emerging stressors like ocean acidification (OA) and strive to better understand their role and potential impacts to the ecosystem. Metrics of OA (pH and Ω_{arag}) continued a multi-decadal decline, indicating more corrosive bottom-water conditions for marine calcifiers, though values improved slightly from 2022 to 2023. At this time, there is no evidence that OA can be linked to recent declines in crab populations. It is worth noting that Ω_{arag} is approaching the threshold value (<1.0) for pteropod shell dissolution that could have subsequent biological significance through the food web (Figure 107).

Northern Bering Sea

Ecosystem-wide impacts have been observed in the northern Bering Sea (NBS) since the two winters (2017/2018 and 2018/2019) of little sea ice and two summers (2018 and 2019) of reduced cold pool extent. Northward shifts in the distribution of groundfish species and concerns about the food web dynamics and carrying capacity have existed since 2018, highlighted by the gray whale Unusual Mortality Event and short-tailed shearwater mass mortality event (Siddon, 2020). Both species feed in the NBS during summer before embarking on long migrations south for breeding.

In 2021, multiple ecosystem 'red flags' occurred in the NBS: (1) the NOAA bottom trawl survey demonstrated a substantial drop in total CPUE between 2019 and 2021 that reflected large decreases in dominant species, including crab and pollock, (2) salmon run failures in the Arctic-Yukon-Kuskokwim region, and (3) seabird die-offs combined with low colony attendance and poor reproductive success (Siddon, 2021). Although the events are coincident, the multi-year warm phase resulted in cumulative impacts of increased thermal exposure and metabolic demands.

Since 2021, like the SEBS, the NBS ecosystem has been transitioning to more average conditions. There have been no prolonged marine heatwaves in the NBS since January 2021 (Figure 17) and sea ice

thickness in 2023 was above the time series average (2011–2023) for the Bering Strait region, Norton Sound, and the area between St. Lawrence Island and St. Matthew Island (Figure 33). SSTs have been within 1SD, therefore organisms have experienced reduced cumulative thermal exposure and metabolic stress (Figure 18). Also similar to the SEBS, the fall and winter 2022/2023 were on the warmer side (Figure 19) with SSTs in the outer domain above average from December 2022 through May 2023 (Figure 21). By summer 2023, bottom temperatures in Norton Sound were below average (Figure 26).

Fewer metrics of benthic habitat condition are currently available for the NBS, but trends in anemones show low biomass in 2023. Sponges are more variable and biomass was moderate in 2023 (Figure 39). Indirect measures of benthic productivity show continued low biomass of eelpouts in 2023 and continued declining trend in poachers since 2017 (Figure 96).

Overall bottom-up productivity indicators showed mixed signals this year, although none were extreme. In the NBS, sea ice retreat regulates the timing of the spring phytoplankton bloom. In general, earlier ice retreat results in an earlier bloom (Waga et al., 2021), except in the years 2018–2019 where ice retreated so early that open water blooms formed in large areas (Nielsen et al. review). In 2023, chlorophyll-a biomass was among the lowest across sub-regions (Figure 45). In fall, the Rapid Zooplankton Assessment noted that small copepods were ubiquitous across the survey area and increased in abundance from south to north. Hot spots of large copepods and euphausiids were observed around St. Lawrence Island (see). The abundance of jellyfish, potential competitors for zooplankton prey, also increased over the NBS shelf (Figures 60 and 61, bottom). Taken together these suggest it is reasonable to assume that there were moderate amounts of prey for planktivorous predators.

Yukon and Kuskokwim River salmon runs have experienced precipitous declines in recent years, largely attributed to ecosystem conditions experienced in both the freshwater and marine residency phases (see), though indicators suggest recent improvement. In 2022, juvenile salmon condition, measured by energy density anomalies, was positive for all species in the NBS (Figure 71). Positive energy stores may contribute to higher overwinter survival (when food is limited) and higher adult returns (see). In fact, slight increases were observed in juvenile Chinook and chum salmon indices in 2023 (see).

Groundfish condition, as measured by length-weight residuals collected during the NBS bottom trawl survey, showed mixed trends precluding an overall assessment of groundfish foraging conditions. Adult pollock (>250mm) condition has increased since 2021 to the highest value in the time series (2010, 2017, 2019 and 2021–2023), while juvenile pollock (100–250mm) condition has decreased since 2021. The condition of Pacific cod increased from a time series low in 2021 to average condition in 2023. Yellowfin sole condition has decreased since 2019 to a time series low in 2023 (Figure 80).

On St. Lawrence Island, qualitative observations indicated that seabirds did well in 2023. Auklet numbers, especially crested auklets, were very high and colonies that had been essentially empty the last few years were at levels comparable to 2016. Together, these observations suggest favorable conditions for seabirds in the NBS (see).

The prevalence of harmful algal blooms (HABs) in marine food webs of the NBS are important indicators of ecosystem health and of potential threats to wildlife and human health. Recent oceanographic changes have made conditions more favorable for HAB species, particularly *Alexandrium catenella* and diatoms in the genus *Pseudo-nitzschia*. Dedicated research has documented a consistent trend of higher prevalence of saxitoxin than domoic acid in Arctic food webs as HABs continue to be observed in all regions, including the Bering Strait (see). This concerning trend will continue to be monitored.

Contents

† indicates new Ecosystem Status Indicator contribution
* indicates Ecosystem Status Indicator contribution updated with 2023 data

List of Tables

List of Figures

Ecosystem Indicators

Noteworthy Topics

Here we present items that are new or noteworthy and of potential interest to fisheries managers.

Highlighting Linkages Among Report Card Indicators

Ecosystem Status Reports (ESRs) compile a wide range of ecosystem indicators and also include qualitative assessments based on current-year indicators that reflect the status and trends of ecosystem components, from physical oceanography to fishes and seabirds. Each ESR also includes a Report Card (see Figure 2 which is a subset of indicators intended to capture main components of the ecosystem. For each Report Card indicator, the mean and trend over the most recent five years are displayed. For more information on the methods for plotting the Report Card indicators, please see 'Methods Description for the Report Card Indicators' (p. 240).

Exploring quantitative linkages among Report Card indicators illustrates how changes in one variable might affect another (i.e., which indicators are stronger/weaker determinants of trends in other ecosystem components). The method proposed here, dynamic structural equation modeling, can also project next year values and can therefore be used as a tool alongside the Spring PEEC (Preview of Ecosystem and Economic Conditions) meeting to identify emergent trends and potential noteworthy topics to track through summer surveys and research efforts.

Understanding ecosystem structure and function usually begins by organizing indicators within a simplified conceptual model, such that ecological relationships among indicators can be expressed, visualized, and discussed. One simplified approach to visualize relationships among variables is a qualitative network model (QNM) (Levins, 1974). QNMs summarize the relationship among multiple variables (represented as boxes) that are linked by hypothesized mechanisms (represented as arrows), where mechanisms are specified as a positive or negative impact of one variable on another. QNMs have been successfully used at the Alaska Fisheries Science Center to identify likely consequences of hypothetical ecosystem changes (Reum et al., 2015, 2021), and can incorporate stakeholder input regarding relevant variables (boxes) and mechanisms (arrows).

Extending QNMs, we develop a time-series model that includes ecosystem indicators (boxes) and hypothesized linkages (arrows), where the strength of linkage can either be specified a priori (i.e., specifying

that a 10% increase in a predator drives a 10% decrease in per-capita production for a prey species) or estimated from available time-series data. This approach - dynamic structural equation modeling (DSEM) - has been demonstrated via application to recruitment modeling for walleye pollock (among other uses) (Thorson et al., in review). DSEM can accommodate a combination of lagged and simultaneous impacts of any variable on any other variable and jointly estimates the strength of impacts (termed "path coefficients").

Additionally, DSEM can estimate missing values within indicator time series, thereby accommodating biennial survey structures, for example. DSEM also addresses potential correlations and complementarity (i.e., trade-offs) among indicators.

We specifically propose a DSEM linking Report Card indicators included in this eastern Bering Sea Ecosystem Status Report. The specified structure for this DSEM is based upon the following design choices:

1. We include the physical variable of sea ice ("Sea.Ice.Extent") and assume greater sea ice extent results in an increase in cold pool extent ("Cold.Pool.Extent"); also years with greater ice extent result in a lower proportion of open-water-associated phytoplankton blooms ("Bloom.Type") that impacts benthic-pelagic coupling;

2. Whether the phytoplankton bloom is associated with open water (higher "Bloom.Type" values) or sea ice (lower "Bloom.Type" values) is hypothesized to cause changes in motile epifauna (e.g., demersal crabs and echinoderms) versus pelagic secondary producers (e.g., euphausiids ("Euphausiids") and zooplankton ("Large.Copepods"));

3. Motile epifauna are assumed to influence apex predators like Pacific cod and arrowtooth flounder and are linked to benthic foragers (flatfishes) as both guilds prey on infauna;

4. Euphausiids and copepods are assumed to drive changes in forage fishes including juvenile gadids (including age-0 pollock), capelin, and herring ("Forage.Fish") and pelagic foragers (adult pollock and herring; "Pelagic.Foragers"), where forage fish in turn drive changes in the reproductive success of a representative fish-eating seabird, the common murre ("COMU"), and pelagic foragers drive changes in fur seal pup production ("Fur.Seal.Pup")

Fitting this conceptual model to time-series data (Figure 3) results in some linkages that are in-line with prior expectations. For example, increased sea ice drives an increase in cold pool extent and a decrease in the proportion of open water blooms. Open-water blooms in turn cause a decrease in motile epifauna and benthic foragers. Periods with more open water blooms are also estimated to cause a decrease in large copepods (because the Report Card time-series show a negative correlation between "Bloom.Type" and "Large.Copepod" indicators). On the other hand, model results also show some linkages that are not consistent with prior expectations. For example, increased euphausiid abundance is estimated to decrease both forage fish and pelagic forager abundance. Similarly, increased forage fish is estimated to decrease the reproductive success of fish-eating seabirds. Finally, we note that DSEM provides interpolated estimates of Report Card indicators in years that are otherwise missing direct measurements (Figure 4). These interpolated estimates seem reasonable in many cases. For example, euphausiid measurements are high in the mid-2000s and low by the mid-2010s, and show relatively little variation around this dominant trend. The model then estimates a high auto-correlation, and interpolates values (and associated uncertainty) that are consistent with this dominant pattern. By

contrast, forage fishes show larger interannual variation, so interpolated values are then estimated with greater uncertainty. DSEM also provides 'historical projections' of Report Card indicators earlier than their first observation. These hindcasts assume that ecosystem dynamics are stationary, analogous to how climate projections are constructed for future decades. However, we do not show these historical projections prior to 1982 for variables without a direct measurement.

We conclude that DSEM provides an avenue to combine a conceptual model for ecosystem function with time-series indicators that are compiled in the ESRs, while compensating for (and interpolating) missing data. We foresee that future research during 2024 could address some estimated linkages that are currently inconsistent with widely understood relationships. For example, we could separate forage fish into taxa with better understood linkages with other variables (e.g., separating cold-associated capelin from warm-associated herring). We also note that estimated linkages involving euphausiids are surprising and generally conflict with assumed dynamics. This suggests that more empirical research is needed to measure euphausiid abundance and consumption to link changes in these variables to both oceanography as well as changes in predator abundance.

Contributed by
James Thorson[1] and Elizabeth Siddon[2]
Indicators provided by
Lewis A.K. Barnett[1], David Kimmel[1], Jens M. Nielsen[1,3], Patrick H. Ressler[1], Sean Rohan[1], Matthew Rustand[4], Rick Thoman[5], Rodney Towell[1], George A. Whitehouse[1,2], and Ellen M. Yasumiishi[1]
Methods development
Alexander G. Andrews III[1] and Scott I. Large[6]

[1]NOAA Fisheries, Alaska Fisheries Science Center, Seattle, WA
[2]NOAA Fisheries, Alaska Fisheries Science Center, Juneau, AK
[3]Cooperative Institute for Climate, Ocean, and Ecosystem Studies (CICOES), University of Washington, Seattle, WA
[4]Alaska Maritime National Wildlife Refuge, U.S. Fish and Wildlife Service, Homer, AK
[5]University of Alaska Fairbanks, International Arctic Research Center, Alaska Center for Climate Assessment and Policy
[6]NOAA Fisheries, Northeast Fisheries Science Center, Woods Hole, MA
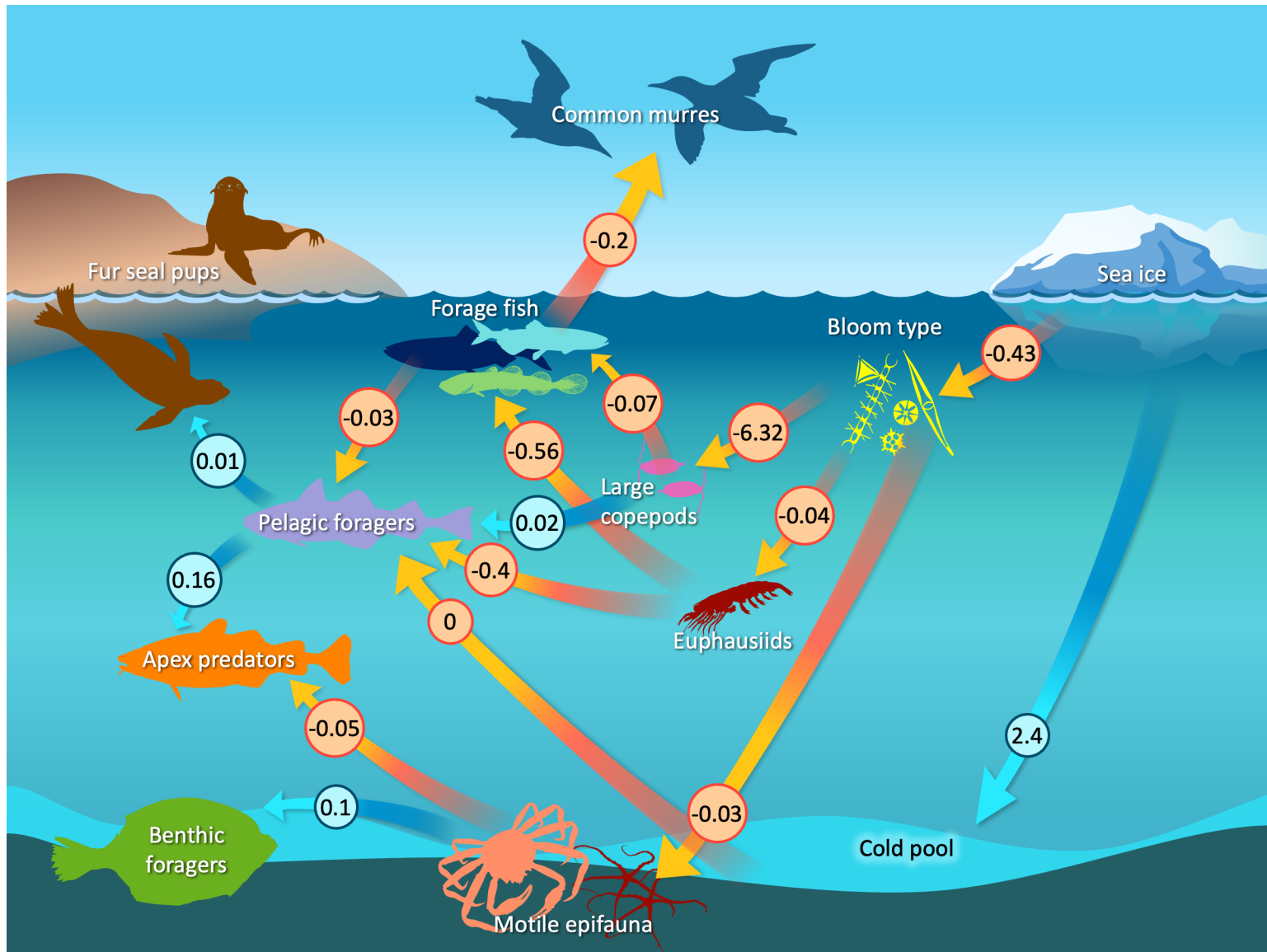
Figure 3: A path diagram showing estimated linkages among ecosystem variables. Arrows correspond to hypothesized relationships, where an arrow pointing from X to Y indicates that a change in X is estimated to cause a change in Y and the number next to each arrow shows the estimated magnitude (using red arrows to indicate negative and blue arrows to indicate positive effects). Each path coefficient also estimates the statistical significance of that hypothesized mechanism (values not shown here to avoid clutter) and future research could conduct model-selection to eliminate non-significant linkages.
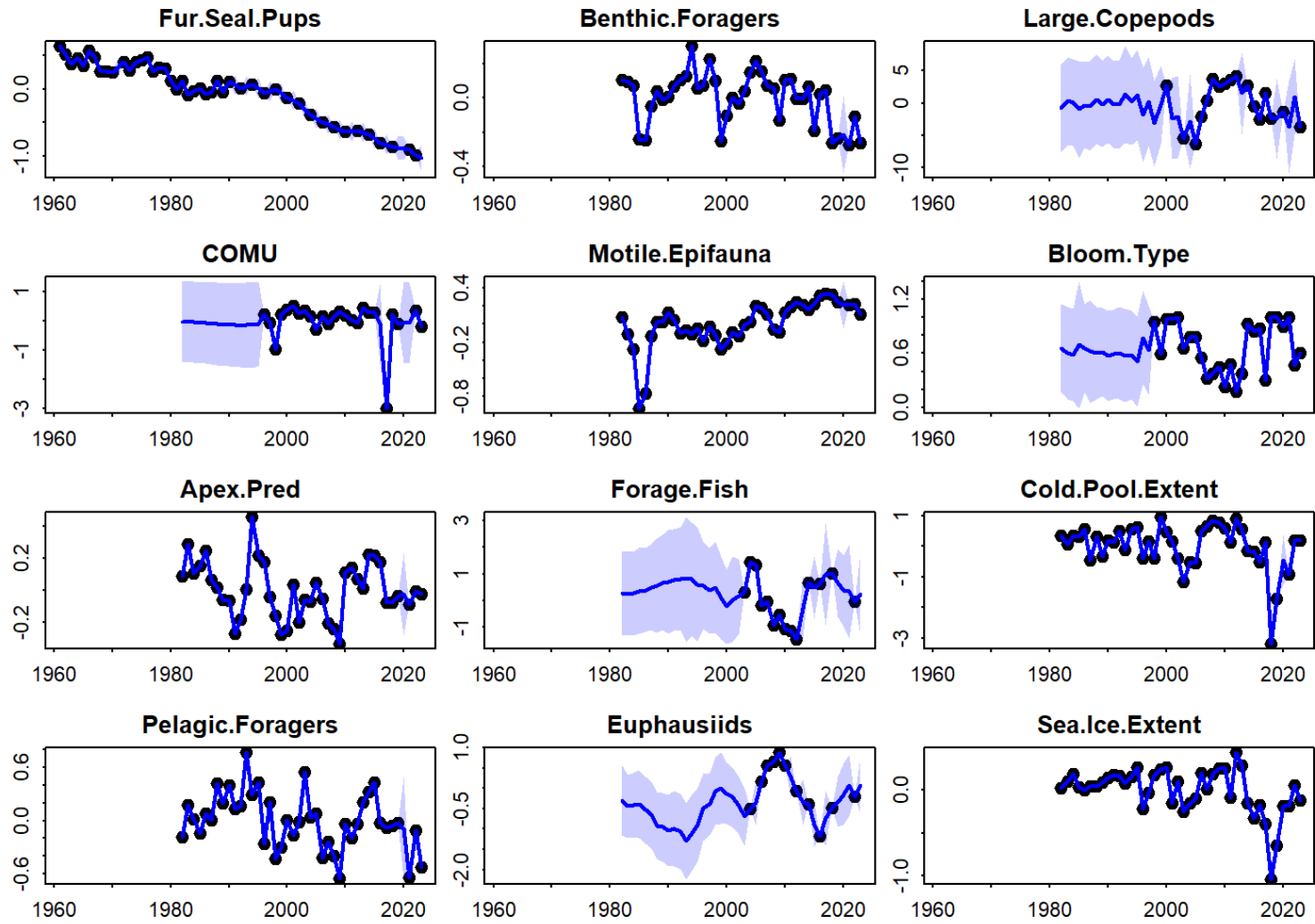
Figure 4: Observed (black dot) and estimated (blue line with 95% confidence interval as shaded area) value for each ecosystem variable included in the DSEM.

Ecosystem Status Indicators

Physical Environment Synthesis

This synthesis section provides an overview of physical oceanographic variables and contains contributions from (in alphabetical order):

Lewis Barnett - NOAA Fisheries, Alaska Fisheries Science Center, Resource Assessment and Conservation Engineering Division
Nick Bond - University of Washington, Cooperative Institute for Climate, Ocean, and Ecosystem Studies [CICOES]
Matt Callahan - Pacific States Marine Fisheries Commission
Lauren Divine - Ecosystem Conservation Office at Aleut Community of St. Paul Island
Tyler Hennon - University of Alaska Fairbanks, College of Fisheries and Ocean Sciences
Kelly Kearney - University of Washington, Cooperative Institute for Climate, Ocean, and Ecosystem Studies [CICOES] and NOAA Fisheries, Alaska Fisheries Science Center, Seattle WA
Emily Lemagie - NOAA Pacific Marine Environmental Lab [PMEL]
Aaron Lestenkof - Ecosystem Conservation Office at Aleut Community of St. Paul Island
Jim Overland - NOAA Pacific Marine Environmental Lab [PMEL]
Sean Rohan - NOAA Fisheries, Alaska Fisheries Science Center, Seattle, WA
Kevin Siwicke - NOAA Fisheries, Alaska Fisheries Science Center, Juneau, AK
Rick Thoman - University of Alaska Fairbanks, International Arctic Research Center, Alaska Center for Climate Assessment and Policy
Muyin Wang - University of Washington, Cooperative Institute for Climate, Ocean, and Ecosystem Studies [CICOES] and NOAA Pacific Marine Environmental Lab [PMEL]

Synthesis compiled by Tyler Hennon
University of Alaska Fairbanks
College of Fisheries and Ocean Sciences

Last updated: October 2023

Introduction
In this section, we provide an overview of the physical oceanographic conditions impacting the eastern Bering Sea (EBS), describe conditions observed from fall 2022 through summer 2023, and place 2023 in the context of recent years. The physical environment impacts ecosystem dynamics and productivity important to fisheries and their management. We merge across information sources, from broad-scale to local-scale, as follows:

Outline

1. Climate Overview

2. Regional Highlights

3. Surface Winds

4. Sea Surface Temperature (SST) and Bottom Temperature

5. Sea Ice

6. Cold Pool

7. Seasonal Projections of SST from the National Multi-Model Ensemble (NMME)

Executive Statement

Observations over the last year (August 2022–August 2023) show that the thermal state of the eastern Bering Sea (EBS) is close to the historical baseline of many metrics. There have been no sustained sea surface temperature (SST) heatwaves since January 2021 over either the northern or southeastern Bering Sea, and modeled EBS bottom temperatures were cool to normal for the 2022–2023 period. For the second year in a row, a summer cold pool of moderate extent was observed, and while it was among the largest in the past several years it was significantly below the large extents common prior to 2014. Similarly, wintertime sea ice extent approached slightly below the 1991–2020 median by mid-winter, though ice formation in late fall was delayed, in part due to ex-Typhoon Merbok. Sea ice thickness during the third week of March was at or exceeded the average from the 2011–2023 record. For projections into 2024, the aggregate estimate from the National Multi-Model Ensemble (NMME) predicts that SST over the EBS is expected to be slightly elevated (anomalies of $<+1$°C relative to the 1982–2010 baseline), though individual models vary from near-normal to moderately above normal.

Synthesis Summary

The recent warm stanza in the eastern Bering Sea (EBS) began in approximately 2014. The 2021–2022 time frame (August to August) represented a relaxation from the extended warm stanza, and 2022–2023 (August to August) continued to be near historical averages across many metrics, including sea surface temperature, wintertime sea ice areal extent and thickness, and cold pool extent.

The NINO3.4 index, which tracks the state of El Niño/Southern Oscillation (ENSO), has been in a negative phase over much of the last three years, which correlated with relaxation from the strong anomalously warm years in 2018–2019 (Figure 5) to the more moderate thermal conditions now present in the EBS. Though there were anomalous sea surface air pressure and wind patterns during the past year (Figures 6 and 8), they did not exhibit the extremes reached during the last marine heatwave (2018–2019). Broad-scale climate indices in 2023 reflected a transition from La Niña conditions to developing El Niño conditions in the tropical Pacific (Figure 5).

Satellite observations of sea surface temperature (SST) have recorded no sustained heatwaves since January 2021 (Figure 17). Similarly, ROMS-based modeled bottom temperatures were fairly consistent with seasonal averages (1986–2016 baseline) from August 2022 to August 2023 over the EBS inner (<50m isobath) and middle (50-100m isobaths) domains in the EBS, though bottom temperatures in the outer domain (>100m isobath) of the southeastern Bering Sea were some of the lowest on record (~0.5°C below the 1986–2016 baseline).

Though sea ice extent in the Bering Sea was unseasonably low in early-winter, for much of the remainder of the ice season it oscillated around 500,000–700,000km^2 (Figure 31). This is among the greater ice extents of recent years, but would still be considered relatively low prior to 2010. The slow early-season ice formation was partially a result of ex-Typhoon Merbok, which made landfall with western Alaska on September 17th, 2022. The intense surface wind stress induced by Merbok mixed relatively deep, warm water up toward the surface, adding heat unfavorable to ice formation. Variability in sea ice extent from February to May is significantly correlated with anomalies in the meridional winds over the Bering Sea, where anomalously southerly winds reduce sea ice extent (and vice versa) (Figure 10).

Sea-ice thickness is evaluated at the 3rd week of March, which is generally when ice extent is at its greatest. During this period, sea-ice thickness across the EBS was close to, or moderately above, the median (2011–present), except the region between St. Lawrence Island and St. Matthew Island, which was the thickest on record (Figures 33 and 34). Regular CTD observations at St. Paul Island had been documenting a steady increase in salinity from 2015–2021 which coincided with reduced sea ice extents during the most recent warm stanza. In 2022 and 2023 this trend has been arrested (Figure 22), likely due to sea ice reaching as far south as the St. Paul Island over the Bering Sea shelf, providing a source of freshwater.

Similar to the prior year, the cool-to-average thermal conditions throughout the water column of the EBS were favorable to cold pool formation (Figures 36 and 35). The extent of the $\leq$-1°C (26,550km^2), $\leq$0°C (62,400km^2), and $\leq$1°C (110,875km^2) isotherms were similar to the 2022 survey, and all larger than their time series averages (1982–present) of 23,579km^2, 54,158km^2, and 102,906km^2, respectively. While these ranges are far greater than the almost nonexistent cold pools in 2018 and 2019, they are still significantly less than extents prior to 2014 (Figure 36).

The National Multi-Model Ensemble (NMME) projections last year (August 2022) predicted a near-normal (compared to the 1982–2010 baseline) SST environment in the Bering Sea for the period of October 2022 to April 2023. This was largely borne out by observations. For the coming year (2023–2024 winter) individual NMME model projections for SST anomalies range from near-normal to moderately above normal on the southeast Bering Sea shelf, though in aggregate they are about +0.25-1.0°C (Figure 37).

1. Climate Overview

Contributed by Nick Bond, *nicholas.bond@noaa.gov*

Climate indices provide a means of characterizing the state of the North Pacific atmosphere-ocean system. The focus here is on five commonly used indices: the NINO3.4 index for the state of the El Niño/Southern Oscillation (ENSO) phenomenon, PDO index (the leading mode of North Pacific SST variability), North Pacific Index (NPI), North Pacific Gyre Oscillation (NPGO) and Arctic Oscillation (AO). The time series of these indices, with the application of three-month running means, from 2013 into spring/summer 2023 are plotted in Figure 5.

The state of the Aleutian Low Pressure System can be encapsulated by the North Pacific Index (NPI), with negative (positive) values signifying relatively low (high) SLP. The NPI was positive during most of 2022 with the strongest anomalies occurring in the boreal fall. The tendency for a mostly positive state to the NPI since 2020 can be ascribed, in part, to the atmospheric tele-connections associated
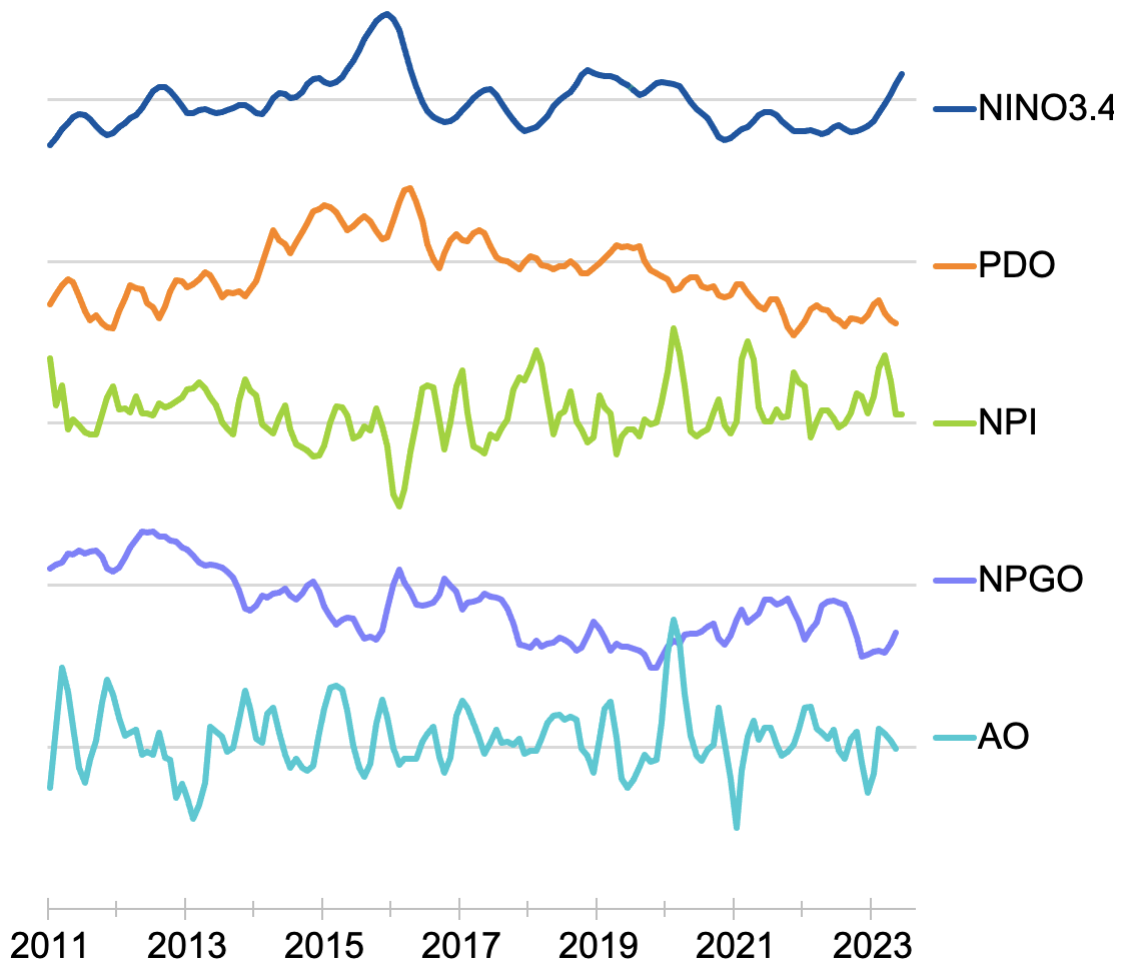
Figure 5: Time series of the NINO3.4, PDO, NPI, NPGO, and AO indices (ordered from top to bottom) for 2011–2023. Each time series represents monthly values that are normalized using a climatology based on the years of 1991–2020, and then smoothed with the application of three-month running means. The distance between the horizontal grid lines represents 5 standard deviations. More information on these indices is available from NOAA's Physical Sciences Laboratory at `https://psl.noaa.gov/data/climateindices/`.

with the extended La Niña. The systematically positive state of the NPI, i.e., weak Aleutian low, can also be linked to the overall decline in the PDO during the interval.

The Arctic Oscillation (AO) represents a measure of the strength of the polar vortex, with positive values signifying anomalously low pressure over the Arctic and high pressure over the North Pacific at a latitude of roughly 45°N. The AO transitioned from a positive state early in 2022 to a negative state by the end of the year. A negative state to the AO often is accompanied by enhanced outbreaks of arctic air to the middle latitudes of the Northern Hemisphere. That phenomenon was not prominent late in 2022, but that period did include relatively warm weather north of the Arctic circle, especially north of Alaska and the Canadian Archipelago.

2. Regional Highlights

Contributed by Nick Bond, *nicholas.bond@noaa.gov*

Alaska Peninsula
The coastal waters in the vicinity of the Alaska Peninsula were cooler than normal, based on averages for the period of 1991–2020, from autumn 2022 through summer 2023. These cool temperatures during the winter of 2022–2023 were associated to the relative lack of mild maritime air masses due to a westward displacement of the storm track; these conditions were maintained by wind anomalies from the northwest during early spring 2023.

Aleutian Islands
The near-surface waters of the Aleutian Islands were generally warmer than normal from late 2022 into spring 2023 before cooling to near normal to slightly below temperatures during summer 2023. It was relatively stormy during the winter of 2022–2023 and summer of 2023. The cooler conditions during 2023 were accompanied by greater upper mixed layer depths than during 2022. Much of the past year included wind anomalies of the sense associated with suppressed northward flow through Unimak Pass.

Eastern Bering Sea
The eastern Bering Sea shelf had a late onset of winter conditions relative to historical norms, as has been typical in recent years. For example, it was not until December 2022 before Bering Strait was closed by sea ice. The maximum ice extent on the eastern shelf was not as great as usual, but there was a rather slow retreat of sea ice in spring 2023. In particular, the month of April 2023 featured some periods of relatively cold weather and westerly winds. More detail on the ocean temperatures and sea ice in this region is included within this Physical Environment Synthesis section. Upper ocean temperatures over the eastern Bering Sea shelf were 0.5-1.0°C below normal in summer 2023.

Bering Sea Deep Basin
Stormy weather prevailed for the deep basin of the Bering Sea during autumn 2022 through the following winter. After a relatively quiet spring, the summer of 2023 also featured active weather. One consequence of the autumn and winter storms was slightly less seasonal cooling than usual in that those storms generally result in periods of mild, maritime versus cold, continental air masses. The wind anomalies were from the west during spring 2023, resulting in equator-ward Ekman transports and little change in the SST anomalies despite the calmer weather.

Arctic
The Arctic region of northern Alaska during the period of fall 2022 through summer 2023 experienced conditions comparable to those that have been typical over the past decade. For the Arctic as a whole, the maximum ice extent in March 2023 was the 5th lowest in the historical record. The minimum ice extent was on the order of 1 million square kilometers less than the climatological average for the period of 1981–2010, but not nearly as low as what occurred in 2020, 2019, or the record year of 2012. There was rapid ice loss north of Alaska in summer 2023 with the ice edge in the Chukchi and Beaufort Seas 100s of kilometers north of its historical position in August 2023. Portions of the Northwest Passage were either open or with low concentrations of sea ice as the end of summer approached.

3. Surface Winds and Air Temperatures

North Pacific Sea Level Pressure Anomalies
Contributed by Nick Bond, *nicholas.bond@noaa.gov*

The state of the North Pacific climate from autumn 2022 through summer 2023 is summarized in terms of seasonal mean sea level pressure (SLP) maps. The SLP anomalies are relative to mean conditions over the period of 1991–2020. The SLP data are from the NCEP/NCAR Reanalysis project and are available from NOAA's Physical Sciences Laboratory (PSL)[5].

The sea level pressure (SLP) over the mid-latitude North Pacific was generally greater than normal from autumn 2022 through summer 2023. The magnitude and position of the high pressure anomaly center varied seasonally but in general, the SLP anomaly pattern supported westerly wind anomalies for Alaskan waters. The positive SLP anomalies over the North Pacific were accompanied by warmer than normal sea surface temperatures (SSTs) between 30°N and 50°N across the western and central portion of the basin.

This warmth extended eastward to near the coast of the Pacific Northwest, and moderated in its intensity in the western portion of the basin, during the summer of 2023. The relatively high SLP in an overall sense, i.e., weak Aleutian low, is consistent with co-occurring conditions in the tropical Pacific, which featured a long-lasting La Niña event ending in the late winter of 2023. The PDO was negative, in large part due to persistent positive SST anomalies in the western and central North Pacific. The climate models used for seasonal weather predictions indicate that El Niño is virtually certain to be present from late 2023 into 2024. In an ensemble sense, the models are also predicting that the first three months of 2024 will include slightly elevated (+0.25°C–1.0°C) SSTs in the Bering Sea and Aleutian Island regions, and warmer than normal temperatures along the west coast of North America from northern California to the southeast GOA. The development of sea ice on the southeast Bering Sea shelf is liable to be delayed, as has been the rule over the past decade, with sea ice eventually expected to extend approximately as far south as St. Paul Island and Mooring M2.

The SLP pattern during autumn (Sep-Nov) of 2022 (Figure 6,a and b) featured a band of strongly positive anomalies extending across the entire North Pacific north of about 35°N, with a center of about +4 millibars (mb) located south of the Alaska Peninsula. Negative SLP anomalies were present from eastern Siberia into the Chukchi Sea. This SLP distribution resulted in wind anomalies of ~2ms^{-1} from the west across the Bering Sea, and easterly wind anomalies of 2-3ms^{-1} between 35°N and 45°N in the central and eastern North Pacific.

During winter (Dec-Feb) of 2022–2023, there were positive SLP anomalies over the central North Pacific, with an anomaly center near 40°N, 150°W (Figure 6d). Lower than normal SLP occurred over eastern Siberia into the western Bering Sea. The associated winds included westerly anomalies of 2 to 3.5ms^{-1} from the southern Sea of Okhotsk through the eastern Aleutian Islands, and a clockwise sense of the anomalies in the GOA. These winds were accompanied by anomalous upwelling in the coastal GOA, and downwelling in the central, deep water portion of the GOA. Anomalous winds from the north were present off the coast of western North America.

Strongly positive SLP anomalies developed over the western and central North Pacific during the spring (Mar-May) of 2023 (Figure 6f), with magnitudes exceeding 7mb south of the Aleutian Islands. This

---

[5]https://www.psl.noaa.gov/cgi-bin/data/composites/printpage.pl.

SLP distribution resulted in westerly wind anomalies of roughly 2ms^{-1} across most of the Bering Sea, northwesterly wind anomalies of 2-3ms^{-1} in the western and central GOA, and easterly wind anomalies of 3-4ms^{-1} in the central portion of the North Pacific between 35°N and 45°N. Near normal winds occurred along the west coast of North America.

The summer (Jun-Aug) of 2023 reflected a transition from a prominent high SLP anomaly during the previous season to a dipole over the western North Pacific with lower than normal SLP extending from the Sea of Okhotsk to the west coast of mainland Alaska, and higher than normal SLP south of 40°N (Figure 6h). The region between these two SLP anomaly centers experienced southwesterly wind anomalies of 2-3.5ms^{-1}. The positive SLP anomalies over the eastern GOA extending southward were accompanied by lower than normal precipitation for the coastal region from SE Alaska to the Pacific Northwest.

Regional Sea Level Pressure Anomalies
Contributed by Jim Overland, *james.e.overland@noaa.gov*, and Muyin Wang *muyin.wang@noaa.gov*

The overall spring (Mar-May) Sea Level Pressure (SLP) patterns are similar to their climatology (Figure 7, left): the Aleutian low center sitting near the tip of Aleutian Islands (contour lines), but with reduced magnitude (shadings: red color indicates SLP anomaly is above its climatology, i.e. weakened Aleutian Low). Lower than average SLP in the western Bering and a ridge of the Gulf of Alaska is a dominant feature in summer (Jun-Aug) (Figure 7, right). This is accompanied by southerly flow in the majority of the Bering Sea and resulted in positive temperature anomalies in most of the eastern Bering Sea and Gulf of Alaska.
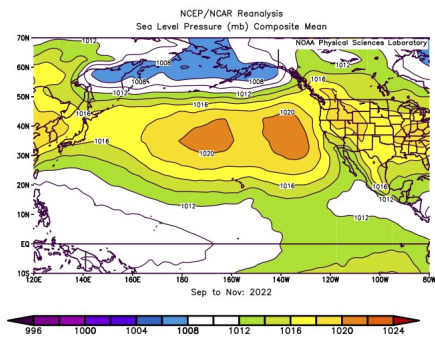
(a) Autumn Mean
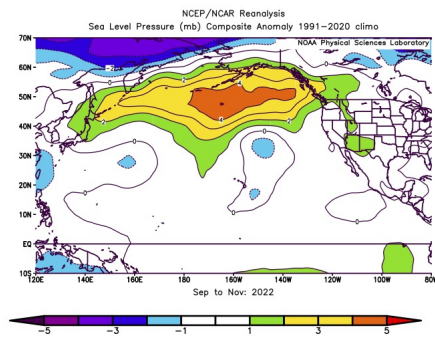
(b) Autumn Anomaly
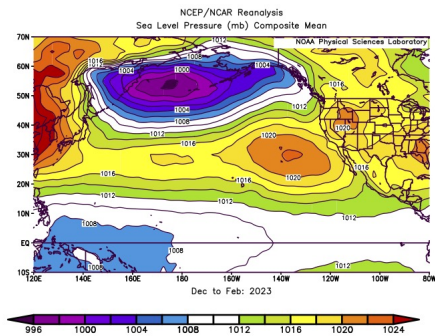
(c) Winter Mean
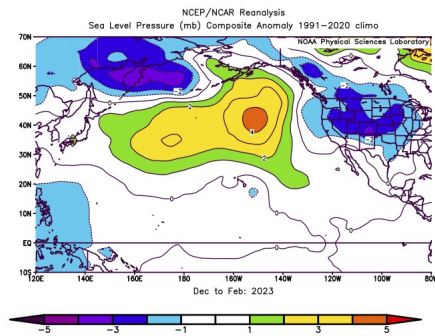
(d) Winter Anomaly
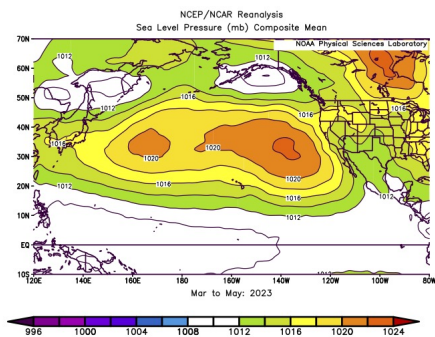
(e) Spring Mean
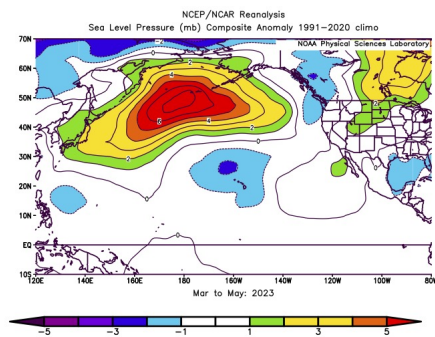
(f) Spring Anomaly
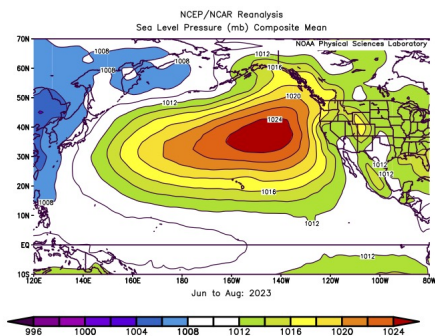
(g) Summer Mean
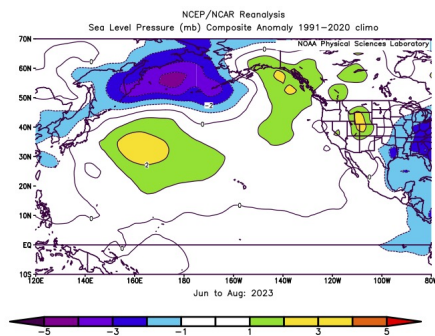
(h) Summer Anomaly

Figure 6: Sea level pressure mean (left column) and anomaly (right column) for autumn (Sept-Nov 2022; a and b), winter (Dec 2022-Feb 2023; c and d), spring (Mar-May 2023; e and f), and summer (Jun-Aug 2023; g and h). The SLP data are from the NCEP/NCAR Reanalysis project and are available by NOAA's Physical Sciences Laboratory (PSL): https://www.psl.noaa.gov/cgi-bin/data/composites/printpage.pl.

2023 MAM   2023 JJA
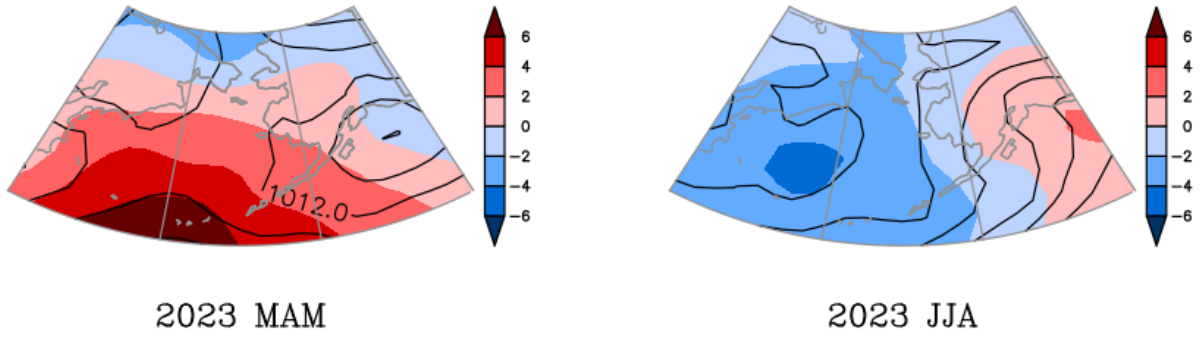
Figure 7: Mean sea level pressure and pressure anomalies averaged for (left) spring (Mar-May) and (right) summer (Jun-Aug) 2023. Black contours are sea level pressure, and the color represents the pressure anomaly.

Winter Wind Speed and Direction
Contributed by Rick Thoman, *rthoman@alaska.edu*

The north-south component of the low level wind for the 2022–2023 winter was weaker (more southerly) than the long term average (Figure 8). This was the sixth time in the past seven winters with weaker than average north winds.
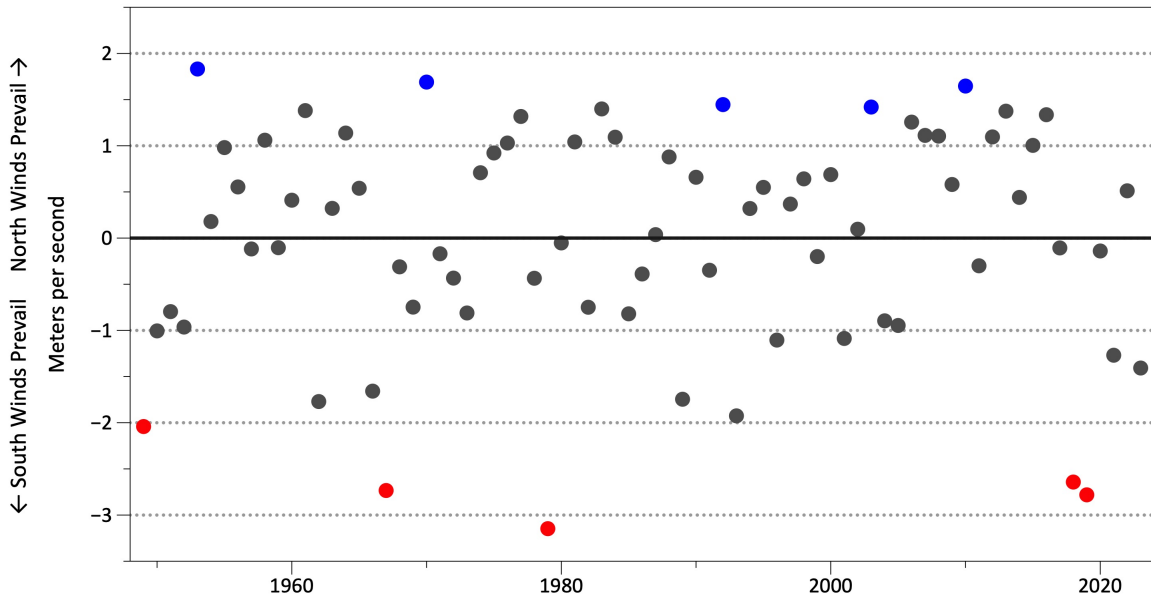
Figure 8: Winter (Nov-Mar) average north-south wind speed anomaly in the Bering Sea, 1949–2023. Red dots denote five years with strongest south winds, blue dots the five strongest north winds. **Note:** the north-south (meridional) component of the wind is plotted inversely to meteorological convention, with south to north as negative values and north to south as positive values. Source: NCEP/NCAR reanalysis.

Spatial Variability of Prevailing Winds in Late-Winter and Early-Spring
Contributed by Tyler Hennon, *tdhennon@alaska.edu*

The NCAR/NCEP 10m wind reanalysis (2000 to present) was used to examine the variability of the prevailing wind anomalies over the Bering Sea. In February of 2018 and 2019, strong and anomalous southerly winds likely were a major factor in the very low sea-ice extent observed during those years. In late winter and early spring of 2023, substantial variability in wind anomalies appear to correlate with shifts in ice extent over the Bering Sea shelf (Figures 9 and 31). Southerly winds in the second half of February coincided with a sudden retreat in sea ice, while northerly winds several weeks later coincided with a substantial rebound in sea-ice extent.
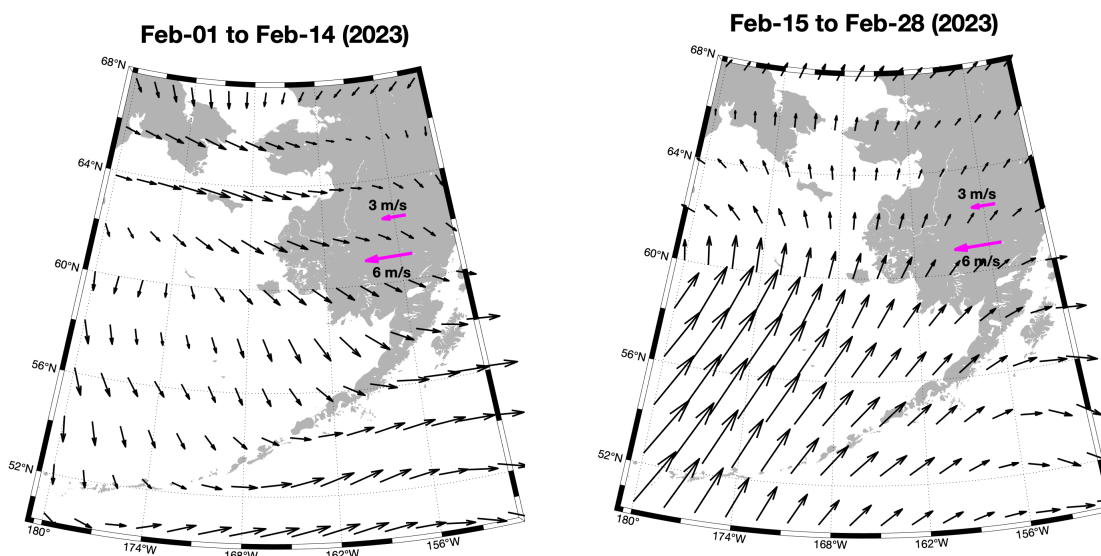
Figure 9: Average 10m wind anomaly vectors (black arrows) during two 2-week periods between February 1st and February 28th 2023. Anomaly is defined as the residual from the average seasonal signal. Magenta arrows indicate vector scales.

Meridional wind anomalies averaged across the Bering Sea (V′) and anomalies in the rate of sea-ice advance/retreat $(dA_{ice}/dt)'$ were significantly correlated (r=-0.44, p<0.01) over the span of January 1st, 2023 to May 1st, 2023 (Figure 10). Meridonal wind anomalies and sea ice advance/retreat anomalies are generally negatively correlated between January 1st to May 1st, with correlations ranging between ∼-0.25 to -0.65 over the last 23 years. The correlation of -0.44 for 2023 sits near the average from 2000 to 2022.
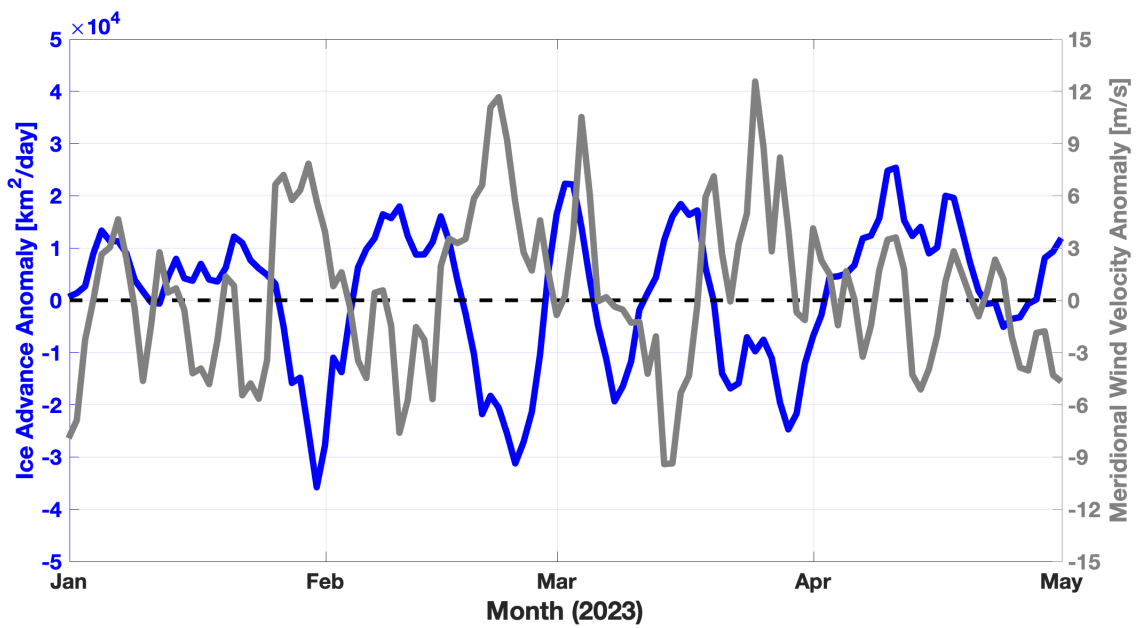
Figure 10: Time series of relative ice advance/retreat (blue) and meridional wind anomaly (gray). Both ice advance/retreat and winds have had the average seasonal cycles removed.

Winds at the Bering Sea Shelf Break
Contributed by Tyler Hennon, *tdhennon@alaska.edu*

NCEP/NCAR wind reanalysis was used to examine the along- and cross-slope wind components along the Bering Sea shelf break. Four-times daily wind data dating back to January 2000 were interpolated to a transect approximating the shelf break (Figure 11), and the zonal and meridional components were rotated into along- and cross-shelf components. These components of wind were then averaged across the whole transect for each month dating back to 2000.
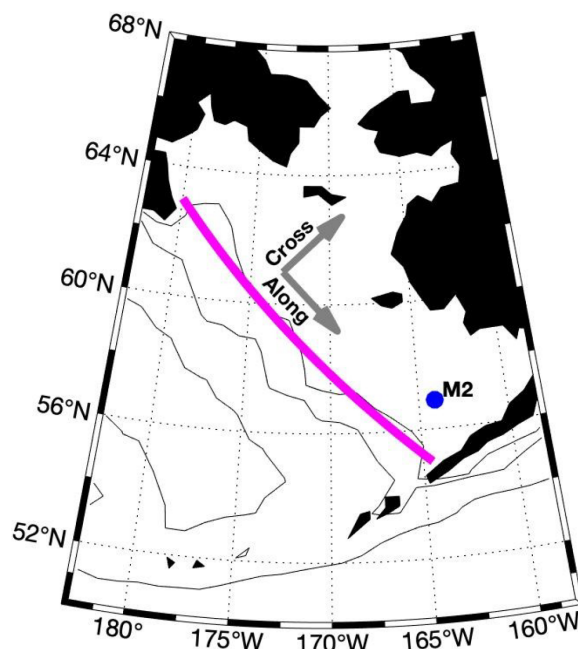
Figure 11: The magenta line shows the line chosen to evaluate along-shelf and cross-shelf wind components in the Bering Sea. Annotation arrows show the direction used to define positive cross and along shelf components of wind. Contours show isobaths at 100m, 500m, and 3500m. The blue dot shows the location of the M2 mooring.

Generally, the Ekman transport associated with cross-shelf winds will be parallel to the shelf break, and could either inhibit or enhance near surface transport associated with the current along the shelf break. Winds oriented along the shelf break will either favor on- or off-shelf transport. Measurements taken at the M2 mooring show that the Ekman layer is not deeper than 30-40 meters from May–October (N. Pelland, pers. comm.). This suggests the cross-shelf transport driven by winds is unlikely to drive upwelling or downwelling at the shelf break, as the water is substantially deeper there. However, the Ekman transport associated with surface wind stress may still be informative for understanding the dispersal of fish larvae and other zooplankton in the upper ocean. In spring (Mar–May) 2023, the along-shelf winds were generally favorable to off-shelf surface transport, while in summer (Jun–Aug) winds were more favorable for on-shelf surface transport (Figure 12).
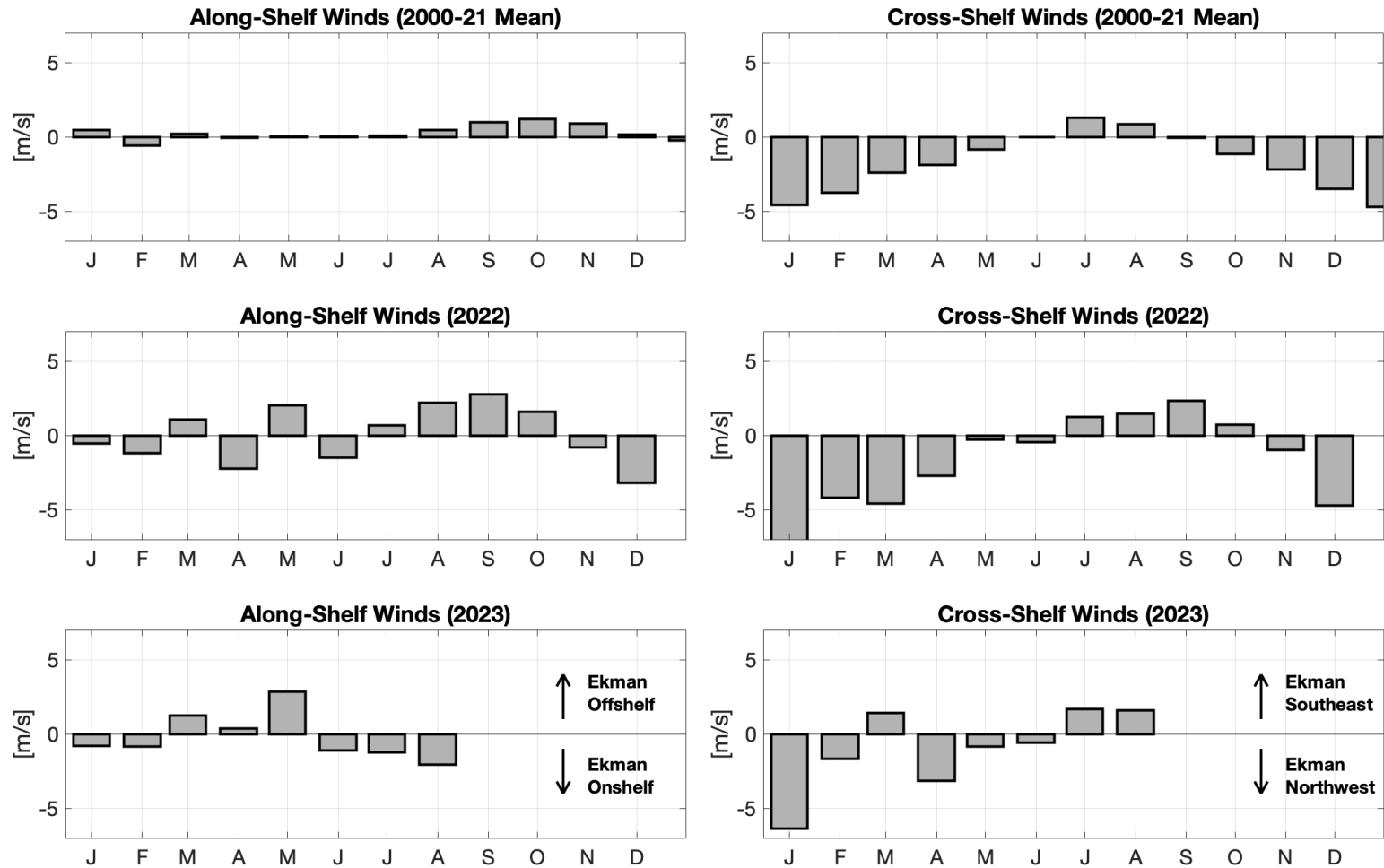
Figure 12: Along-shelf (left set of panels) and cross-shelf (right set of panels) wind components averaged along the magenta line in Figure 11. Top panels show the monthly averages across the period of record. Middle panels show the monthly averages for 2022, and bottom panels show the monthly average for 2023. Positive along-shelf winds are defined as blowing to the southeast, and positive cross-shelf winds are defined as blowing to the northeast.

St. Paul and Bering Sea Air Temperature Anomalies
Contributed by Jim Overland, *james.e.overland@noaa.gov* and Muyin Wang, *muyin.wang@noaa.gov*

The St. Paul Island surface air temperature time series has been updated to August 2023 and is based on GHCN v4, archived by NASA GISS[6]. Positive temperature anomalies have dominated the region over the last decade (Figure 13). A linear trend of 0.62°C/decade [0.45°C/decade to 0.79°C/decade] has been found for the period 1981 to 2023, a slight increase from last year due to positive temperature anomalies throughout the whole year. Starting from 2014, St Paul's temperature has been above its climatology almost every single month, with few exceptions.
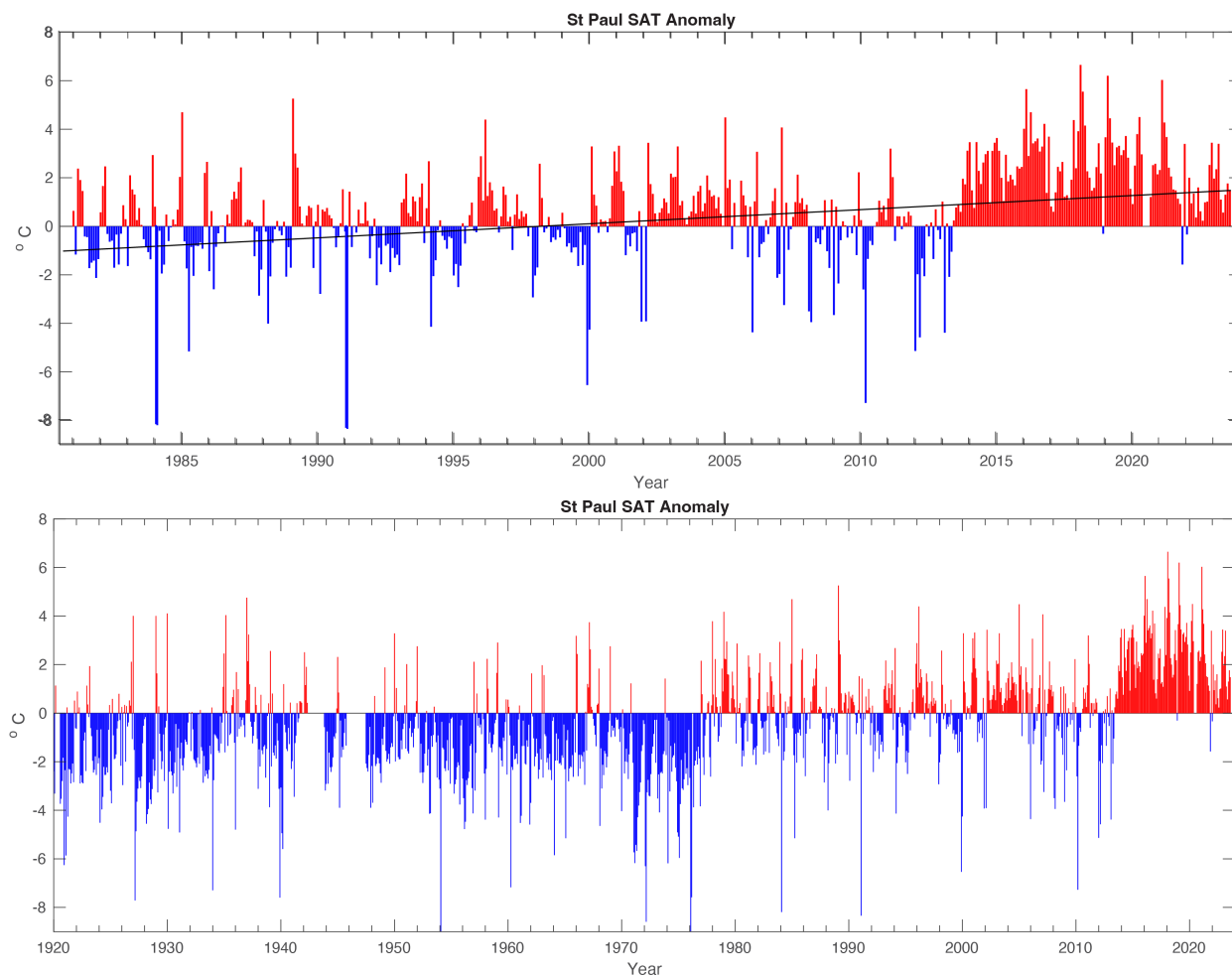
Figure 13: St. Paul air temperature anomalies updated to August 2023.

More broadly, springtime (Mar-May) air temperatures (at 925mb) in the Alaskan region were close to average conditions with slight positive anomalies in the Bering Sea and slight negative anomalies over Alaska land areas and the Gulf of Alaska (Figure 14, left). In the summer (Jun-Aug), lower than average sea level pressure in the western Bering and a ridge in the Gulf of Alaska (Figure 7, right) was accompanied by southerly flow over the majority of the Bering Sea, which resulted in positive temperature anomalies in the Bering Sea (Figure 14, right). The warm summer is part of overall warmer conditions around the world, as NASA announced that summer 2023 was the hottest on record[7]. The negative temperature anomalies in eastern Russia are part of the cold spell extension from the Eurasian land.
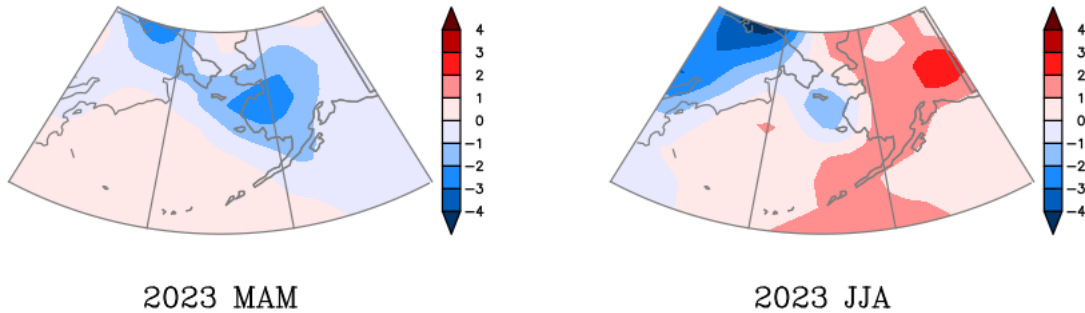
Figure 14: Air temperature anomaly at 925mb for spring (Mar-May; left) and summer (Jun-Aug; right) 2023.

---

[7]https://www.nasa.gov/press-release/nasa-announces-summer-2023-hottest-on-record

4. Sea Surface Temperature (SST) and Bottom Temperature

North Pacific Sea Surface Temperature (SST) Anomalies
Contributed by Nick Bond, *nicholas.bond@noaa.gov*

The state of the North Pacific climate from autumn 2022 through summer 2023 is summarized in terms of seasonal sea surface temperature (SST) anomaly maps. The SST anomalies are relative to mean conditions over the period of 1991–2020. The SST data are from NOAA's Extended SST V5 (ERSST) analysis and are available from NOAA's Physical Sciences Laboratory (PSL)[8].

The autumn (Sep-Nov) of 2022 featured a broad band of warmer than normal SST that extended across the entire North Pacific (Figure 15a), with anomalies exceeding 2.5°C near 40°N and the dateline. Cooler water relative to seasonal norms was present in the Sea of Okhotsk and the eastern Bering Sea shelf. The central and eastern tropical Pacific was cooler than normal in association with moderate La Niña conditions.

The positive SST anomalies in the central North Pacific persisted through the winter (Dec-Feb) of 2022–2023 (Figure 15b), with moderation in the warm temperatures in the western North Pacific. During this season, Alaskan waters were mostly within 0.5°C of normal. La Niña weakened, with only a small region of water 1°C cooler than normal near the dateline in the equatorial Pacific.

A band of warm water centered along 40°N across all but the far eastern portion of the North Pacific was present during spring (Mar-May) of 2023 (Figure 15c). Regions of cooler water reappeared in the Sea of Okhotsk and on the eastern Bering Sea shelf. The tropical Pacific had mostly near-normal SSTs with the exception of the immediate vicinity of the coast of South America, where positive anomalies began developing.

The summer (Jun-Aug) of 2023 brought marked moderation of the positive SST anomalies in the western North Pacific between 30°N and 50°N but also an eastward extension of warm anomalies to the Pacific Northwest coast. This season also included a continuation of cool conditions in the eastern Bering Sea, the development of negative SST anomalies in the GOA, and cooling southwest of Baja California into the subtropical eastern North Pacific (Figure 15d). The tropical Pacific featured strong warming east of 140°W, with the SSTs meeting the threshold for El Niño in June 2023, according to NOAA's Climate Prediction Center (CPC).

---

[8]https://www.psl.noaa.gov/cgi-bin/data/composites/printpage.pl.
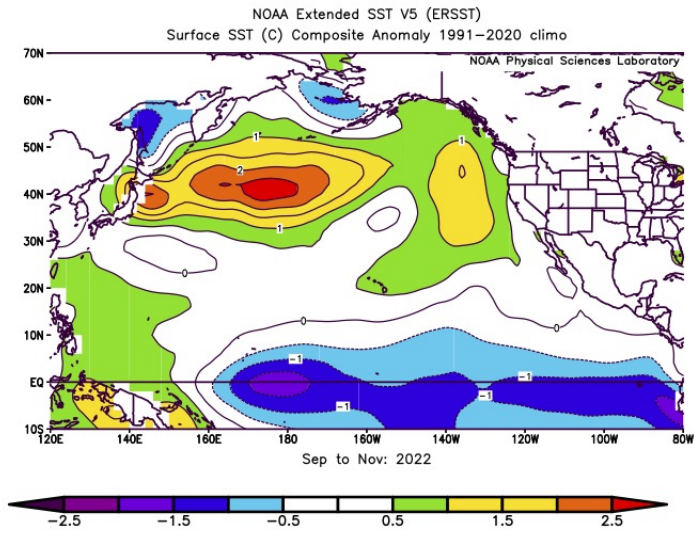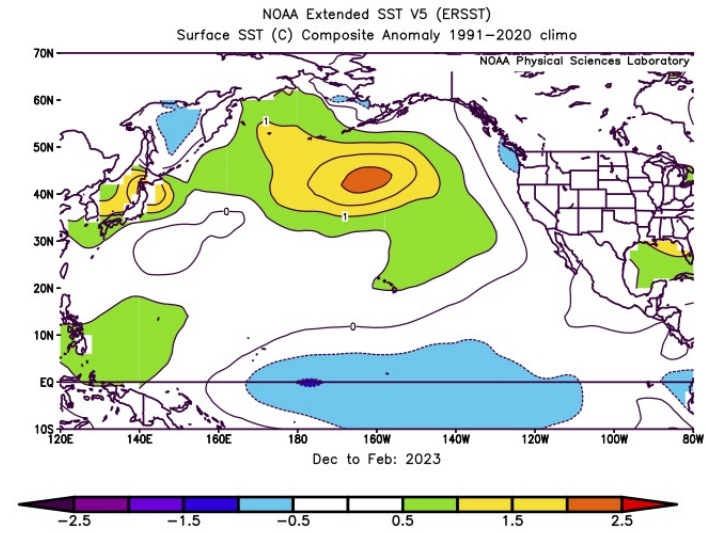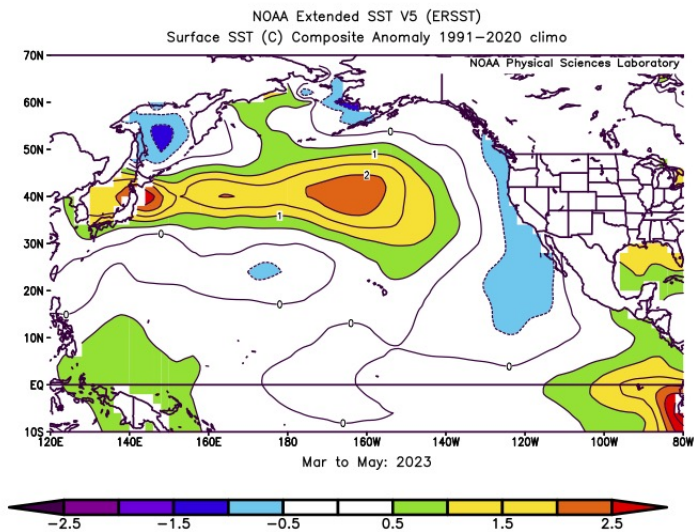
(a) Autumn

(b) Winter

(c) Spring
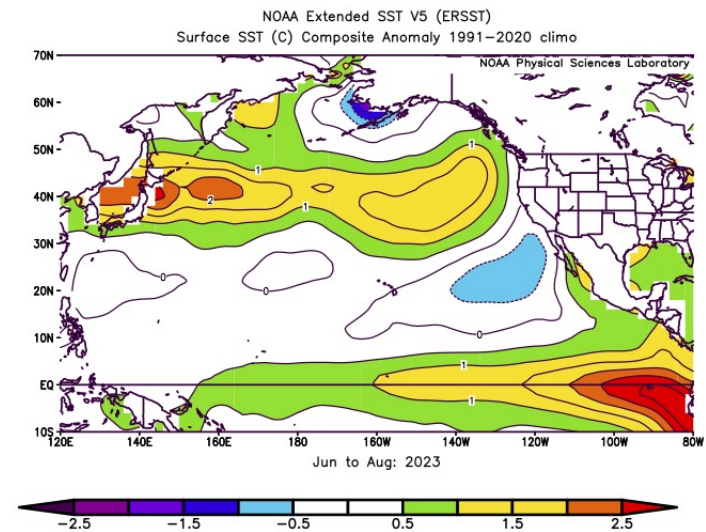
(d) Summer

Figure 15: Sea surface temperature anomalies for (a) autumn (Sept-Nov 2022), (b) winter (Dec 2022-Feb 2023), (c) spring (Mar-May 2023), and (d) summer (Jun-Aug 2023).

Bering Sea SST Anomalies
Contributed by Emily Lemagie, *emily.lemagie@noaa.gov* and Matt Callahan, *matt.callahan@noaa.gov*

Satellite SST data (source: NOAA Coral Reef Watch Program) were accessed via the Alaska Fisheries Information Network (AKFIN). Daily data were averaged within the southeastern (south of 60°N) and northern (60°–65.75°N) Bering Sea shelf (10–200m depth). Detailed methods are available online[9].

Trend analysis removed seasonality and variability from the SST time series (Edullantes, 2019) to better illustrate the long term trends in the SST data (Figure 16). Trends are compared to the mean (± 1 standard deviation) from a 30-yr baseline (1985–2014) and demonstrate that both the northern and southeastern Bering Sea cooled relative to the recent persistent warm stanza. In the most recent data, the trend is within 1 standard deviation of the mean. Note: The time series trend analysis requires truncation of the ends of the time series (due to differencing) so the trend line extends only into March 2023.
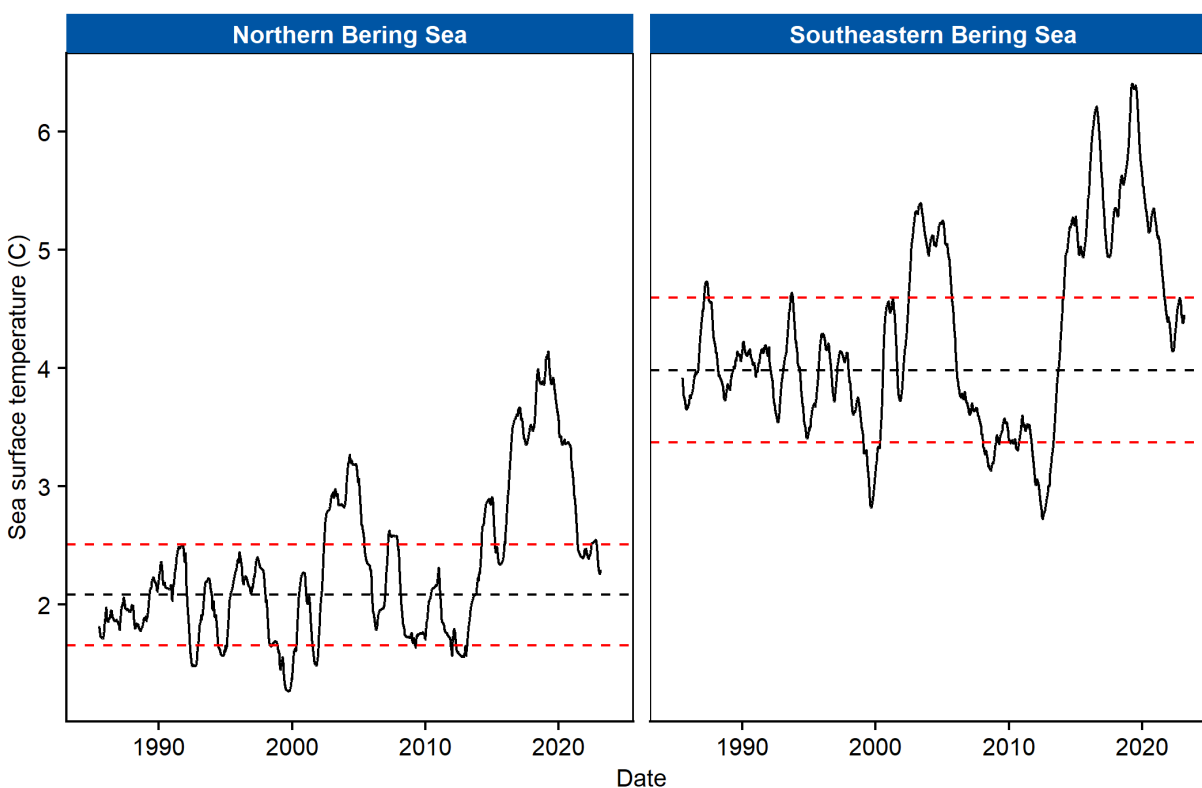
Figure 16: Time series trend of SST (seasonality and noise removed) for the northern (left) and southeastern (right) Bering Sea shelves. The black horizontal dotted line is the 30-year mean (1985–2014) of the trend and the red lines are ± 1 SD.

Marine Heatwave Index
Contributed by Emily Lemagie, *emily.lemagie@noaa.gov*, and Matt Callahan, *matt.callahan@noaa.gov*

There were no marine heatwaves (MHWs) in 2023 (Figure 17). Since January 2021 there have been only a few brief and predominantly moderate events over the eastern Bering Sea shelf. Note, this MHW index is based on SST, which is strongly influenced by sea ice and stratification in the Bering Sea, particularly over the middle shelf where surface and bottom temperature dynamics can be decoupled much of the year (Ladd and Stabeno, 2012). Bottom temperature in the Bering Sea is an important ecosystem indicator (Stabeno and Bell, 2019).
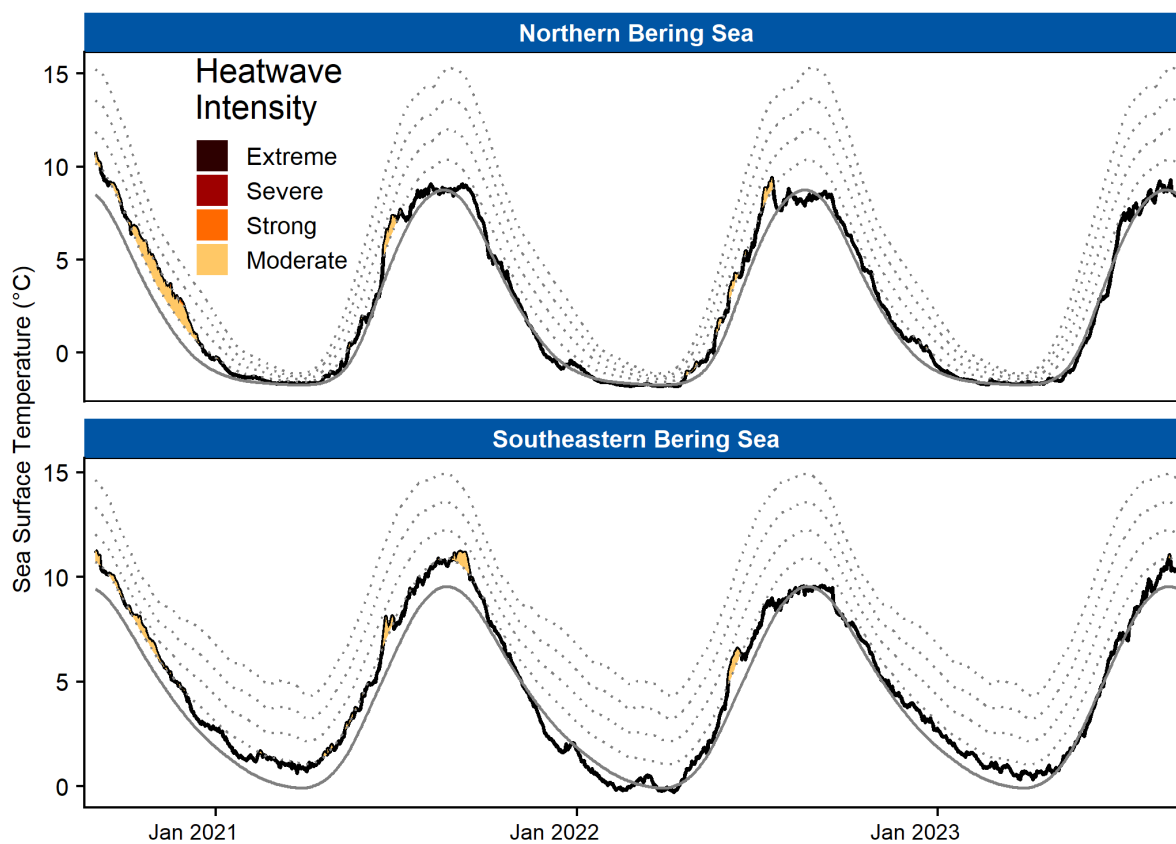
Figure 17: Marine heatwaves in the northern and southeastern Bering Sea since September 2020. The smoothed solid black line represents the baseline average temperature (i.e., climatology) for each day during the 30-yr baseline period (1 Sept 1985 to 31 Aug 2014). The jagged solid black line is the observed (satellite-derived) SST for each day. Dotted lines illustrate thresholds for increasing MHW intensity categories (moderate, strong, severe, extreme). Colored portions indicate periods during which MHW occurred, with intensity increasing as colors darken.

Annual and Seasonal SST Trends
Contributed by Emily Lemagie, *emily.lemagie@noaa.gov*, and Matt Callahan, *matt.callahan@noaa.gov*

The cumulative SSTs for 2023 were within 1 standard deviation of average for the second consecutive year (Figure 18). Such cumulative warming as experienced in 2014–2021 may represent important conditions for the ecology of these systems in that the total thermal exposure for organisms was higher than historically average conditions. Protracted warming may lead to elevated metabolic rates, higher growth rates, and higher prey demands. At the seasonal level, mean SST patterns were within one standard deviation of the long-term mean in both 2022 and 2023 (Figure 19; note mean and standard deviations not shown for clarity).
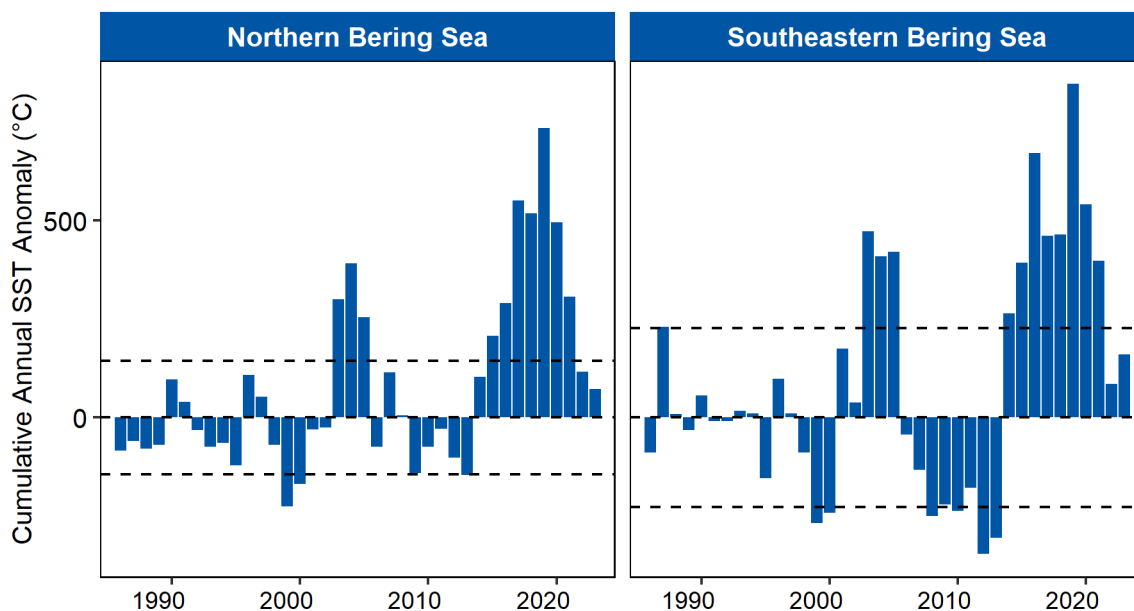
Figure 18: Cumulative annual SST anomalies (sum of daily temperatures). Horizontal lines are ± 1 standard deviation from the mean during the 30-yr baseline period (1 Sept 1985 to 31 Aug 2014).
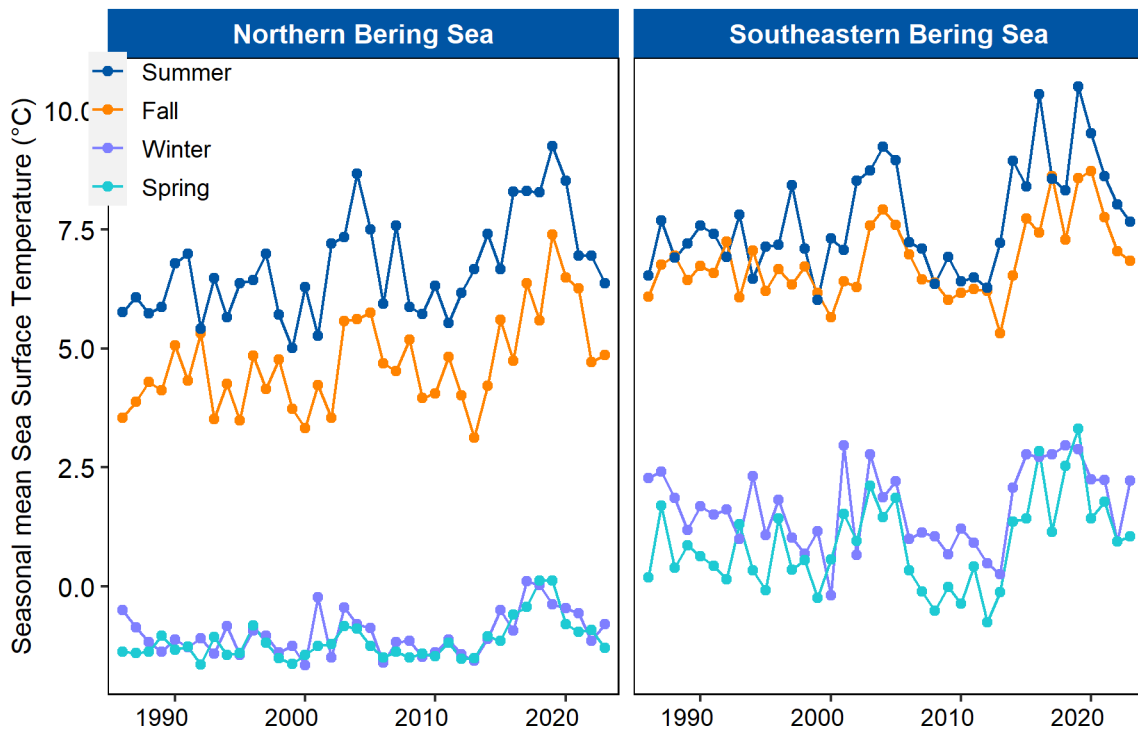
Figure 19: Seasonal mean SSTs for each year, apportioned by season: summer (Jun–Aug), fall (Sep–Nov), winter (Dec–Feb), and spring (Mar–May). Negative values are due to sea surface temperatures below zero.

Bering Sea SST and Bottom Temperature Trends
Contributed by Emily Lemagie, *emily.lemagie@noaa.gov*, Matt Callahan, *matt.callahan@noaa.gov*, and
Kelly Kearney, *kelly.kearney@noaa.gov*

Estimates of bottom temperature are derived from the Bering 10K Regional Ocean Modeling System
(ROMS) hindcast simulation, which was extended to the near-present, using reanalysis-based input
forcing. This hindcast simulation now extends from Jan 15, 1970 to Aug 16, 2023.

After an eight year warm stanza, SST over the past year (September 2022–August 2023) in the northern
Bering Sea (NBS) and southeastern Bering Sea (SEBS) (see Figure 20 for domains) broadly returned to
within 1 standard deviation of the 30-year baseline (1985–2014) (Figure 21, top two rows). Exceptions
to near-normal thermal conditions include a relatively warm winter across all regions. Above-average
temperatures lasted through spring over the outer domain and over the middle domain (50-100m) of
the SEBS.

Similar to SST, ROMS-estimated bottom temperatures in the NBS and SEBS were near historical aver-
ages much of the prior year over most domains (Figure 21, bottom two rows). Two notable exceptions
include: 1) the outer (100–200m isobaths) southern domain, where temperatures were consistently near
the coldest on record ($\sim$0.5°C below the seasonal average), and 2) the inner domain ($<$50m) for both
NBS and SEBS regions, which were moderately cooler than average from about mid-April through
August 2023. For the outer southern domain, the cool bottom temperatures were a continuation from
the prior year, and since the outer domain SST was slightly above average for the 2022–2023 winter,
waters were more vertically thermally stratified than average. For the inner northern and southern do-
mains, both surface and bottom temperatures were near or slightly above their seasonal averages for
the 2022–2023 winter, when the water column tends to be well mixed from top to bottom, coupling
the surface and bottom temperatures. However, beginning in mid-spring, a combination of freshwater
melt and surface warming causes stratification, decoupling the surface and bottom regimes. After this
springtime stratification, surface temperatures in the inner domains remained near the seasonal average,
while bottom temperatures showed delayed warming, and hence, were cooler than average for the 2023
spring and summer.
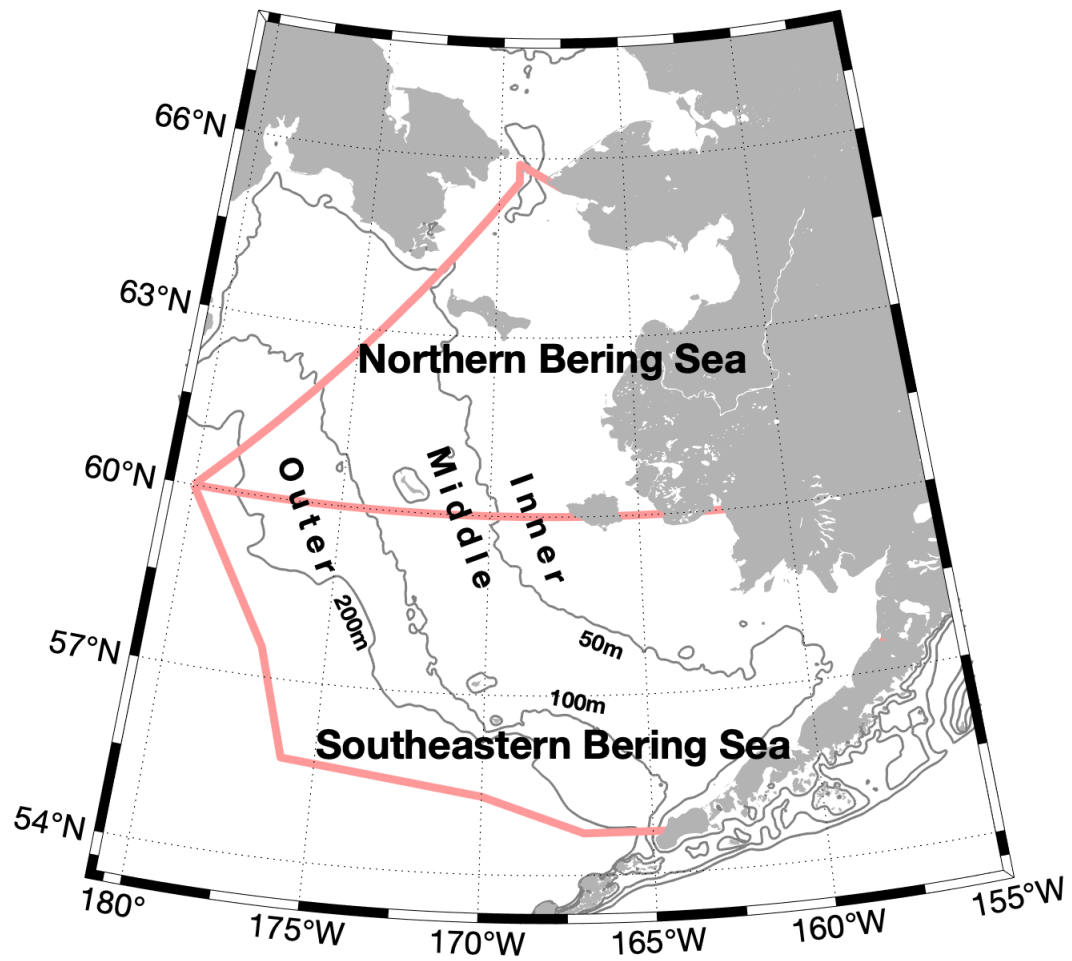
Figure 20: Map of the eastern Bering Sea. The inner (¡50m isobaths), middle (50–100m isobaths), and outer (100–200m isoboaths) domains are shown. The southeastern and northern Bering Sea are delineated at 60°N.
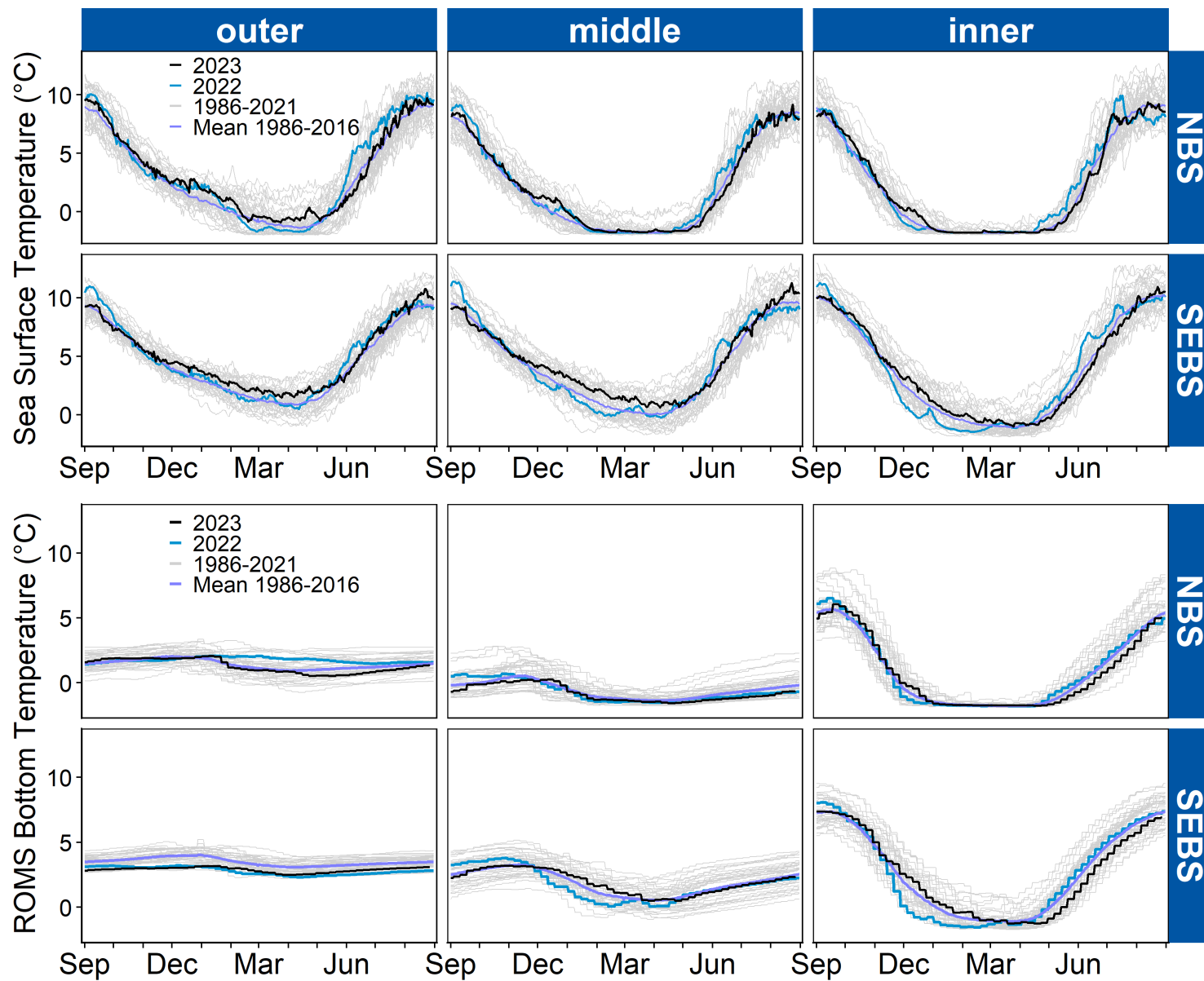
Figure 21: Top 2 rows: Mean daily SST for the northern (NBS) and southeastern (SEBS) outer, middle, and inner shelf domains. Bottom 2 rows: Mean weekly bottom temperature for the NBS and SEBS outer, middle, and inner shelf domains. The most recent year (2022–2023; through August 2023) is shown in black, 2021–2022 is shown in blue, and the historical mean is shown in purple. Individual years in the time series are shown in light gray.

St. Paul Island Temperature, Salinity, and Chlorophyll-a
Contributed by Lauren Divine, *lmdivine@aleut.com*, Aaron Lestenkof, *aplestenkof@aleut.com*
and Tyler Hennon, *tdhennon@alaska.edu*

Community-led monitoring of temperature and salinity from North Dock on the St. Paul Island break-water have been made since 2014 using CTD data loggers (Figure 22). Instrumentation used since 2015 has also had a sensor for chlorophyll-a fluorescence, which provides a measure of phytoplankton concentration. Water depth at the sample site is approximately 8m. Water column profiles are collected nominally weekly and have been averaged into monthly means with the annual signal removed (Figure 23).

Following the trends exhibited elsewhere, temperature anomalies over the last ~12 months at St. Paul Island show relatively cool conditions compared to the preceding years. Anomalies occasionally exceeded 1°C cooler than the seasonal average (Figure 23). It is important to note, however, that across the North Pacific as a whole, 2014 through 2021 has been appreciably warmer than the long-term average, such that the baseline temperature in this record is significantly warmer than other time series with a longer period-of-record (e.g., Danielson et al., 2020).

Until about 2021, salinity had been generally increasing over the period of record. As noted in the 2022 Eastern Bering Sea Ecosystem Status Report (Siddon, 2022), this trend appeared to undergo reversal from August 2021 to August 2022. Similarly during the span of August 2022 to August 2023, salinities remain significantly below the highs reached in ~2019–2021 (Figure 23). Contributing factors to salinity variability on the EBS shelf include river discharge, precipitation, evaporation, ice advection, inflows from the Gulf of Alaska, and cross-slope exchanges with the basin (Aagaard et al., 2006). It is not completely clear what is responsible for the reversal in the salinity trend, but it is likely that the increased presence of sea ice over the prior two years is a factor (see Figure 30).

Chlorophyll-a fluorescence measurements show year-to-year variability in the timing of the spring phy-toplankton bloom. While several years (e.g., 2018, 2019) show a relatively late and weak bloom, chlorophyll-a data from St. Paul Island in 2023 suggest the weakest bloom since at least 2017 (Figure 24), which corroborates satellite-derived chlorophyll a concentrations observed over the EBS shelf (see p. 79).
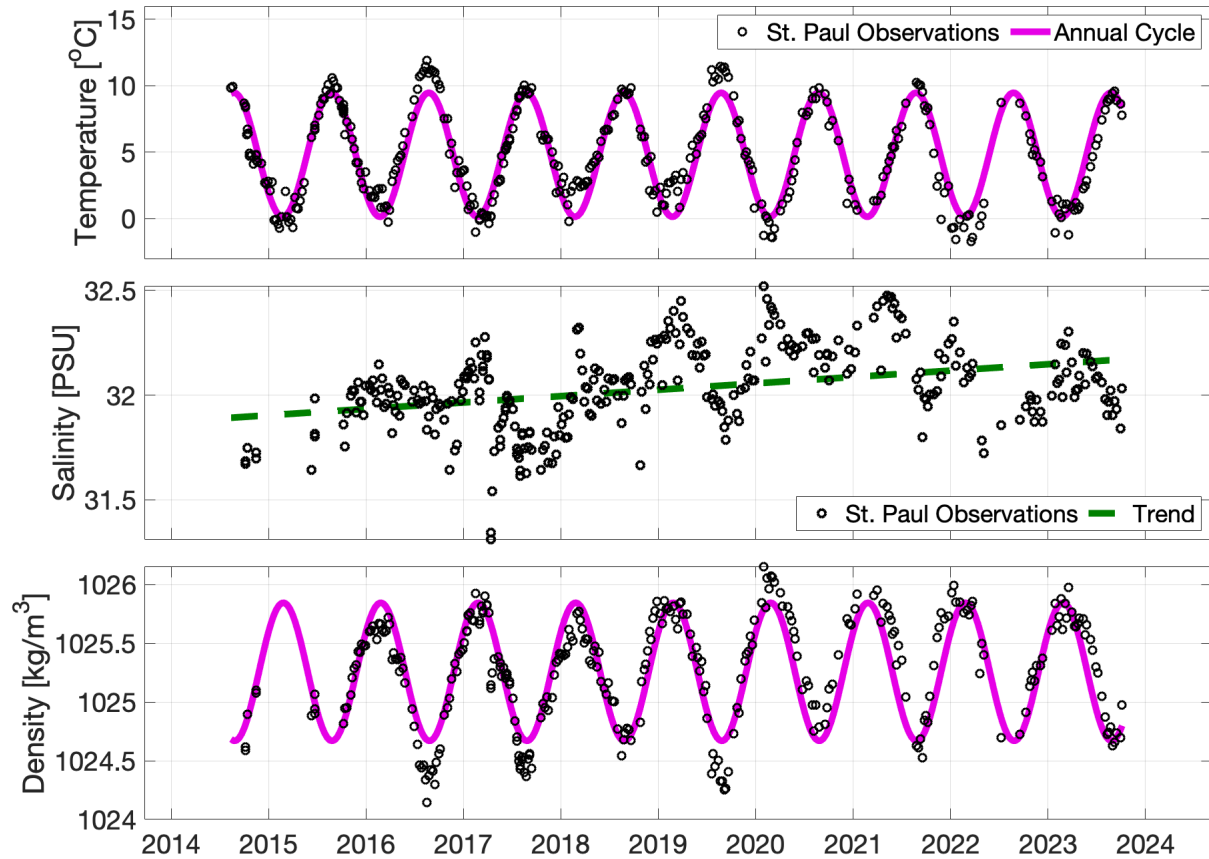
Figure 22: Observations of temperature (top), salinity (middle), and density (bottom) collected at St. Paul Island (black dots). Fitted annual cycles in temperature and density are in magenta, and the long term linear trend in salinity over the time series is represented by the dashed green line (p<0.01), though the most recent years suggest a potential reversal.
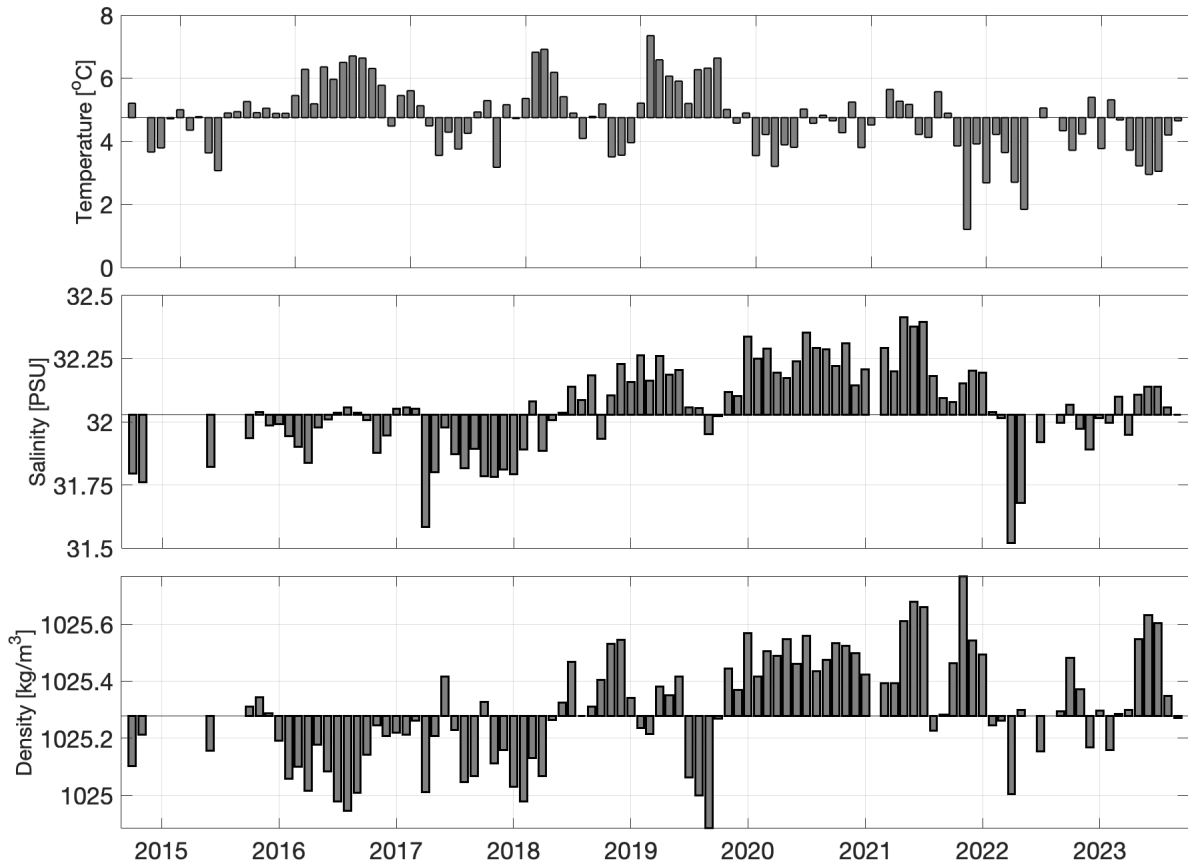
Figure 23: Monthly averages with the seasonal cycle removed for temperature (top), salinity (middle), and density (bottom) from St. Paul Island.
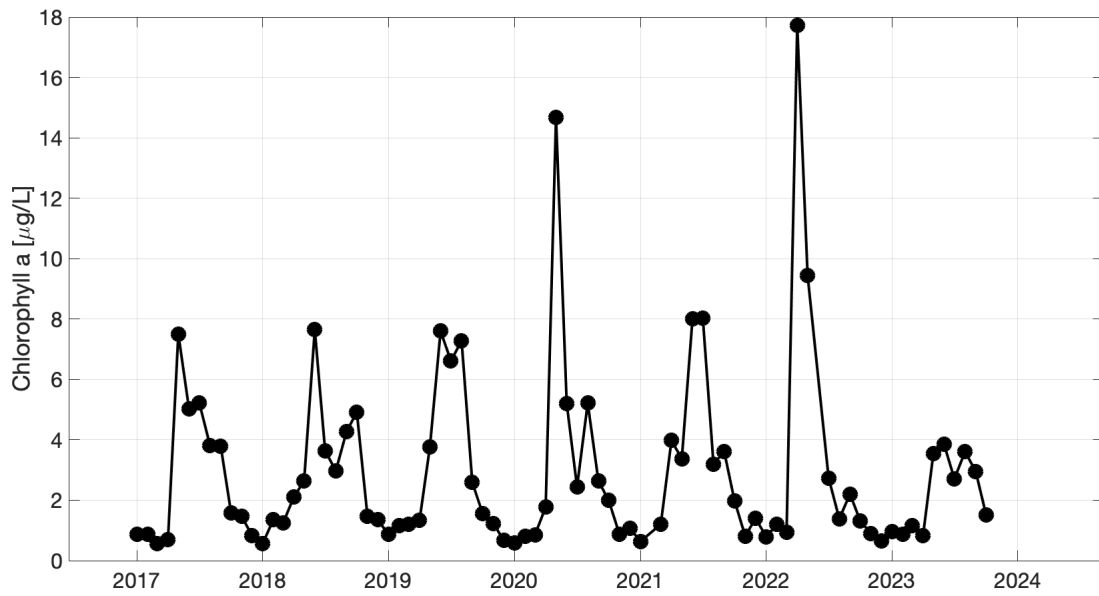
Figure 24: Monthly average of chlorophyll-a concentrations collected at St. Paul Island through August 2023.

Summer Surface and Bottom Temperatures
Contributed by Sean Rohan, *sean.rohan@noaa.gov* and Lewis Barnett, *lewis.barnett@noaa.gov*

Annual mean surface and bottom temperatures are calculated from spatially interpolated data collected during AFSC summer bottom trawl surveys of the EBS shelf (1982–2023, except 2020) and NBS (2010, 2017–2019, 2021–2023). Temperature data are not adjusted for effects of seasonal heating. Temperature data are interpolated using ordinary kriging with Stein's parameterization of the Matern semivariogram model (Rohan et al., 2022). Code, figures, and data products presented in this contribution are provided in the coldpool R package version 3.2-2[10].

In the EBS, the mean surface temperature (6.34°C) was near the time series average (6.75°C) and 1.12°C colder than in 2022. The 2023 mean bottom temperature in the EBS (2.28°C) was near the time series mean of 2.49°C and 0.28°C colder than the mean bottom temperature in 2022 (Figure 25). The near-average bottom temperatures in 2022 and 2023 are a departure from extremely warm conditions in 2016–2021, which included four of the five warmest years in the time series. In the NBS, the mean surface temperature (9.07°C) was near the time series average (9.17°C) and the mean bottom temperature (3.71°C) was near the time series average (3.91°C). However, the time series for the NBS includes only six years, which is extremely short compared to the 41 years of temperature data from the EBS.
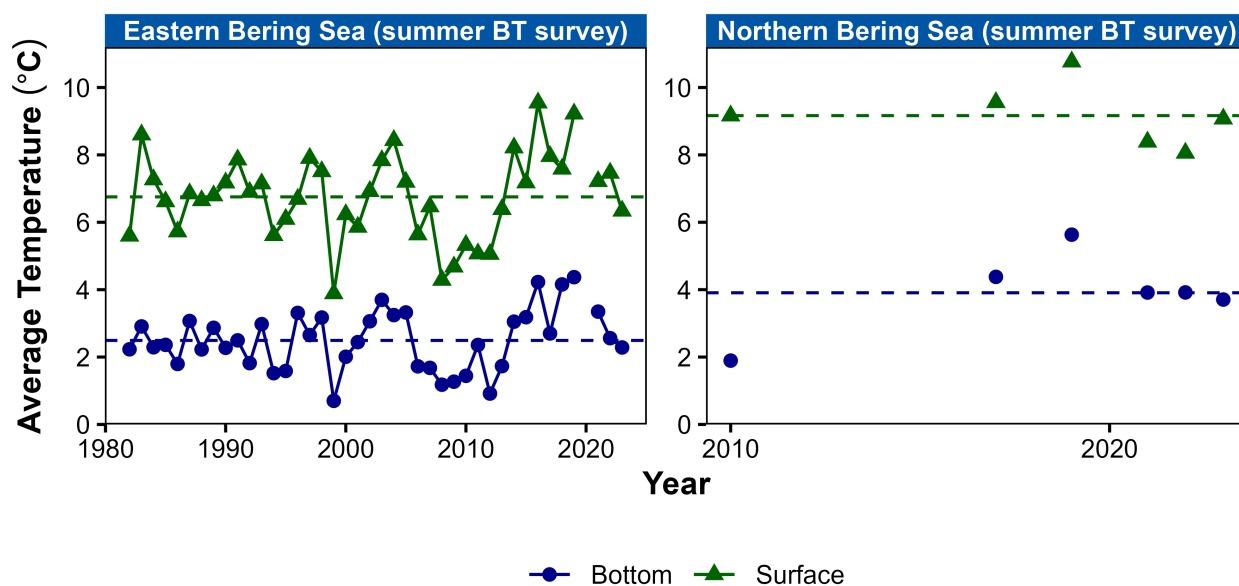
Figure 25: Average summer surface (green triangles) and bottom (blue circles) temperatures (°C) on the eastern Bering Sea shelf based on data collected during standardized summer bottom trawl surveys from 1982–2023. Dashed lines represent the time series mean.

In 2023, bottom temperatures ≤-1°C were observed south of St. Matthew Island for the first time since 2015 (Figure 26). The average bottom temperature in the inner domain of the EBS survey area (2.17°C) was the coldest observed since 2013 (1.64°C). The coldest bottom temperatures within the combined EBS shelf and NBS survey areas were in the middle shelf (between 50–100m isobaths), extending from

---

[10]https://github.com/afsc-gap-products/coldpool

south of St. Matthew Island at ~ 61.5°N to the U.S.-Russia maritime boundary. This area of cold water was considerably larger than in 2019 and 2021, when bottom temperatures ≤0°C were confined to a small area along the U.S.-Russia Convention Line.

The warmest bottom temperatures were along the coast of the Alaska mainland between Nunivak Island and Norton Sound. However, the area north of Nunivak Island at 60.5°N is sampled at the end of the survey and reflects seasonal warming since sampling occurs 35–45 days later than in the area directly south.
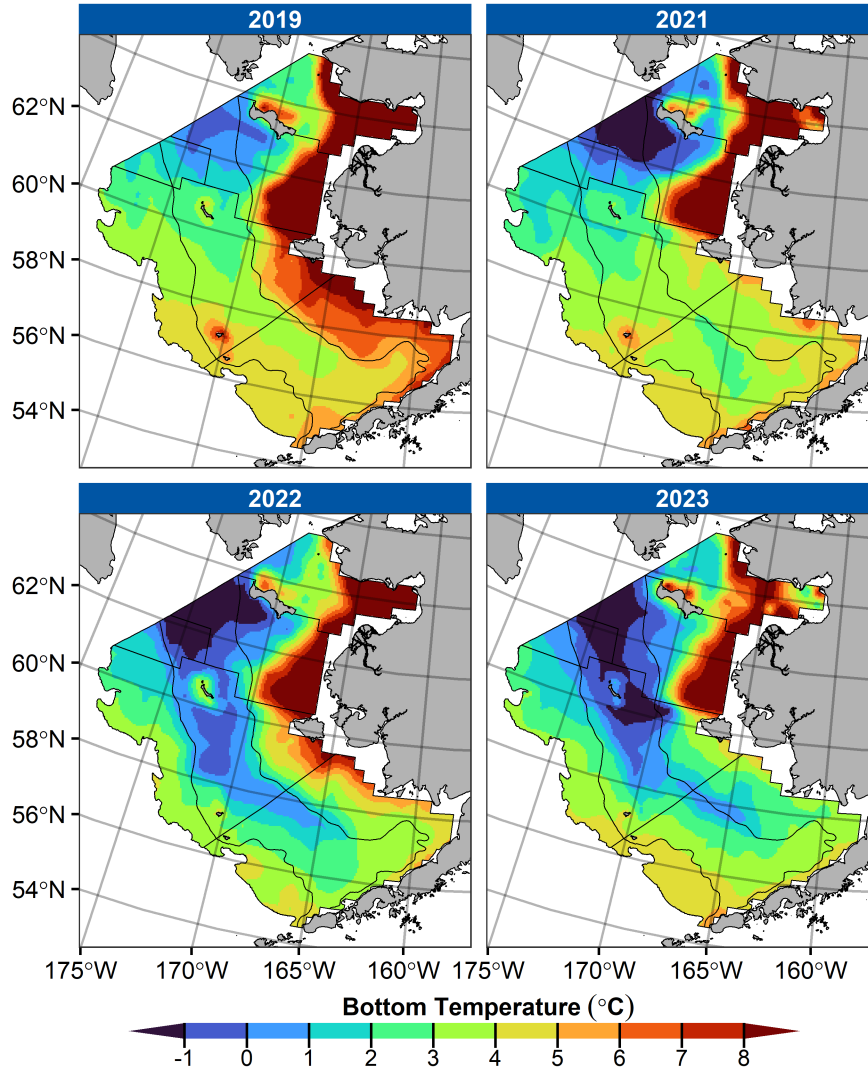
Figure 26: Contour maps of bottom temperatures from the 2019, 2021, 2022, and 2023 eastern Bering Sea shelf and northern Bering Sea bottom trawl surveys.

Bottom Temperatures Along the EBS Shelf Break
Contributed by Kevin Siwicke, *kevin.siwicke@noaa.gov* and Tyler Hennon, *tdhennon@alaska.edu*

Since 2005 bottom temperatures have been measured during the EBS longline survey, generally between June and August. Thermistors are mounted to longline equipment, and remain on the bottom for several hours before recovery. Longline surveys are conducted on the Bering shelf break every odd year, and the bottom depths sampled there range between about 250m to 500m (Figure 27).

Though the period of record is relatively short for the Bering Sea shelf break, the bottom temperature averaged across all EBS stations during the last five survey years (between 2015 and 2023) are markedly higher than from 2009 to 2013 (Figure 28). While the water temperatures ≤200m across the EBS have seen a relaxation from the most recent warm stanza, the trends in the slightly deeper longline survey data may suggest that vertical stratification has decoupled the deeper water from shallower processes, allowing the relatively warm conditions to persist.
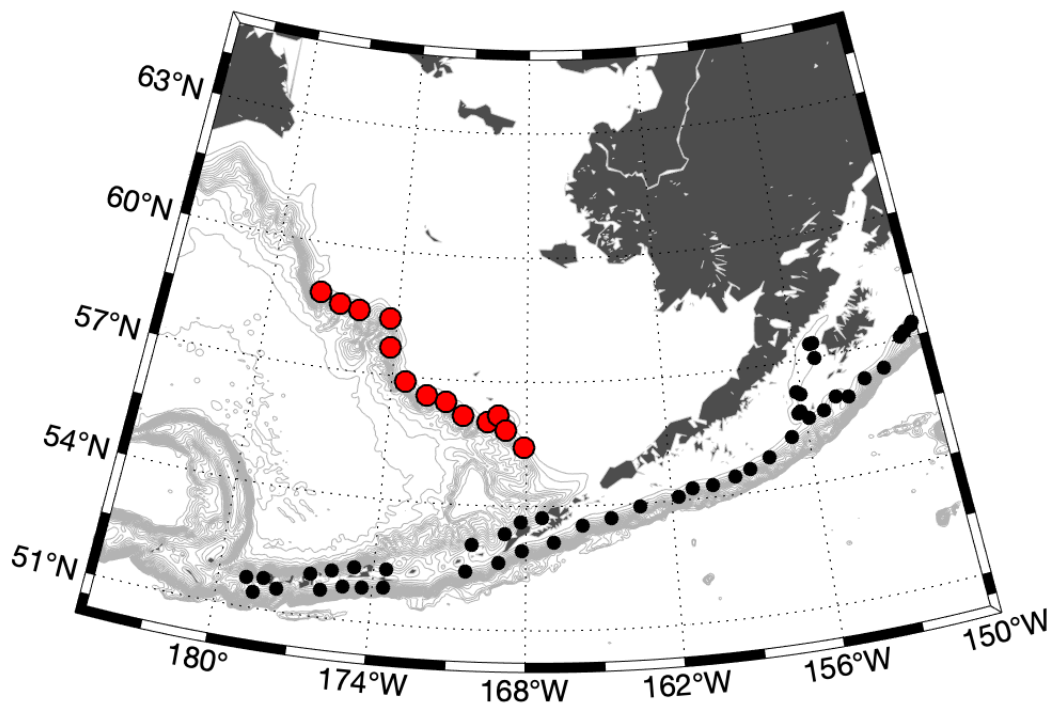
Figure 27: Location of stations for longline survey bottom temperature measurements in the eastern Bering Sea (red) and elsewhere (black). Bathymetric contours are every 200m.
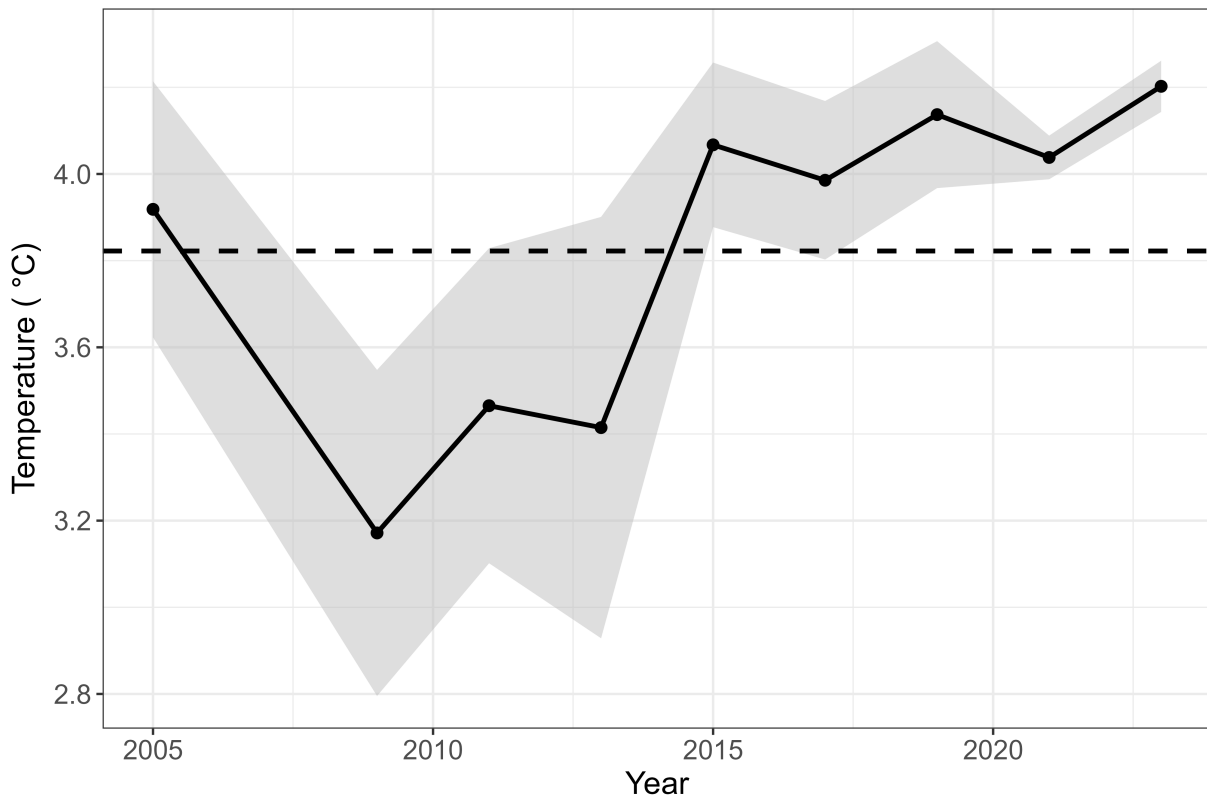
Figure 28: Average bottom temperature during the longline survey in the eastern Bering Sea (black line) ± 1 standard deviation (shaded area). Beginning in 2005, surveys have been conducted in the eastern Bering Sea every odd year (except 2007). The dashed line is the average over the period of record.

5. Sea Ice

Early Season Sea-Ice Extent
Contributed by Rick Thoman, *rthoman@alaska.edu*

Early season ice extent was similar to most years since 2013 except for 2022's very high values and lower than any year prior to 2007 (Figure 29). Over the 45 year period of record, early season mean ice extent has decreased by 55%.
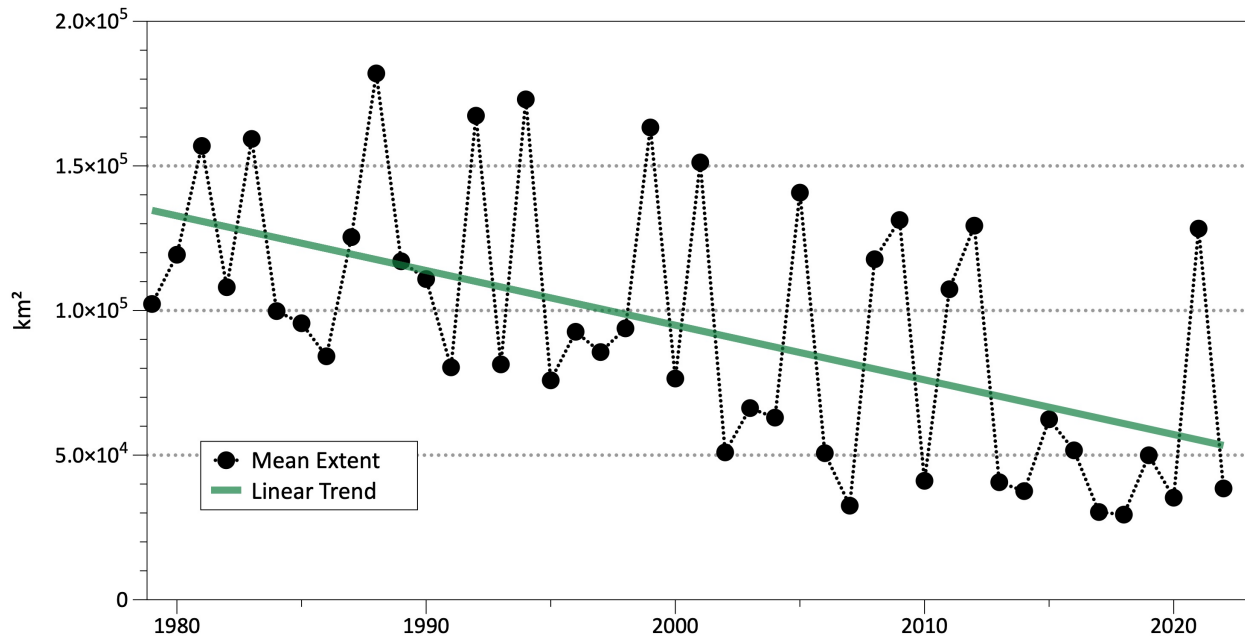
Figure 29: Early (15 Oct-15 Dec) mean sea-ice extent in the Bering Sea, 1979–2023. Source: National Snow and Ice Data Center Sea Ice Index version 3.

Annual and Daily Bering Sea Sea-Ice Extent

The 2022–2023 average sea ice extent was slightly lower than 2021–2022 (Figures 30 and 31). While a significant recovery from the extreme 2017–2018 and 2018–2019 seasons, the 12-month average extent was similar to what were considered "low ice stanza" years prior to 2010.
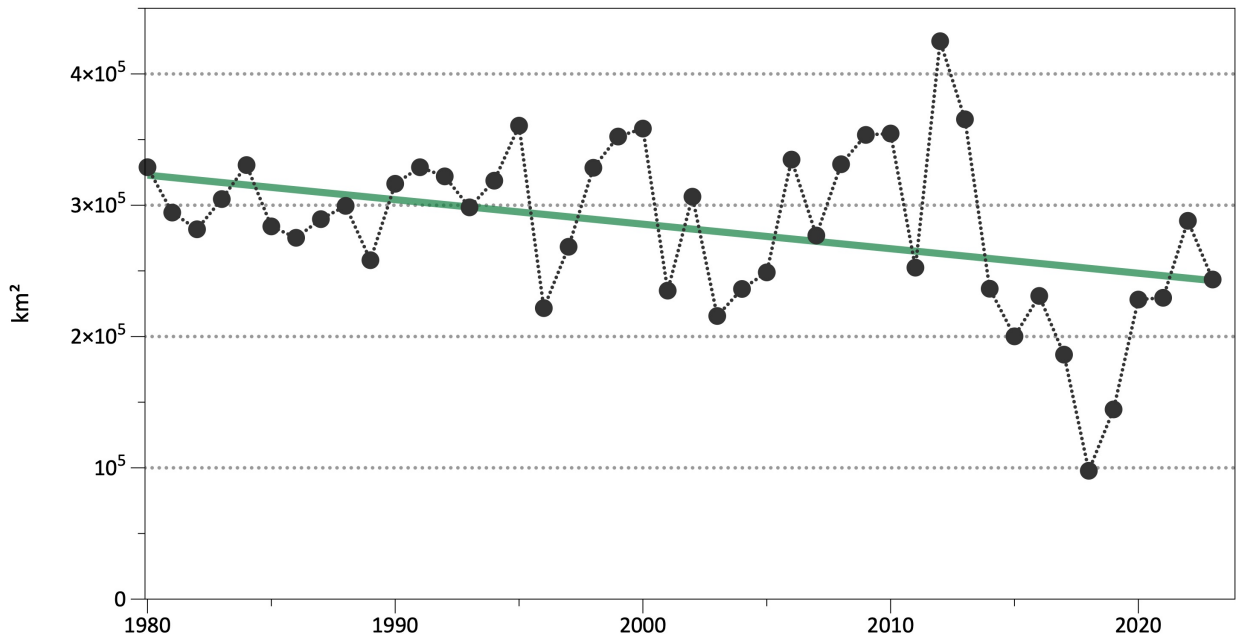
Figure 30: Mean sea-ice extent in the Bering Sea from 1 August to 31 July, 1979/1980–2022/2023.
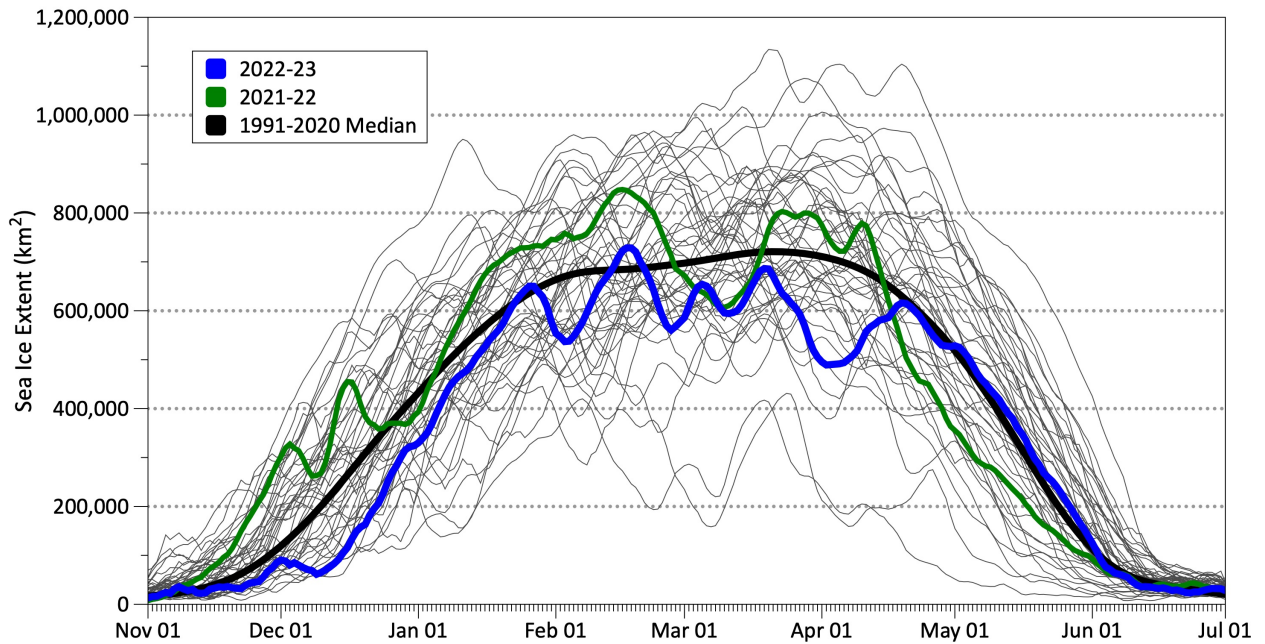
Figure 31: Daily sea ice extent in the Bering Sea. The most recent year (2022–2023) is shown in blue, 2021–2022 in green, and the historical median in black. Individual years in the time series are shown in gray.

Sea-Ice Thickness

This year's report uses version 2.05 of the combined CryoSat-2/SMOS sea ice thickness from the Alfred Wegener Institute. The main difference between this version and version 2.04 used for last year's report is the uncertainty estimates have been narrowed for some earlier years. Figure 32 delineates the different domains where sea ice thickness is quantified.

For the week of March 15-21, sea ice thickness was higher in Norton Sound than 2022. For the area between St. Lawrence Island and St. Matthew Island, ice thickness for this week was the highest since 2013. Other regions were close to the 13-year median (Figures 33 and 34).
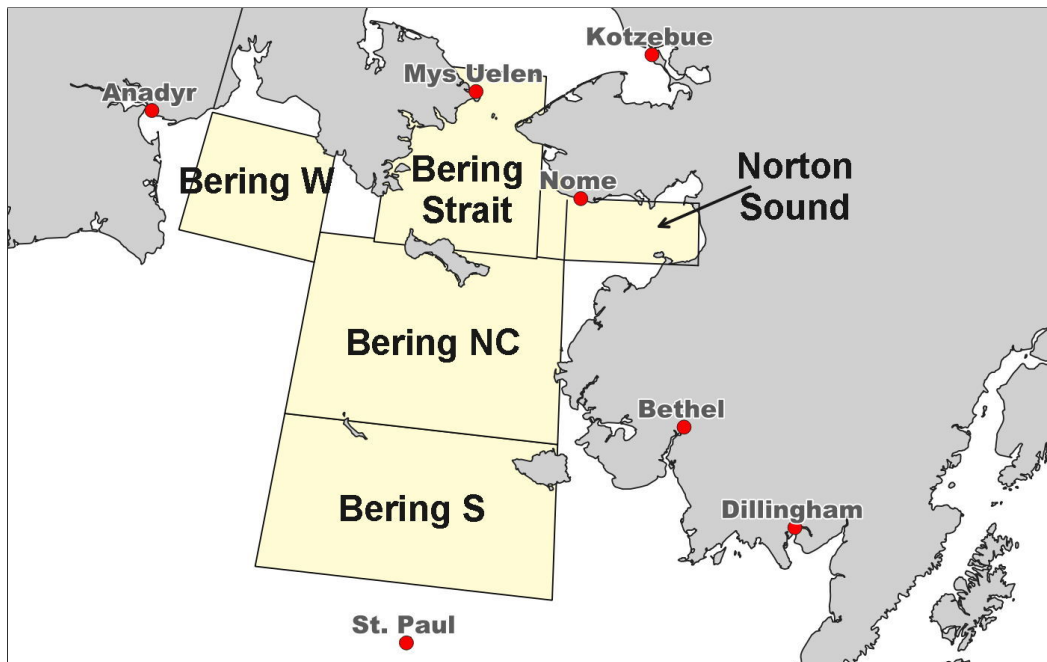
Figure 32: Map showing the five areas over the Bering Sea within which ice thickness indices were calculated: Gulf of Anadyr (Bering W), Bering Strait, Norton Sound, St. Lawrence Island to St. Matthew Island (Bering NC), and St. Matthew Island to St. Paul Island (Bering S).
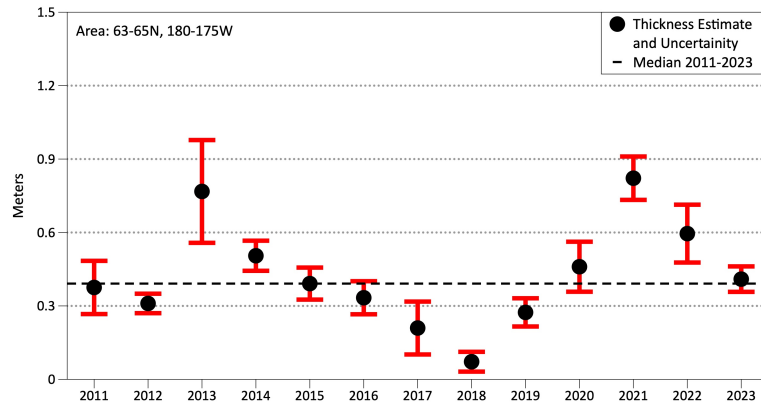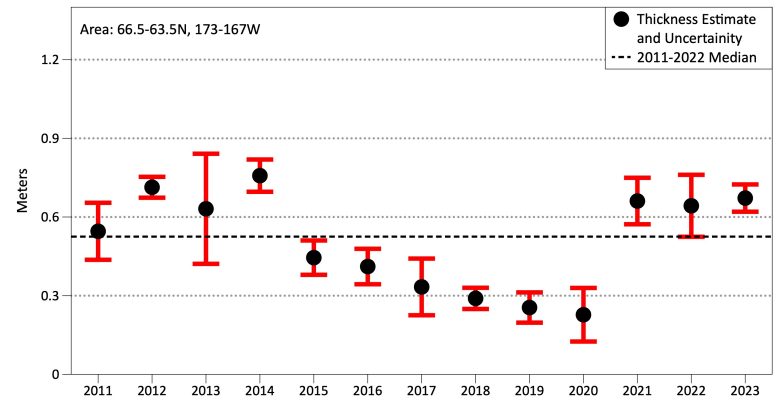
Figure 33: Sea-ice thickness in the Bering Sea for (a) Gulf of Anadyr, (b) Bering Strait, (c) St. Lawrence Island to St. Matthew Island, and (d) Norton Sound. Source: Alfred Wegener Institute. Details on how uncertainty in sea-ice thickness was quantified are available at: `https://www.meereisportal.de/en/`
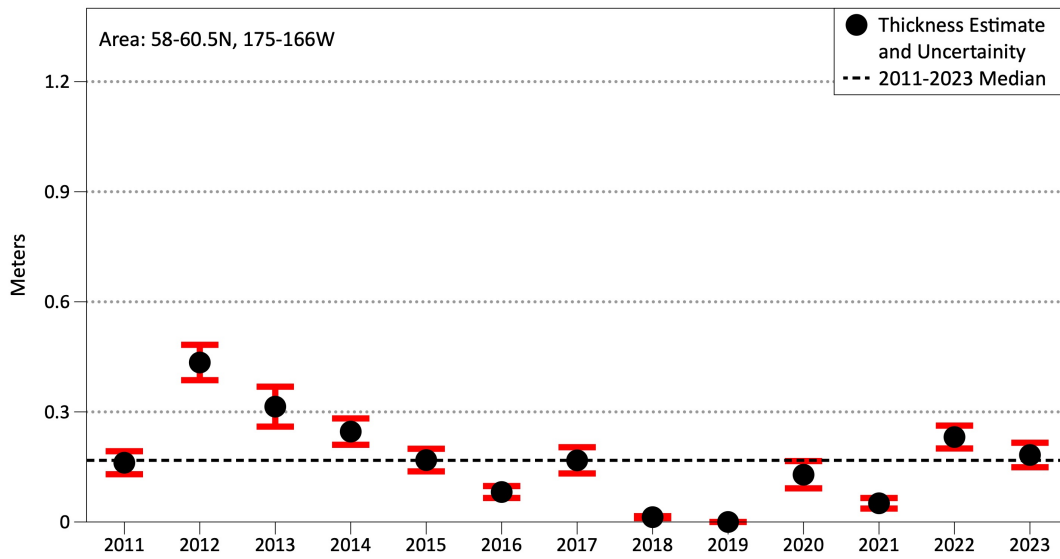
Figure 34: Sea-ice thickness between St. Matthew Island and St. Paul Island. Source: Alfred Wegener Institute. Details on how uncertainty in sea-ice thickness was quantified are available at: `https://www.meereisportal.de/en/`

6. Cold Pool

Cold Pool Extent - ROMS
Contributed by Kelly Kearney, *kelly.kearney@noaa.gov*

As in 2022, 2023 simulated conditions fall toward the historical mean of 1970–2023 (Figure 35). The mean SEBS bottom temperature was 2.28°C, about half a degree below the historical mean of 2.77°C. The 2°C cold pool index was 0.4 and the 0°C index was 0.13, likewise just to the cool side of the historical means of 0.35 and 0.11, respectively. Our cluster analysis revealed some similarities with other middle-of-the-road years, though no particularly close analogues: the bottom temperature spatial patterns across the shelf resembled those seen in 2020 and 2011 as well as a few years in the late 1990s (1995, 1997, 2000), and the seasonal evolution of the cold pool indices clustered with 2017, 1984–1986, and 1994.

Cold Pool Extent - AFSC Bottom Trawl Survey
Contributed by Sean Rohan, *sean.rohan@noaa.gov* and Lewis Barnett, *lewis.barnett@noaa.gov*

The cold pool extent is calculated from spatially interpolated bottom temperature data collected during AFSC summer bottom trawl surveys of the EBS shelf (1982–2023, except 2020). See 'Summer Surface and Bottom Temperatures' contribution above for more details.

The spatial footprint of the cold pool in 2023 was similar to the most recent near-average years in 2011, 2017, and 2022 (Figure 36). North of ∼57.5°N, the cold pool covered nearly the entire middle domain of the survey area between the 50m and 100m isobaths. The extents of the $\leq$-1°C (26,550km^2) and $\leq$0°C (62,400km^2) isotherms were larger than they have been since the 2015 survey. The extent of the $\leq$1°C isotherm (110,875km^2) was the largest it's been since 2013. The extents of the $\leq$-1°C, $\leq$0°C, and $\leq$1°C isotherms were all larger than their time series averages of 23,579km^2, 54,158km^2, and 102,906km^2, respectively.
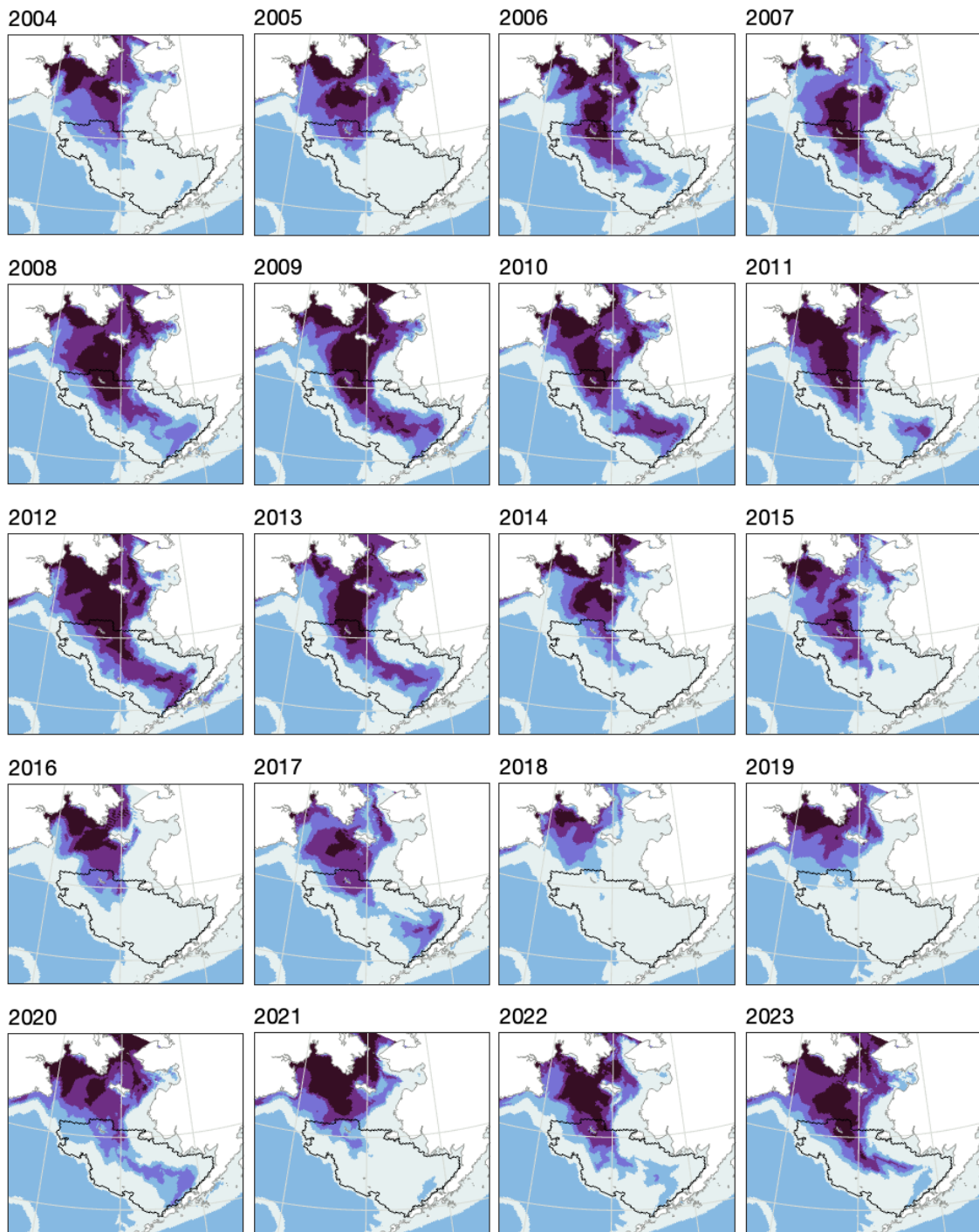
Figure 35: Bering 10K ROMS hindcast of cold pool extent, extracted on July 1 of each year, for the Bering Sea, 2004–2023. The black outline denotes the standard bottom trawl survey grid.
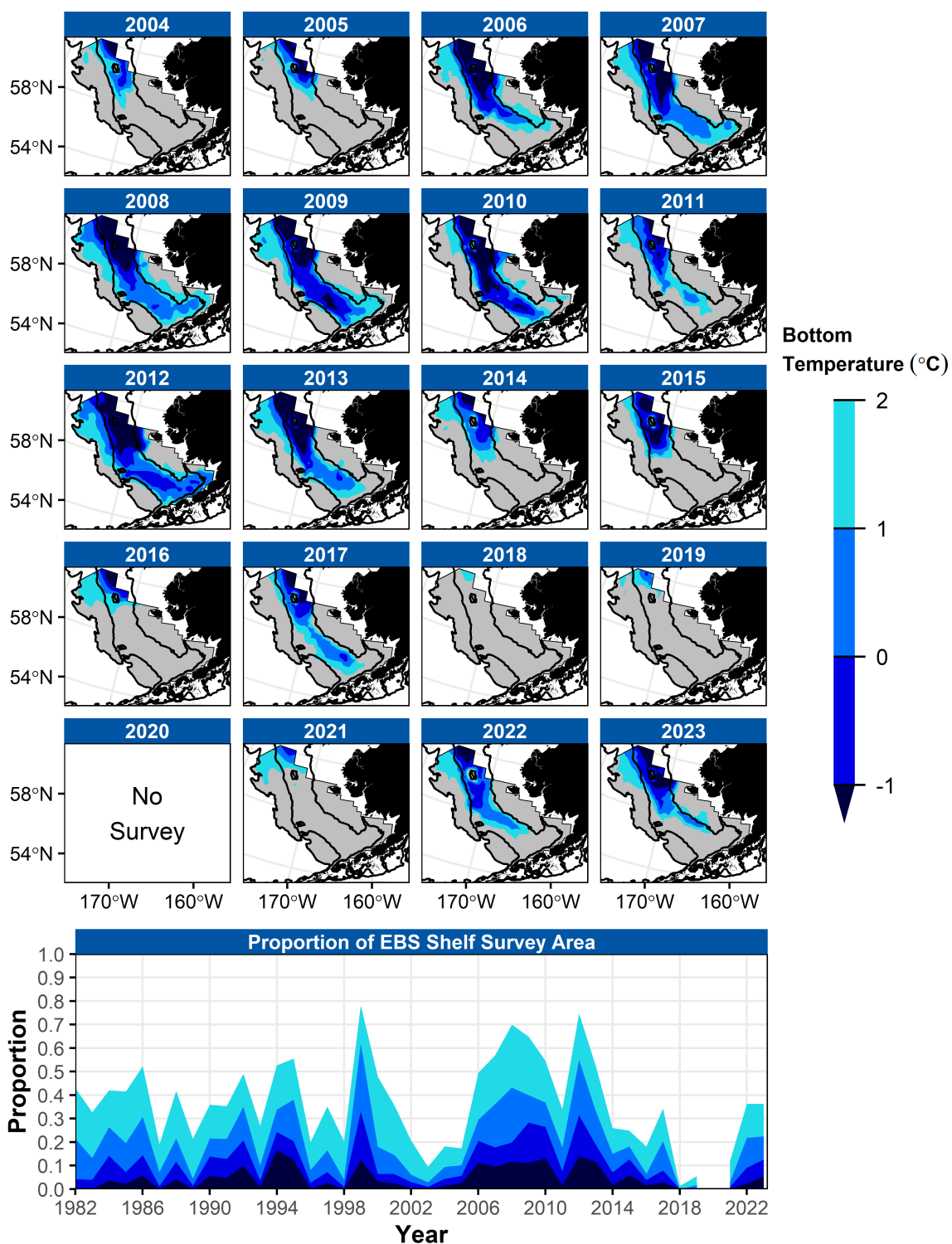
Figure 36: Cold pool extent in the eastern Bering Sea (EBS), as measured using observations from the EBS bottom trawl survey. Upper panels: Maps of cold pool extent in the EBS shelf survey area from 2004–2023. Lower panel: Extent of the cold pool in proportion to the total EBS shelf survey area from 1982–2023. Fill colors denote bottom temperatures ≤2°C, ≤1°C, ≤0°C, and ≤-1°C.

7. Seasonal Projections from the National Multi-Model Ensemble (NMME)

Contributed by Nick Bond, *nicholas.bond@noaa.gov*

Seasonal projections of SST from the National Multi-Model Ensemble (NMME) are shown in Figures 37a-c. An ensemble approach incorporating different models is particularly appropriate for seasonal and longer-term simulations; the NMME represents the average of eight climate models. The uncertainties and errors in the predictions from any single climate model can be substantial. More detail on the NMME and projections of other variables are available at the National Weather Service Climate Prediction Center website[11].

First, the model projections from a year ago are reviewed. The consensus of the model forecasts from September 2022 for the following fall and winter indicated a continuation of positive SST anomalies across the North Pacific south of 50ºN and near to weakly cooler than normal temperatures on the southeast Bering Sea shelf. They also indicated negative anomalies of 0.5-1ºC for the northern Gulf of Alaska (GOA). The extended range projections for spring 2023 showed essentially maintenance of the anomaly distributions established during the previous winter. The performance of the climate models as a group demonstrated mostly positive skill. For the first period considered of October through December 2022, they correctly forecast warmth in the central North Pacific and weakly negative anomalies in the Bering Sea. But the GOA was warmer than predicted. The overall SST anomaly pattern was forecast to remain similar for the following winter (Dec-Feb) with additional cooling for the southeast Bering Sea shelf and GOA. As with the previous forecast, the models captured the overall pattern for the North Pacific, but over-predicted the cool temperatures in the GOA. The consensus of the model forecasts for February-April 2022 included slight warming for the southeast Bering Sea shelf and modest cooling for the eastern GOA. The Bering shelf actually cooled (in association with a delay in ice retreat); the projection for the GOA was fairly accurate. In summary, the model predictions were quite good for the mid-latitude North Pacific, but were less skillful in terms of the details in season-to-season changes for Alaskan waters.

These NMME forecasts of three-month average SST anomalies indicate a continuation of El Niño in the tropical Pacific and a large region of relatively warm water in the central and western North Pacific between 30ºN and 50ºN through the end of the calendar year (Nov 2023-Jan 2024; Figure 37a). Positive temperature anomalies are also predicted for the western Aleutian Islands and coastal Alaskan waters extending from the southeast Bering Sea shelf to the Beaufort Sea. The models also are indicating an atmospheric circulation pattern that would bring reduced storminess to the GOA (not shown). The ensemble of model predictions for January through March 2024 (Figure 37b) shows some moderation in tropical Pacific temperatures but still enough warmth to constitute Niño. As is typical with these events, the projections show warming in the coastal zone of the eastern GOA. Moderation is indicated in the warm anomalies elsewhere in the coastal regions of Alaska. The projections for March through May of 2024 (Figure 37c) indicate continued decreases in tropical Pacific SST anomalies. On the other hand, substantial warming is forecast for the GOA and northern Bering Sea. It bears mentioning that the individual model predictions yield rather consistent outcomes for the GOA but range from near-normal to moderately above normal temperatures for the southeast Bering Sea shelf. Nevertheless, these solutions also indicate conditions should not be extreme relative to the past 20–30 years with the result that sea

---

[11]http://www.cpc.ncep.noaa.gov/products/NMME/

ice should extend south of 60°N, perhaps all the way to Mooring M2, and as far south as Bristol Bay along the coast. The retreat of the sea ice on the southeast Bering Sea shelf in the spring of 2024 is apt to occur earlier than usual.

(a) Months Nov-Dec-Jan

(b) Months Jan-Feb-Mar

(c) Months Mar-Apr-May
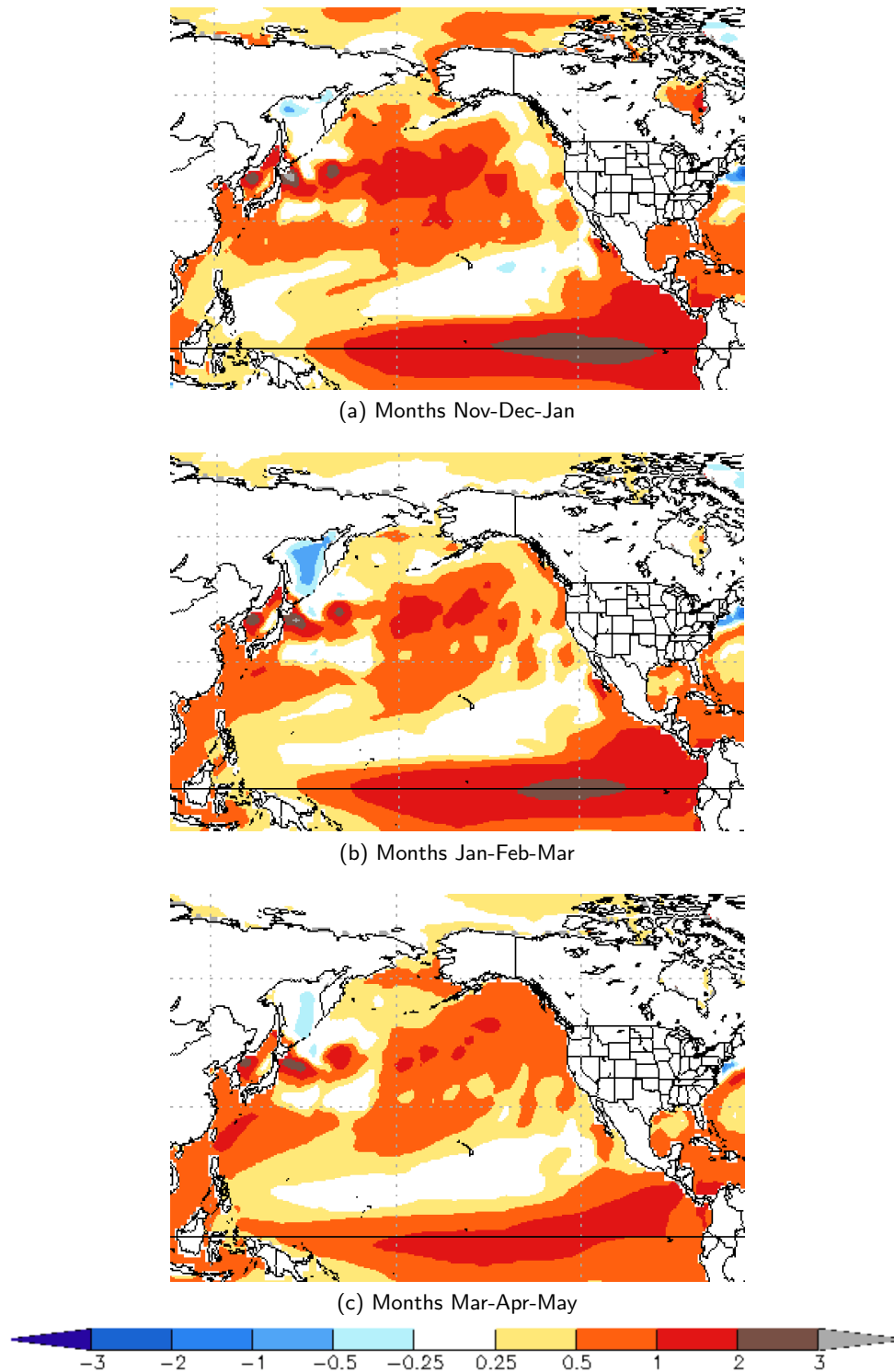
Figure 37: Predicted SST anomalies (°C) from the National Multi-Model Ensemble (NMME) for Oct-Dec 2022 (1 month lead), Dec 2022-Feb 2023 (3-month lead), and Feb-Apr 2023 (5-month lead). See text for details.

Habitat

Eastern and Northern Bering Sea – Structural Epifauna

Contributed by Thaddaeus Buser
Resource Assessment and Conservation Engineering Division, Alaska Fisheries Science Center
National Marine Fisheries Service, NOAA
Contact: thaddaeus.buser@noaa.gov
Last updated: September 2023

Description of indicator: Groups considered to be structural epifauna include: sea whips, corals, anemones, and sponges. Corals are rarely encountered in the eastern or northern Bering Sea so they were not included here; sea whips are rarely encountered in the northern Bering Sea so they are only shown for the eastern Bering Sea shelf survey. Relative CPUE by weight (kg per hectare) was calculated and plotted for each species group by year for 1982–2023 for the eastern Bering Sea survey and for 2010–2023 for the northern Bering Sea survey. Catch methods for the northern Bering Sea were standardized in 2010, so the catches from previous years do not provide comparable data and are excluded. Relative CPUE was calculated by setting the largest biomass in the time series to a value of 1 and scaling other annual values proportionally. The standard error (± 1) was weighted proportionally to the CPUE to produce a relative standard error.

Status and trends:

Eastern Bering Sea:
As in 2022, the relative catch rates for sea anemones (Actiniaria) were similar to those observed during 2010–2015, compared to lower catch rates observed from 2016–2021. Likewise, sea whip (Pennatulacea) estimates for 2023 are similar to those observed in 2021 and 2022, which together represent an increase from 2019 observations and a return to a catch rate similar to that observed 1999–2005 and 2013–2016. The catch rate of sponges (Porifera) in 2023 continues the very low catch level observed since 2021, which was the lowest level observed in the time series, but similar to results observed intermittently during the early years of the time series, 1984–1992. These trends should be viewed with caution because the consistency and quality of their enumeration have varied over the time series (Stevenson and Hoff, 2009; Stevenson et al., 2016). Moreover, the identification of trends is uncertain given the large variability in relative CPUE (Figure 38).

Northern Bering Sea:
The relative catch rates of sea anemones are consistent across the time series except for 2022, which was much larger than all other years. This differs slightly from the trend observed in the eastern Bering Sea from 2010–2023, which showed relatively high catch rates from 2010–2013 and 2022–2023, with relatively low catch rates in between. The catch rate of sponges in the NBS is highly variable across the time series, with high relative catch rates 2010, 2017, 2022, and 2023 and low catch rates in 2019 and 2021 (Figure 39).

Factors influencing observed trends: It is difficult to identify trends, given that the NBS survey has been conducted intermittently and only recently (i.e., starting in 2017) been conducted on a more regular schedule. Further research in several areas would benefit the interpretation of structural epifauna trends including systematics and taxonomy of Bering Sea shelf invertebrates, survey gear selectivity, and the life history characteristics of the epibenthic organisms captured by the survey trawl.

Implications: Understanding the trends as well as the distribution patterns of structural epifauna is important for modeling habitat to develop spatial management plans for protecting habitat, understanding fishing gear impacts, and predicting responses to future climate change (Rooper et al., 2016). More research on the eastern Bering Sea shelf will be needed to determine if there are definitive links.
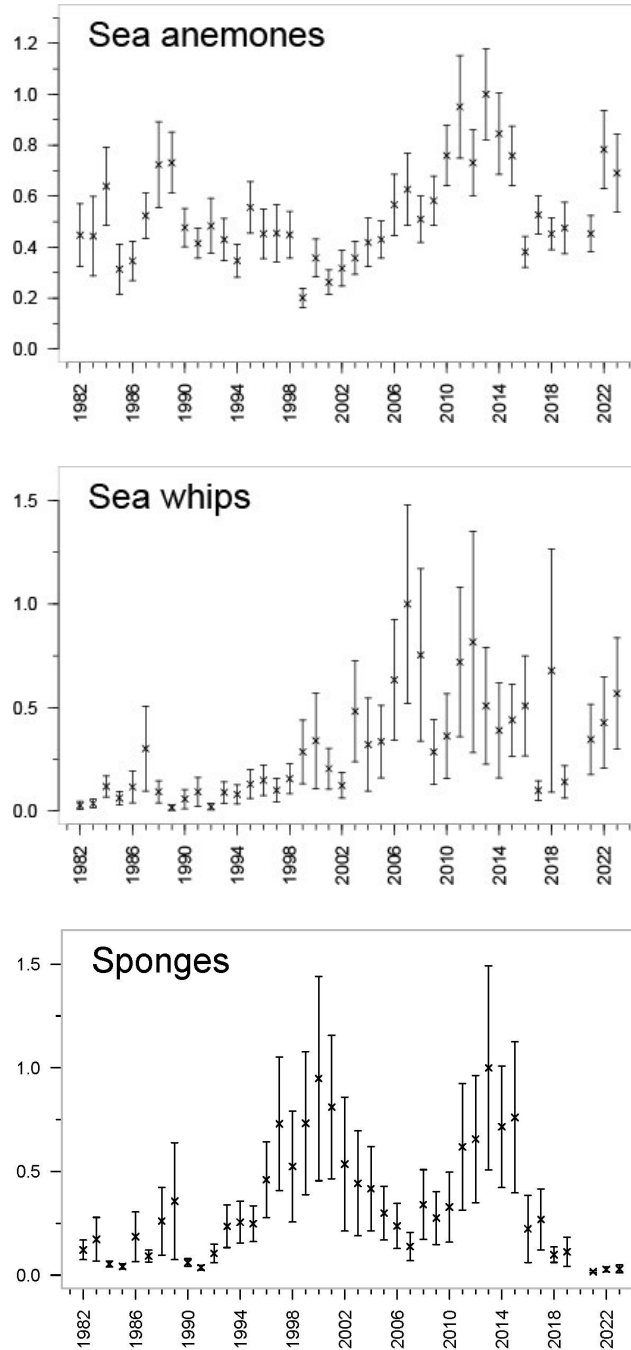
Figure 38: AFSC eastern Bering Sea shelf bottom trawl survey relative CPUE for three groups of benthic epifauna during the May to August time period from 1982–2023.
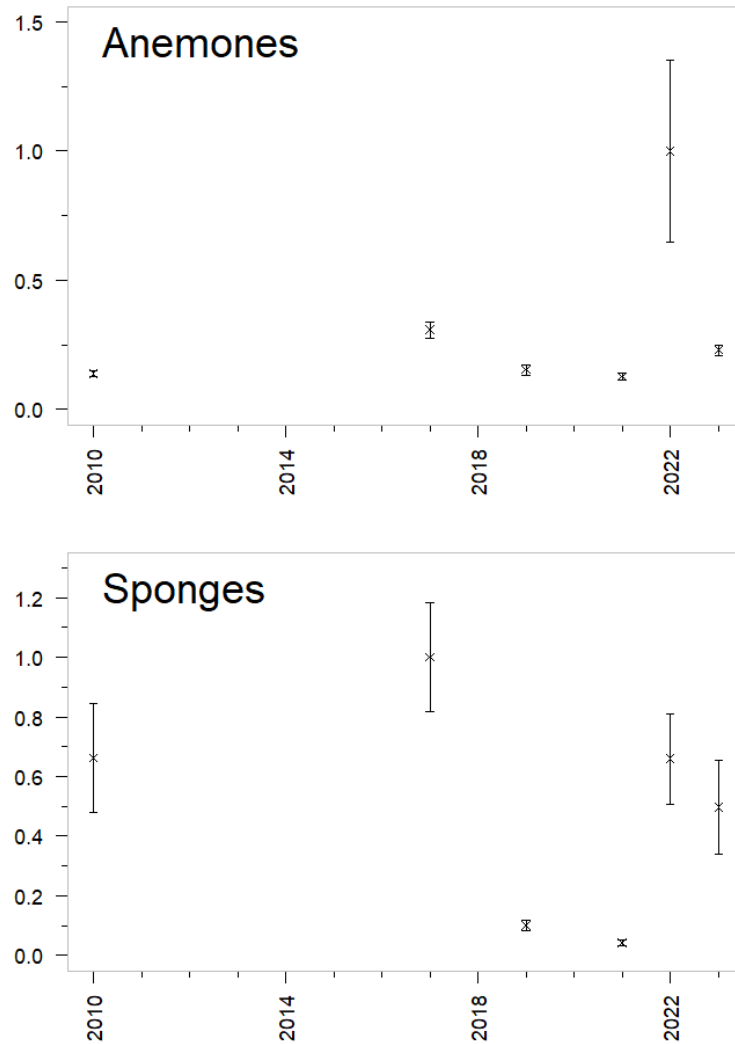
Figure 39: AFSC northern Bering Sea shelf bottom trawl survey relative CPUE for two groups of benthic epifauna during the July to August time period from 2010–2023.

Primary Production

Phytoplankton Biomass and Size Structure During Late Summer / Early Fall in the Eastern Bering Sea

Contributed by Lisa Eisner[1], Jens Nielsen[2,3], Jeanette Gann[1]
[1]Auke Bay Laboratories, Alaska Fisheries Science Center, NOAA Fisheries
[2]Resource Assessment and Conservation Engineering Division, Alaska Fisheries Science Center, NOAA Fisheries
[3]Cooperative Institute for Climate, Ocean, and Ecosystem Studies (CICOES), University of Washington, Seattle, WA
Contact: jens.nielsen@noaa.gov
Last updated: September 2023

Description of indicator: Southeastern (SE Bering; BASIS) and Northern Bering Sea (NBS) fisheries oceanography surveys were conducted over the Bering Sea shelf from mid-August to late-September for three early warm years (2003–2005), six cold years (2007–2012), six recent warm years (2014–2016, 2018, 2019, 2021), and four average years (2006, 2013, 2017, 2022). Variations in chlorophyll-a (chla) were used to evaluate spatial and interannual differences in late summer total phytoplankton biomass (excluding 2021, 2022) and size structure (an indication of phytoplankton species). The ratio of large ($>10\mu$m) phytoplankton biomass to total biomass ($>10\mu$m chla/total chla) were estimated from discrete water samples filtered through GFF and 10μm filters and analyzed with standard fluorometric methods (Parsons et al., 1984). Integrated chla values were estimated from CTD fluorescence profiles calibrated with discrete chla (GFF) samples. Chla data were averaged over the top 50m of the water column or to the bottom for shallower stations for integrated chla, and generally over the top 30m or less for size fractionated samples. Mean values of integrated chla and $>10\mu$m/total chla at each station in the middle shelf were averaged over early warm, cold, recent warm, and average years with the most recent year. Friction velocity cubed (u*[3]), a proxy for wind mixing, was obtained from NCEP reanalysis around Mooring M2[12]. Normalized anomalies of u*[3], integrated chla, and large size fraction chla are shown for the southeastern Bering Sea middle shelf for the period 2003–2022 (Figure 40).

Status and trends: In general, the highest phytoplankton biomass was observed in the south outer shelf with highest values inshore of Bering Canyon, near the Pribilof Islands, along the Aleutian Islands for the average, cold, and early warm years, and north of St. Lawrence Island and on the south inner shelf for all temperature stanzas (Figure 41, top). Larger phytoplankton were observed in higher proportions on the inner shelf and near the Pribilof Islands. In contrast, smaller phytoplankton were predominant on the south middle and outer shelf, with expansion across the shelf in the early warm years compared to other temperature stanzas, including the recent warm years (Figure 41, bottom).

Integrated chla on the middle shelf varied 3-fold among all years (Figure 42, top). For the earlier years (2003–2012), higher fractions of large phytoplankton were associated with higher integrated chla. In the south, the mean size of phytoplankton assemblages was larger in early warm (2003–2005) than in cold (2006–2012) years. In contrast to both the early warm and cold period, in 2014–2016 and 2018 (recent warm years) integrated chla was average, whereas large size fraction ratios were below average

---

[12]https://psl.noaa.gov/data/gridded/data.ncep.reanalysis.surface.html

	u^{*3}	Int chla	Large chla ratio
2003	-0.4	0.3	1
2004	0.6	0.5	1.6
2005	3.1	2.9	2.1
2006	0.1	-0.3	-0.3
2007	-0.6	-1.1	-0.8
2008	-1.7	-1.1	-0.8
2009	0.4	-0.1	-0.3
2010	-0.3	-0.9	-0.6
2011	0.1	0.5	-0.5
2012	-0.1	0.3	-0.6
2013	-0.1	NA	NA
2014	-1.2	-1	-1.3
2015	0.1	0.3	-0.4
2016	-0.9	-0.5	-0.6
2017	1.1	NA	NA
2018	0	0.1	1.1
2019	-0.3	NA	NA
2020	-0.1	NA	NA
2021	-0.7	NA	NA
2022	1.1	NA	0.4

Figure 40: Normalized anomalies (mean yearly value minus time series average, normalized by standard deviation) for 2003 to 2022 for the south middle shelf (Bering Project Regions 3 and 6, Ortiz et al., 2012). Anomalies were calculated for integrated chla and ratio of large ($>10\mu$m) to total chla over the top 50m for August–September from BASIS surveys, and friction velocity cubed (u^{*3}) for August at a region around M2. Year is colored as red for warm, black for average, and blue for cold. Shading indicates if anomaly is positive (dark gray, >0.5), small (no shading, -0.5 to 0.5), or negative (light gray, $<$-0.5).

in 2014–2016, but above average in 2018 (Figure 40). In 2022, a year with average temperatures, large fraction chla were average in the south. In the north, the large size fraction was highest in 2021, a year with above average integrated chla. The lowest percent large (highest % small) phytoplankton for our time series in the south was seen in 2014, and in the north in 2014, 2018, 2019, all warm years, and in 2022 (Figure 42, bottom).

Factors influencing observed trends: Wind and temperature influence interannual and spatial variations in phytoplankton biomass. For the south middle shelf, a positive association was observed between August $u*^3$ (wind mixing 2–3 weeks prior to chla sampling) and integrated chla in the top 50m (Figure 43). Years with low wind mixing had a greater proportion of small cells compared to years with high wind mixing which had a greater proportion of large particles (Figure 40). During periods of high winds and low water column stability, deep nutrient-rich waters may be mixed to the surface to fuel production of large assemblages (e.g., diatoms). The highest chla and largest size fractions were seen in 2005, a period with very high August wind mixing (Figures 40 and 42). The small size fractions observed in 2014 were due to an extensive coccolithophore bloom over the north and south middle shelf (see p. 83). In the north, low integrated chla and low ratios of large (high ratios of small) phytoplankton were observed in 2018 and 2019, years with the warmest sea temperatures and lowest ice on record for this region (see p. 28), conditions that are known to favor small cells.

Implications: Phytoplankton size structure is a primary determinant of the amount and quality of food available to zooplankton and higher trophic levels, and are thus important to ecosystem function. For example, smaller phytoplankton assemblages may lead to longer food webs and a less efficient transfer of energy to sea birds, fish, and marine mammals and reductions in the quantity and quality of food sinking to the benthos. The low percent of large phytoplankton cells in the north in 2018 and 2019 is consistent with other measures of low productivity in this region (e.g., few large copepods, lower abundances of forage fish, extensive sea bird die-offs, Duffy-Anderson et al., 2019). Phytoplankton size and biomass data can help discern relevant ecosystem processes during the critical late summer period prior to the overwintering of key forage fish (e.g., juvenile pollock, cod, salmon) (Eisner et al., 2015).
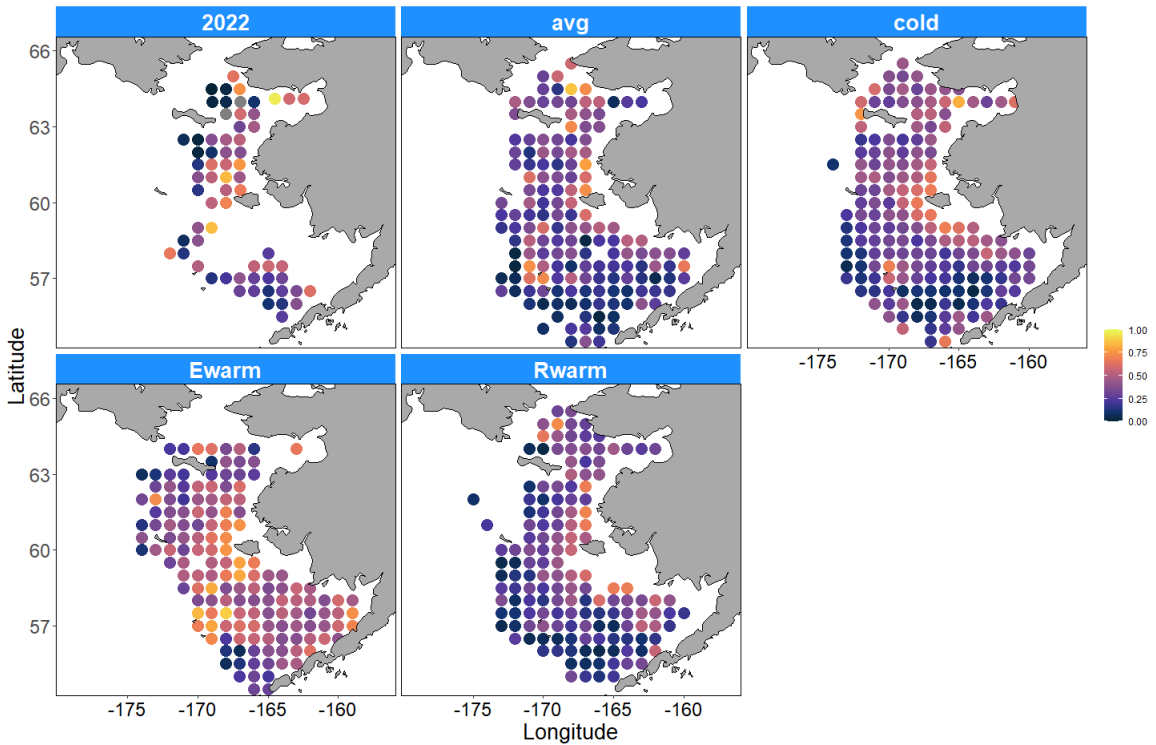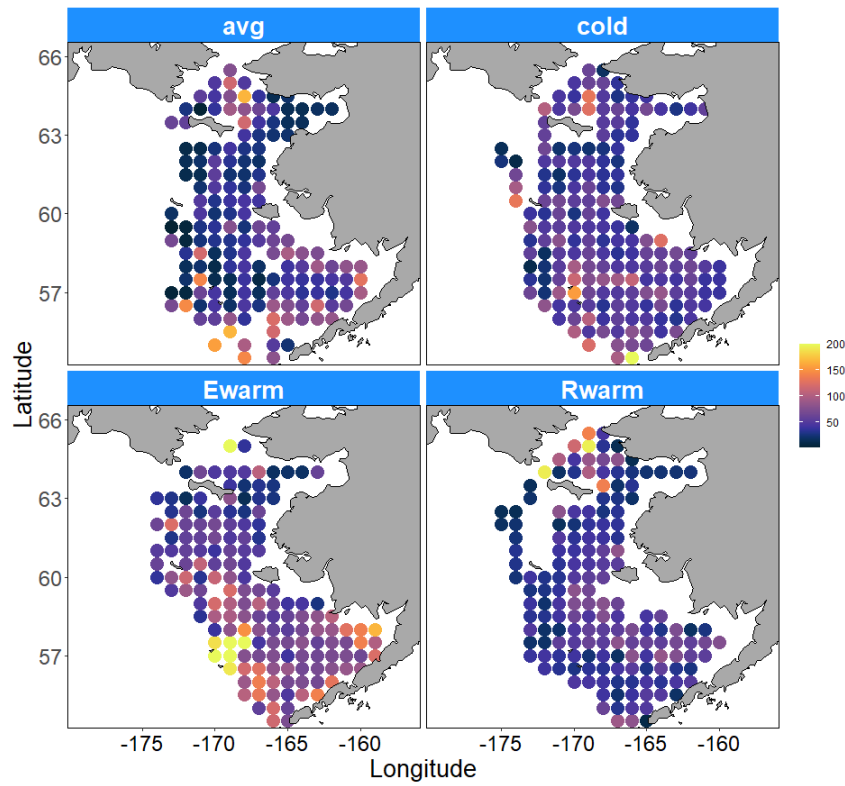
Figure 41: (Top) Mean integrated chla by station for years classified as average temperature (2006, 2013, 2017), cold (2007–2012), early warm (Ewarm, 2003–2005), and recent warm (Rwarm, 2014–2019), and (Bottom) large phytoplankton ratio ($>10\mu$m chla/total chla) by station for the recent year, 2022, and means for average, cold, Ewarm, and Rwarm years. No data for 2020.

76
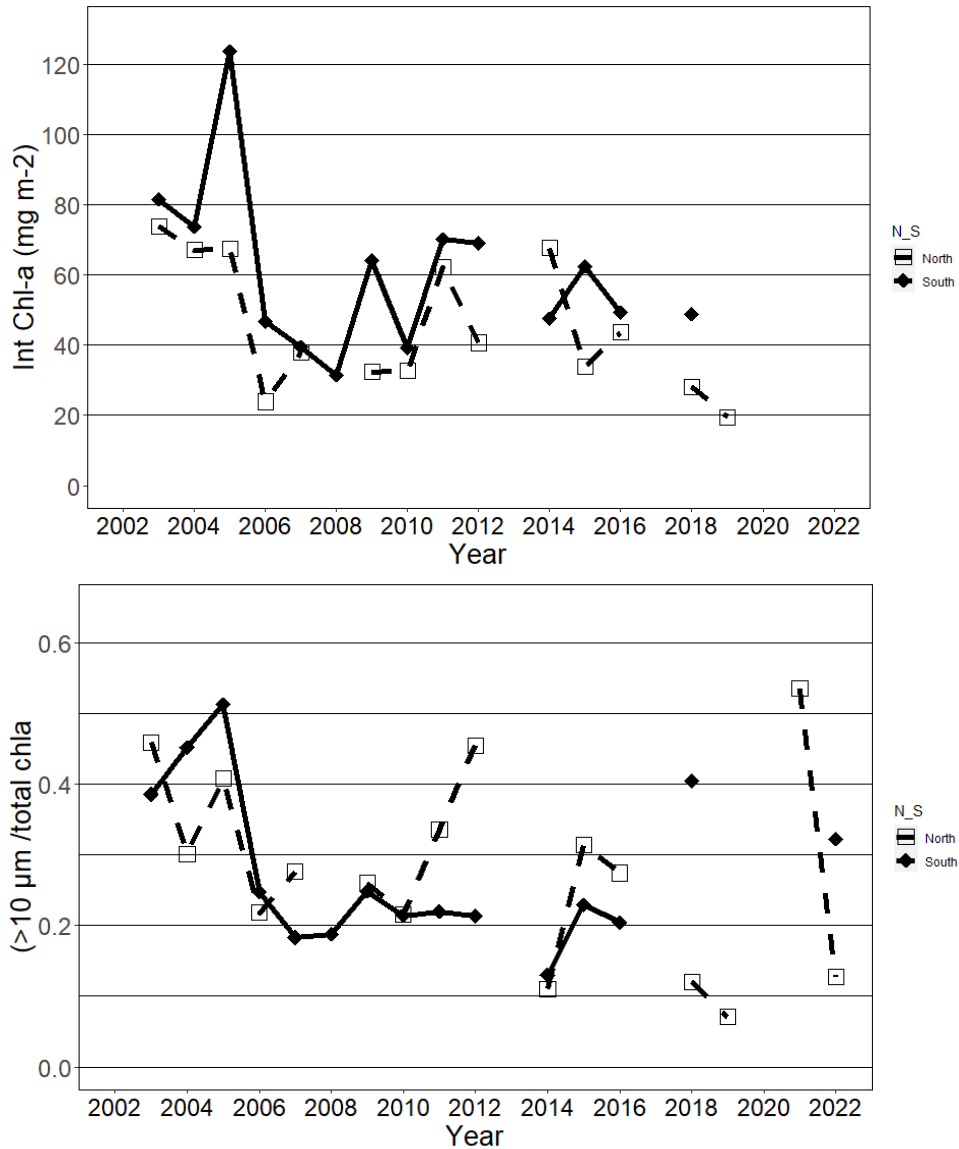
Figure 42: (Top) Integrated total chla and (Bottom) ratio of large assemblages to total ($>10\mu$m chla/total chla) for the middle shelf in the south (S, 54.5–59.5°N, Bering Sea Project Regions 3 and 6) and north (N, 60–62.5°N, Regions 9 and 10) for 2003–2022. No data included for 2013, 2017, or 2020. Note that north middle shelf data were sparse, 6, 5, and 6 stations for (A) and 6, 5, and 4 stations for (B) for 2015, 2016, and 2018 respectively. 2022 for (B) was also sparse with 5 stations.
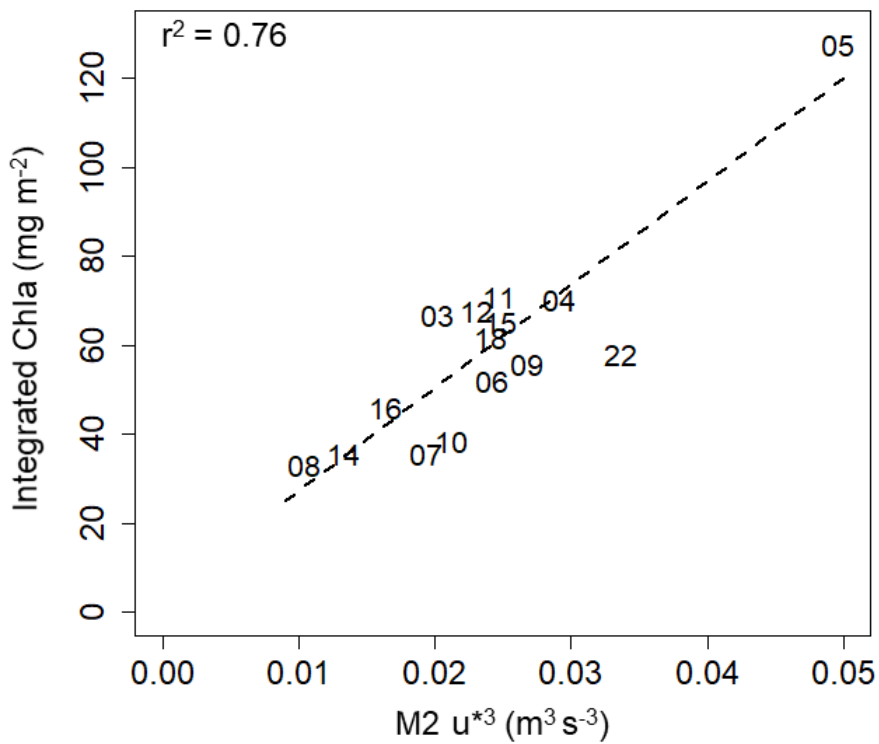
Figure 43: Linear regression between mean August u^{*3}, an indicator of wind mixing, at M2 and integrated chla for the south middle shelf in Bering Sea Project Region 3 (region around M2) for 2003–2012, 2014–2018, and 2022. For 2018, chla data were collected ~3 weeks later (September 28) compared to other years (mean 2003–2016=September 5, SD=8.5 days). To account for this delay, we estimated the mean u^{*3} for the period August 23–September 22 for 2018, instead of August 1–31 as used for other years.

Spring Satellite Chlorophyll-a Concentrations in the Eastern Bering Sea

Contributed by Jens M. Nielsen[1,2], Matt W. Callahan 3, Lisa Eisner[4], Jordan Watson[5], Jeanette C. Gann[4], Calvin W. Mordy[2,6], Shaun W. Bell[6],and Phyllis Stabeno[6]

[1]Resource Assessment and Conservation Engineering Division, Alaska Fisheries Science Center, NOAA Fisheries
[2]Cooperative Institute for Climate, Ocean, and Ecosystem Studies (CICOES), University of Washington, Seattle, WA
[3]Pacific States Marine Fisheries Commission - Alaska Fish Information Network
[4]Auke Bay Laboratories, Alaska Fisheries Science Center, NOAA Fisheries
[5]Pacific Islands Ocean Observing System, University of Hawai'i Manoa, 1680 East West Rd. POST 815, Honolulu, HI 96822, USA
[6]Pacific Marine Environmental Laboratory, NOAA Research, Seattle, WA, USA
Contact: jens.nielsen@noaa.gov
Last updated: September 2023

Description of indicator: In subarctic systems, such as the eastern Bering Sea, the timing and magnitude of the spring phytoplankton bloom can have large and long-lasting effects on biological production with subsequent impacts on higher trophic levels including commercial fish stocks (Platt et al., 2003). The fate of the spring bloom (pelagic grazing or sinking to benthos), and it's timing also impact benthic feeders in the Bering Sea (Hunt et al., 2002). Warm years with open water blooms tend to result in fewer large copepods and reduced pollock retruitment (Hunt et al. 2011). Recent climatic changes in the Bering Sea have included reduced sea ice and warming ocean temperatures (Stabeno and Bell, 2019), with consequent changes to the food web (Duffy-Anderson et al., 2019). Understanding annual changes in spring phytoplankton biomass and peak timing dynamics are thus important metrics for depicting ecosystem changes.

Here, we used ocean color satellite data from 1998–2023. 8-day satellite chlorophyll-a (chl-a, μg/L) at a 4 km-resolution from The Hermes GlobColour website[13] was used (Maritorena et al., 2010). This is a standardized merged chl-a product, combining remote sensing data from SeaWiFS, MERIS, MODIS, VIIRS, and OLCI.

We estimate: 1) average spring (Apr–Jun) chlorophyll-a concentrations (chl-a, an estimate of phytoplankton biomass in the surface layer) and 2) peak timing of the spring bloom for major regions in the eastern Bering Sea. In the southeastern Bering Sea, sustained observations at the M2 mooring (56.9°N, -164.1°W) provide good representation of the south middle shelf biophysical conditions. Thus, the long-term chl-a fluorescence mooring measurements were compared to the bloom peak timing estimates calculated from the satellite data.

We focus on the spring period as this is an important time for providing basal resources for zooplankton and thus energy for higher trophic level species. The April–June time period was chosen as this period consistently includes the pelagic spring bloom peak. We further divided the eastern Bering Sea into 8 distinct regions split between approximately north and south of 60°N and defined by oceanographic fronts and water mass characteristics based on Ortiz et al. (2012) (Figure 44). There are several advantages of satellite data, including high spatial and temporal coverage. However, these products are

---

[13]http://hermes.acri.fr/

also limited to measurements within the surface ocean and also have missing data due to ice and cloud cover, particularly in high latitude systems such as the Bering Sea. We used 8-day composite data for the biomass estimates and timing estimates.

Spring bloom peak timing was estimated from data binned and averaged into ∼0.5° (56 km) latitude × 1° (47–65 km) longitude spatial grid cells. We then calculated the average and standard deviation of all estimated bloom peaks within a specific region, which allowed for calculation of variability for each of the 8 areas.
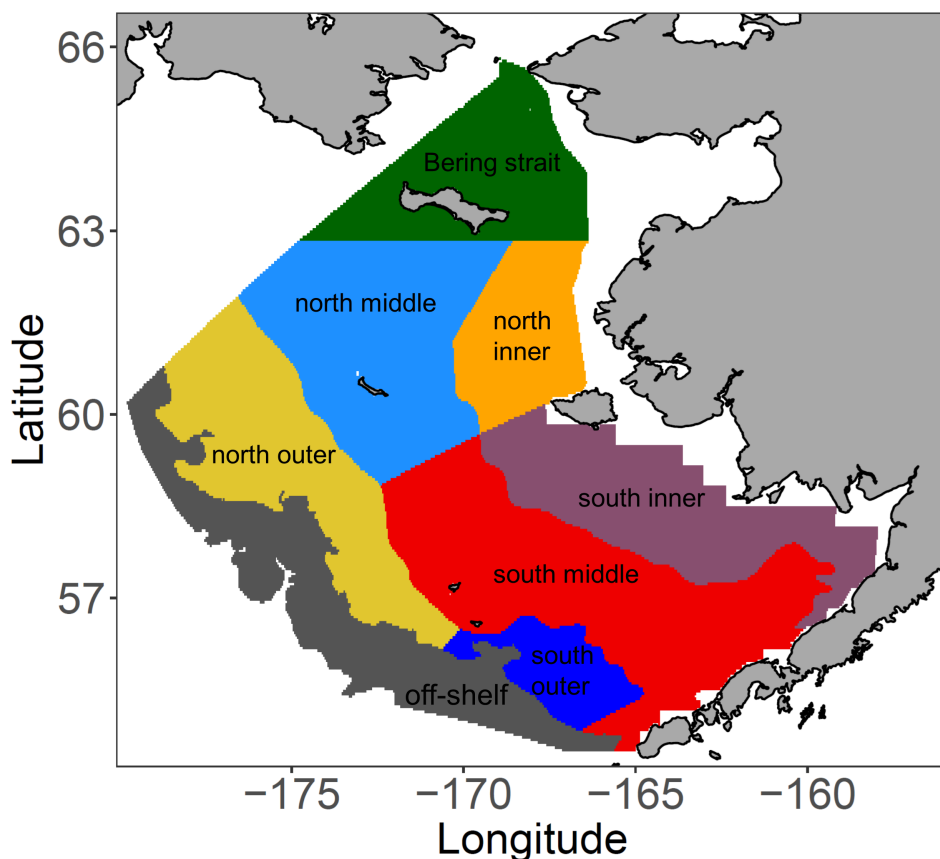
Figure 44: Map of the 8 shelf regions used for satellite chlorophyll-a analyses: south inner (purple), south middle (red), south outer (dark blue), off-shelf (dark gray), north inner (orange), north middle (light blue), north outer (yellow), and the Bering Strait (dark green). Off-shelf denotes regions on the shelf break and slope deeper than 200m (Ortiz et al., 2012).

Status and trends: There was a high degree of interannual variability in satellite chl-a from 1998–2023. Both the south inner (<50m) and south outer shelf (100–180m) had below average values in 2023, similar to values in the period 2016–2022. Values in the south middle (50–100m), north inner, and north middle shelf region were also low for 2023. Values along the shelf–break (off-shelf region) were low in 2023, continuing an apparent decreasing trend since 2015 (Figure 45). Combined results show spring chl-a concentrations were near all-time lows (based on data since 1998) in almost all regions. Data coverage in the southern regions was generally good across all years, however further north, in some years data from April were particularly scarce due to extended ice coverage. Consequently, estimates in spring should be considered with caution during the years when coverage was limited.
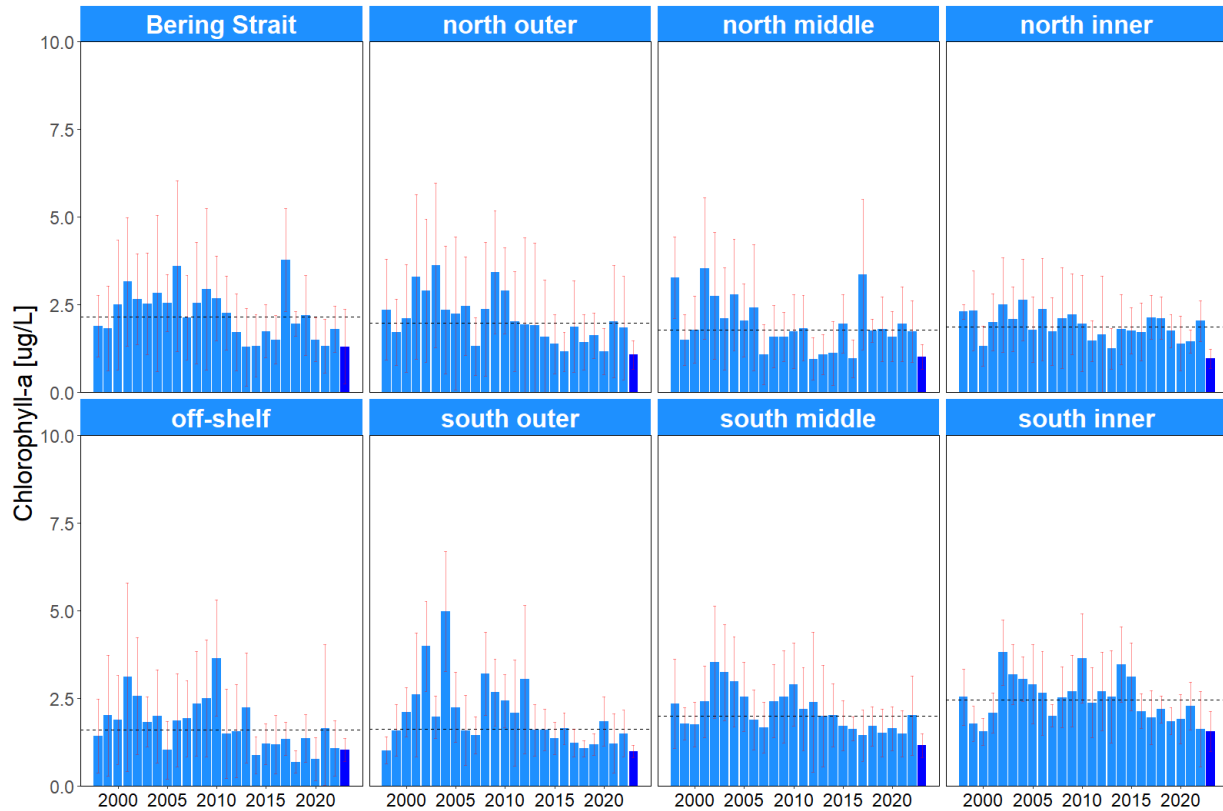
Figure 45: Average and standard deviation (SD) from spring (Apr–Jun) chlorophyll-a concentrations for 8 regions in the eastern Bering Sea. Dotted black line denotes the long-term median (1998–2023) for each region. **Note:** For plotting purposes, the minimum error bar is set at 0.01 and the maximum at 9.99. In a few cases, the +standard deviation was >10 (south outer in 2004 was 18.9; north middle in 2015 was 13.8; south outer in 2012 was 11.6).

Analyses of the pelagic spring bloom peak timing suggest that 2023 was similar to the long-term overall, with average timing observed in the south inner, south middle, and south outer shelf regions (Figure 46). Overall, annual timing estimates from 1998 to 2023 from the M2 mooring align well with estimates based on satellite chla at the mooring (0.5 lon x 0.5 lat box with M2 in the center). In the off-shelf region the bloom peak in 2023 was later than the long-term average. However, the magnitude of off-shelf spring chl-a concentrations were, as mentioned above, low overall (Figure 45). Due to lack of consistent data coverage, no bloom satellite peak estimates were done for the northern regions.

Factors influencing observed trends: Previous studies have highlighted the strong coupling between temperature and sea ice dynamics and spring bloom timing. For example, in the southern Bering Sea, ice present after mid-march commonly results in an early and prominent ice-associated bloom, while lack of ice normally results in a delayed open water bloom in mid- to late- May (Sigler et al., 2014). The bloom type indicator (see Report Card metric in Figure 2) suggests that 2022 and 2023 had more ice associated blooms compared to the recent warm period (2014–2021). Increased ice associated blooms tend to correlate positively with higher abundances of large zooplankton and have been suggested to favor pollock recruitment (Hunt et al., 2011).
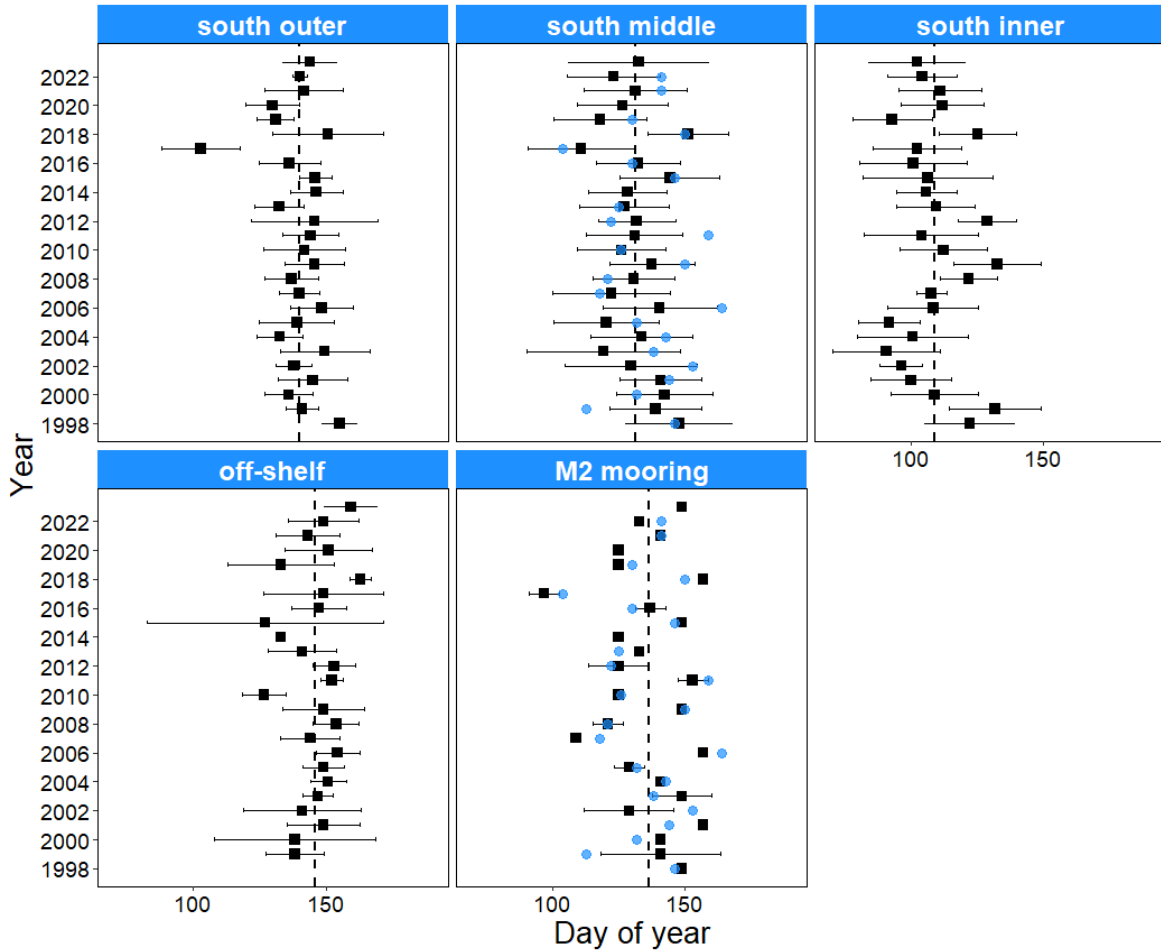
Figure 46: Average and SD of peak spring bloom timing estimated from areas within 4 southern regions in the eastern Bering Sea. Blue dots are the M2 fluorescence peak timing estimates, which are compared to both the south middle shelf data and specifically to satellite data near M2 [1° latitude x 1° longitude].

On the southern middle shelf, we observed an earlier spring bloom in the cold years of 2007–2012 (excluding 2009) and in the average years of 2013 and 2017. However, spring bloom timing varied considerably in recent warm years (2018–2021), suggesting that the timing of the bloom in those years was impacted by other factors besides ice. Recent analyses suggest that in years where ice is not the driving factor, wind intensity influences bloom timing (Nielsen et al. in review). In low ice years, variations in springtime winds influence the setup of stratification (e.g., higher winds can delay stratification, Stabeno et al. (2016)), which in turn affects light availability and the timing of the bloom. Analysis of chl-a biomass, though informative in depicting spring bloom timing, does not directly provide information of primary productivity (growth rates), though biomass levels in spring generally align well with the timing of production peak estimates.

Implications: Our analyses show no significant long-term change in the bloom peak timing among low and high ice years combined for most of the southern Bering Sea (<60°N). For the northern Bering Sea, sea ice retreat regulates the timing of the bloom. In general, earlier ice retreat results in an earlier bloom (Waga et al., 2021), except in the years 2018–2019 where ice retreated so early that open water blooms formed in large areas in this region (Nielsen et al. review).

Our analyses indicate spring 2023 chl-a concentrations were near an all-time low (1998–2023) for most of the regions. At the time of writing it is unclear what caused this pattern. Bloom timing for most regions were near the long-term average, suggesting that the low chl-a concentrations observed in 2023 are not because the bloom occurred outside the period Apr-June. Whether the low chl-a concentrations observed in 2023 is a result of low primary production during that period needs to be assessed, as low primary production during spring will influence consumers such as zooplankton. The declining trend in chl-a biomass observed along the shelf-break in recent warm years (2015–2023) deserves further investigation. This area includes the "greenbelt", a known region of high production (Springer et al., 1996), and it will be important to understand the mechanism behind these apparent changes.

Coccolithophores in the Bering Sea

Contributed by Jens Nielsen[1,2] and Lisa Eisner[3]
[1]Resource Assessment and Conservation Engineering Division, Alaska Fisheries Science Center, NOAA Fisheries
[2]Cooperative Institute for Climate, Ocean, and Ecosystem Studies (CICOES), University of Washington, Seattle, WA
[3]Auke Bay Laboratories, Alaska Fisheries Science Center, NOAA Fisheries
Contact: jens.nielsen@noaa.gov
Last updated: October 2023

Description of indicator: Blooms of coccolithophores, a unicellular calcium carbonate-producing phytoplanktonic organism, are easily observed by satellite ocean color instruments due to their high reflectivity. Coccolithophores produce calcium carbonate plates (coccoliths) that contribute to particulate inorganic carbon (PIC) in the ocean (Matson et al., 2019). Blooms are most commonly observed and cloud cover is typically lower during September than other months, allowing for better quantification (Iida et al., 2012). An interannual index of the average area (km^2) covered by coccolithophores during the month of September is calculated with monthly average mapped PIC data (Balch et al., 2005; Gordon et al., 2001) from satellite observations. We use monthly PIC data from the blended (multisensor) GlobColour product[14]. This extends the timeseries from 1997 to the present. Comparisons of the GlobColour calculations show very similar trends to estimates based on MODIS-Aqua satellite data (2003–2020, r^2=0.96-0.98) and from the VIIRS-SNPP satellite (2012–2021, r^2=0.97-0.98) provided by NASA Goddard Space Flight Center, Ocean Ecology Laboratory (NASA, 2019).

PIC>0.0011 mol/m^3 was used to estimate the areal coverage of coccolithophore blooms. This threshold was derived by Matson et al. (2019). Highly reflective waters in shallow water near the coast can be due to re-suspended diatom frustules rather than coccoliths (Broerse et al., 2003). Thus, the index is calculated from the region south of 60°N and greater than 30m depth to avoid contamination by shallow regions around St. Matthew and St. Lawrence islands and along the Alaskan coast, as well as sediment associated with the Yukon and Kuskokwim rivers. Because blooms are often largely confined to either the middle shelf or the inner shelf (Ladd et al., 2018), two indices are calculated, one for the middle shelf (50–100m isobaths) and one for the inner shelf (30–50m isobaths).

---

[14]https://hermes.acri.fr/index.php?class=archive

Before 1997, coccolithophore blooms in the eastern Bering Sea were rare. A large bloom (primarily *Emiliania huxleyi*) occurred in 1997 (Napp and Hunt, 2001; Stockwell et al., 2001) and for several years thereafter. During the 1997 bloom, the bloom coincided with a die-off of short-tailed shearwaters (*Puffinus tenuirostris*), a seabird commonly seen in these waters (Baduini et al., 2001). It was thought that the bloom may have made it difficult for the shearwaters to see their zooplankton prey from the air (Lovvorn et al., 2001). Since then, coccolithophore blooms in the eastern Bering Sea have become more common. Satellite ocean color data suggest that blooms are only found where water depths are between 20 and 100m. Blooms typically peak in September, though they can occur in August, and interannual variability is related to both very weak and strong stratification (Iida et al., 2012; Ladd et al., 2018).

Status and trends: Annual images (Figure 47) show the spatial and temporal variability of coccolithophore blooms in September. Annual indices are obtained from satellite data by averaging spatially over the inner and middle shelf (Figure 48). Coccolithophore blooms were particularly large during the early part of the record, 1997, 1998 and 2000 (Figure 48). The index was low and remained low ($<$80,000 km^2) through 2006. In 2007, the index rose to almost double that observed in 2006 ($\sim$125,000 km^2). A higher index ($>$100,000 km^2) was observed in 2007, 2009, 2011, 2014, 2016, 2020, 2021, 2022, and 2023 for the middle shelf and in 2011, 2014, 2022, and 2023 ($>$ 40,000 km^2) for the inner shelf. In 2023, the coccolithophore index for both the inner and middle shelf was similar to 2022 and among the highest ever observed in the timeseries (Figures 47 and 48). Commonly for years with high index values (e.g., 2014, 2016, 2020, 2022, 2023) blooms were also observed in August (e.g., scientists conducting shipboard sampling on the middle shelf noted an extensive bloom in August 2022). September 2017 exhibited the lowest index of the record. The bloom index remained below average in 2018 and 2019 but increased for the 4th consecutive year, particularly on the middle shelf, in 2020, 2021, 2022, and in 2023.

Factors influencing observed trends: It has been suggested that the strength of density stratification is the key parameter controlling variability of coccolithophore blooms in the eastern Bering Sea (Iida et al., 2012; Ladd et al., 2018). Stratification influences nutrient supply to the surface layer. Stratification in this region is determined by the relative properties (both temperature and salinity) of two water masses formed in different seasons, the warm surface layer formed in summer and the cold bottom water influenced by ice distributions the previous winter. Thus, the strength of stratification is not solely determined by summer temperatures and warm years can have weak stratification and vice versa (Ladd and Stabeno, 2012).

Implications: Coccolithophore blooms can have important biogeochemical implications. The Bering Sea can be either a source or a sink of atmospheric CO_2, with the magnitude of coccolithophore blooms and the associated calcification playing a role (Iida et al., 2012) In addition, variability in the dominant phytoplankton (diatoms vs. coccolithophores) is likely to influence trophic connections with the smaller coccolithophores resulting in longer trophic chains. Coccolithophores may be a less desirable food source for microzooplankton in this region (Olson and Strom, 2002). As noted previously, the striking milky aquamarine color of the water during a coccolithophore bloom may also reduce foraging success for visual predators, such as surface-feeding seabirds and fish.
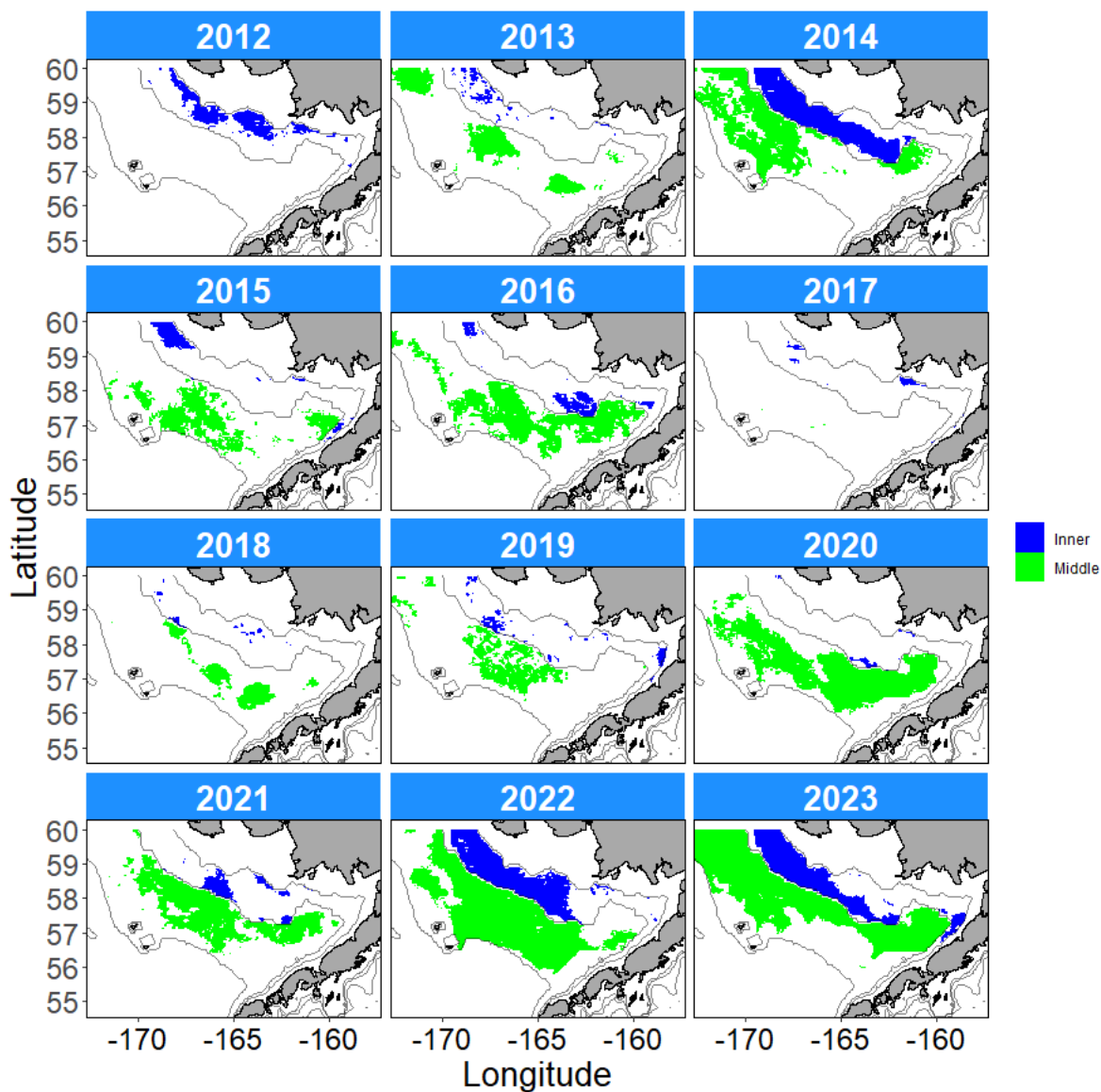
Figure 47: Maps illustrating the location and extent of coccolithophore blooms in September of each year from globcolour data. Color: satellite ocean color pixels exceeding the threshold (PIC>0.0011 mol/m³) indicating coccolithophore bloom conditions. Blue: inner shelf (30–50m depth), Green: middle shelf (50–100m depth). These data are used to calculate the areal index in Figure 48.
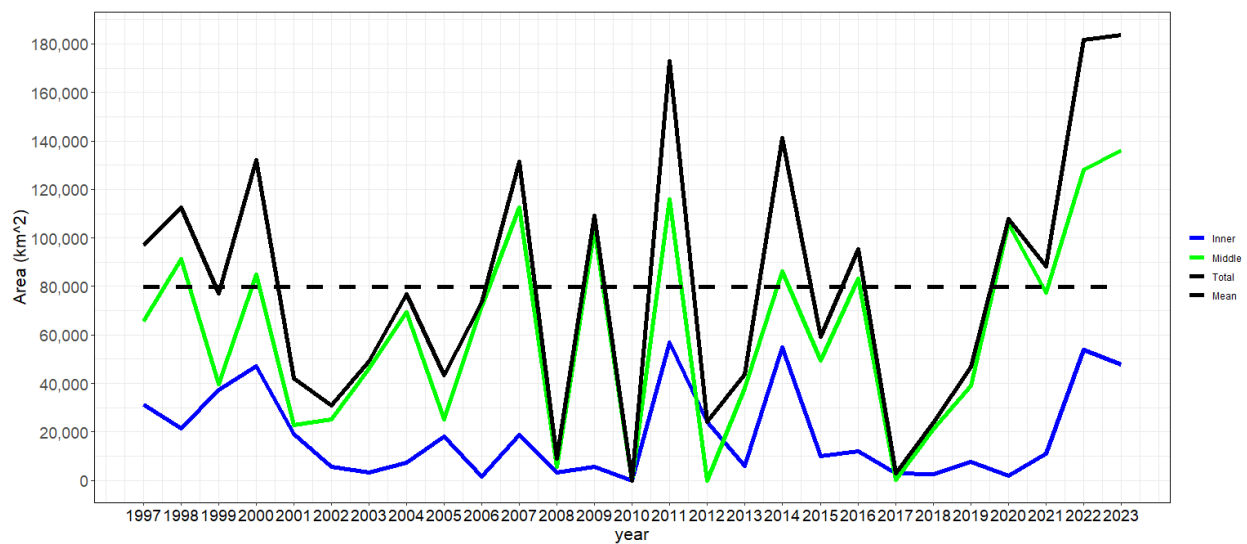
Figure 48: Coccolithophore index for the southeastern Bering Sea shelf (south of 60°N) calculated from the GlobColour blended PIC product. Blue: average over the inner shelf (30–50m depth), Green: average over the middle shelf (50–100m depth), Black: total. The black dotted line is the time series average.

Zooplankton

Continuous Plankton Recorder Data from the Eastern Bering Sea

Contributed by Clare Ostle[1] and Sonia Batten[2]
[1]CPR Survey, The Marine Biological Association, The Laboratory, Citadel Hill, Plymouth, Devon, PL1 2PB, UK
[2]PICES, 4737 Vista View Cr, Nanaimo, BC, V9V 1N8, Canada
Contact: claost@mba.ac.uk
Last updated: July 2023

Description of indicator: Continuous Plankton Recorders (CPRs) have been deployed in the North Pacific routinely since 2000. Two transects are sampled seasonally, both originating in the Strait of Juan de Fuca, one sampled monthly ($\sim$April–September) which terminates in Cook Inlet, the second sampled 3 times per year (in spring, summer, and autumn) which follows a great circle route across the Pacific terminating in Asia. Several indicators are now routinely derived from the CPR data and updated annually.

As well as the regular Pacific CPR sampling, the icebreaker *Sir Wilfrid Laurier* (SWL) has now sampled a transect through the Bering Strait, and the western Chukchi and Beaufort Seas during the summer months for the last 5 years 2018–2022. The SWL is currently towing a CPR in the same region for 2023. We do not (at present) have the funds to complete the sample analysis for the year 2023, however, we are looking for long-term funding to continue sampling in these areas in the future, as they provide important information on this transition area.

This report highlights the Arctic route that started in 2018 and transects the Bering Strait during the summer months of July and September. We present CPR data from the eastern Bering Sea region (Figure 49) as the following indices: the abundance per sample of large diatoms (the CPR only retains large, hard-shelled phytoplankton so while a large proportion of the community is not sampled, the data are internally consistent and may reveal trends), mean Copepod Community Size (see Richardson et al., 2006 for details but essentially the length of an adult female of each species is used to represent that species and an average length of all copepods sampled calculated) as an indicator of community composition, and mesozooplankton biomass (estimated from taxon-specific weights and abundance data). Annual anomaly time series of each index have been calculated using a standard z-score calculation: z-score = $(x - \mu)/\sigma$ where x is the value and μ is the mean, and σ is the standard deviation (Glover et al., 2011). Scores of zero are equal to the mean, positive scores signify values above the mean, and negative scores values below the mean.

Status and trends: Figure 50 shows that the copepod community size and annual anomaly for 2021 and 2022 was positive, where it had been negative in 2020. The mean diatom abundance and meso-zooplankton biomass anomalies were negative in 2022.

Factors influencing observed trends: As there are only 5 years of consistent data, it is difficult to determine any trend. Analysis of summer CPR data in this region has revealed a general alternating (and opposing) pattern of high and low abundance of diatoms and large copepods (indicated in Figure 50 by copepod community size). This is a similar finding to the analysis from Batten et al. (2018) which was
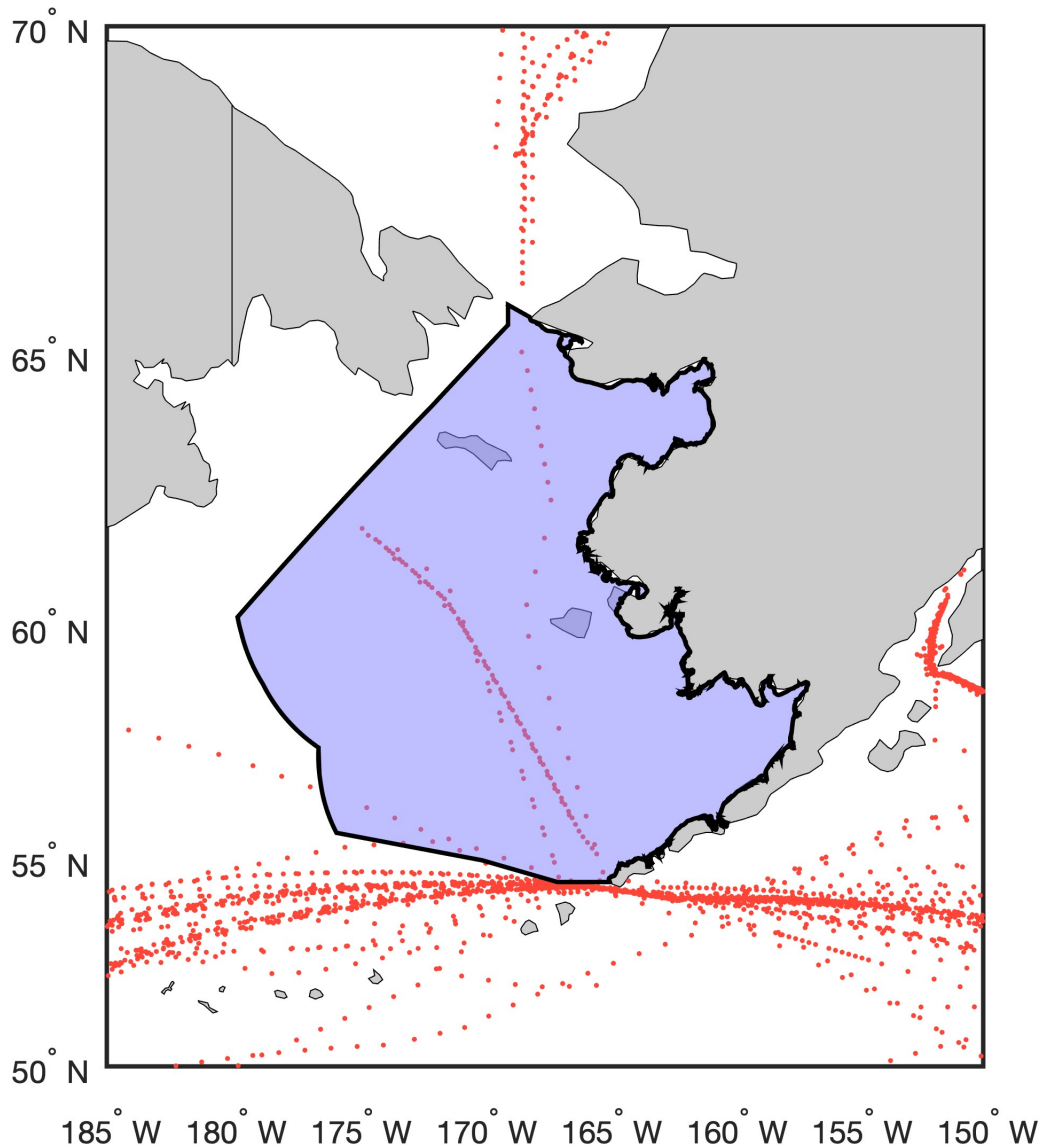
Figure 49: Location of CPR data. The EBS region selected for analysis is highlighted in purple. Red dots indicate actual sample positions and may overlay each other.

carried out in the southern Bering Sea and Aleutian Islands and concluded that this alternation was the result of a trophic cascade caused by maturing pink salmon present in the region. The zooplankton data in Figure 50 consist of more taxa than just large copepods but it is likely that there is some top-down influence of the pink salmon also present in these data.

Implications: This region appears to be subjected to top-down influence by pink salmon as well as bottom up forcing by ocean climate, the combination of which is particularly challenging to interpret. Changes in community composition (e.g., abundance and composition of large diatoms, prey size as indexed by mean copepod community size) may reflect changes in the nutritional quality of the organism to their predators. Changes in abundance or biomass, together with size, influences availability of prey to predators.
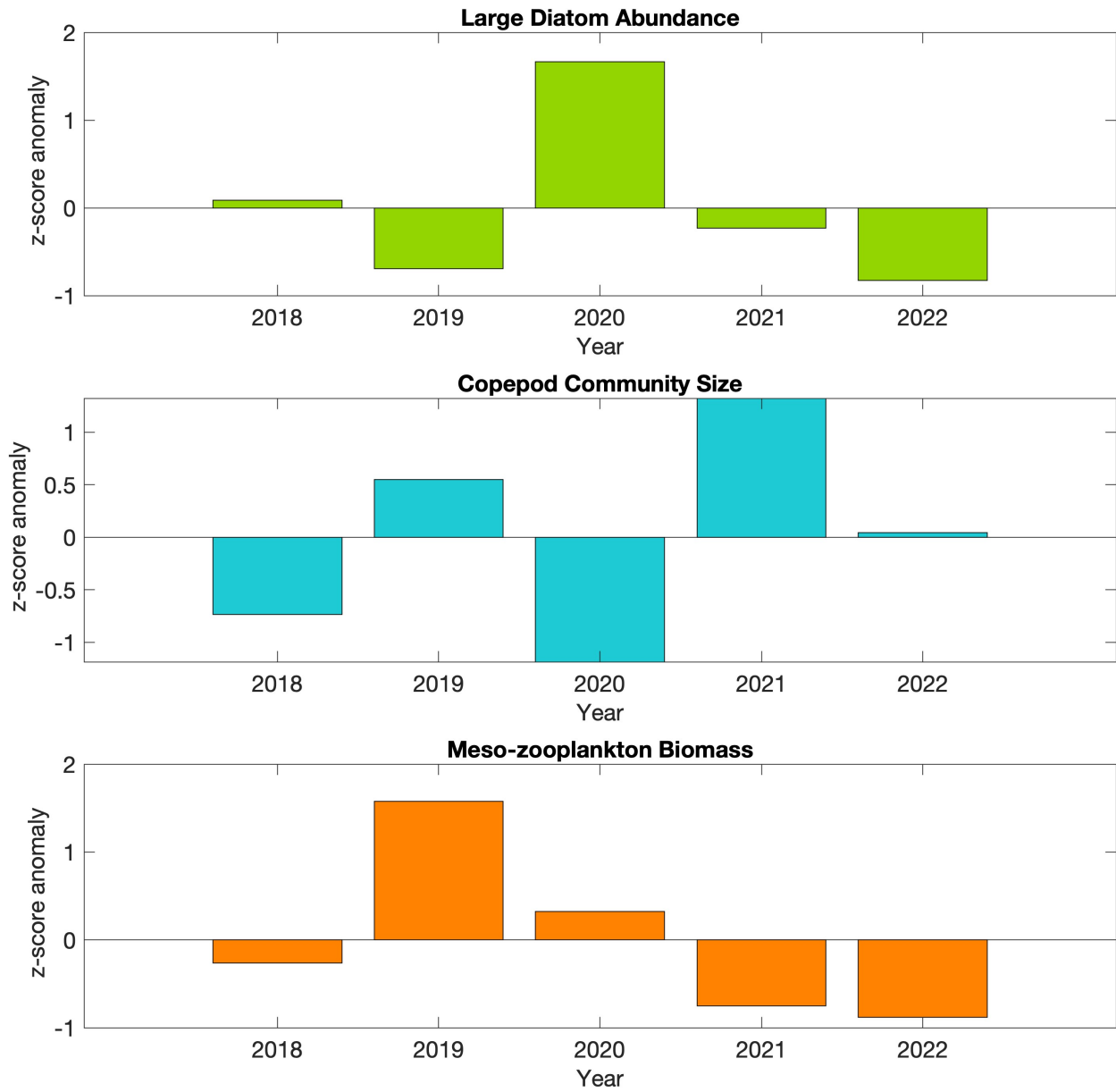
Figure 50: Annual anomalies of three indices of lower trophic levels (see text for description and derivation) for the region shown in Figure 49.

Current and Historical Trends for Zooplankton in the Bering Sea

Contributed by David Kimmel[1], Daniel Cooper[1], Bryan Cormack[2], Colleen Harpold[1], James Murphy[2], Melanie Paquin[1], Cody Pinger[2], Brooke Snyder[1], and Robert Suryan[2]
[1]Resource Assessment and Conservation Engineering Division, Alaska Fisheries Science Center, National Marine Fisheries Service, NOAA
[2]Auke Bay Laboratories, Alaska Fisheries Science Center, National Marine Fisheries Service, NOAA
Contact: david.kimmel@noaa.gov
Last updated: October 2023

Description of indicator: In 2015, NOAA's Alaska Fisheries Science Center (AFSC) implemented a method for an at-sea Rapid Zooplankton Assessment (RZA) to provide leading indicator information on zooplankton composition in Alaska's Large Marine Ecosystems. The rapid assessment, which is a rough count of zooplankton (from paired 20/60 cm oblique bongo tows from 10m off bottom or 300 m, whichever is shallower), provides preliminary estimates of zooplankton abundance and community structure. The method employed uses coarse categories and standard zooplankton sorting methods (Harris et al., 2000). The categories are small copepods (<2mm; example species: *Acartia* spp., *Pseudocalanus* spp., and *Oithona* spp.), large copepods (>2mm; example species: *Calanus* spp. and *Neocalanus* spp.), and euphausiids (<15mm; example species: *Thysanoessa* spp.). Small copepods were counted from the 153μm mesh, 20cm bongo net. Large copepods and euphausiids were counted from the 505μm mesh, 60cm bongo net. Other, rarer zooplankton taxa were present but were not sampled effectively with the on-board sampling method.

RZA abundance estimates may not closely match historical estimates of abundance as methods differ between laboratory processing and ship-board RZA, particularly for euphausiids which are difficult to quantify accurately (Hunt et al., 2016). Rather, RZA abundances should be considered estimates of relative abundance trends overall. Detailed information on these taxa is provided after in-lab processing protocols have been followed (1 year post survey).

Here, we show RZA maps for three surveys: (1) the spring 70m isobath survey (May 2023), (2) the fall 70m isobath survey (August/September 2023), and (3) the northern Bering Sea survey (NBS, August/September 2023). We also show RZA time-series for the spring and fall 70m isobath surveys over the southern middle shelf (Ortiz et al., 2012) as well as the northern Bering Sea. We have revised our time-series approach to separate 70m surveys from gridded surveys, thus we present individual time-series for each ongoing survey as opposed to spring and summer combined time-series as in the past. Separating out the two different surveys allows a better understanding of any changes in trends of taxa abundances during the time-series. We also revised the time-series to correct error-bar miscalculations and standardize all gear types across the time-series.

In addition to abundance estimates, the total lipid content for the zooplankton categories of large copepods and euphausiids was estimated. Zooplankton were collected separately in glass vials from each station, stored frozen, and analyzed at NOAA's Auke Bay Laboratories. Briefly, the measured lipid content was compared to the respective wet-weight for the zooplankton in each vial. Lipid analysis was performed via a rapid colorimetric technique employing a modified version of the sulfo-phospho-vanillin (SPV) assay. This method was shown to be highly accurate for analyzing zooplankton lipids in a recent inter-laboratory cross validation study (Pinger et al., 2022).

Status and trends:

Spring 70m isobath survey

Overall, the RZA abundances were low in spring (Figure 51). Large copepods were very low in abundance along the 70m isobath; however, greater numbers were observed in the Unimak Pass region (Figure 51a). Small copepods were also low in abundance with highest estimates in the most southeastern station of the 70 m isobath (Figure 51b). Euphausiids (<15mm) were largely absent from RZA estimates, with only one sampling location having a high abundance near Unimak Pass (Figure 51c). Despite this, larger euphausiids (>15mm) were present in small numbers throughout the sampling area. Larger euphausiids are more difficult to estimate accurately with RZA sub-sampling methods, thus abundances are not reported here.

Large copepod estimates were very low relative to the long-term average (Figure 52). Values were similar to the recent warm years and well below the moderate estimates during the prolonged cold period from 2006–2013 and well below the highest values during the 2014–2016 warm period (Figure 52a). Small copepod values were moderate relative to the historical record and values were lowest in spring during the cold years (2006–2013) and increased during recent warming (Figure 52b). Euphausiid values are variable in the spring over time and values in 2023 were near zero (Figure 52c).

A total of 12 and 23 samples of large copepods and euphausiids were analyzed, respectively, for percent lipid per wet weight (Figure 53). Large copepod lipid content was low overall (mean=3.12%, SD=1.89), with only one sample having a high value (6.8%) (Figure 53a). Euphausiid average lipid content was also low (mean=2.75%, SD=0.84) (Figure 53b). **Note**: euphausiids estimated for lipid content were large euphausiids (>15mm) and therefore do not match with the zeros shown in the estimates of abundance map (Figure 51c) which reports small (<15mm) euphausiids.
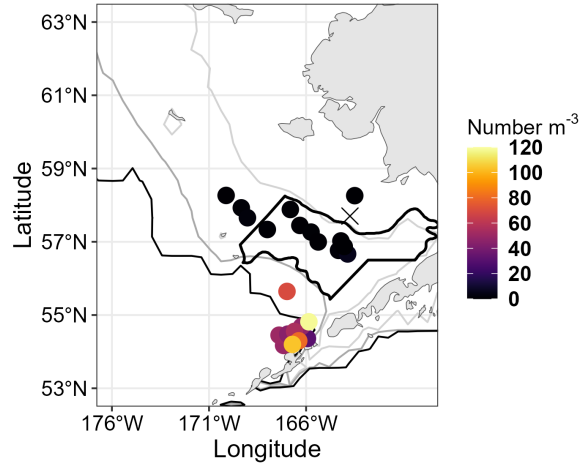
(a) Large copepods (>2mm)
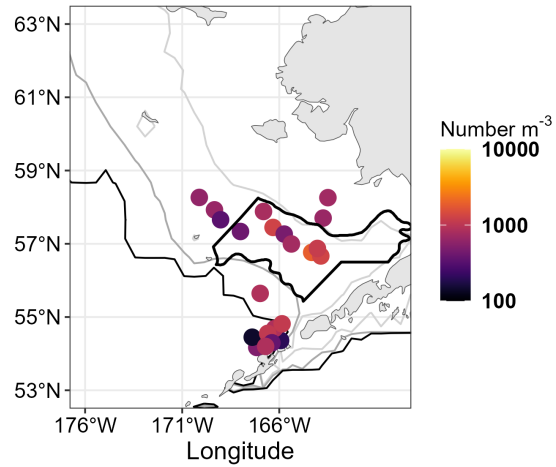
(b) Small copepods (<2mm)
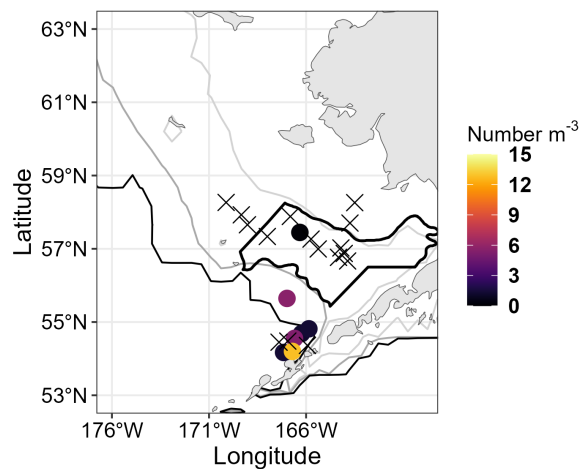
(c) Euphausiids (<15mm)

Figure 51: Maps show the abundance estimated by the RZA during the spring 70m isobath survey. **Note**: all maps have different abundance scales (Number m^{-3}). X indicates a sample with abundance of zero individuals m^{-3}. Black polygon shows the core sampling area used to estimate the time-series.
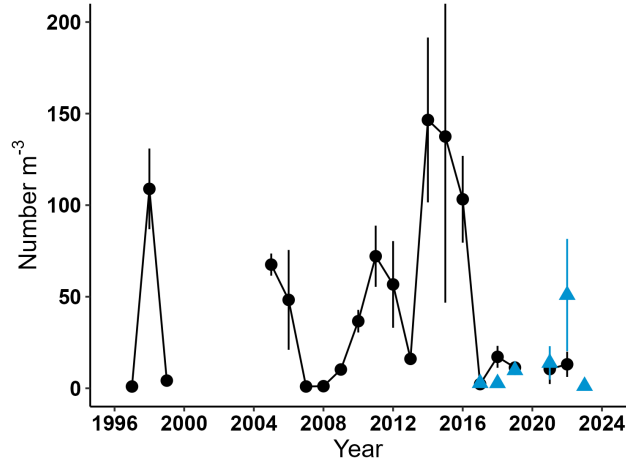
(a) Large copepods (>2mm)
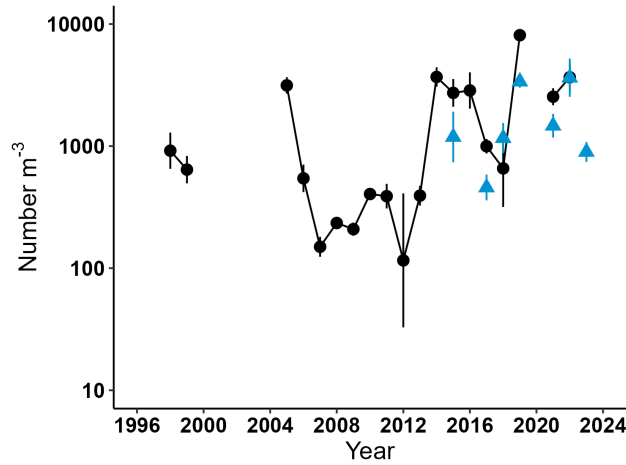
(b) Small copepods (<2mm)
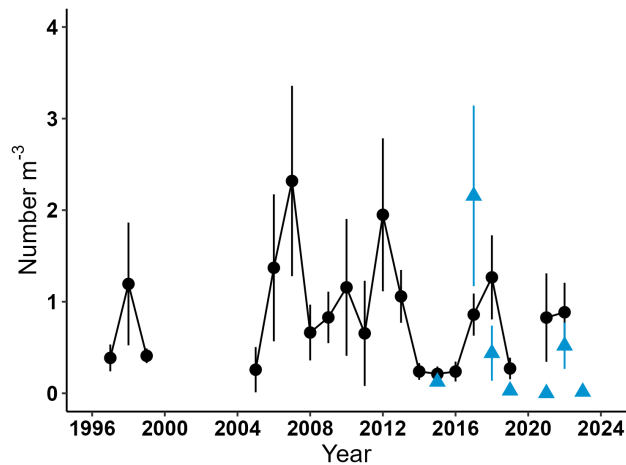
(c) Euphausiids (<15mm)

Figure 52: Mean abundance along the 70m isobath during spring. Black circles represent laboratory processed data, blue triangles represent vessel-based RZA data. Line ranges are the standard error of the mean. **Note** differences in scale.
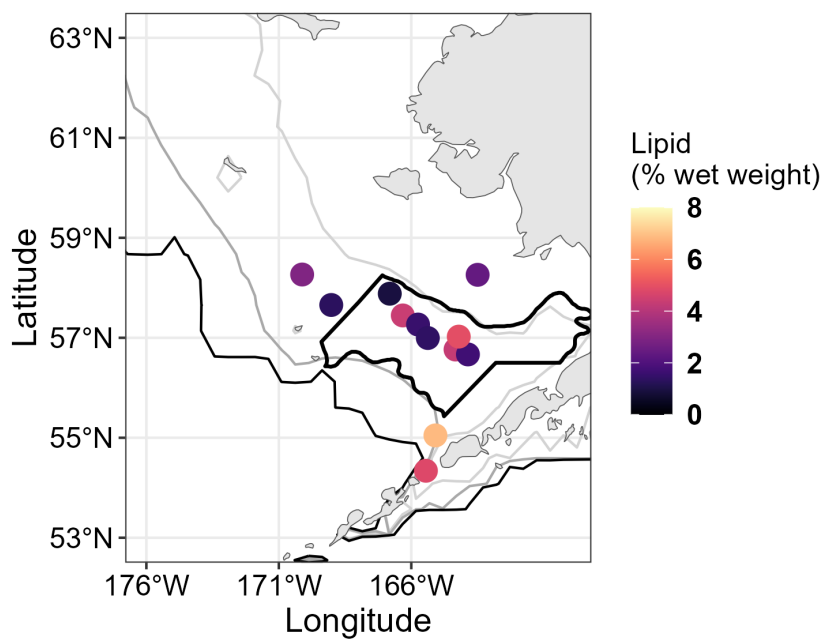
(a) Large copepods (>2mm)
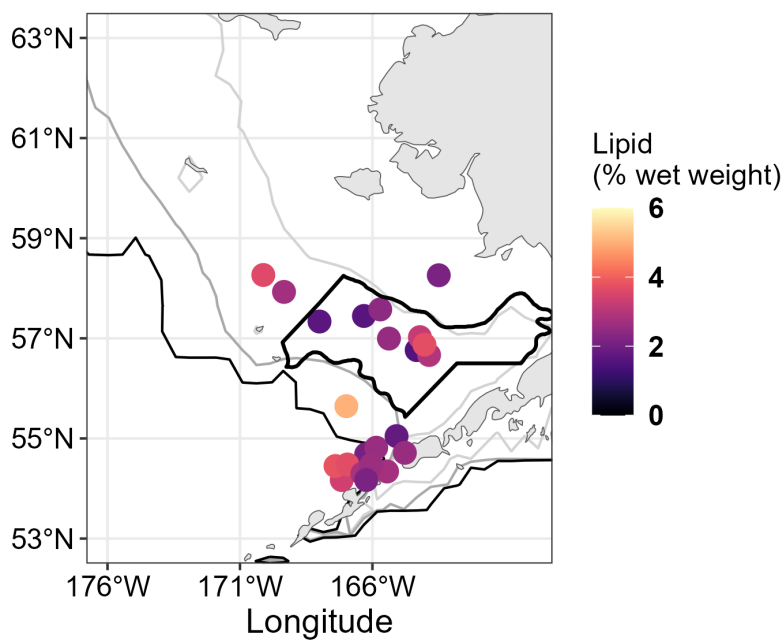
(b) Euphausiids (>15mm)

Figure 53: Lipid content (% wet weight) for large copepods (>2mm, *Calanus* spp.) and euphausiids (>15mm, *Thysanoessa* spp.) for the spring 70m isobath survey. Black polygon shows the core sampling area used to estimate the time-series, for reference; however, not enough samples have been collected to produce a lipid time-series at present.

Fall 70m isobath survey

In fall, large copepod abundances were very low in the times-series sampling region, but increased in the northern portion of the 70m isobath survey (Figure 54a). Small copepods had similar abundances spatially along the 70m isobath (Figure 54b). Euphausiid abundances were similar in pattern to those of large copepods, with low values in the southern portion of the 70m isobath survey and increasing numbers in the northern portion of the survey (Figure 54c).

Only a total of three samples were collected within the time-series polygon, thus the estimate for the time-series should be viewed with caution. Here we place the 2023 RZA estimate on the time-series to provide some information about the status and trend (Figure 55). Large copepod numbers were very low on the southeastern shelf, well-below the peak values observed during the cold period (2006–2013). These values are similar to the low numbers observed during recent warm periods (Figure 55a). Small copepod abundances were about average relative to the historical record, above those of the cold period (2006–2013) and below those of the recent warm period, with the exception of 2017 (Figure 55b). Euphausiid abundances were similar to most years in the data record, having low abundance in the fall (Figure 55c).

A total of 13 and 11 samples of large copepods and euphausiids were analyzed, respectively, for percent lipid per wet weight. Large copepod lipid content increased compared to spring (mean=16.62%, SD=3.42) (Figure 56a). Euphausiid average lipid content also increased (mean=8.99%, SD=2.55) (Figure 56b). Lipid values for copepods were elevated in the northern portion of the 70m isobath, coincident with higher abundance values, whereas euphausiid values were variable (Figure 56).
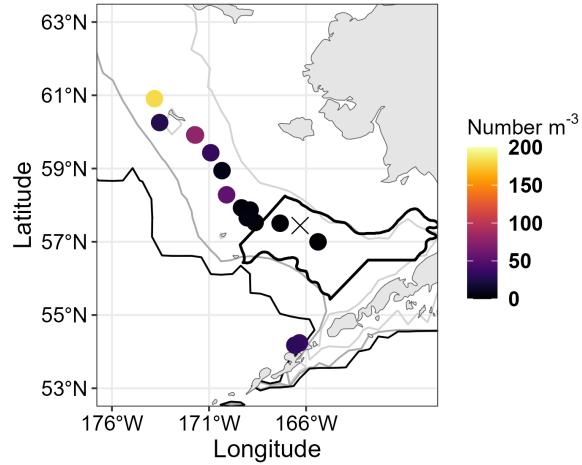
(a) Large copepods (>2mm)
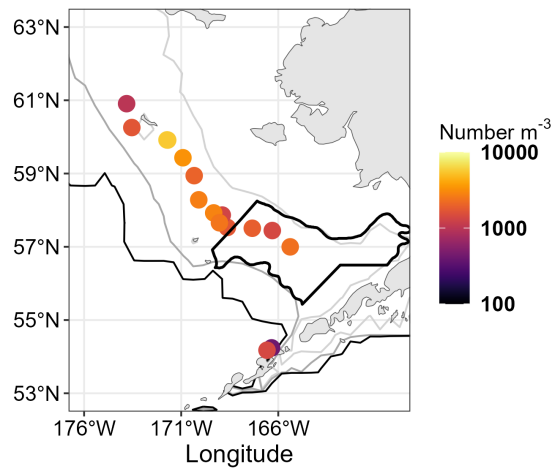
(b) Small copepods (<2mm)
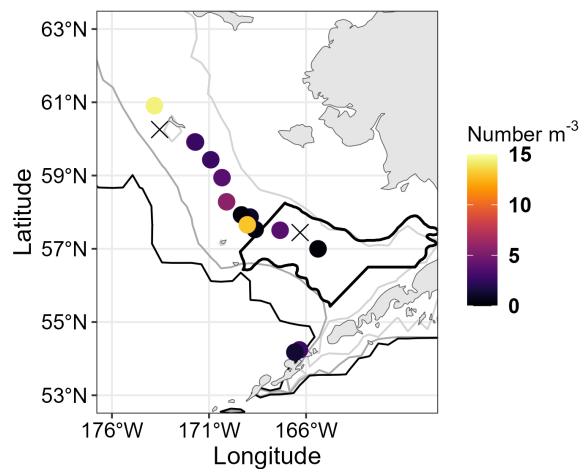
(c) Euphausiids (<15mm)

Figure 54: Maps show the abundance estimated by the RZA during the fall 70m isobath survey. **Note**: all maps have different abundance scales (Number m^{-3}). X indicates a sample with abundance of zero individuals m^{-3}. Black polygon shows the core sampling area used to estimate the time-series.
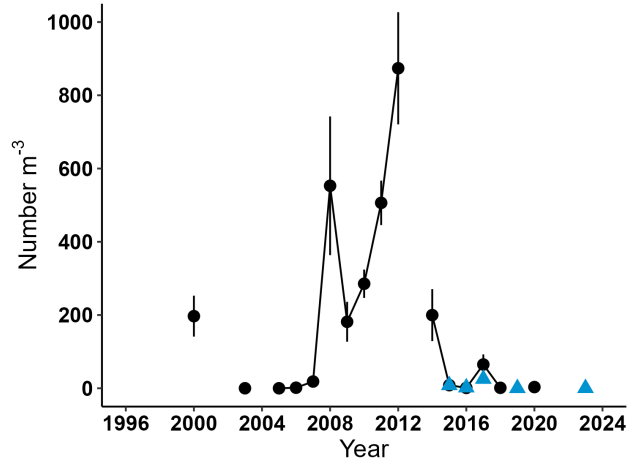
(a) Large copepods (>2mm)
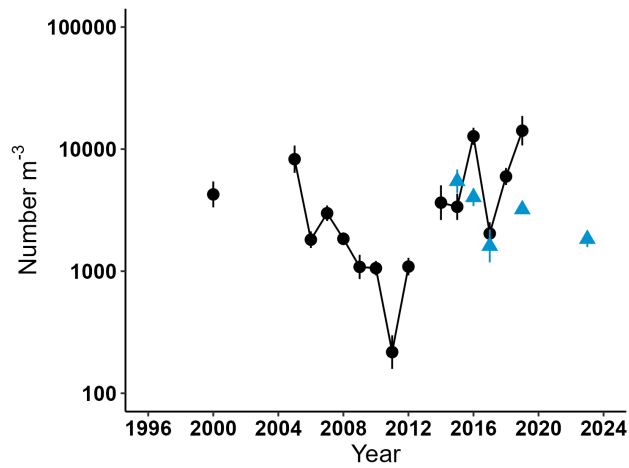
(b) Small copepods (<2mm)
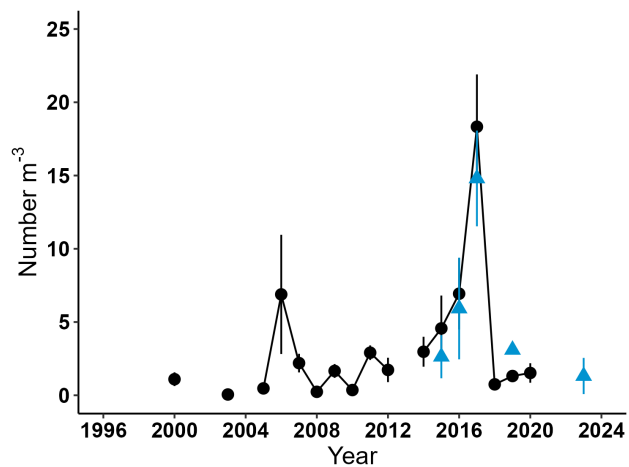
(c) Euphausiids (<15mm)

Figure 55: Mean abundance along the 70m isobath during fall. Black circles represent laboratory processed data, blue triangles represent vessel-based RZA data. Line ranges are the standard error of the mean. **Note** differences in scale.
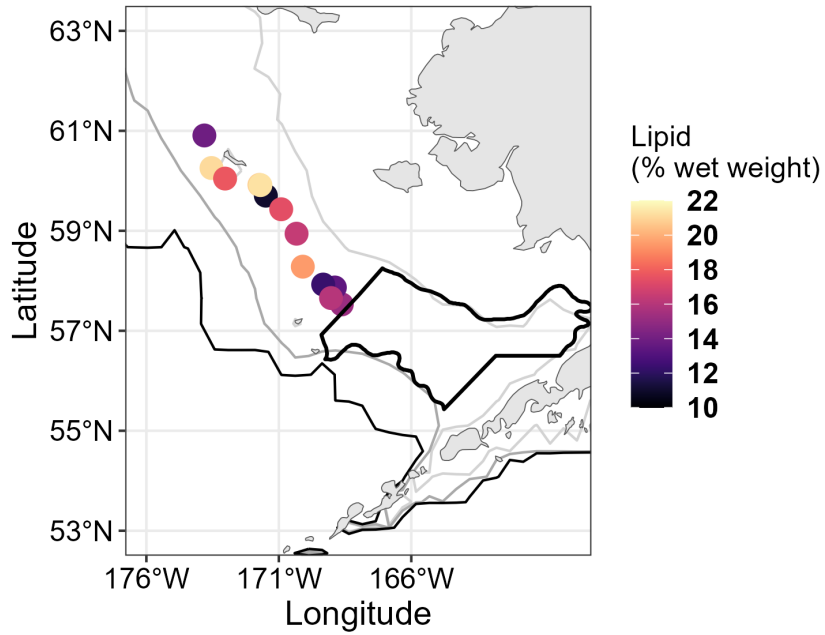
(a) Large copepods (>2mm)
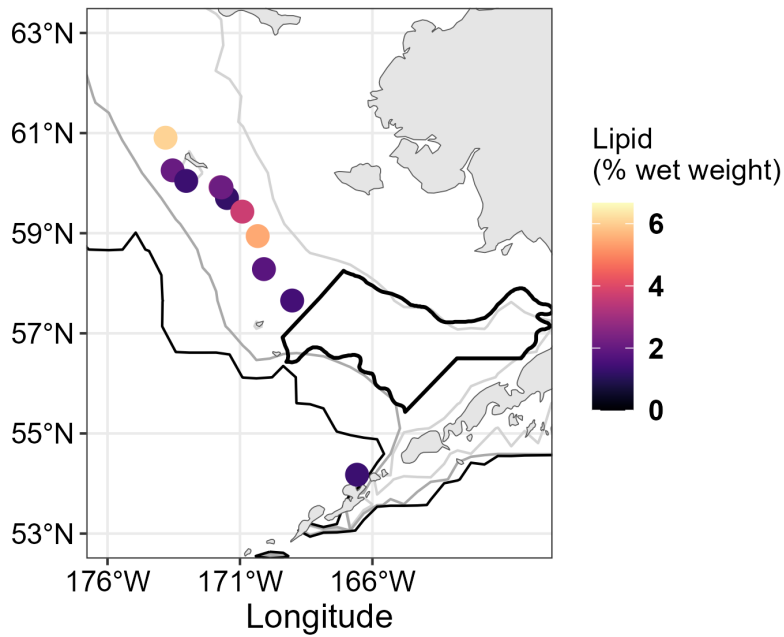
(b) Euphausiids (>15mm)

Figure 56: Lipid content (% wet weight) for large copepods (>2mm, *Calanus* spp.) and euphausiids (>15mm, *Thysanoessa* spp.) for the fall 70m isobath survey. Black polygon shows the core sampling area used to estimate the time-series, for reference; however, not enough samples have been collected to produce a lipid time-series at present.

Northern Bering Sea survey
Large copepod abundances in the northern Bering Sea were patchy throughout the sampling region with the highest values north and south of St. Lawrence Island (Figure 57a). Small copepods increased in abundance moving from south to north within the survey grid (Figure 57b). Euphausiids were abundant in the same locations as large copepods, i.e. in the vicinity of St. Lawrence Island (Figure 57c).

Large copepod abundances were similar to those reported during the last three surveys and higher than the low values observed in 2018–2019 (Figure 58a). Small copepods were near average in value and lower than observed during the recent warm period (2014–2018) (Figure 58b). Euphausiid abundance estimates were higher than recent years with an upward trend since 2021 and the 2023 estimate is the highest recorded in the time-series (with the exception of 2007) (Figure 58c).

A total of 27 and 16 samples of large copepods and euphausiids were analyzed, respectively, for percent lipid per wet weight (Figure 59). Large copepod lipid content was low overall (mean=6.87%, SD=4.28), particularly when compared to values from the northern portion of the fall 70m isobath survey (Figures 56a and 59a). Euphausiid average lipid content (mean=3.28%, SD=1.68) was also lower than values observed on the fall 70 m isobath survey (Figures 56b and 59b).
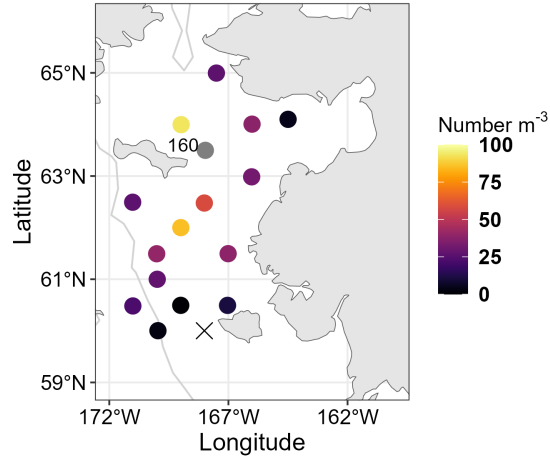
(a) Large copepods (>2mm)
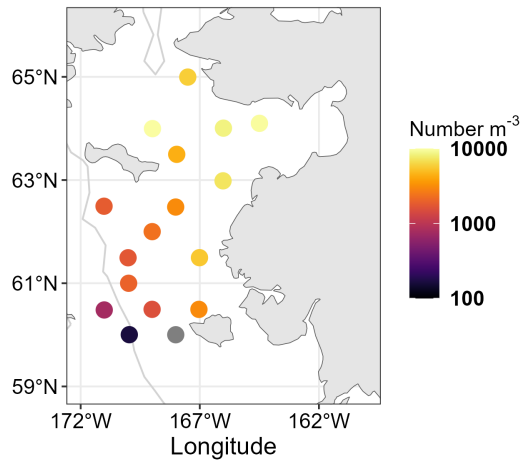
(b) Small copepods (<2mm)
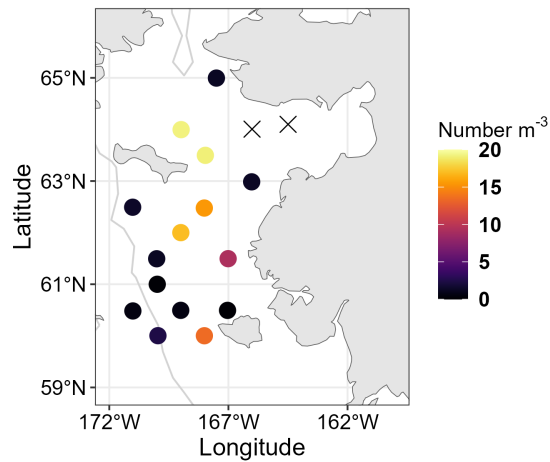
(c) Euphausiids (<15mm)

Figure 57: Maps show the abundance estimated by the RZA during the northern Bering Sea survey in fall. **Note**: all maps have different abundance scales (Number m^{-3}). X indicates a sample with abundance of zero individuals m^{-3}. Time-series is estimated from the whole sample region. Note one value for large copepods was beyond the legend scale and is indicated as 160 individuals m^{-3}.
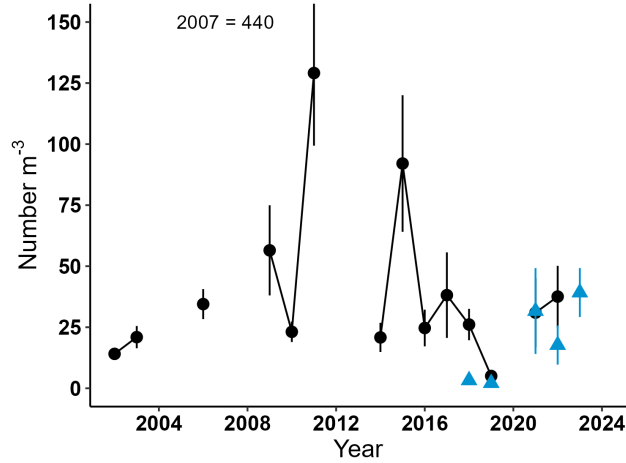
(a) Large copepods (>2mm)
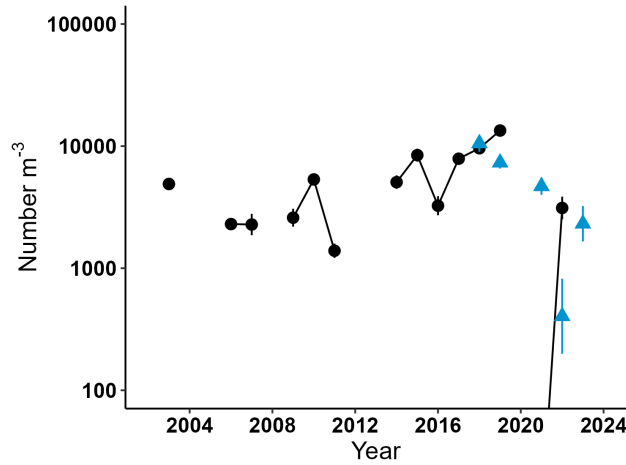
(b) Small copepods (<2mm)
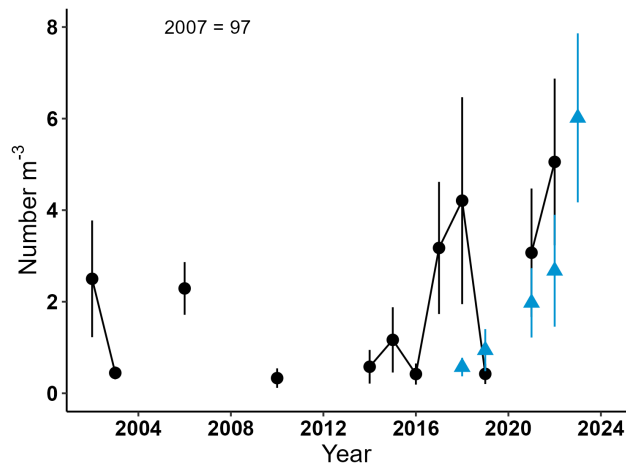
(c) Euphausiids (<15mm)

Figure 58: Mean abundance in the northern Bering Sea during fall. Black circles represent laboratory processed data, blue triangles represent vessel-based RZA data. Line ranges are the standard error of the mean. **Note** differences in scale.
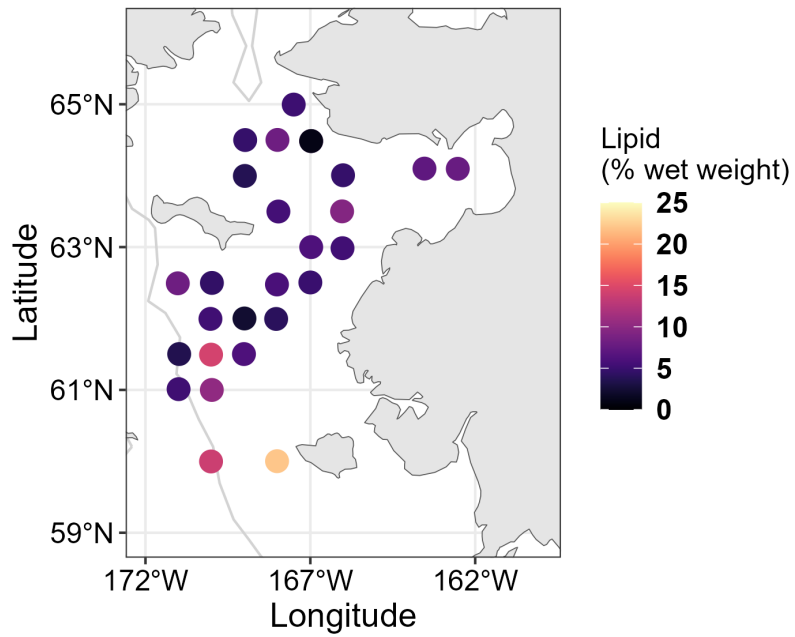
(a) Large copepods (>2mm)
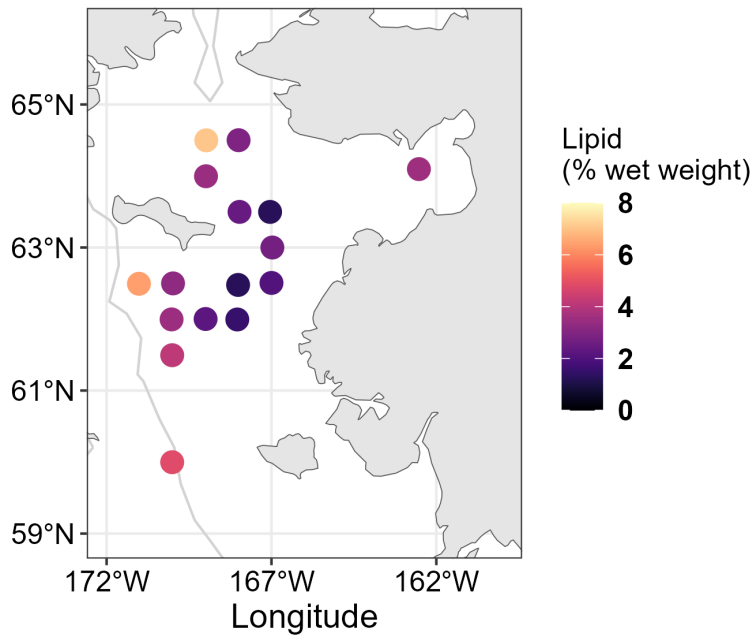
(b) Euphausiids (>15mm)

Figure 59: Lipid content (% wet weight) for large copepods (>2mm, *Calanus* spp.) and euphausiids (>15mm, *Thysanoessa* spp.) for the northern Bering Sea survey. Not enough samples have been collected to produce a lipid time-series at present.

Factors influencing observed trends: The 70m isobath survey in spring showed very low values of abundance for the zooplankton community overall. The survey encountered significant ice coverage and very cold temperatures, and this appeared to limit the development of the zooplankton community in spring (Figures 51 and 52). Given the presence of spring ice, conditions appeared favorable for *Calanus* spp. population accumulation in summer/fall if the ice extent resulted in a large cold pool. Small copepod numbers were moderate in abundance overall with a downward trend during the past warm years, but lower than recent warm years (Figure 52). Colder temperatures reduce development rates and slow population increases for copepods (Kiorboe and Sabatini, 1995). Euphausiids <15mm were largely absent from the samples; however, larger euphausiids were present as indicated by the lipid samples and this suggest that reproduction may have been occurring on the shelf. Lipid content during the spring was low, as was expected, as large copepods such as *Calanus* spp. were represented by earlier life history stages and euphausiids were preparing for spring reproduction, meaning energy was not being stored as lipid (Figure 53). Compared to prior years, the lipid content of *Calanus* spp. in spring has averaged around 4% by wet mass, similar to this year's average of 3.12%.

Though conditions did appear favorable in the spring, low numbers of large copepods (*Calanus* spp.) were seen on the southeastern shelf during the fall 70m isobath survey (Figure 54a). This can be attributed to bottom temperatures in excess of 3.5°C on the southeastern shelf. When bottom temperatures decreased below 2°C in the northern portion of the 70m isobath line, *Calanus* spp. was present in greater numbers, as were euphausiids (Figures 54a and 54c). The cold pool extent is one of the most important factors that correlates to the presence of *Calanus* spp. (Eisner et al., 2018; Kimmel et al., 2018). Small copepod abundances in fall were moderate and did not show a spatial gradient from south to north (Figure 54b). The lower abundances of small copepods compared to more recent warm years suggests water temperatures were reduced compared to recent warming periods (Figure 55b). Euphausiid abundances were higher than those observed in spring and this suggests that euphausiids had reproduced in spring and euphausiids <15mm were present. Their numbers also appeared to increase with declining bottom water temperatures; however, correlations with euphausiids and temperature are not strong (Bi et al., 2015) and population dynamics of euphausiids remain difficult to estimate (Hunt et al., 2016).

The lack of large copepods on the southeastern shelf was in contrast to the northern Bering Sea survey which found higher abundances (Figure 57a). Values were similar to recent years, but below those of the cold period (2006–2013) (Figure 58a). This result was similar to 2022 where a reduced cold pool to the south resulted in moderate numbers present in the northern Bering Sea. The northern Bering Sea appears to be more stable across warm and cold periods in comparison to the southeastern shelf, with at least a small population of *Calanus* spp. present annually. It should be noted that the *Calanus* spp. numbers are also lower in this inner shelf region compared to middle shelf numbers. Small copepod numbers were elevated in the northern Bering Sea as would be expected in inner shelf waters (Figure 57b); however, values were lower than the high estimates observed during the peak of the warming period from 2014–2018 when large numbers of neritic species were observed across the northern Bering Sea (Kimmel et al., 2023). Euphausiid values were high in the northern Bering Sea relative to the historical record and appear to be elevated when large copepod numbers are lower (Figures 58a and 58c). There is no clear explanation for this trend at the present time.

Lipid data for the fall 70m isobath survey showed that copepods were higher in lipid than was reported in the spring (Figures 53a and 56a). The high values observed in the northern portion of the fall 70m isobath survey suggest that these copepods were nearing entry into diapause as the wet weight values translated to a mean of 61.4% lipid per dry weight, similar to values of copepodite stage 5 *C. glacialis*

in European waters (Mayzaud et al., 2016). Interestingly, the *Calanus* spp. from the northern Bering Sea were lower in overall lipid (Figure 59a) averaging 6.87% lipid per wet weight (30.7% lipid per dry weight). These *Calanus* spp. were in warmer, inshore waters and this appeared to impact lipid accumulation, in contrast to 2022 when lipid values for *Calanus* spp. were high in this region. Lipid values for euphausiids were consistent across all three surveys, though those captured in the fall 70m isobath survey had the highest lipid content (Figure 56b).

Implications: Smaller copepods and their early life history stages (nauplii) form the prey base for larval to early juvenile walleye pollock, as well as other fish species, during spring (Figures 51b and 52b) on the eastern Bering Sea middle shelf. Warm years result in larger estimates for small copepods in the spring (Figure 52b) and this led to the formulation of the first Oscillating Control Hypothesis (OCH) (Hunt et al., 2002) as this supports larval pollock production. While small copepod numbers were reduced in 2023 relative to the warm years, they were still abundant overall and this suggests that adequate food for larval fish was present during spring 2023.

Large copepods and euphausiids are more important to late juvenile pollock as shown in the second iteration of the OCH (Hunt et al., 2011). While large copepods were absent on the southeastern shelf in fall, they were present in moderate abundances further north in both the fall 70m isobath survey (Figures 54a and 54c) and northern Bering Sea surveys (Figures 57a and 57c). This suggests forage for juvenile pollock would be present in the northern portion of the Bering Sea on the middle shelf, but scarce in the southeastern shelf. Euphausiid numbers were low in the fall 70m isobath survey, but elevated in the northern Bering Sea surveys relative to prior years (Figures 55c and 58c). Euphausiids have been more prevalent in age-0 pollock diets during warm years, thus have been proposed as an alternative diet item in the absence of *Calanus* spp. (Duffy-Anderson et al., 2017). Exact estimates of euphausiid abundances remain semi-quantitative. Euphausiid estimates should be treated with caution as bongo nets are effectively avoided by euphausiids. Furthermore, it should be noted that the RZA and processed estimates of abundances do differ and this is expected due to the patchy nature of euphausiid distribution and the difficulty in accurately estimating euphausiid abundances (Hunt et al., 2016).

Lipid values showed a contrast between species and locations. Lipid values for *Calanus* spp. were elevated in the northern portion of the 70m isobath survey in fall (Figure 56a), suggesting that lipid rich forage was present in this region and this was in contrast to the low lipid values observed for *Calanus* spp. on the inner shelf from the northern Bering Sea survey (Figure 59a). Euphausiid lipid values from the northern Bering Sea survey were lower compared to copepods, particularly on the inner shelf (Figure 59b). These values also highlight the difference in total lipids between *Calanus* spp. and euphausiids, with *Calanus* spp. providing nearly double the lipid content per unit mass. In prior years with low large copepod numbers, the proportion of euphausiids increased in age-0 pollock diets; however, this correlated with lower overall condition of age-0 pollock (Heintz et al., 2013).

In summary, the large ice extent observed during the spring 70m isobath survey had differing impacts on the zooplankton community. It reduced zooplankton levels early in the year, particularly for small copepods which had been elevated during the recent warm period. Despite this, adequate numbers appeared to be present, suggesting that larval fish in the early portion of the year experienced sufficient forage. The sea ice did not translate into an extension of the cold pool over the southeastern shelf during late summer, but was present further north along with increased abundances of large copepods and euphausiids. The *Calanus* spp. that were found further north were rich in lipid along the middle shelf, but not in the inner shelf region. Cold pool dynamics continue to play a key role in the degree of spatial overlap between age-0 pollock and these prey species that are important to their survival (Siddon et al., 2013; Eisner et al., 2020).

Jellyfish

Trends in the Biomass of Jellyfish in the South- and Northeastern Bering Sea During Late-Summer Surface Trawl Surveys, 2004–2023

Contributed by Ellen Yasumiishi, Alex Andrews, Jim Murphy, Andrew Dimond, and Ed Farley
NOAA Fisheries, Alaska Fisheries Science Center, Ecosystem Monitoring and Assessment Program, Juneau, AK
Contact: ellen.yasumiishi@noaa.gov
Last updated: September 2023

Description of indicator: Annual indices of juvenile groundfish, juvenile salmon, forage fish, and jellyfish biomass (metric tonnes) and abundance (numbers) of juvenile sockeye salmon (*Oncorhynchus nerka*) in surface waters were estimated for the Alaska Fisheries Science Centers' (AFSC) Bering Arctic Subarctic Integrated Survey (BASIS). BASIS is an integrated fisheries oceanography survey in the south- and northeastern Bering Sea during late summer, 2003–2023. Primary jellyfish taxa include *Chrysaora melanaster*, *Cyanea* sp., *Aequorea* sp., *Aurelia labiata*, *Phacellophora camtschatica*, and *Staurophora mertensii*. Unidentified or non-dominant jellyfish species were included in the total jellyfish catch.

Pelagic fish and jellyfish were sampled using a trawl net towed in the upper 25m. For the estimates of species abundance, the BASIS survey (373,404 km^2) was within the region south to north from 54.54ºN to 59.50ºN and west to east from -173.08ºW to -159.00ºW for years 2003–2012, 2014, 2016, 2018, and 2022. The northern Bering Sea survey (197,868 km^2) was within the region south to north from 59.97ºN to 65.50ºN and west to east from -172.00ºW to -161.50ºW for years 2003–2007, 2009–2019, 2021–2023. A trawl was towed for approximately 30 minutes. Area swept was estimated from horizontal net opening and distance towed. For 2024, authors plan to present density rather than biomass and abundance estimates to account for differences in survey area in the north and south

Annual indices of relative biomass (metric tonnes) and numbers (abundance) were estimated using a single-species spatio-temporal model with the VAST package version 3.10.1, INLA version 22.04.16, TMB version 1.9.2, FishStatsUtils version 2.12.1, R software version 4.11.3, and RStudio version 2023.06.1 (RTeam, 2023; Thorson et al., 2015; Thorson and Kristensen, 2016; Thorson, 2019*a*). We used the VAST package to reduce bias in biomass estimates due to spatially unbalanced sampling across years, while propagating uncertainty resulting from predicting density in unsampled areas. Spatial and spatio-temporal variation for both encounter probability and positive catch rate components were specified at a spatial resolution of 500 knots. We used a Poisson-link, or conventional, delta model and a gamma distribution to model positive catch rates and specified a bias-corrected estimate (Thorson et al., 2019). Parameter estimates were within the upper and lower bounds and final gradients were less than 0.0005. Julian day was added as a normalized covariate with a spatially constant and linear response due to changes in the timing of the survey among years.

Status and trends: During 2023, the estimated biomass of jellyfish in pelagic waters was high in the northeastern Bering Sea during late summer (Figure 60). Trends in jellyfish biomass were similar in the north and south, except during 2012–2018. There was no southeastern Bering Sea survey in 2023. Higher levels of jellyfish biomass in the south occurred during 2012, 2014, 2016, and 2018.
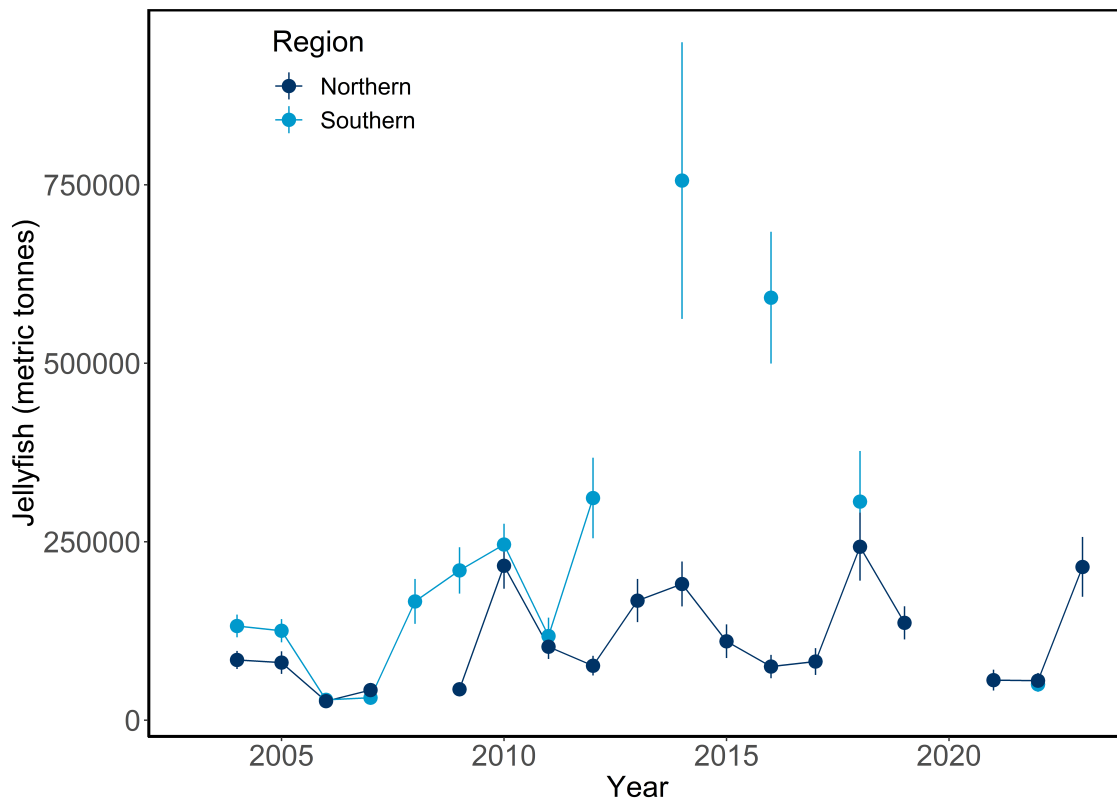
Figure 60: Estimated biomass (metric tonnes) of jellyfish in surface waters surveyed in the eastern Bering Sea during late summer, 2004–2023.

Factors influencing observed trends: Jellyfish feed primarily on small fish and zooplankton, and jellyfish production tracks forage fish production. Lower forage fish biomass, such as age-0 pollock, during 2022 may have contributed to lower jellyfish production, however in 2023, a cool year, jellyfish biomass was high and forage fish biomass low (see 2023 EBS Forage Report). In addition, the higher levels of jellyfish biomass in the south from 2012 to 2018 corresponded with a relatively warm period and higher biomass of age-0 pollock and forage fish, both prey items of jellyfish.

Implications: Jellyfish are competitors, predators, and act as shelters for forage fishes. During 2023, the higher abundance of jellyfish may indicate favorable environmental conditions for the growth and survival of jellyfish and other species in the eastern Bering Sea during late summer. Higher jellyfish biomass may also not favor other species by increased competition for food and predation pressure.

Eastern and Northern Bering Sea – Jellyfishes

Contributed by Thaddaeus Buser
Resource Assessment and Conservation Engineering Division, Alaska Fisheries Science Center
National Marine Fisheries Service, NOAA
Contact: thaddaeus.buser@noaa.gov
Last updated: September 2023

Description of indicator: The time series for jellyfishes (Scyphozoa, but primarily *Chrysaora melanaster*) relative CPUE by weight (kg per hectare) was updated for 2023 from both the eastern (Figure 61, top) and northern (Figure 61, bottom) Bering Sea surveys. Catch methods for the Northern Bering Sea (NBS) were standardized in 2010, so the catches from previous years do not provide comparable data and are consequently excluded. Relative CPUE was calculated by setting the largest biomass in the time series to a value of 1 and scaling other annual values proportionally. The standard error (± 1) was weighted proportionally to the CPUE to produce a relative standard error.

Status and trends:
Eastern Bering Sea:
The relative CPUE for jellyfishes in the eastern Bering Sea in 2023 is virtually unchanged from the 2022 survey estimate, similar to the catch rates observed 1992–1999 and in 2018. There is an apparent pattern of cyclical rise and fall of CPUE values across the time series. The relatively low biomass estimated throughout the 1980's was followed by a period of increasing biomass of jellyfishes throughout the 1990s (Brodeur et al., 1999). A second period of relatively low CPUE estimates from 2001 to 2008 was then followed by a second period with relatively higher CPUE values from 2009 to 2015. It is worth noting that, prior to this year, jellyfish CPUE estimates in the EBS have been relatively inconsistent over the past several survey years.

Northern Bering Sea:
The relative CPUE for jellyfishes in the northern Bering Sea is inconsistent across the time series. While an apparent pattern of cyclical rise and fall of jellyfish CPUE values exists in the EBS time series, gaps in sampling years across the northern Bering Sea time series makes identifying multi-year trends difficult.

Factors influencing observed trends: The fluctuations in jellyfish biomass and their impacts on forage fish, juvenile walleye pollock (*Gadus chalcogrammus*), and salmon in relation to other biophysical indices were investigated by Cieciel et al. (2009) and Brodeur et al. (2002, 2008). Ice cover, sea-surface temperatures in the spring and summer, and wind mixing all influence jellyfish biomass, and affect jellyfish sensitivity to prey availability (Brodeur et al., 2008).

Implications: Jellyfish are pelagic consumers of zooplankton, larval and juvenile fishes, and small forage fishes. A large influx of pelagic consumers such as jellyfish can decrease zooplankton and small fish abundance, which in turn can affect higher trophic levels causing changes to the community structure of the ecosystem.
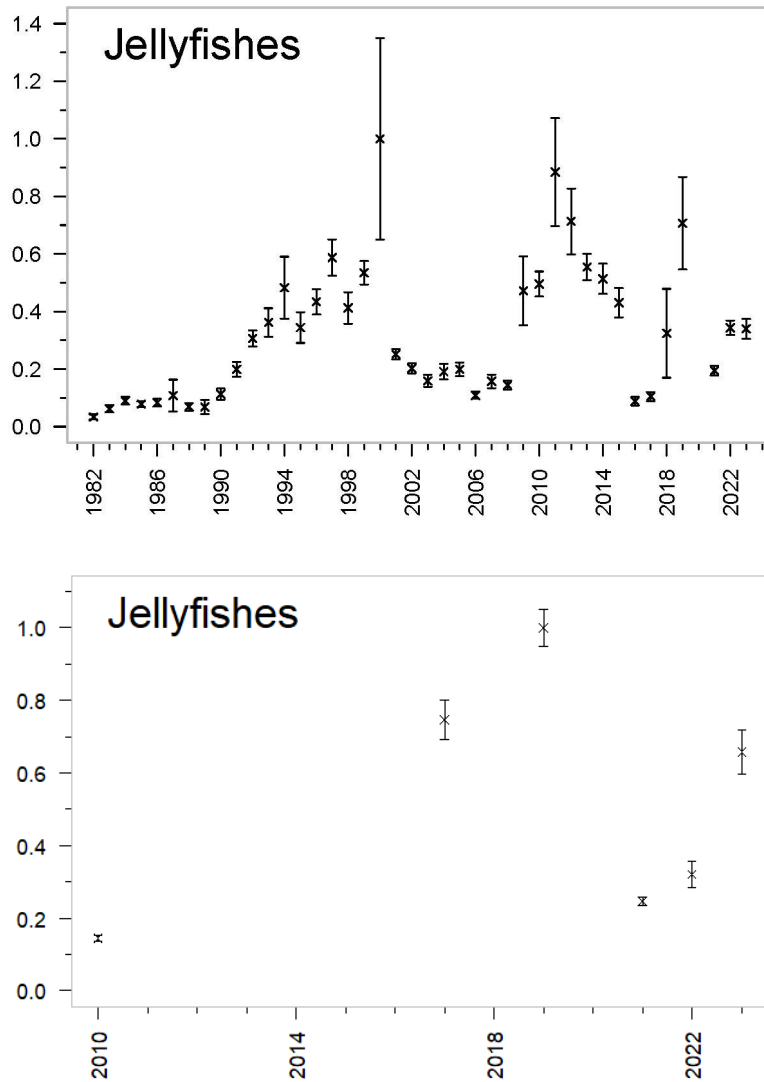
Figure 61: AFSC eastern (top) Bering Sea shelf bottom trawl survey relative CPUE for jellyfish during the May–August time period from 1982–2023 and for the northern (bottom) Bering Sea shelf survey during the July–August time period from 2010–2023.

Forage Fish

Highlights of the 2023 Bering Sea and Aleutian Islands Forage Report

Contributed by Cody Szuwalski
Resource Ecology and Fisheries Management Division, Alaska Fisheries Science Center, NOAA Fisheries
Contact: Cody.Szuwalski@noaa.gov
Last updated: October 2023

The abundance of forage species (e.g., fishes, squids, euphausiids, and other invertebrates) in the eastern Bering Sea (EBS) is difficult to measure. There are no dedicated surveys for these species, and the existing surveys are limited in their ability to assess forage species due to gear selectivity (e.g., mesh size) or catchability (e.g., vertical distribution).

Nevertheless, these surveys can be used to discern general trends in abundance, which were mixed in 2023. Estimated capelin and eulachon density and prevalence from the NMFS bottom trawl surveys were near all-time lows in 2023. Pacific herring density and prevalence has been above average for the last several years. Shrimp densities have been trending upward since the mid-1990s; prevalence peaked in 2010. Total incidental catches of the FMP forage group were low in 2022 and 2023 compared to historical values. Total shrimp catches decreased in 2022, but were near all time highs in 2023. Prohibited species catch of herring has been higher than average since 2020, with the third highest catches ever observed in 2023.

Fall Condition of Young-Of-The-Year Walleye Pollock in the Southeastern and Northern Bering Sea, 2002–2023

Contributed by Johanna Page, Jacek Maselko, Robert Suryan, Todd Miller, Elizabeth Siddon, Cody Pinger, Emily Fergusson, and Bryan Cormack
Auke Bay Laboratories, Alaska Fisheries Science Center, National Marine Fisheries Service, NOAA
Contact: johanna.vollenweider@noaa.gov
Last updated: September 2023

Description of indicator: Several metrics of body condition of young-of-the-year (YOY) walleye pollock (*Gadus chalcogrammus*) in the Bering Sea are presented, including length-weight residuals, percent lipid, and energy density. **Note**: values from 2023 are from a preliminary subsample of fish. Fish were sampled primarily by surface trawl from late-summer surveys in the southeastern and northern Bering Sea, with a relatively small number of fish from opportunistic surveys. Fish <100mm total length were assumed to be YOY (Bailey, 1989).

Fish length, weight, percent lipid, and energy density were measured at Auke Bay Laboratories, Juneau, AK, following respective standard protocols described in Vollenweider et al. (2011) and Pinger et al. (2022). Fish weight is strongly correlated with length, therefore, annual length-weight residuals were calculated from the linear regression of log transformed length (total length, mm) and weight (whole
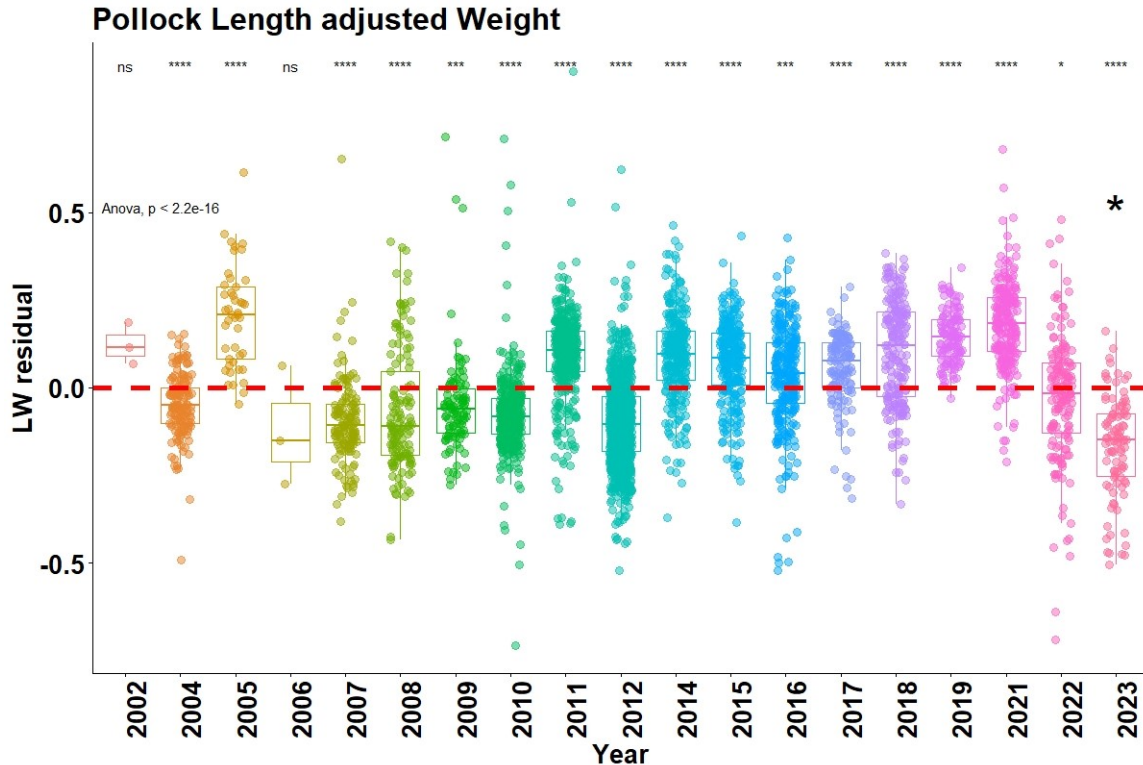
Figure 62: Annual length-weight residuals from log-transformed length-weight regressions for young-of-the-year walleye pollock. The horizontal line indicates the mean of all residuals, the significance of deviations from the mean are denoted by stars above the given year, and "ns" indicates not significant. Length is total length (mm) and mass is total body wet mass (grams). The asterisk above 2023 data indicates that these are preliminary results.

wet mass, g). Similarly, annual length-energy density residuals were calculated from the linear regression of log transformed length and energy density (kJ/g dry mass). There was no correlation between fish length and percent lipid, therefore percent lipid was not length-corrected.

Status and trends: From 2006–2010 YOY pollock had below average wet weight for a given length (Figure 62), but above average lipid content (Figure 63) and energy density (Figure 64). In contrast, during recent warm years 2014–2019, they were heavier than average, but had low lipid content and energy density. Since 2021, body condition has trended back towards the mean of the time series, but is still variable. Preliminary data from 2023 indicates fish weighed less for a given size and also had lower lipid content and energy densities, which is different than previous patterns.

Factors influencing observed trends: YOY pollock transition from an energetic strategy favoring growth during early summer, which reduces size-dependent predation, to a strategy of lipid storage during late summer for winter survival (Siddon et al., 2013). Ocean temperatures, which impact physiological thermal responses and the availability of lipid-rich prey, influence growth and lipid storage of juvenile pollock (Koenker et al., 2018; Laurel et al., 2016). In the Bering Sea, fluctuating thermal regimes between alternating warm and cold periods result in changes to zooplankton community composition (Kimmel et al., 2023). During warm regimes, energetic stress of increased metabolic demands is compounded by a community of lipid-poor zooplankton species dominated by small copepods as opposed to a high abundance of lipid-rich *Calanus* spp. during cold regimes (Kimmel et al., 2023).
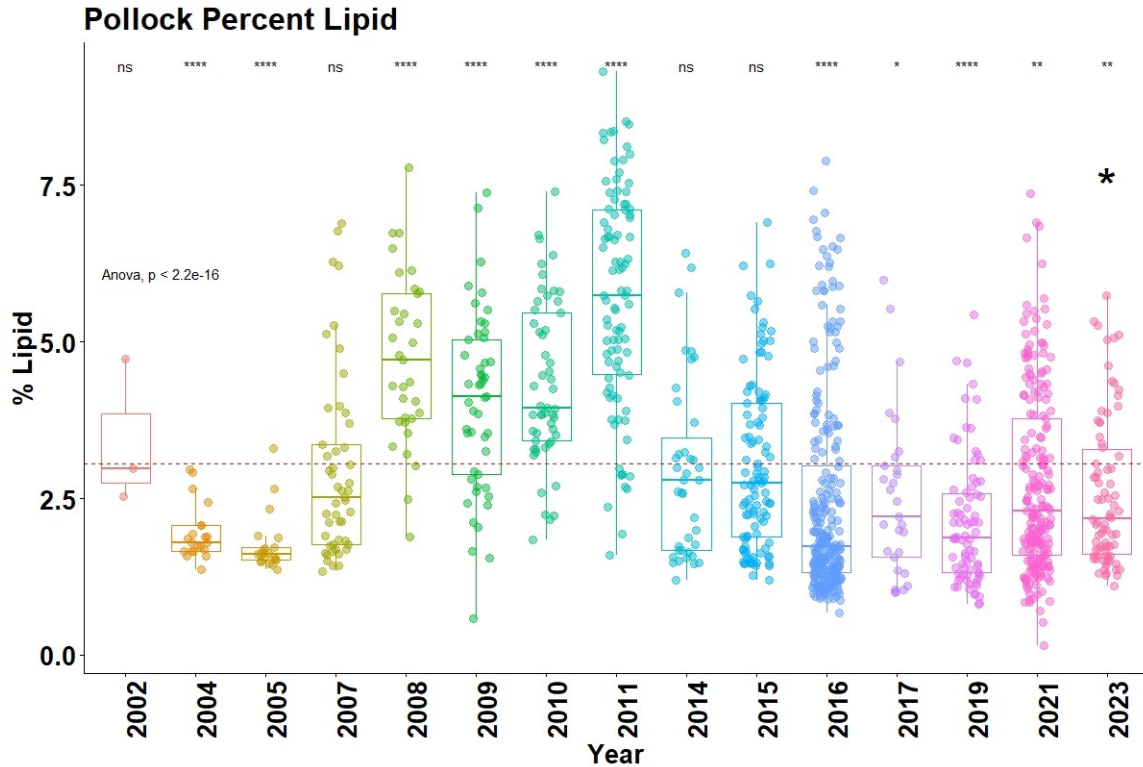
Figure 63: Annual lipid content (% lipid/gram wet fish mass) of young-of-the-year pollock. The horizontal line indicates the mean percent lipid for all years, the significance of deviations from the mean are denoted by stars above the given year, and "ns" indicates not significant. The asterisk above 2023 data indicates that these are preliminary results.

Consequently, the energetic content of YOY pollock diets is reduced during warm years resulting in poor body condition of YOY pollock (Andrews III et al., 2019).

Implications: Summer environmental conditions and the ability of YOY pollock to balance the synonymous energetic demands to grow and store lipid is reflected in their body condition prior to winter. Winter survival is dependent on their ability to grow large enough for predator avoidance while simultaneously having acquired sufficient lipid stores to sustain them through cold winters when food is relatively scarce. In the Bering Sea, first winter survival of YOY pollock to age-1 recruits has been shown to vary during cold and warm regimes (Heintz et al., 2013).
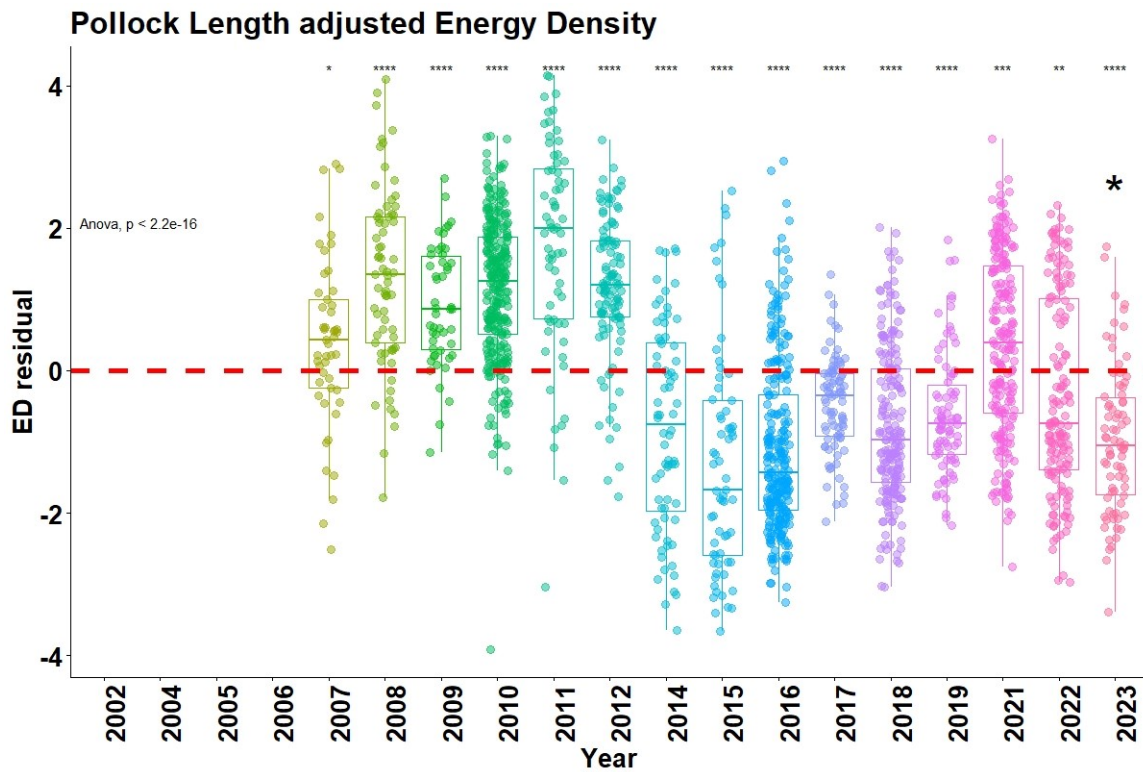
Figure 64: Annual length-adjusted energy density (kJ/gram fish dry mass) of young-of-the-year pollock. The horizontal line indicates the mean of all residuals, the significance of deviations from the mean are denoted by stars above the given year. The asterisk above 2023 data indicates that these are preliminary results.

Vertical Distribution of Age-0 Pollock in the Southeastern Bering Sea

Contributed by Adam Spear[1] and Alexander G. Andrews III[2]
[1]Resource Assessment and Conservation Engineering Division
[2]Auke Bay Laboratories
Alaska Fisheries Science Center, National Marine Fisheries Service, NOAA
Contact: adam.spear@noaa.gov
Last updated: September 2023

Description of indicator: Vertical distribution of age-0 pollock was estimated through the calculation of an abundance-weighted mean depth during a range of water temperature phases (cold, warm, average). The abundance of age-0 pollock in the southeastern Bering Sea was estimated using acoustic-trawl methods. The process involved assigning trawl-catch data to acoustic-backscatter data that was measured along the transect line. The trawl catch information was manually assigned to backscatter from a single surface, oblique, or midwater-trawl depending on proximity, tow depth, and backscatter characteristics. Scrutinized backscatter was echo-integrated into 0.5 nautical mile (nmi) by 5 m bins, and output as nautical area scattering coefficient, m^2/nmi^2 (NASC). The species-specific compositions from each catch were used to convert NASC to species-specific abundance (individuals/nmi^2) using published measurements of the acoustic properties of these species.
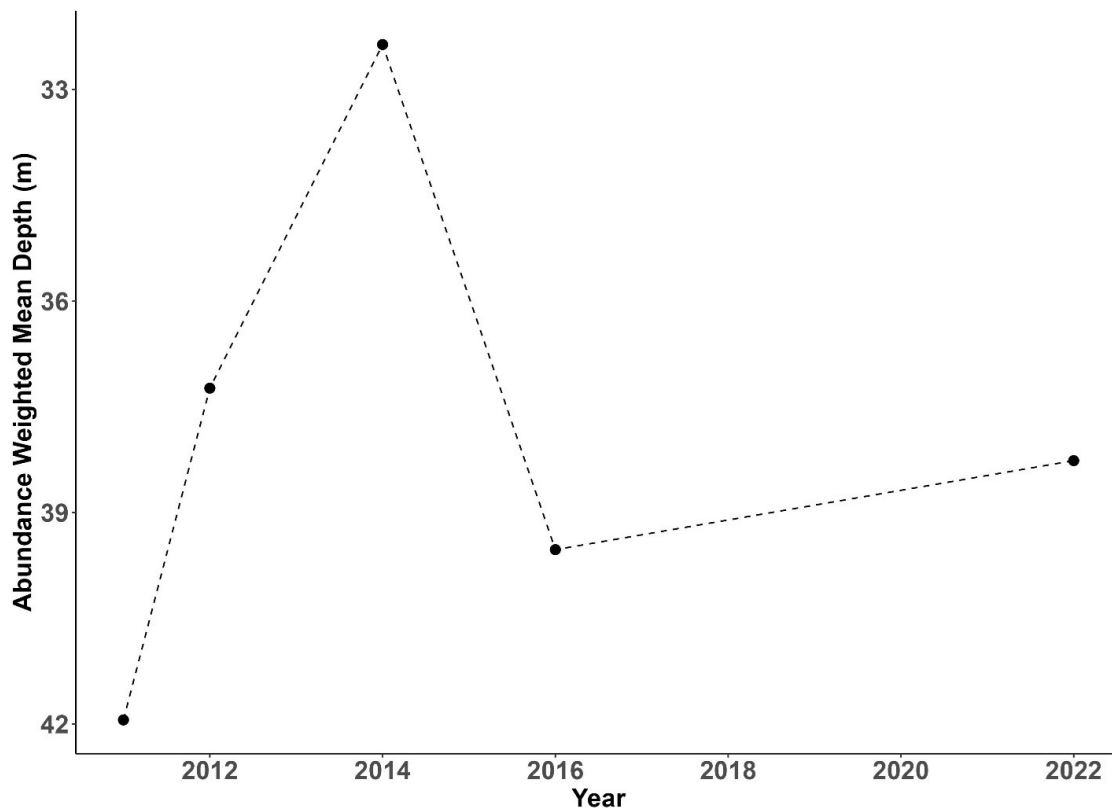
Figure 65: Annual abundance-weighted mean depth of age-0 pollock during late summer in the southeastern Bering Sea.

The middle domain (50 to 100m isobaths; Coachman, 1986) was the most consistent region surveyed across all years. Thus, to account for survey bias, values were constrained to those sampled over the middle domain. Age-0 pollock abundance was summed over each depth bin to calculate the weighted mean depth. Here, we show yearly abundance-weighted mean depths during the late summer over the southeastern Bering Sea middle domain.

Status and trends: Age-0 pollock were deeper in the water column in 2011 (~37m) and 2012 (42m; cold years), and closer to the surface in 2014 (~32m; warm year) by 10 and 5 meters respectively. The trend was less apparent in 2016 (warm year) with a weighted mean depth of 39m, which was similar to colder years. In 2022 (average temperatures), the weight mean depth was 38m, which was also similar to colder years (Figure 65).

Factors influencing observed trends: From the five data points, 2011 and 2012 represented two anomalously colder years, while 2014 and 2016 represented two warmer years, and 2022 represented an average year in the southeastern Bering Sea. Changes in oceanographic phases result in changes in the vertical distribution of age-0 pollock (Spear et al., 2023). Energy densities of age-0 pollock collected in trawls from these surveys showed that pollock collected in cold years had higher energy densities than those collected in warm years (see p. 109), suggesting improved feeding and provisioning conditions at depth in colder-than-average thermal conditions. Colder years have greater abundances of larger lipid-rich prey which result in higher dietary percentages of lipid and energy densities of age-0 pollock (Coyle et al., 2011; Heintz et al., 2013; Kimmel et al., 2018). This is partially explained by larger lipid-rich prey vertically migrating deeper in the water column during the day. Deeper age-0 pollock in 2016 is likely attributed to extreme surface temperatures that reached >15°C in the southeastern Bering Sea (Stabeno et al., 2017), which is within the range where they exhibit thermal stress (Laurel et al., 2016).

Implications: Vertical distribution shifts may impact predator-prey overlap between age-0 pollock and their lipid-rich prey (e.g., calanoid copepods, euphausiids), resulting in different feeding conditions that ultimately define fish body condition prior to the onset of winter. As the climate warms further, or these warm phases potentially lengthen in time, there may be a compounding problem of poor condition and recruitment, thus significantly reducing the standing stock of pollock.

Herring

Togiak Herring Population Trends

Contributed by Phil Joy[1], Sherri Dressel[1], Sara Miller[1], Caroline Brown[2], and Jack Erickson[1]
[1]Alaska Department of Fish & Game, Commercial Fisheries Division
[2]Alaska Department of Fish & Game, Subsistence Section
Contact: philip.joy@alaska.gov
Last updated: September 2023

Description of indicator: A time-series of catch-at-age model estimates of mature Pacific herring (*Clupea pallasii*) biomass (1980–2022) spawning in the Togiak District of Bristol Bay serves as an index of mature population size. An integrated statistical catch-at-age model is used to estimate Togiak herring biomass (Funk et al., 1992; Funk and Rowell, 1995). The data used in the model includes aerial survey estimates of biomass (Lebida and Whitmore, 1985) weighted by a confidence score (Figure 66), age composition and weight-at-age information collected from the purse seine and gillnet fisheries, and harvest from these fisheries.

Recruitment of Togiak herring to the fishery begins at age-4 and fish are estimated to be fully recruited into the fishery at age-8. Togiak herring are an important prey species for piscivorous fish, seabirds, and marine mammals, an important resource for subsistence harvesters, the basis for a directed Togiak commercial herring sac roe fishery and a directed commercial Dutch Harbor bait fishery. Additionally, they are a prohibited species catch (PSC) in the eastern Bering Sea (EBS) groundfish fisheries. The PSC limit for BSAI groundfish fisheries is set at 1% of the EBS mature herring biomass (age 4+) forecast, and Togiak herring comprise a majority of the nine-stock combined EBS mature herring biomass.

Status and trends: Mature Togiak herring biomass, as estimated by the model, increased steeply from 1980 to 1983 (Figure 66), declined through the late-1990s, remained stable through 2020, and has been increasing in recent years as a result of strong age-4 recruitment in 2020 and 2021. Recruitment has been near or above the long-term median (128 million fish) since 2017 with two of the largest recruitment events since the 1980s occurring in 2020 and 2021 (the 2016- and 2017-year classes; Figure 67). The growth and maturation of these fish has driven the recent increase in biomass (Figure 66) and suggests that the population has increased to levels not observed since the mid-1980s.

Based on observer data, the predominant size of herring caught as PSC in the EBS pollock fishery in 2020 (150g; Siddon, 2020) and 2023 (300g; observer data through September 7), which were both years of high herring PSC, align with the 2017 Togiak year class, supporting the recent strong increase in EBS herring biomass. ADF&G subsistence surveys show variable harvest pounds per capita from 1999–2019 (Coiley-Kenner et al., 2003; Fall et al., 2012; Jones et al., 2021), but Togiak respondents noted that the quantity of herring spawn on kelp available for harvest was improved in 2019 in comparison to resource availability since the early 1990s.

Factors causing observed trends: Togiak herring biomass trends are dependent upon highly variable recruitment and are influenced by the environment. The large biomass estimates in 1983–1987 and in recent years resulted from the large age-4 recruitments in 1981, 1982, 2020, and 2021. Williams and Quinn (2000) demonstrated that Pacific herring populations in the North Pacific are closely linked to environmental conditions, particularly water temperature. Tojo et al. (2007) demonstrated how the
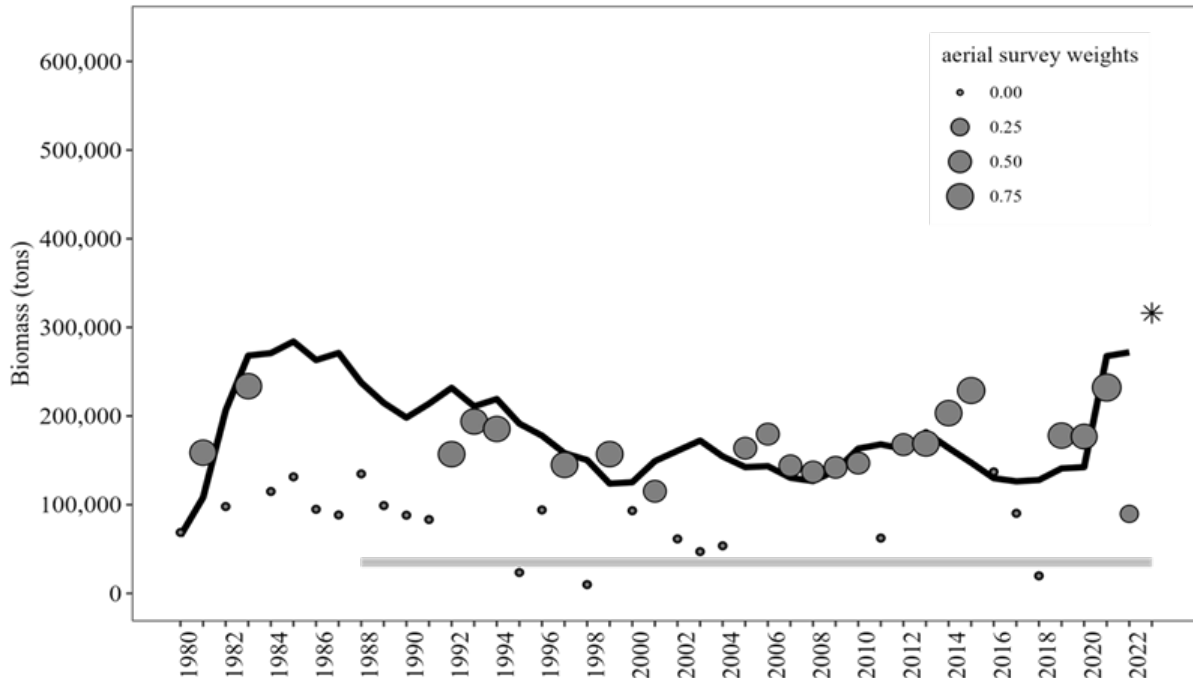
Figure 66: Aerial survey-estimated herring biomass plus pre-peak catch that were included in the model (grey points), model-estimated mature biomass (black solid line), and model-estimated mature biomass forecast (black asterisk). The size of the grey points reflects the confidence weighting of each aerial survey estimate in the model based on weather, number of surveys, quality of surveys, and timing of surveys relative to the spawn (ranging from 0 = no confidence to 1 = complete confidence). Aerial surveys are effectively removed from the model (have no impact) if they are rated at 0. The confidence ranking in 2022 was 0.25 out of 1.0.

complex reproductive migration of EBS herring is related to temperature and the retreat of sea ice and how it has changed since the 1980s. Wespestad and Gunderson (1991) suggest that recruitment variation in the EBS relates to the degree of larval retention in near-coastal nursery areas where temperatures and feeding conditions are optimal for rapid growth. Specifically, they indicate that above average year-classes occur in years with warm sea surface temperatures when the direction of transport is north to northeast (onshore) and wind-driven transport velocity is low. The shift to warm sea surface temperatures from 2014 to 2021 (see Physical Oceanography Synthesis in Siddon, 2022) and the northward onshore springtime drift in June 2017 (Wilderbuer, 2017) may have contributed to support the exceptional 2016- and 2017-year classes.

Implications: The strength of the 2016- and 2017-year classes has resulted in an increase of biomass in the Togiak stock to levels not seen since the mid-1980s, affecting both directed and non-target fisheries. The 2023 forecast was the second highest on record at 316,203 tons (forecasting began in 1993; Brannian et al., 1993) and showed a 16% increase from the model hindcast of 2022 biomass (271,875 tons; Figure 66). The large forecast has provided for continued high allowable harvest in the State of Alaska 2023 directed sac roe and Dutch Harbor food and bait fisheries and may have resulted in increased spawn on kelp available for subsistence harvest. Despite the high allowable harvest in 2023, there was no sac roe fishery in Togiak for the first time since 1976 and the Dutch Harbor food and bait fishery took only 30% of its allocation.
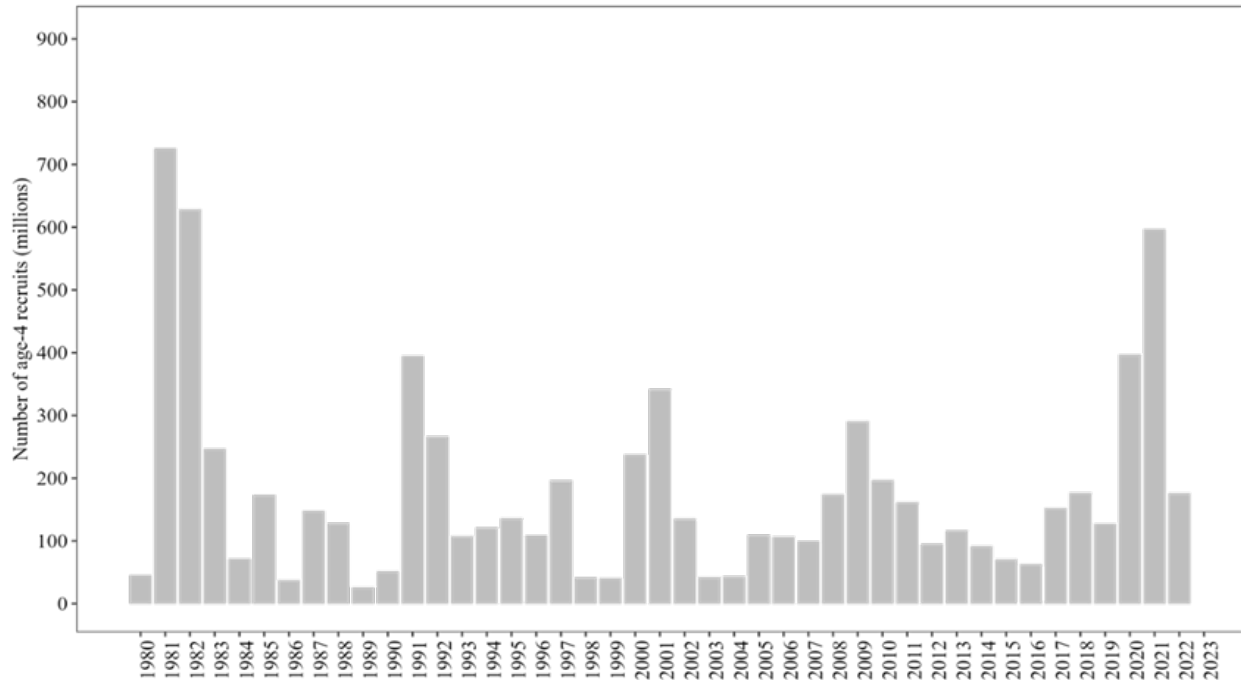
Figure 67: Model estimates of age-4 herring recruit strength (millions of age-4 mature and immature fish).

The strength of the 2017-year class appears to have contributed to high PSC in the EBS pollock fishery in 2020 and 2023. In 2020 the pollock fishery exceeded its PSC allocation with the weight composition of the PSC herring suggesting a majority were 3-year old fish from the 2017-year class. The pollock fishery is again near its PSC allocation in 2023 (2,980 mt harvested from a 3,066 mt allocation as of September 9) with the majority of herring around 300 g, a size that also aligns with the now 6-year old 2017-year class. It is unclear why the 2017-year class was not encountered in high numbers by the pollock fishery in 2021 and 2022, but a reduced footprint of fishing by pollock vessels in 2021 and 2022 (Martell, pers. comm.) may have contributed to the lower PSC in these years. The 2023 pollock fishery has further noted encountering herring deeper and in more variable areas than in the past (Zagorski, pers. comm.) while flatfish fisheries also encountered herring at higher rates than normal.

Rock sole, flathead sole, Alaska plaice, and other flatfish fisheries exceeded their combined PSC allocation in 2023 (99 mt) and directed fishing was closed in the Summer and Winter Herring Savings Areas (HSAs) from June 15, 2023, through March 1, 2024. This is the first time a HSA has been closed to directed fishing from a flatfish fishery since the yellowfin sole fishery exceeded their PSC limit in 1992. High PSC in the 2023 pollock fishery, coupled with the appearance of high catches in flatfish fisheries, suggests shifting patterns of herring distribution in 2023.

The 2017-year class is now approaching full size and maturity and should begin to age out of the population as natural mortality accrues in coming years. However, changing spatial distributions of herring biomass and/or changes in the distributions of directed pollock and flatfish fisheries could result in exceeding PSC limits when and if exceptionally large year classes occur in the future.

Salmon

Salmon Summary and Synthesis

Contributions to the 2023 Eastern Bering Sea (EBS) Ecosystem Status Report provide information on the status of both juvenile and adult salmon of all species. Due to the variable age structure and complex life cycles of Pacific salmon, which span multiple habitats, it can be difficult to disentangle the impacts of environmental conditions experienced across different life stages on their population dynamics. However, some salient patterns do emerge from the contributions to the 2023 EBS Ecosystem Status Report, most notably signs of negative impacts from the anomalously warm conditions in 2019 on adult returns of some stocks, and evidence of favorable effects from a return to cooler temperatures in subsequent years on juveniles.

As has been the case since 2020, adult returns of Yukon and Kuskokwim chum salmon were low in 2023, likely due at least partly to marine heatwave conditions during 2019 (see p. 128). The most common ages of maturity in Yukon and Kuskokwim chum salmon are four and five, such that most adults returning in 2023 are the product of spawning events that occurred in 2018 and 2019. Adult salmon returning to spawn in 2019 suffered direct negative impacts from heatwave conditions through elevated river temperatures and low water levels, with reports of substantial pre-spawning mortality. Heatwave conditions of 2019 adversely affected juvenile chum salmon during marine residency as well. Immature western Alaska chum salmon typically rear in the Bering Sea during summer and fall of their ocean residency and overwinter in the Gulf of Alaska. Heatwave conditions of 2019 negatively impacted juvenile chum salmon rearing in the Bering Sea through reduced prey quality and elevated metabolic stress, leading to poor juvenile condition and survival. Juveniles were likely similarly impacted by heatwave conditions when overwintering in the Gulf of Alaska as well, compounding the negative effects on cohort survival. However, there are indications that returns to cooler temperatures beginning in 2020 are having a positive impact on juvenile chum salmon in the ocean. Survey data from the Northern Bering Sea (NBS) indicates an increased (though still well below average) abundance of juvenile upper Yukon fall chum salmon in 2023 from 2022 (Figure 69). Furthermore, data on energy density, an indicator of body condition, increased substantially in juvenile chum salmon sampled from the NBS in 2021–2022 (the most recent years of data currently available) compared to markedly low values observed during marine heatwave conditions of 2019 (Figure 71). These patterns in juvenile condition over time are coherent with the lipid content of large copepods, suggesting that improved prey quality and reduced metabolic demands arising from cooler sea surface temperatures have led to improved juvenile chum salmon condition.

Preliminary data from 2023 indicates that adult returns of Chinook salmon in the Arctic-Yukon-Kuskokwim (AYK) region also remained low, and likely will not meet management escapement targets (see p. 131). Survey data from the NBS also indicate below average numbers of juvenile Chinook salmon in 2023, similar to 2022 levels (Figure 68). While the energy density of juvenile Chinook salmon in the NBS also increased in 2021–2022 compared to 2019 levels (Figure 71), juvenile energy density of Chinook in the NBS does not appear to have been as strongly adversely affected in 2019 compared to other species. While the causes of the declines of AYK Chinook salmon are still being explored, there is strong evidence that stressors such as heat and low water levels affecting adults during their upriver spawning migrations play a large role.

While AYK chum and Chinook salmon have exhibited low returns in recent years, Bristol Bay sockeye

salmon have shown some of the strongest returns on record during this time period (see p. 125). In 2023, returns of Bristol Bay sockeye salmon remained exceptionally high relative to the long-term average, but lower than the recent record high numbers observed in 2021 and 2022. Such large adult returns suggest that early ocean survival for Bristol Bay sockeye salmon continues to be favorable, although the decline in run size from 2022 to 2023 and predominance of ocean age-3 relative to ocean age-2 fish in the 2023 run suggests early ocean conditions faced by the 2019 brood year cohort in 2021–2022 may have been less favorable than those experienced by the 2018 cohort in 2020–2021. While the correlation between juvenile condition and adult run strength is mixed for Bristol Bay sockeye, it is worth noting that the energy density of mixed stock sockeye salmon juveniles in the southeastern Bering Sea was considerably lower than average in 2022 (Figure 70).

Compiled by Lukas DeFilippo
NOAA Fisheries
Alaska Fisheries Science Center
Last updated: October 2023

Northern Bering Sea Juvenile Salmon Abundance Indices

Contributed by Jim Murphy[1], Sabrina Garcia[2], Andrew Dimond[1], Dan Cooper[3], Elizabeth Lee[2], and Kathrine Howard[2]
[1]Auke Bay Laboratories, Alaska Fisheries Science Center, NOAA
[2]Alaska Department of Fish & Game, Anchorage, AK
[3]Resource Assessment and Conservation Engineering Division, Alaska Fisheries Science Center
Contact: jim.murphy@noaa.gov
Last updated: October 2023

Description of indicator: Mixed-stock juvenile (first year at sea) Chinook salmon (*Oncorhynchus tshawytscha*) abundance indices are estimated from late summer (September) surface trawl catch-per-unit-effort (CPUE) data and adjusted for mixed-layer depth in the northern Bering Sea (NBS). This mixed-stock index provides a rapid assessment of all juvenile Chinook salmon stocks present in the NBS and is different from the stock-specific abundance estimates of Yukon River Chinook salmon that are used to forecast future run sizes.

Abundance indices for Yukon River Fall chum salmon (*O. keta*, Upper Yukon River genetic stock group) are based on CPUE data from surveys in both the northern and southern Bering Sea. The preliminary 2023 abundance index was generated using the average genetic stock proportion from 2016 to 2021 and will change once stock compositions from 2022 and 2023 become available.

Status and trends: The mixed-stock abundance of juvenile Chinook salmon in the NBS was below average in 2023 (1.7 million), and has ranged from 1.4 million to 5.8 million with an overall average of 2.9 million (Figure 68). The preliminary index of juvenile Yukon River Fall chum salmon was below average in 2023 (29) and has ranged from a low of 14 in 2022 to a high of 118 in 2009 with an overall average of 60 (Figure 69).

Factors influencing observed trends: Early life-history (freshwater and early marine) survival and adult spawning escapement are the key factors that determine juvenile salmon abundance in the NBS.
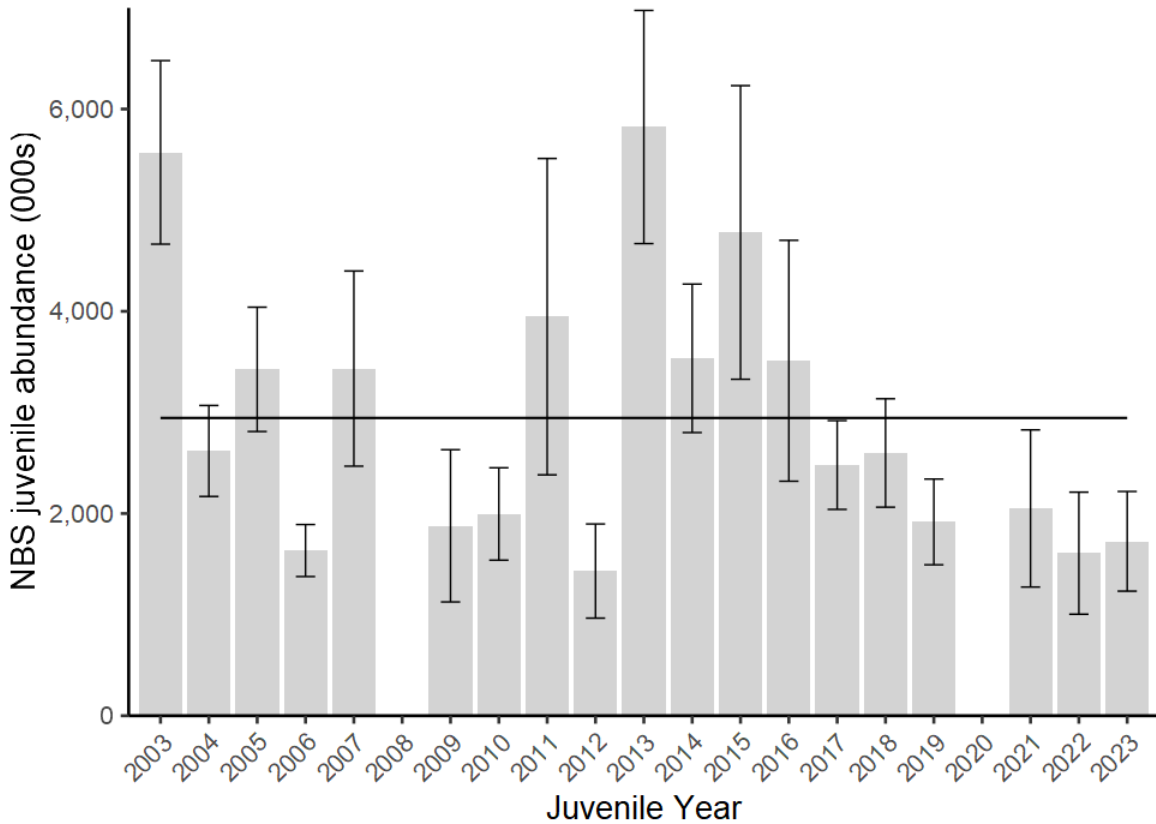
Figure 68: Juvenile Chinook salmon abundance estimates in the northern Bering Sea, 2003–2023. Error bars are one standard deviation above and below juvenile abundance estimates.

Implications: Juvenile Chinook salmon abundance has been related to adult returns (Murphy et al., 2017; Howard et al., 2019, 2020; Murphy et al., 2021). Below average juvenile abundance is expected to contribute to below average adult Chinook salmon returns to the Yukon River three to four years in the future (juveniles typically remain at sea for three to four years before returning to freshwater to spawn). Models assessing the relationship between juvenile and adult Yukon River Fall chum salmon are currently in development. Preliminary model results identify that fluctuations in marine mortality, likely driven by rapid changes in the marine environment, have contributed to recent poor run sizes to the Yukon River, complicating the relationship between juvenile and adult abundance. Future iterations of model development will require ecosystem covariates (e.g., sea surface temperature) to account for changes in natural mortality in chum salmon.
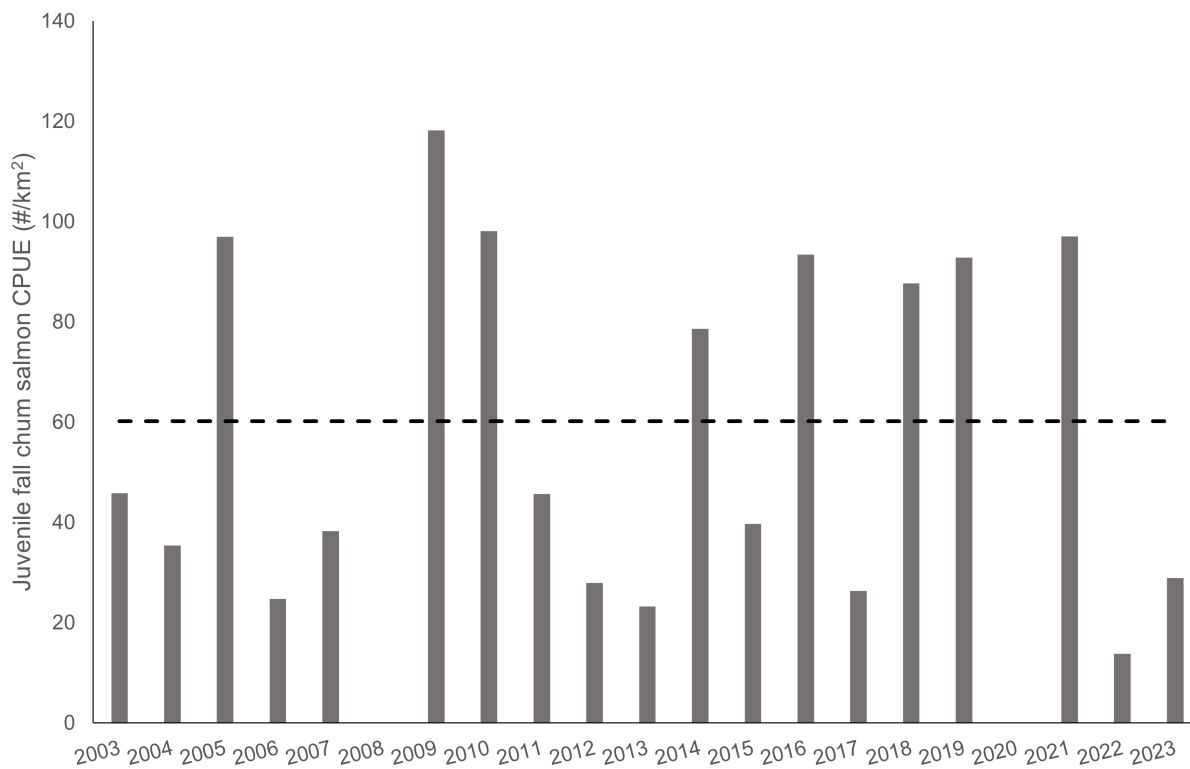
Figure 69: Juvenile chum salmon abundance index (#/km²) for the Upper Yukon River (fall chum) stock group, 2003–2023. No surveys occurred in 2008 and 2020. The 2022 and 2023 abundance indices were generated using the average genetic stock proportion from 2016 to 2021 and will change once stock compositions from 2022 and 2023 become available. Dashed line indicates the average juvenile chum salmon index across years 2003–2022.

Juvenile Salmon Condition Trends in the Eastern Bering Sea

Contributed by Emily Fergusson, Rob Suryan, Todd Miller, Jim Murphy, and Alex Andrews
Auke Bay Laboratories, Alaska Fisheries Science Center, NOAA
Contact: emily.fergusson@noaa.gov
Last updated: September 2023

Description of indicator: The eastern Bering Sea surface trawl surveys consist of multidisciplinary research in the southeastern Bering Sea (SEBS) and northern Bering Sea (NBS) that support sampling of fish, zooplankton and lower trophic levels, and oceanographic conditions. The SEBS survey occurs biennially in late summer (odd years, August–September) within the middle to outer domains (50–200m, 55°N–60°N). The NBS survey occurs annually in late summer (September) and covers the inner domain (bottom depths generally <55m) waters between 60°N–66.5°N.

Juvenile pink (*Oncorhynchus gorbuscha*), chum (*O. keta*), sockeye (*O. nerka*), coho (*O. kisutch*), and Chinook (*O. tshawytscha*) salmon nutritional condition data have been collected from the two fisheries-independent surveys. This report presents 2022 energy density anomalies (ED, kJ/g dry weight) of juvenile salmon in relation to the past 5 to 14 year time series of fish condition from these surveys.

Status and trends: For the SEBS in 2022, ED anomalies in 2022 for juvenile pink, chum, sockeye, and Chinook salmon were negative, and most notably so for pink, chum, and sockeye salmon (Figure 70). No juvenile coho salmon were available for ED analysis in the SEBS.

For the NBS in 2022, ED anomalies for all five species were positive (Figure 71). For juvenile pink, chum, coho, and Chinook salmon, ED was similar to 2021 values. For juvenile sockeye, ED decreased from 2021 values but remained positive. For pink, chum, and sockeye, this represents at least two years of improved condition following some of the lowest values recorded in 2019.

Factors influencing observed trends: During early marine entry and residency, juvenile salmon must grow quickly to avoid predation while also acquiring enough lipid reserves to survive winter when food is severely limited (Beamish and Mahnken, 2001; Moss et al., 2005). The SEBS ED anomaly trends were not in-step with NBS salmon, with SEBS ED anomalies responding more variably to sea surface temperature (SST) conditions. This is also reflected in the SEBS large copepod percent lipid (see Figures 53 and 56), where there is no discernible relationship between warm-cool years and having respective low-high lipids.

For the NBS, the anomalously high ED values from all salmon species in 2021 and 2022, and relatively lower values from 2018 and 2019, indicate a shared functional response to variable SST values in the Bering Sea. This trend is also seen in lipid composition of large copepods (*Calanus* spp.) from the same years in the NBS, with highest total lipids observed in 2021 and 2022 (see Siddon, 2022), and lowest values in the warm year of 2018. As a mechanism for salmon condition, direct effects of SST on metabolic demands reduce energy available for reserves, while indirect effects of reduced availability of lipid-rich prey further constrains the capacity to build reserves for overwinter survival.
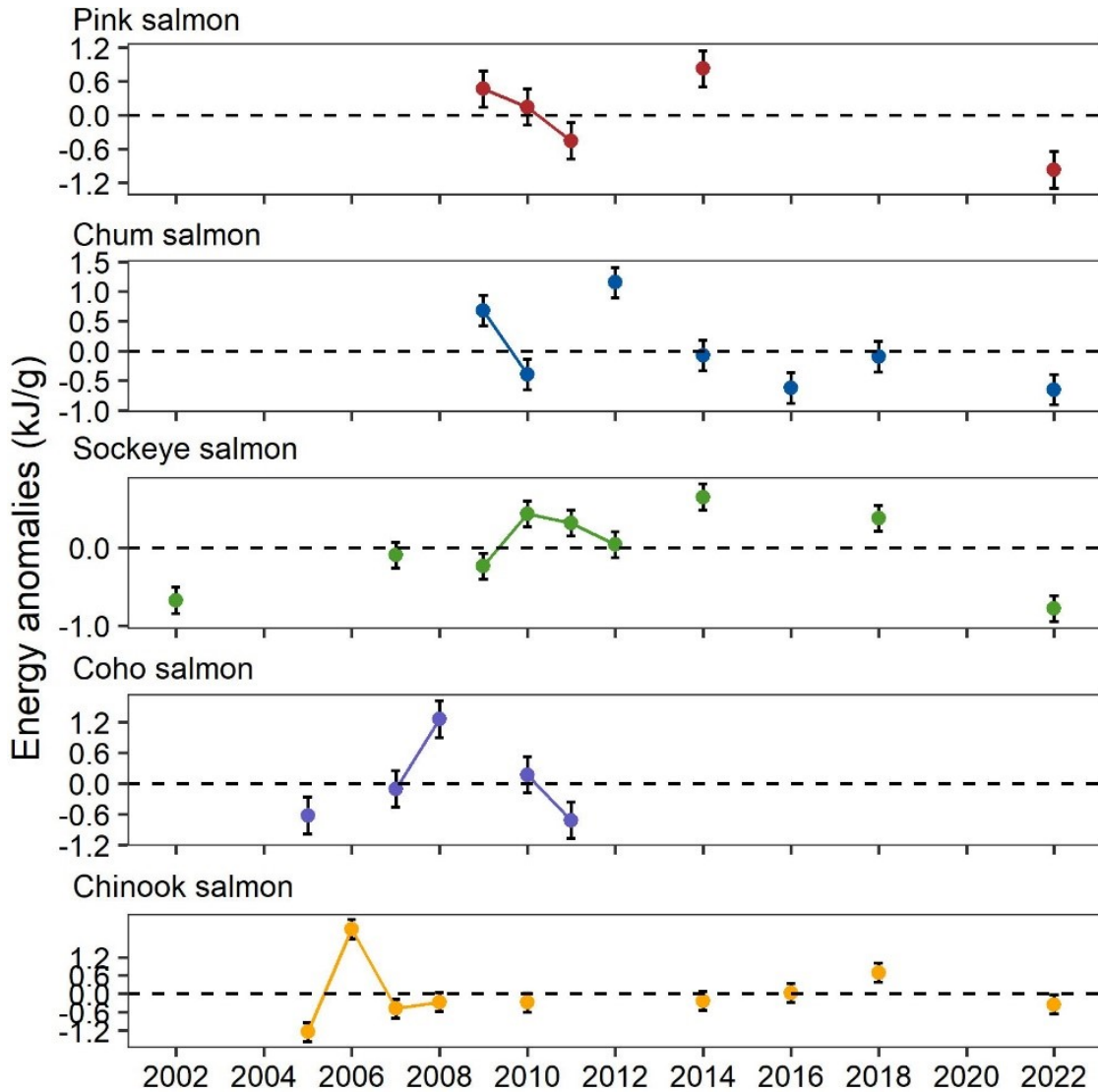
Figure 70: Energy density anomalies (kJ/g, dry weight; ±1 SE) of juvenile salmon captured in the southeastern Bering Sea, 2002–2022. Time series average is indicated by the dashed line.

Implications: Energy density trends over time can represent the condition of juvenile salmon and other taxa in response to climate and ocean conditions during their early marine residency. Juvenile pink, chum, sockeye, coho, and Chinook salmon in the SEBS in 2022 showed ED anomaly values that were more consistent with lower energy stores and a reduced capacity for overwinter survival. Conversely, salmon entered the NBS in 2022 with positive energy stores, which may contribute to higher overwinter survival (when food is limited) and higher adult returns.
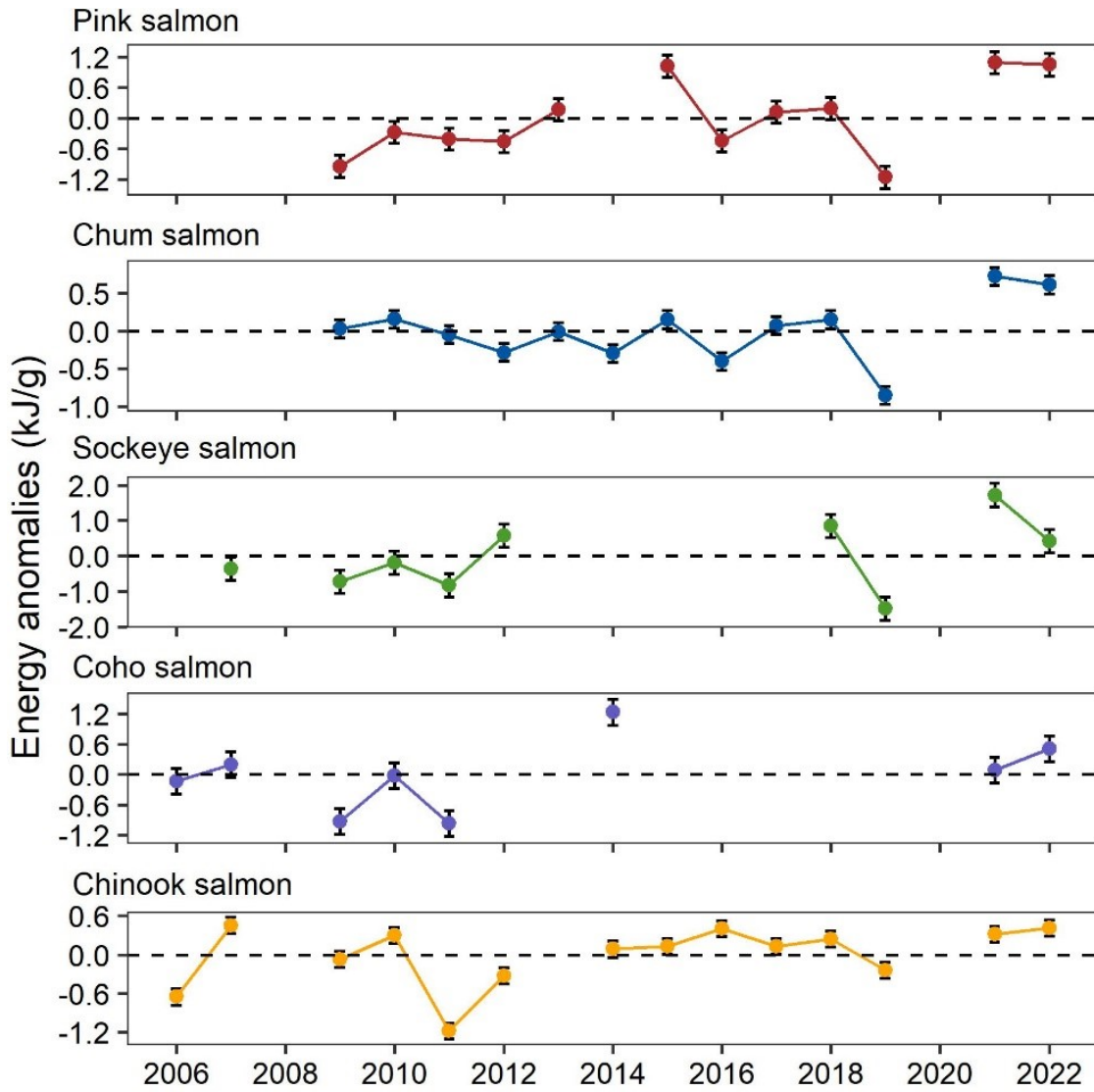
Figure 71: Energy density anomalies (kJ/g, dry weight; ±1 SE) of juvenile salmon captured in the northern Bering Sea, 2006–2022. Time series average is indicated by the dashed line.

Temporal Trend in the Annual Inshore Run Size of Bristol Bay Sockeye Salmon (Oncorhynchus nerka)

Contributed by Curry J. Cunningham[1] and Stacy Vega[2]

[1]College of Fisheries and Ocean Sciences, University of Alaska Fairbanks, Juneau, Alaska

[2]Alaska Department of Fish & Game, Anchorage, Alaska

Contact: cjcunningham@alaska.edu

Last updated: September 2023

Description of indicator: The annual abundance of adult sockeye salmon (*Oncorhynchus nerka*) returning to Bristol Bay, Alaska is enumerated by the Alaska Department of Fish and Game (ADF&G). The total inshore run in a given year is the sum of catches in five terminal fishing districts plus the escapement of sockeye to nine major river systems. Total catch is estimated based on the mass of fishery offloads and the average weight of individual sockeye within time and area strata. Escapement is the number of fish successfully avoiding fishery capture and enumerated during upriver migration toward the spawning grounds, or through post-season aerial surveys of the spawning grounds (Elison et al., 2018). Although there have been slight changes in the location and operation of escapement enumeration projects and methods over time, these data provide a consistent index of the inshore return abundance of sockeye salmon to Bristol Bay since 1963.
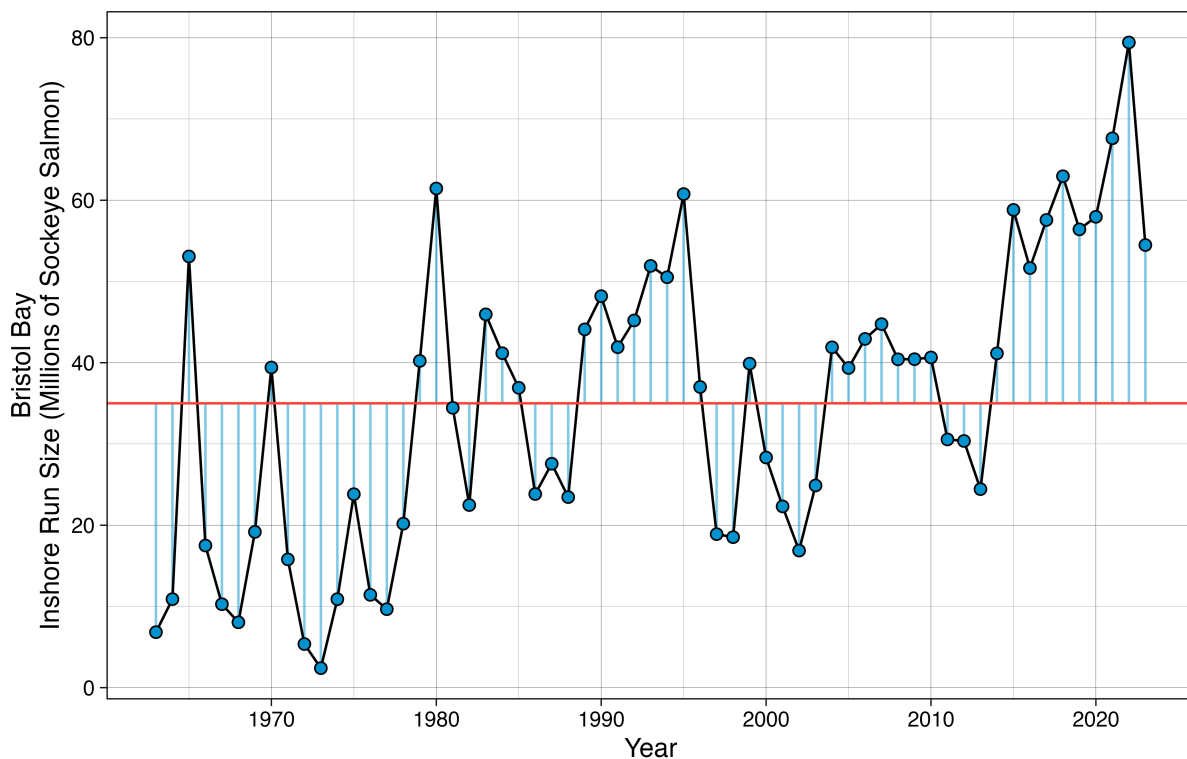
Figure 72: Annual Bristol Bay sockeye salmon inshore run size 1963–2023. Red line is the time series average of 35.0 million sockeye.

Status and trends: The 2023 Bristol Bay preliminary inshore run estimate of 54.5 million sockeye salmon is 2.5% lower than the recent 10-year average of 55.8 million sockeye, and 55.6% higher than the 1963–2022 average of 35.0 million sockeye salmon. The 2023 inshore run represents a decrease from the record high Bristol Bay run sizes observed in 2021–2022 (Figure 72). The temporal trend in Bristol Bay sockeye salmon indicates a large increase beginning in 2015 and continuing for the recent 9 years, with inshore run sizes in 2015-2023 all exceeding 50 million salmon and above long-term average. The current period of high Bristol Bay sockeye salmon production now exceeds the previous high production stanza that occurred 1989–1995.

Note: *At the time of printing, the 2023 Bristol Bay inshore run size numbers are preliminary and subject to change.*

Factors influencing observed trends: The return abundance of Bristol Bay sockeye salmon is positively correlated with the Pacific Decadal Oscillation (Hare et al., 1999), specifically with Egegik and Ugashik district run sizes increasing after the 1976/1977 regime shift (Figure 73). However, recent research has highlighted that relationships between salmon population dynamics and the PDO may not be as consistent as once thought, and may in fact vary over time (Litzow et al., 2020*a,b*). The abundance and growth of Bristol Bay sockeye salmon has also been linked to the abundance of pink salmon (*Oncorhynchus gorbuscha*) in the North Pacific (Ruggerone and Nielsen, 2004; Ruggerone et al., 2016).

Implications: The high inshore run of Bristol Bay sockeye salmon in 2023 and the preceding 8-year period indicate positive survival conditions for these stocks while in the ocean. Given evidence that the critical period for sockeye salmon survival occurs during the first summer and winter at sea (Beamish and Mahnken, 2001; Farley et al., 2007, 2011) and the predominant age classes observed for Bristol Bay stocks are 1.2, 1.3, 2.2, and 2.3 (European designation: years in freshwater – years in the ocean), the larger than average 2023 Bristol Bay sockeye salmon inshore run suggests these stocks experienced positive conditions at entry into the eastern Bering Sea in the summers of 2020 and 2021, and winters of 2020–2021 and 2021–2022. However, the predominance (>82%) of 3-ocean sockeye salmon in the 2023 Bristol Bay run, combined with the decline in overall run size from 2022 to 2023 may suggest that survival for the brood year 2019 cohort may be lower than was observed for the 2018 cohort, and/or conditions at ocean entry were more favorable in the winter of 2020–2021 compared with the winter of 2021-2022.
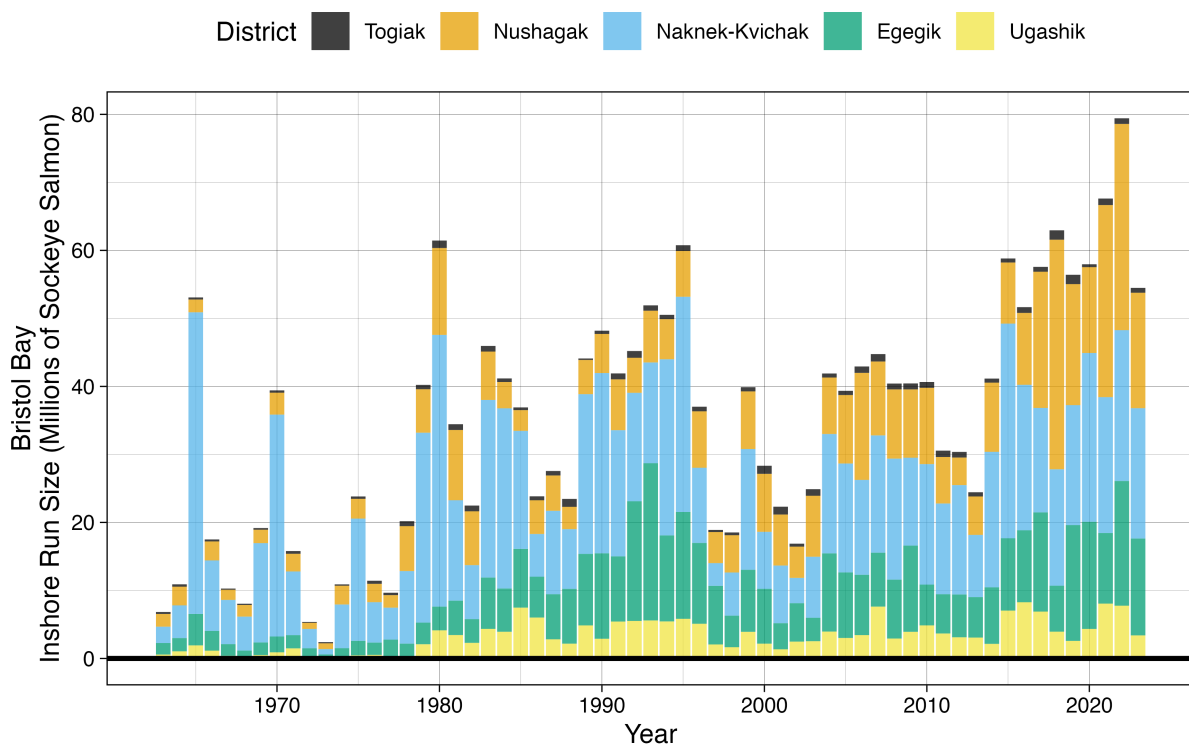
Figure 73: Annual Bristol Bay sockeye salmon inshore run size 1963–2023 by commercial fishing district.

Factors Affecting 2023 Yukon & Kuskokwim Chum Salmon Runs and Subsistence Harvests

Contributed by Kevin Whitworth[1], Terese Vicente[1], Andrew Magel[1], Kathrine Howard[2], Vanessa von Biela[3], Megan Williams[4], and Patricia Chambers[4]
[1]Kuskokwim River Inter-Tribal Fish Commission
[2]Alaska Department of Fish & Game
[3]U.S. Geological Survey, Alaska Science Center
[4]Ocean Conservancy
Contact: kevinwhitworth@kritfc.org
Last updated: October 2023

Yukon and Kuskokwim chum salmon (*Oncorhynchus keta*) runs are in a fourth year of low returns (2020–2023; KRITFC, 2022; Donnellan, 2023). Salmon are integral to the Western Alaska ecosystem, bridging marine and freshwater habitats, filling both prey and predator niches, and supporting vital subsistence harvests and Indigenous ways of life (Courtney et al., 2019; KRITFC, 2022). Figure 74 highlights likely factors that may have contributed to the low 2023 run sizes of chum salmon across the Yukon and Kuskokwim regions as evidenced by Western science, Indigenous Knowledge, and community observations. This figure tracks the life cycle of chum salmon returning to spawn as adults in 2023, beginning with their parents in 2018 or 2019, depending on age class.

Cumulative ecosystem factors since 2018 or 2019 have potentially impacted parent spawning adults, marine-stage juveniles and immature fish, and ultimately returning adults in 2023. Parent spawners returning in 2019 were exposed to warm ocean temperatures associated with a marine heatwave (MHW) in the Gulf of Alaska (Ferriss and Zador, 2022) and Bering Sea (Siddon, 2022) and likely experienced associated increased metabolic rates (Barbeaux et al., 2020; Piatt et al., 2020; Murphy et al., 2021; Suryan et al., 2021). Yukon and Kuskokwim chum salmon return as either summer or fall run populations, and premature mortality of Yukon and Kuskokwim chum salmon was observed during unusually warm river water temperatures in summer 2019 (von Biela et al., 2022), with the potential to influence 2023 and 2024 summer chum salmon returns. Fall-run chum salmon populations return later when river temperatures are typically cooler.

Marine phase juvenile chum salmon experienced MHW conditions during their first summer in the Bering Sea in 2019, and again during their first winter at sea in the Gulf of Alaska in 2019–2020. During these MHW conditions, low zooplankton productivity (Siddon, 2022) contributed to decreased fish condition and empty stomachs; the 2019 stomach fullness index was the lowest on record for juvenile chum salmon in the northern Bering Sea (Murphy et al., 2021). Temperatures returned to more normal conditions in the Bering Sea (Siddon, 2022) and Gulf of Alaska (Ferriss and Zador, 2022) in 2020 and 2021. However, it is reasonable to anticipate that juvenile chum salmon in 2020 could have carryover effects from the poor environmental conditions experienced by parents in 2019 during egg yolk provisioning and development for a number of key reasons: chum have little to no freshwater rearing, chum out-migrate to sea shortly after hatching, and chum rely on residual yolk sac lipids as the only potential source of stored energy (Burril et al., 2018).

During the immature and maturing adult life stages, a total of 107,235 Western Alaska chum salmon (Coastal Western Alaska, Upper- and Mid-Yukon River stocks) were caught as bycatch in federal fisheries

in the Bering Sea during the summer and fall of 2021 and 2022 combined[15]. Additionally, South Alaska Peninsula fisheries in 2022 caught an estimated 105,320 Western Alaska and Upper Yukon chum salmon (Dann and Foster, 2023).

The chum salmon that returned in 2023 likely benefited from marine temperatures that largely relaxed to normal conditions during 2020–2023 (see p. 28) because cooling tends to have a positive effect on adult body condition. However, chum salmon returns in 2023 remained well below the long-term average, which led to yet another year of restricted subsistence fisheries with minimal harvest opportunities for chum salmon in Yukon and Kuskokwim communities. Poor run size and restricted harvest means that escapement goals, food security needs, and rebuilding goals for chum salmon populations are unlikely to be met on these rivers in 2023, and the practice of culture and tradition and health of in-river ecosystems remain on the line.

---

[15]https://meetings.npfmc.org/CommentReview/DownloadFile?p=5b15695d-d544-4385-87cb-b5cdfee54909.
pdf&fileName=C4%20Chum%20Salmon%20Bycatch%20Analysis.pdf

FACTORS AFFECTING 2023 YUKON & KUSKOKWIM CHUM SALMON RUNS AND SUBSISTENCE HARVESTS

SALMON LIFECYCLE

(A)

PARENT SPAWNERS & EGGS
2018-2019

2019 poor forage conditions during MHW, 2019 returning parents also experienced premature mortality associated with low water levels and warm river temperatures.

(B)

MARINE JUVENILES
Summer EBS and winter GOA
2019-2021

2019 empty stomachs and poor juvenile salmon condition in EBS associated with MHW; GOA winter MHW 2019; 2020-2021 temperatures return to more average conditions in the GOA and EBS.

(C)

IMMATURES AND MATURING ADULTS
EBS/GOA | 2021-2022

Total bycatch of 107,235 Western Alaska and Yukon chum in the EBS 2021 and 2022; Harvest of 105,320 Coastal Western Alaska and Upper Yukon chum salmon in the South Peninsula Area M fishery in 2022; Competition for food likely occurring.

(D)

MATURING ADULTS AND ADULTS
EBS | 2023

River temperatures variable for 2023 returning adults; WAK chum returns remain well below long-term average and most escapement goals still not being met; food security, culture, and ecosystem health impacted.

OBSERVED IMPACTS TO SUBSISTENCE HARVESTS*

"There's the climate change part, there's bycatch and things like that. And then not only the ocean life, but also what's happening in our spawning rivers. The health of those because of climate change; too much snow, not enough snow; too cold, too warm. How different everything is changing. I think there's a lot of things that come into play."

"2019 was a very bad year. We were finding a lot of dead fish because the water was getting very warm, and there was a lot of bacteria in the water. That's really unusual."

"There were more chums in the river [in 2023] and people were catching more; but when compared to the past 40 years and even just 10 years ago, there were far less chums in the river running and being caught by the poeple now. We should not pretend that this season's slight increase means the chum run has significantly improved."

"When the chum returns were good, it was just stink, and fish were everywhere. I don't think people realize the importance they have to the ecosystem. The river's health, the plants. I think of all the bears, and if they have no fish, they're eating berries; but that's not going to hold them off, so they have to eat more baby moose; and then we get back to where we are still: trying to conserve moose up here."

"This used to be a chum river. In the old days, [their] uses were multifold. We ate them and our dogs ate them. And I still think of what the old people say: You use them, they will come back in numbers."

*Observations are kept anonymous

INDICES OF CHUM SALMON RUN SIZE OVER TIME
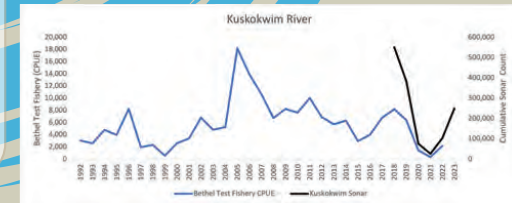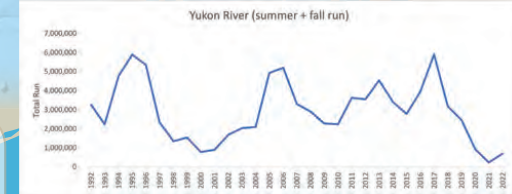
Figure 74: Factors Affecting 2023 Yukon & Kuskokwim Chum Salmon Runs and Subsistence Harvests.

Trends in Alaska Commercial Salmon Catch – Bering Sea

Contributed by George A. Whitehouse
Cooperative Institute for Climate, Ocean, and Ecosystem Studies (CICOES), University of Washington, Seattle WA
Contact: andy.whitehouse@noaa.gov
Last updated: October 2023

Description of indicator: This contribution provides historic and current commercial catch information for salmon of the Bering Sea. This contribution summarizes data and information available in current Alaska Department of Fish & Game (ADF&G) agency reports (e.g., Donnellan, 2023) and on their website[16].

Pacific salmon in Alaska are managed in four regions based on freshwater drainage basins[17]: Southeast/Yakutat, Central (encompassing Prince William Sound, Cook Inlet, and Bristol Bay), Arctic-Yukon-Kuskokwim, and Westward (Kodiak, Chignik, and Alaska peninsula). ADF&G prepares harvest projections for all areas rather than conducting run size forecasts for each salmon run. There are five Pacific salmon species with directed commercial fisheries in Alaska; they are sockeye (*Oncorhynchus nerka*), pink (*O. gorbuscha*), chum (*O. keta*), Chinook (*O. tshawytscha*), and coho (*O. kisutch*) salmon.

Status and trends:

Statewide
Combined catches from directed fisheries on the five salmon species have fluctuated over recent decades but in total have been generally strong statewide (Figure 75). The salmon commercial harvests from 2022 totaled 163.2 million fish, which was 2.6 million more than the preseason forecast of 160.6 million fish. The 2022 total commercial harvest was elevated by the harvest of 75.5 million sockeye salmon, primarily from Bristol Bay. Preliminary data from ADF&G for 2023 indicates a statewide total commercial salmon harvest of about 227 million fish (as of 27 September 2023), which is well above the preseason projection of 189.4 million fish. The 2023 harvest has been bolstered by the catch of 134.5 million pink salmon, primarily from Prince William Sound and Southeast Alaska.

Bering Sea
Salmon harvests in the Bering Sea are numerically dominated by the catch of sockeye in Bristol Bay (Figure 76). The 2022 Bristol Bay sockeye salmon run of 79.2 million and the harvest of 60.5 million were both the highest recorded. Escapement goals for sockeye salmon in 2022 were met or exceeded in every drainage in Bristol Bay where escapement was defined. For more information on 2022 Bristol Bay sockeye salmon, see Cunningham et al., p. 125. Preliminary data for 2023 from ADF&G indicates that the commercial harvest of Bristol Bay sockeye salmon is strong again, at more than 43 million fish. The 2022 commercial harvest of other species in the Bering Sea were 8,700 Chinook salmon, 780,000 chum salmon, 115,000 pink salmon, and 18,000 coho salmon.

Chinook salmon abundance in the Arctic-Yukon-Kuskokwim region has been low since the mid-2000s and remains low. From 2008 to 2022 no commercial periods targeting Chinook salmon were allowed in the Yukon Management Area. In 2022, Chinook salmon did meet the drainage-wide sustainable escapement goal for the Kuskokwim River. Preliminary data for 2023 indicate that Chinook salmon escapement goals will not likely be met for the Yukon Area.

---

[16]https://www.adfg.alaska.gov/
[17]https://www.adfg.alaska.gov/index.cfm?adfg=commercialbyfisherysalmon.salmonareas

Summer chum salmon did not meet escapement goals in the Yukon Area in 2022 and there was no commercial harvest. Additionally, there were no commercial harvests for salmon during fall 2022 in the Yukon Management Area due to the low run size for fall chum and coho salmon. Preliminary data for the Yukon River in 2023 indicates that fall chum are again unlikely to meet escapement goals. For more information on factors affecting the 2023 Yukon and Kuskokwim chum salmon runs and subsistence harvest, see Whitworth et al., p. 128.
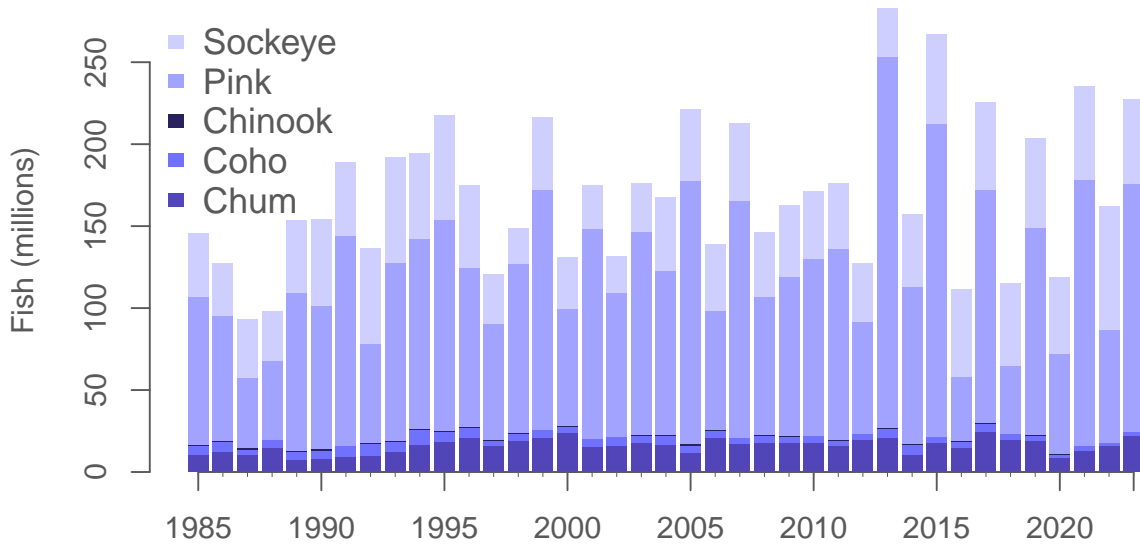
Figure 75: Alaska statewide contemporary commercial salmon catches, 2023 values are preliminary. Source: ADF&G, http://www.adfg.alaska.gov. ADF&G not responsible for the reproduction of data, subsequent analysis, or interpretation.
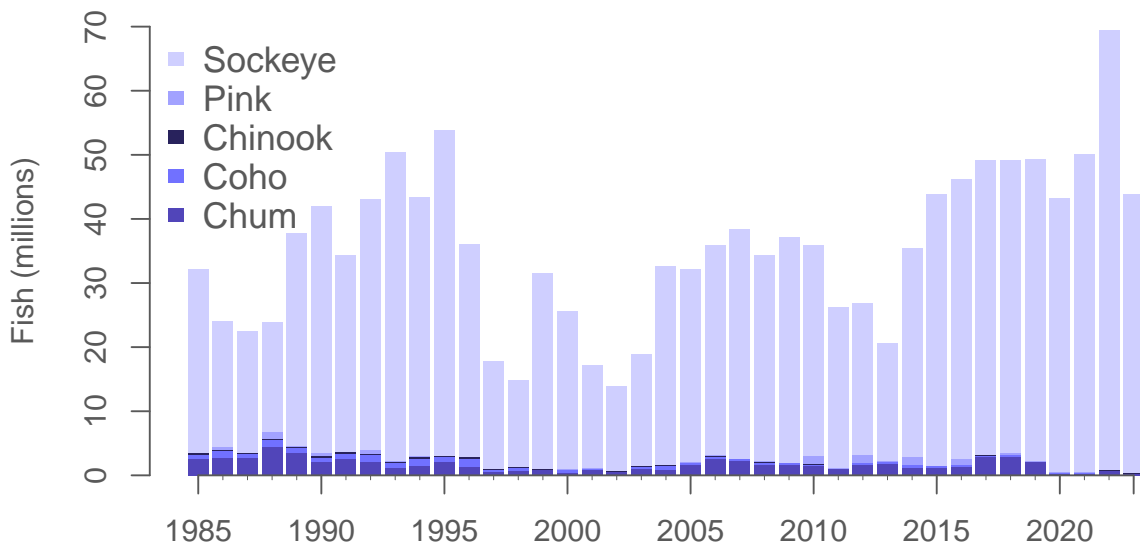
Figure 76: Contemporary commercial salmon catches in the eastern Bering Sea, 2023 values are preliminary. Source: ADF&G, http://www.adfg.alaska.gov. ADF&G not responsible for the reproduction of data, subsequent analysis, or interpretation.

Factors influencing observed trends: Salmon have complex life histories and are subject to stressors in the freshwater and marine environments, and anthropogenic pressures. These forces do not affect all species and stocks equally or in the same direction, and resolving what is driving the population dynamics of a particular stock is challenging (Rogers and Schindler, 2011). Interannual variation in Alaska statewide total salmon abundance is partly due to the even-year, odd-year cycle in pink salmon, particularly production from the Prince William Sound stock of pink salmon, which typically have larger runs in odd years. Chinook salmon runs have been declining statewide since 2007. Size-dependent mortality during the first year in the marine environment is thought to be a leading contributor to low Chinook salmon run sizes (Beamish and Mahnken, 2001; Graham et al., 2019). Rising sea temperatures and loss of sea ice may lead to slower growth for juvenile Chinook salmon in the eastern Bering Sea (Yasumiishi et al., 2020). Additionally, warming water temperatures and low stream discharges during adult spawner migrations may reduce Chinook salmon reproductive success (Howard and von Biela, 2023).

Salmon may also be caught as bycatch in Bering Sea groundfish trawl fisheries, most of which are Chinook and chum salmon. The North Pacific Fishery Management Council has implemented a number of management measures and incentives that have largely been successful at reducing Chinook salmon bycatch in groundfish trawl fisheries since their peak in 2007 (Stram and Ianelli, 2015). However, the bycatch of non-Chinook salmon (i.e., chum) has trended upward since 2012 and in 2021 was at its highest level since 2005[18].

In the Bering Sea, sockeye salmon are the most abundant salmonid and since the early 2000s, they have had consistently strong runs, which have supported large harvests. Bristol Bay sockeye salmon display a variety of life history types and utilize a diverse range of habitats for spawning (Hilborn et al., 2003). Productivity within these various habitats may be affected differently depending upon varying conditions, such as climate (Mantua et al., 1997), so more diverse sets of populations provide greater overall stability (Schindler et al., 2010). The abundance of Bristol Bay sockeye salmon may also vary over centennial time scales, with brief periods of high abundance separated by extended periods of low abundance (Schindler et al., 2006).

Implications: Salmon have important influences on Alaska marine ecosystems through interactions with marine food webs as predators on lower trophic levels and as prey for other species such as Steller sea lions. In years of great abundance, salmon may exploit prey resources more efficiently than their competitors. In odd years when pink salmon are most abundant they can initiate pelagic trophic cascades (Batten et al., 2018) which may negatively impact the population dynamics of several other species, including other salmonids, forage fishes, seabirds, and whales (Ruggerone et al., 2023). A biennial pattern in seabird reproductive success has been attributed to a negative relationship with years of high pink salmon abundance (Springer and van Vliet, 2014). Directed salmon fisheries are economically important for the state of Alaska. The trend in total statewide salmon catch in recent decades has been for generally strong harvests, despite annual fluctuations and lower catches for some species in specific management areas.

Measures to reduce salmon bycatch can affect the spatial distribution of groundfish trawl fisheries through area closures and incentives to avoid bycatch. When the aggregate Chinook salmon run size in the Kuskokwim, Unalakleet, and Upper Yukon Rivers is less than 250,000, a lower limit to Chinook salmon bycatch is imposed on the pollock fishery.

---

[18]https://www.npfmc.org/wp-content/PDFdocuments/bycatch/BeringSeaSalmonBycatchFlyer.pdf

Groundfish

Eastern and Northern Bering Sea Groundfish Condition

Contributed by Bianca Prohaska and Sean Rohan
Resource Assessment and Conservation Engineering Division
Alaska Fisheries Science Center, NOAA Fisheries
Contact: sean.rohan@noaa.gov
Last updated: October 2023

Description of indicator: Length-weight residuals represent how heavy a fish is per unit body length and are an indicator of somatic growth variability (Brodeur et al., 2004). Therefore, length-weight residuals can be considered indicators of prey availability, growth, general health, and habitat condition (Blackwell et al., 2000; Froese, 2006). Positive length-weight residuals indicate better condition (i.e., heavier per unit length) and negative residuals indicate poorer condition (i.e., lighter per unit length) (Froese, 2006). Fish condition calculated in this way reflects realized outcomes of intrinsic and extrinsic processes that affect fish growth which can have implications for biological productivity through direct effects on growth and indirect effects on demographic processes such as reproduction and mortality (e.g., Rodgveller, 2019; Barbeaux et al., 2020).

The groundfish morphometric condition indicator is calculated from paired fork lengths (mm) and weights (g) of individual fishes that were collected during bottom trawl surveys of the eastern Bering Sea (EBS) shelf and northern Bering Sea (NBS), which were conducted by the Alaska Fisheries Science Center's Resource Assessment and Conservation Engineering (AFSC/RACE) Groundfish Assessment Program (GAP). Fish condition analyses were applied to walleye pollock (*Gadus chalcogrammus*), Pacific cod (*G. macrocephalus*), arrowtooth flounder (*Atheresthes stomias*), yellowfin sole (*Limanda aspera*), flathead sole (*Hippoglossoides elassodon*), northern rock sole (*Lepidopsetta polyxystra*), and Alaska plaice (*Pleuronectes quadrituberculatus*) collected in bottom trawls at standard survey stations (Figure 77). For these analyses and results, survey strata 31 and 32 were combined as stratum 30; strata 41, 42, and 43 were combined as stratum 40; and strata 61 and 62 were combined as stratum 60. Northwest survey strata 82 and 90 were excluded from these analyses.

To calculate indicators, length-weight relationships were estimated from linear regression models based on a log-transformation of the exponential growth relationship, $W = aL^b$, where W is weight (g) and L is fork length (mm) for all areas for the period 1997–2023 (EBS: 1997–2023, NBS: 2010, 2017, 2019, 2021–2023). Unique intercepts (a) and slopes (b) were estimated for each survey stratum, sex, and interaction between stratum and sex to account for sexual dimorphism and spatial-temporal variation in growth and bottom trawl survey sampling. Length-weight relationships for 100–250 mm fork length walleye pollock (corresponding with ages 1–2 years) were calculated separately from adult walleye pollock (>250 mm). Residuals for individual fish were obtained by subtracting observed weights from bias-corrected weights-at-length that were estimated from regression models. Length-weight residuals from each stratum were aggregated and weighted proportionally to total biomass in each stratum from area-swept expansion of mean bottom-trawl survey catch per unit effort (CPUE; i.e., design-based stratum biomass estimates). Variation in fish condition was evaluated by comparing average length-weight residuals among years. To minimize the influence of unrepresentative samples on indicator calculations, combinations of species, stratum, and year with a sample size <10 were used to fit length-weight regressions, but were excluded

from calculating length-weight residuals for both the EBS and NBS. Morphometric condition indicator time series, code for calculating the indicators, and figures showing results for individual species are available through the *akfishcondition* R package and GitHub repository[19].
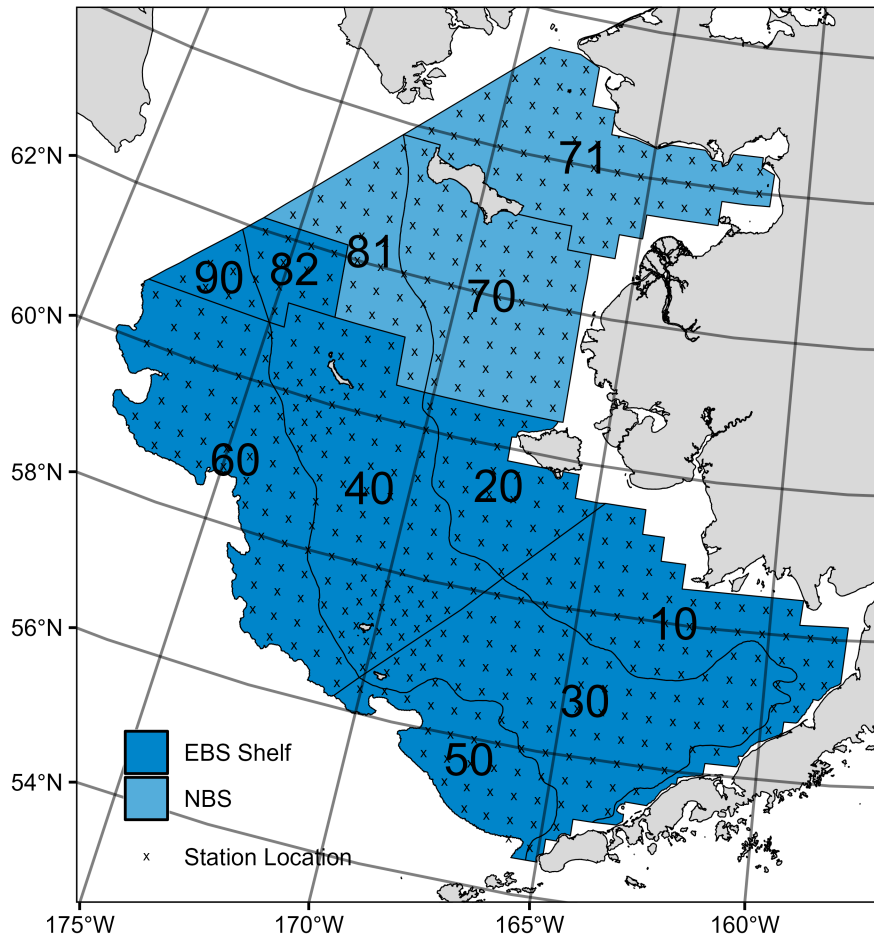
Figure 77: NOAA Alaska Fisheries Science Center summer bottom trawl survey strata (10–90) and station locations (x) on the eastern Bering Sea (EBS) shelf and in the northern Bering Sea (NBS).

Methodological Changes:

In Groundfish Morphometric Condition Indicator contributions to the 2022 Eastern Bering Sea and Aleutians Islands Ecosystem Status Reports, historical stratum-biomass weighted residuals condition indicators were presented alongside condition indicators that were calculated using the R package VAST following methods that were presented for select GOA species during the Spring Preview of Ecological and Economic Conditions (PEEC) in May 2020. The authors noted there were strong correlations between VAST and stratum-biomass weighted condition indicators for most EBS and NBS species (r=0.79–0.98). The authors received the following feedback about the change from the BSAI Groundfish Plan Team meeting during their November 2022 meeting:

"The Team discussed the revised condition indices that now use a different, VAST-based condition index, but felt additional methodology regarding this transition was needed. The Team recommended a short presentation next September to the Team to review the methods and tradeoffs in approaches.

---

[19]https://github.com/afsc-gap-products/akfishcondition

The Team encouraged collaboration with the NMFS longline survey team to develop analogous VAST indices."

Based on feedback from the Plan Team, staff limitations, and the lack of a clear path to transition condition indicators for longline survey species to VAST, analyses supporting the transition to VAST were not conducted during 2023. Therefore, the 2023 condition indicator was calculated from statum-biomass weighted residuals of length-weight regressions.

Stratum-biomass weighted residuals for NBS strata are presented for the first time in 2023. NBS length-weight samples were previously pooled across strata to calculate region-wide length-weight residuals because of the lack of samples from regular survey sampling prior to 2017. The authors have opted to present stratum-biomass weighted residuals for the NBS in 2023 because of the accumulation of regular length-weight samples in recent years.

Status and trends: Fish condition, indicated by length-weight residuals, has varied over time for all species examined in the EBS (Figures 78 and 79). In 2023 a downward trend in condition from 2022 was observed for all species in the EBS, with large walleye pollock (>250 mm) and arrowtooth flounder decreasing since 2019; however, all species were still within one standard deviation of the mean except for large walleye pollock (>250 mm) which was negative but within two standard deviations of the mean (Figure 78). Large walleye pollock (>250 mm) exhibited the second worst condition observed over the full time series with the lowest observed condition occurring in 1999 (Figure 78). In 2019, an upward trend in condition was observed for most species relative to 2017–2018 with positive weighted length-weight residuals relative to historical averages for large walleye pollock (>250 mm), northern rock sole, yellowfin sole, arrowtooth flounder, and Alaska plaice; however, in 2021 condition had a downward trend in most species examined. In 2022 in the EBS, conditions were near the historical mean, or positive for all species examined except for arrowtooth flounder and large walleye pollock (>250 mm). While their conditions were below average, the mean for both groups fell within one standard deviation of the historical mean (Figure 78).

In the EBS in 2023, condition was negative for large walleye pollock (>250 mm), arrowtooth flounder, and flathead sole across most strata (Figure 79). In 2023, there was a divergence in small walleye pollock (100-250 mm) condition among strata with more positive condition observed on the inner shelf (stratum 10), and more negative condition observed on the middle shelf (stratum 30).

In the NBS in 2023, positive condition was observed for large walleye pollock (>250 mm), which has been increasing since 2021. The remaining species exhibited near-average condition in the NBS in 2023, except for yellowfin sole which exhibited negative condition, and has been declining since 2019 (Figure 80).

In 2023 large walleye pollock (>250 mm) condition was positive in all NBS strata, whereas condition was previously negative in all strata from 2021–2022 (Figure 81). Pacific cod, small walleye pollock (100-250 mm), Alaska plaice, and yellowfin sole condition have been consistently negative across all strata since 2021, with a notable exception in 2023 of positive condition for Pacific cod in the inner southern NBS shelf (stratum 70), and Alaska plaice in the northern inner NBS shelf and Norton Sound (stratum 71; Figure 81).
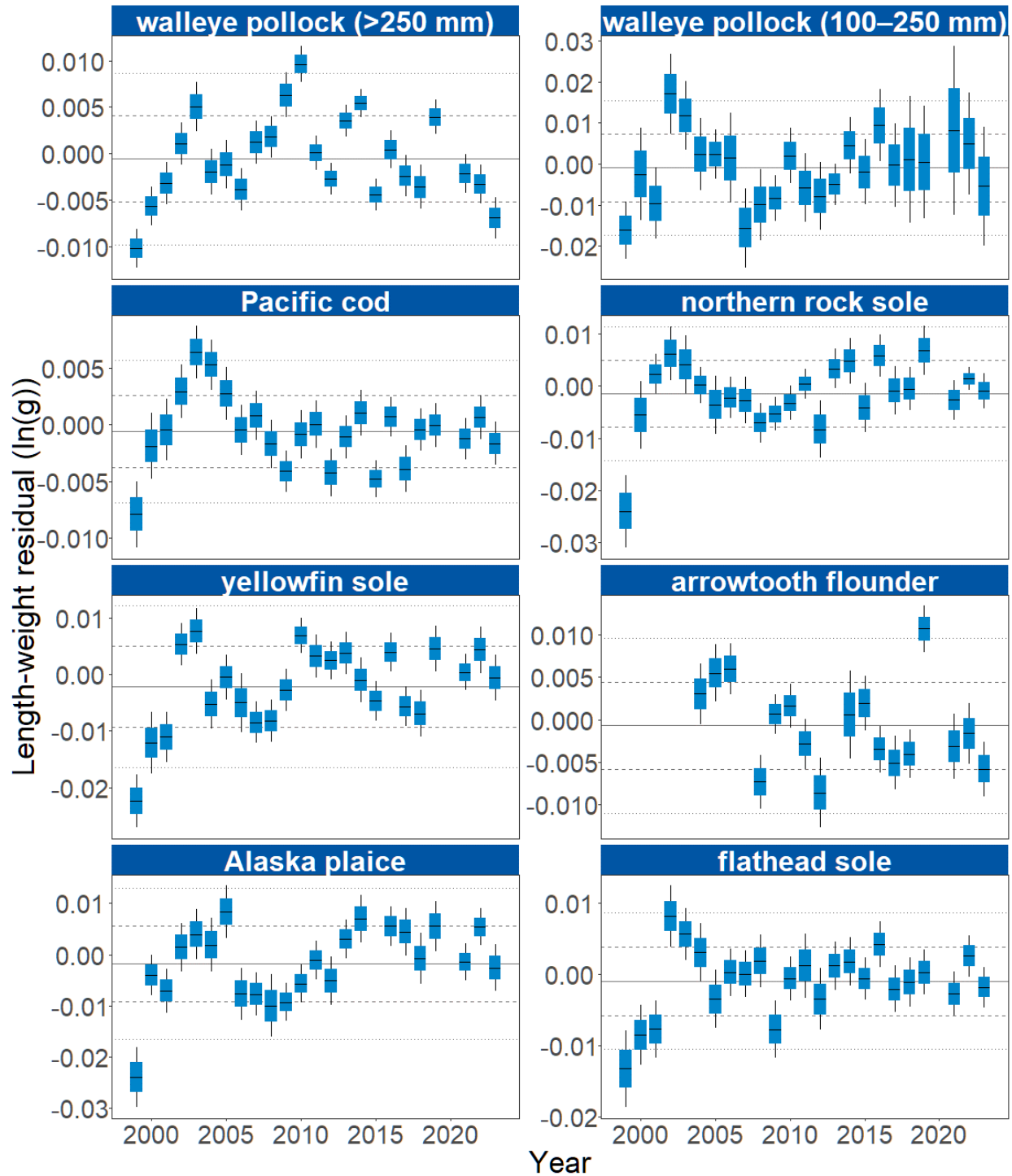
Figure 78: Morphometric condition of groundfish species collected during AFSC/RACE GAP standard summer bottom trawl surveys of the eastern Bering Sea shelf (1999–2023) based on residuals of length-weight regressions. The dash in the blue boxes denote the mean for that year, the box denotes one standard error, and the lines on the boxes denote two standard errors. Lines on each plot represent the historical mean, dashed lines denote one standard deviation, and dotted lines denote two standard deviations.
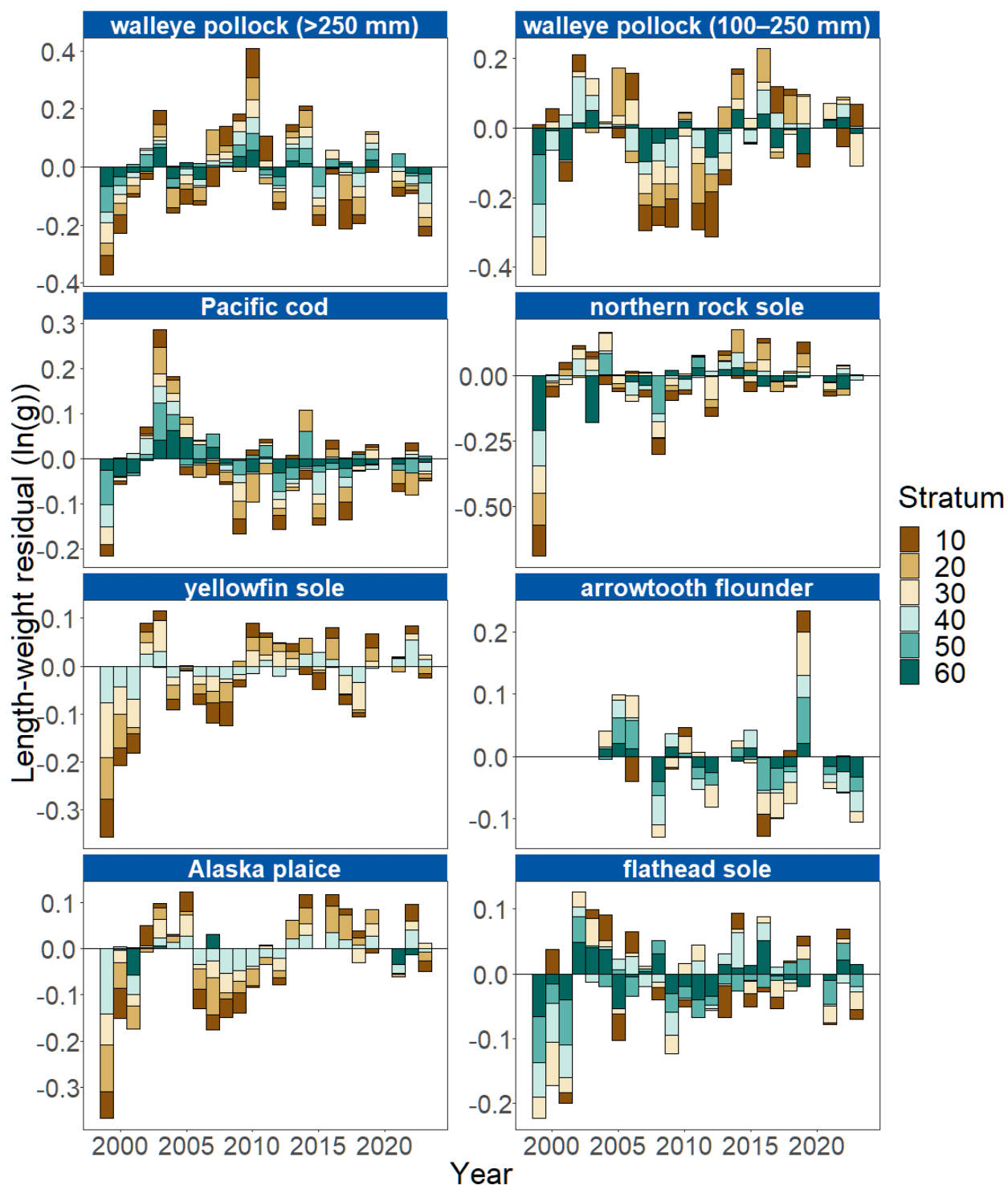
Figure 79: Length-weight residuals by survey stratum (10–60) for seven eastern Bering Sea shelf groundfish species and age 1–2 walleye pollock (100–250 mm) sampled in the AFSC/RACE GAP standard summer bottom trawl survey, 1999–2023. Length-weight residuals are not weighted by stratum biomass.
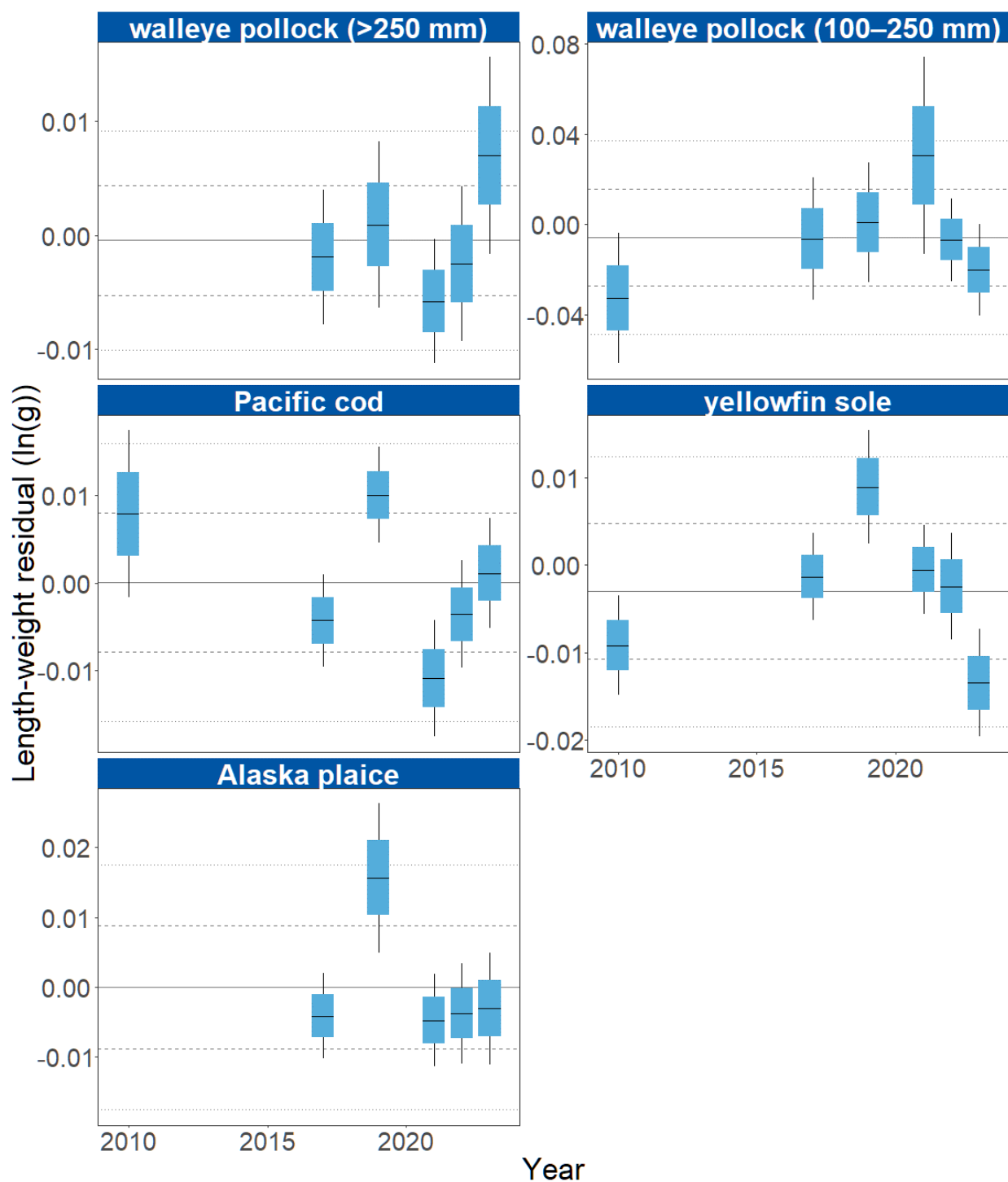
Figure 80: Morphometric condition of groundfish species collected during AFSC/RACE GAP standard summer bottom trawl surveys of the northern Bering Sea shelf (2010, 2017, 2019 and 2021–2023) based on residuals of length-weight regressions. The dash in the blue boxes denote the mean for that year, the box denotes one standard error, and the lines on the boxes denote two standard errors. Lines on each plot represent the historical mean, dashed lines denote one standard deviation, and dotted lines denote two standard deviations.

139
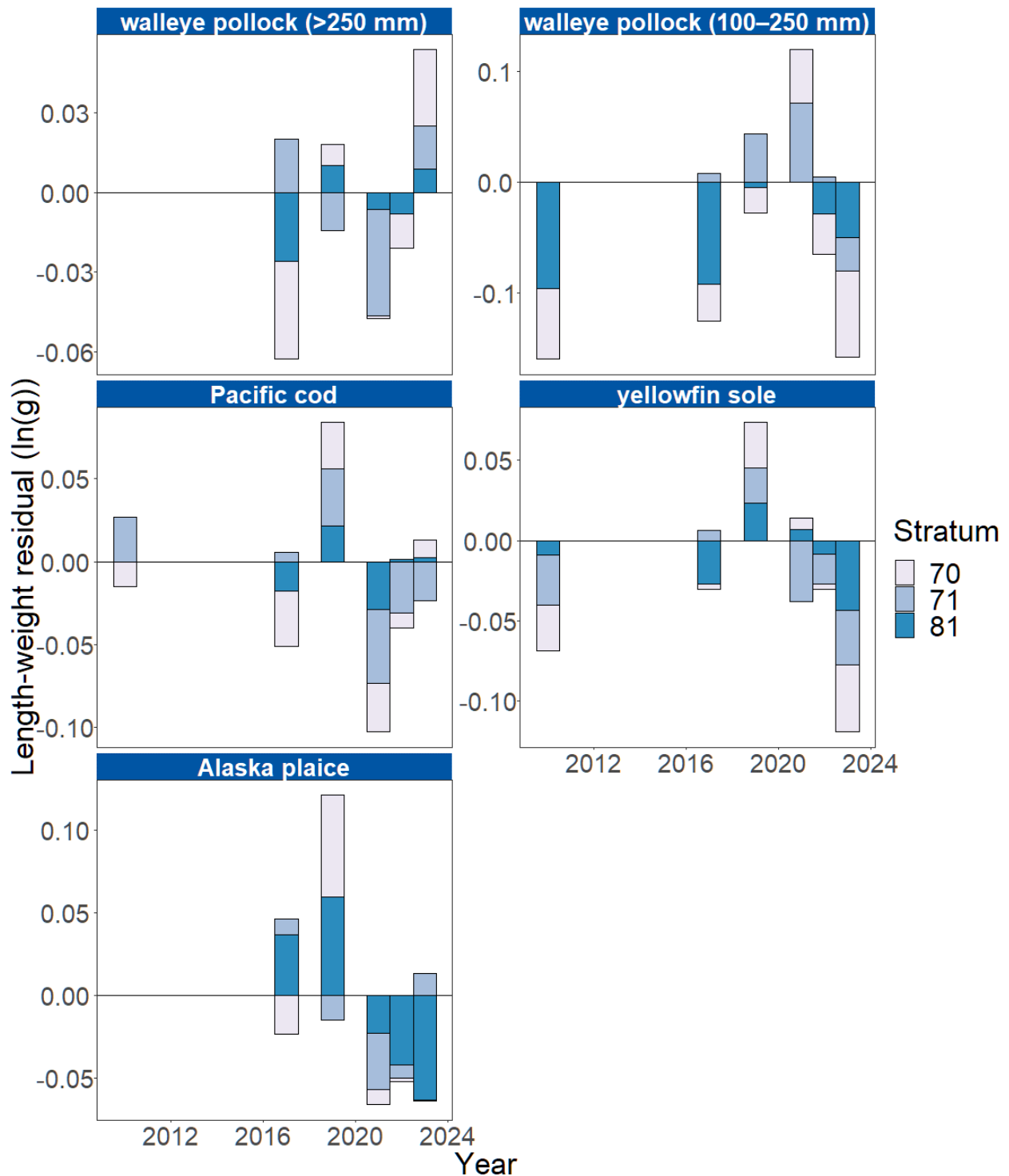
Figure 81: Length-weight residuals by survey stratum (70, 71, and 81) for four northern Bering Sea shelf groundfish species and age 1–2 walleye pollock (100–250 mm) sampled in the AFSC/RACE GAP standard summer bottom trawl survey during 2010, 2017, 2019, and 2021–2023. Length-weight residuals are not weighted by stratum biomass.

Factors influencing observed trends: Temperature appears to influence morphological condition of several species in the EBS and NBS, so near-average cold pool extent and water temperatures in 2023 likely played a role in the near-average condition (within 1 S.D. of the mean) for most species in the EBS and NBS. Historically, particularly cold years tend to correspond with negative condition, while particularly warm years tend to correspond to positive condition. For example, water temperatures were particularly cold during the 1999 Bering Sea survey, a year in which negative condition was observed for all species that data were available. In addition, spatiotemporal factor analyses suggest the morphometric condition of age-7 walleye pollock is strongly correlated with cold pool extent in the EBS (Grüss et al., 2021). In recent years, warm temperatures across the Bering Sea shelf, since the record low seasonal sea ice extent in 2017–2018 and historical cold pool area minimum in 2018 (Stabeno and Bell, 2019), may have influenced the positive trend in the condition of several species from 2016 to 2019. However, despite near-average temperature in 2023 large walleye pollock (>250 mm) condition in the EBS was the second lowest recorded over the time series.

Although warmer temperatures may increase growth rates if there is adequate prey to offset temperature-dependent increases in metabolic demand, growth rates may also decline if prey resources are insufficient to offset temperature-dependent increases in metabolic demand. The influence of temperature on growth rates depends on the physiology of predator species, prey availability, and the adaptive capacity of predators to respond to environmental change through migration, changes in behavior, and acclimatization. For example, elevated temperatures during the 2014–2016 marine heatwave in the Gulf of Alaska led to lower growth rates of Pacific cod and lower condition because available prey resources did not make up for increased metabolic demand (Barbeaux et al., 2020).

Other factors that could affect morphological condition include survey timing, stomach fullness, fish movement patterns, sex, and environmental conditions (Froese, 2006). The starting date of annual length-weight data collections has varied from late May to early June and ended in late July-early August in the EBS, and mid-August in the NBS. Although we account for some of this variation by using spatially-varying coefficients in the length-weight relationship, variation in condition could relate to variation in the timing of sample collection within survey strata. Survey timing can be further compounded by seasonal fluctuations in reproductive condition with the buildup and depletion of energy stores (Wuenschel et al., 2019). Another consideration is that fish weights sampled at sea include gut content weights, so variation in gut fullness may influence weight measurements. Since feeding conditions vary over space and time, prey consumption rates and the proportion of total body weight attributable to gut contents may be an important factor influencing the length-weight residuals.

Finally, although the condition indicators characterize temporal variation in morphometric condition for important fish species in the EBS and NBS, they do not inform the mechanisms or processes behind the observed patterns.

Implications: Fish morphometric condition can be considered an indicator of ecosystem productivity with implications for fish survival, maturity, and reproduction. For example, in Prince William Sound, the pre-winter condition of herring may determine their overwinter survival (Paul and Paul, 1999), differences in feeding conditions have been linked to differences in morphometric condition of pink salmon in Prince William Sound (Boldt and Haldorson, 2004), variation in morphometric condition has been linked to variation in maturity of sablefish (Rodgveller, 2019), and lower morphometric condition of Pacific cod was associated with higher mortality and lower growth rates during the 2014–2016 marine heat wave in the Gulf of Alaska (Barbeaux et al., 2020). Condition can also be an indicator of stock status relative to carrying capacity because morphometric condition is expected to be high when the stock is at low abundance and low when the stock is at high abundance because of the effects of density-dependent

competition (Haberle et al., 2023). Thus, the condition of EBS and NBS groundfishes may provide insight into ecosystem productivity as well as fish survival, demographic status, and population health. However, survivorship is likely affected by many factors not examined here.

Another important consideration is that fish condition was computed for all sizes of fishes combined, except in the case of walleye pollock. Examining condition of early juvenile stage fishes not yet recruited to the fishery, or the condition of adult fishes separately, could provide greater insight into the value of length-weight residuals as an indicator of individual health or survivorship (Froese, 2006), particularly since juvenile and adult walleye pollock exhibited opposite trends in condition in the EBS this year.

The near-average condition for most species in 2023 may be related to the near historical average temperatures observed. However, trends in recent years such as prolonged warmer water temperatures following the marine heat wave of 2014–2016 (Bond et al., 2015) and reduced sea ice and cold pool areal extent in the eastern Bering Sea (Stabeno and Bell, 2019) may affect fish condition in ways that have not yet been determined. Additionally, periods of high fishing mortality that reduce population biomass are likely to increase body condition because of the compensatory alleviation of density-dependent competition (Haberle et al., 2023). As we continue to add years of length-weight data and expand our knowledge of relationships between condition, growth, production, survival, and the ecosystem, these data may increase our understanding of the health of fish populations in the EBS and NBS.

Research priorities:
Research is being planned and implemented across multiple AFSC programs to explore standardization of statistical methods for calculating condition indicators, and to examine relationships among putatively similar indicators of fish condition (i.e., morphometric, bioenergetic, physiological). Research is underway to evaluate connections between morphometric condition indices, temperature, and density-dependent competition.

Patterns in Foraging and Energetics of Walleye Pollock, Pacific Cod, Arrowtooth Flounder, and Pacific Halibut

Contributed by Kirstin K. Holsman[1], Cheryl Barnes[1], Kerim Aydin[1], Ben Laurel[2], Tom Hurst[2], and Ron Heintz[3]
[1]NOAA Fisheries, Alaska Fisheries Science Center, Resource Ecology and Fishery Management Division
[2]NOAA Fisheries, Alaska Fisheries Science Center, Resource Assessment and Conservation Engineering Division
[3]Sitka Sound Science Center
Contact: kirstin.holsman@noaa.gov
Last updated: November 2023

Description of indicator: We report trends in metabolic demand from an adult bioenergetics model for groundfish in the eastern Bering Sea (EBS) (Ciannelli et al., 1998; Holsman et al., 2019; Holsman and Aydin, 2015) and patterns in diet composition from the NOAA Fisheries Alaska Fisheries Science Center's Food Habits database of fish diets collected during summer bottom trawl surveys in the SEBS and NBS. *This work is part of a submitted manuscript (Holsman et al. submitted) and the authors request that the images and data reported herein not be duplicated or shared outside of this Ecosystem Status Report until the publication is complete.* Bioenergetics-based indices were calculated for individual predator stomach samples using bioenergetics models. Samples were averaged by 1-cm predator bins across stations within a strata and then extrapolated to the population level using annual proportional biomass for each bin in each strata based on bottom trawl surveys (see Ciannelli et al., 1998; Holsman et al., 2019; Holsman and Aydin, 2015, and Livingston et al., 2017 for more information).

Bioenergetic diet indices collectively indicate changes in foraging and growing conditions; relative foraging rate (RFR) reflects the ratio of observed food consumption (specific consumption rate; C_ggd) to a theoretical temperature and size-specific maximum consumption rate from laboratory feeding experiments. Declines in this index can reflect decreases in prey availability or prey switching to more energetically valuable prey. Therefore we also present mean diet energy density ($mnEDJ\_g$) which reflects the average energetic density of prey in stomachs sampled from across the EBS in a given year. Less favorable foraging patterns would be reflected in declines in RFR when $mnEDJ\_g$ remains the same or also declines in a given year. Metabolic demand (R_ggd) generally increases with temperature and indicates the basal energetic requirements of the fish. Finally, scope for growth (G_ggd) integrates metabolic demand, prey energy, and relative consumption rates to indicate how changes in temperature and foraging collectively influence (potential) growth.

Status and trends: We observe directional trends in consumption and potential growth that reflect climate-driven changes to metabolic demand and trophic interactions and which indicate declining conditions for groundfish in the SEBS and NBS during recent marine heatwave (MHW) years. All six indices suggest that MHWs across the EBS resulted in poor foraging conditions for walleye pollock (*Gadus chalcogrammus*; hereafter "pollock") and Pacific cod (*Gadus macrocephalus*; hereafter "P. cod"). For adult pollock, prey limitation is indicated by multiple consumption indices including observed and relative foraging rates ('C_ggd' and 'RFR', respectively), and is reflected in a low scope for growth (i.e., 'G_ggd' or "growth potential") index for pollock in recent years, although initial limited observations from 2022 indicate more favorable growth conditions associated with the recent return to cooler conditions. Growth potential for P. cod remains below the historical averages, while Pacific halibut (*Hippoglossus stenolepis*) appears to have offset warming impacts with increases in consumption of energetically valuable prey.

Thermal experience (biomass weighted bottom temperature; 'TempC') of all four groundfish species in the EBS has increased in recent years (Figure 82), with adult P. cod thermal experience in 2018 the highest in the 30+ year timeseries (Figure 83). In contrast, juvenile P. cod sought out cold refugia during the MHW, as is reflected in lower metabolic demand during those years. Relative metabolic demand ('R_ggd') reflects the climate- and behaviorally- mediated changes to thermal experience. Accordingly, we observe divergent trends in metabolic demand in the NBS relative to the SEBS, and between juvenile and adults of each species. In the NBS, metabolic demand for adult groundfish continues to increase relative to historical (1990–2010) rates with 2019–2022 rates approximately 2X and 15X fold higher than historical values for pollock and P. cod, respectively. In the SEBS, metabolic demand for adult groundfish has returned to more average conditions (1990–2010) (Figure 84), and is lower than in the recent warm period with 2019–2022 rates approximately -15% and -10% lower than historical values for pollock and P.cod, respectively.

There is evidence of recent declines in foraging efficiency of multiple groundfish species in the EBS (Figures 83 and 84). Specifically, observed consumption rates (g of prey consumed per g body weight of the predator per day) and Relative Foraging Rates (i.e., the ratio of observed consumption rates relative to theoretical maximum consumption rates given the size and thermal experience of the fish) have both declined recently (2019–2022) for juvenile and adult pollock by -43% and -61%, respectively. Additionally, both indices have declined for juvenile P. cod as well ('RFR'=-48% and 'C_ggd'=-44%) suggesting potential declines in prey availability for these groundfish species and life-history stages. In contrast, adult P. cod continue to exhibit foraging rates near the long-term average, suggesting redistribution to the NBS during MHW years may have helped reduce metabolic demand and maintained sufficient access to prey.

Associated with slightly cooler temperatures, average energetic content of sampled diets of juvenile fish have declined -10% and -44%, respectively, in recent years (2019–2022), reflecting a switch to less energetically valuable prey species. The energetic content of adult pollock diets also declined -37% across the EBS. In contrast, adult P. cod ate slightly more energetically valuable prey in recent years (11% above average), up considerably from low energetic indices during the MHW years of 2016–2019.
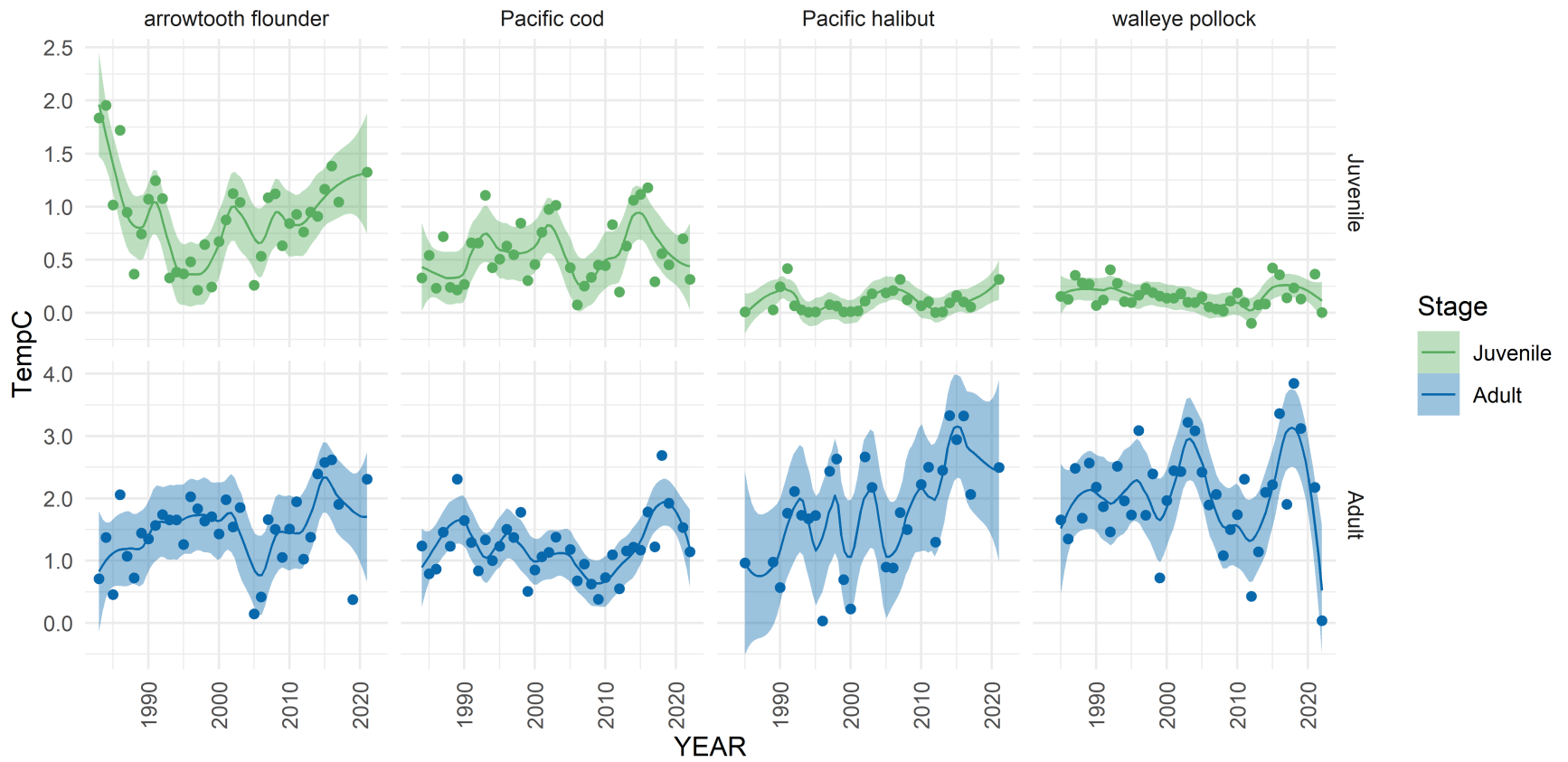
Figure 82: Average thermal experience (TempC) for 5-cm size bins of groundfish species in EBS. The spline represents a loess smoother for juvenile (top row) and adult (bottom row) fish. Data are based on biomass-weighted bottom temperature for samples collected during NOAA NMFS AFSC bottom-trawl summer surveys.

Figure 83: Normalized (i.e., Z-score scaled) bioenergetic diet indices for juvenile (<45cm) groundfish species over time including thermal experience ('TempC'), metabolic demand ('R_ggd'), Relative Foraging Rate ('RFR'), observed specific consumption rate ('C_ggd'), mean diet energy density ('mnEDJ_g'), and scope for growth ('G_ggd'). Mean values for each year and bin are shown as dots, while recent sampled years are highlighted for reference (large triangles and squares). The spline represents a loess smoother. Data is based on biomass-weighted indices for samples collected during NOAA NMFS AFSC bottom-trawl summer surveys.
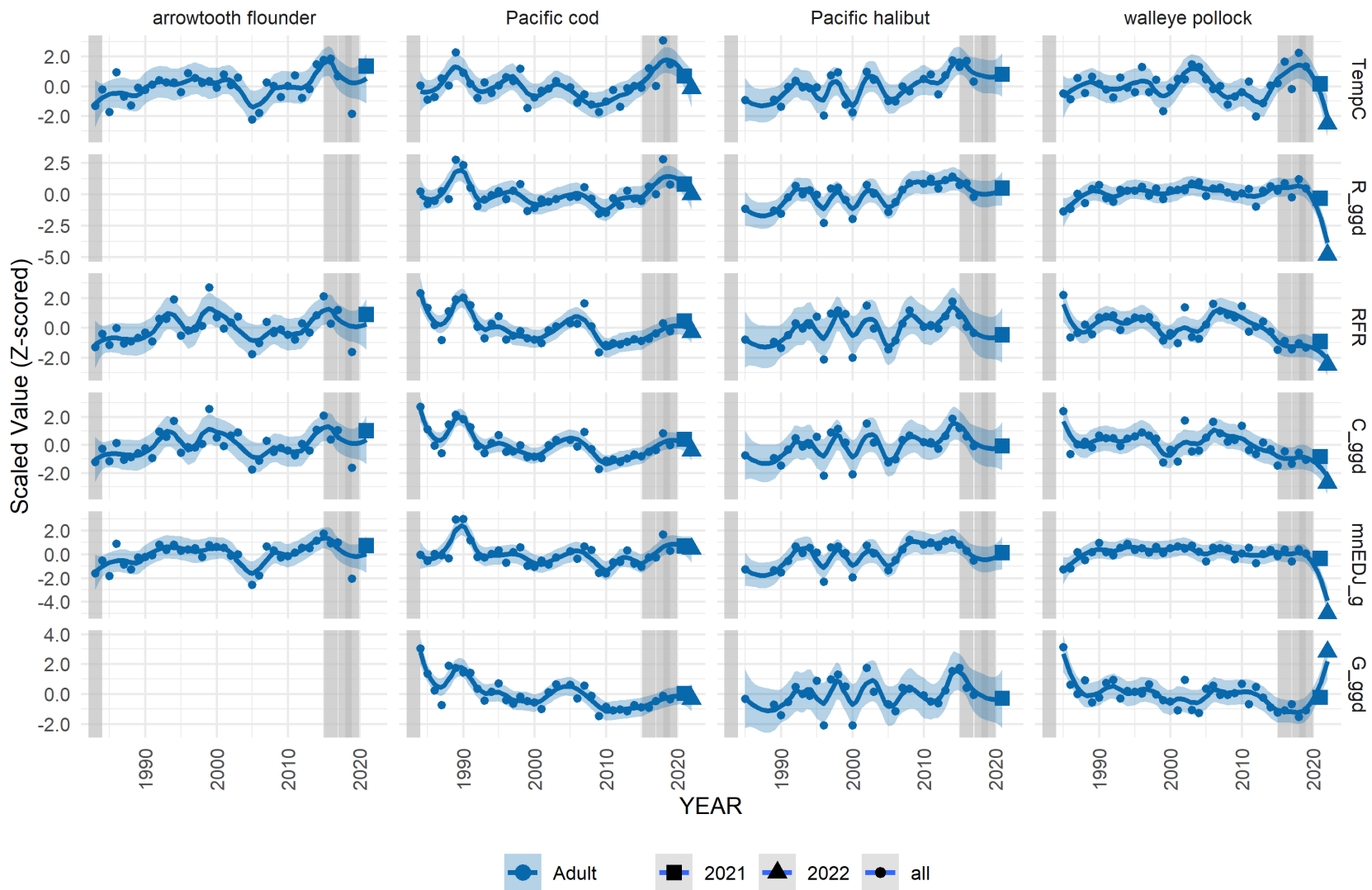
Figure 84: Normalized (i.e., Z-score scaled) bioenergetic diet indices for adult groundfish species over time including thermal experience ('TempC'), metabolic demand ('R_ggd'), Relative Foraging Rate ('RFR'), observed specific consumption rate ('C_ggd'), mean diet energy density ('mnEDJ_g'), and scope for growth ('G_ggd'). Mean values for each year and bin are shown as dots, while recent sampled years are highlighted for reference (large triangles and squares). The spline represents a loess smoother. Data is based on biomass-weighted indices for samples collected during NOAA NMFS AFSC bottom-trawl summer surveys.

The average energetic content of sampled diets generally increases linearly with thermal experience for juvenile and adult arrowtooth, P. cod, and P. halibut, but while this holds true for juvenile pollock, adult pollock diets have exhibited considerably little variation across years or EBS bottom temperatures. Similarly, observed consumption rates for these species also tend to increase linearly with increasing bottom temperature, again except for pollock where consumption rates decline above 1.5°C (bottom temperature) and to a lesser extent for juvenile P. cod. The integrated outcome of these changes, combined with exponential increases in metabolism with warming, is a linear increase in adult P. cod and P. halibut scope for growth with increasing bottom temperature, while juvenile P. cod and adult and juvenile pollock scope for growth decreases with warming temperatures (Figure 85). This is reflected in annual patterns, where we observed an overall decline in scope for growth for both pollock and P. cod in recent years, especially for juvenile pollock and P. cod during the MHW (2016–2019), adult P. cod since 2010, and adult pollock in 2021 (Figures 83 and 84). Initial limited sampling from 2022 collections suggest higher growth potential for pollock in that year, although these early samples should be interpreted cautiously.

Trends in energetic densities in recent years may reflect temporal shifts in diet composition of groundfish in response to changing climate conditions (Figure 86). In particular, for P. cod (as predators), there is a notable increase in the proportion diets composed of snow crab (*Chionoecetes opilio*) and decrease in the proportion composed of pollock since 2013.

Factors influencing observed trends: Metabolic demands for ectothermic fish like pollock, P. cod, arrowtooth flounder, and P. halibut are largely a function of thermal experience and body size and tend to increase exponentially with increasing temperatures. Fish can minimize metabolic costs through behaviors such as movement to thermally optimal temperatures (e.g., movement to climate refugia in the NBS or at depth), or can increase consumption of food energy (quality and/or quantity of prey) to meet increasing metabolic demands. The latter requires sufficient access to abundant or high energy prey resources. By examining patterns in diets of fish across the EBS we are able to derive indices of potential increases in metabolic demand, foraging rate, and growth potential (or "scope for growth") which provides insight into ecological changes associated with marine heatwaves and long-term warming in the region.

Implications: For both species in the EBS during recent anomalously warm years, metabolic demands were elevated while foraging rates and scope for growth were reduced (Figures 82 and 83), this pattern was most pronounced for juvenile and adult pollock, and juvenile P. cod (Figure 84). This has important implications, as to offset metabolic demands these fish would have had to (1) consume more food or more energetically rich food, (2) access energetic reserves leading to net body mass loss, or (3) move to more energetically favorable foraging grounds. There are a few lines of evidence to support all three of these potential responses to climate-driven changes in the EBS, including observations of large numbers of P. cod in the NBS surveys in 2017–2023.
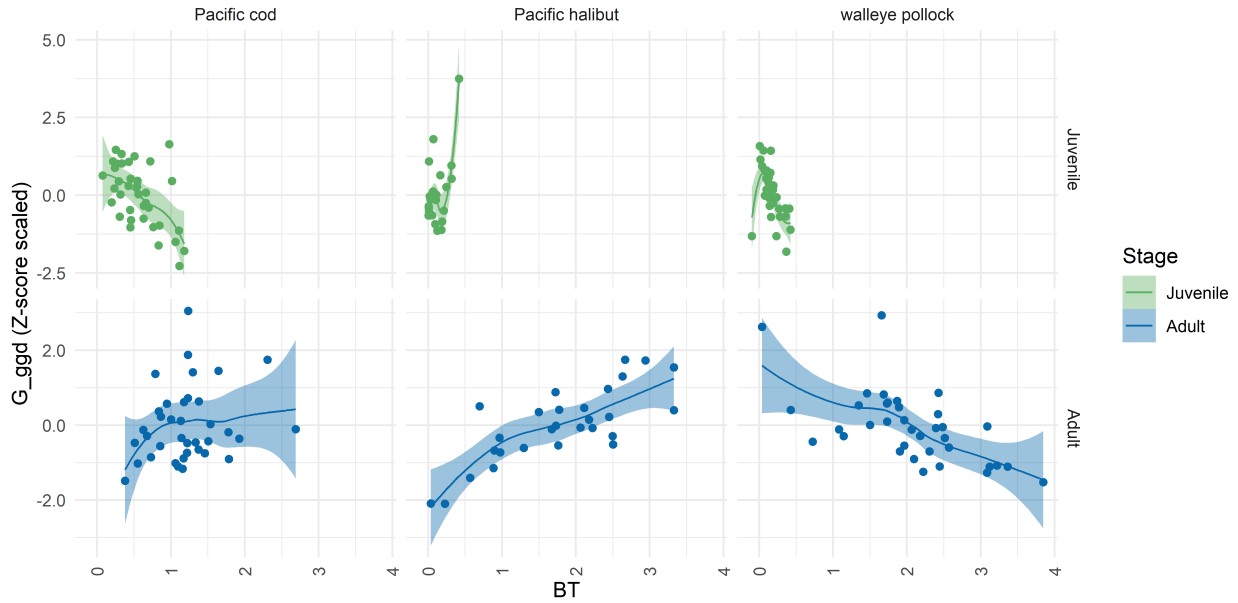
Figure 85: Normalized (i.e., Z-score scaled) bioenergetic (potenital) scope for growth ('G_ggd') for juvenile and adult fish as a function of survey bottom temperature (BT; °C). Data is based on biomass-weighted indices for samples collected during NOAA NMFS AFSC bottom-trawl summer surveys for the NBS and SEBS.
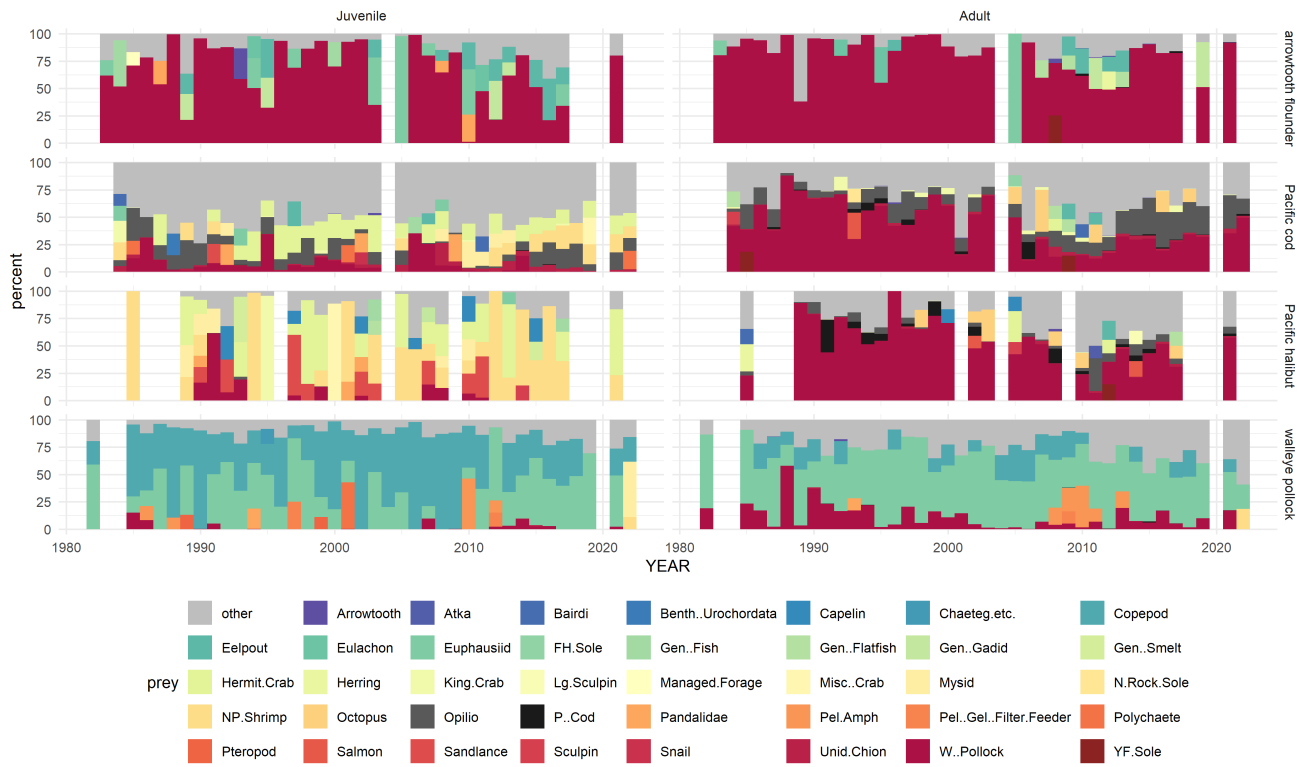
Figure 86: Diet composition of juvenile and adult groundfish across the Bering Sea. Data is based on biomass-weighted indices for samples collected during NOAA NMFS AFSC bottom-trawl summer surveys for the NBS and SEBS. **Note** that recent years (2021–present) have fewer processed samples.

Multispecies Model Estimates of Time-varying Natural Mortality

Contributed by Kirstin K. Holsman, Jim Ianelli, Kerim Aydin, Kalei Shotwell, Kelly Kearney, Ingrid Spies, Steve Barbeaux, and Grant Adams
Resource Ecology and Fishery Management Division, Alaska Fisheries Science Center, National Marine Fisheries Service, NOAA
Contact: kirstin.holsman@noaa.gov
Last updated: November 2023

Description of indicator: We report trends in age-1 total mortality for walleye pollock (*Gadus chalcogrammus*, 'pollock'), Pacific cod (*Gadus macrocephalus*, 'P. cod'), and arrowtooth flounder (*Atheresthes stomias*, 'arrowtooth'), from the eastern Bering Sea (EBS). Total mortality rates are based on residual mortality inputs (M1) and model estimates of annual predation mortality (M2) produced from the multi-species statistical catch-at-age assessment model (known as CEATTLE: Climate-Enhanced, Age-based model with Temperature-specific Trophic Linkages and Energetics). See Appendix 1 of the BSAI pollock stock assessment for 2023 as well as Holsman et al. (2016), Holsman and Aydin (2015), Ianelli et al. (2016), and Jurado-Molina et al. (2005) for more information.

Status and trends: The CEATTLE model estimates of age-1 natural mortality (i.e., M1+M2) for pollock, P. cod, and arrowtooth continue to decline from the 2016 peak mortality. For all three species, age-1 predation mortality rates have remained similar to 2022. At 1.2 yr^{-1}, age-1 mortality estimated by the model was greatest for pollock and lower for P. cod and arrowtooth, with total age-1 natural mortality at around 0.65 and 0.66 yr^{-1} for P. cod and arrowtooth, respectively. The 2023 age-1 natural mortality across species was 11% to 39% lower than in 2016 and is near average for pollock (relative to the long-term mean) (Figure 87). Similarly, P. cod and arrowtooth age-1 mortality are well below the long-term mean.

Patterns in the total biomass of each species consumed by all three predators in the model (typically 1–3 yr old fish) exhibit divergent trends from predation mortality in 2023. Pollock and P. cod biomass consumed by all predators in the model is trending upward (i.e., indicating more pollock and P. cod were consumed this year than in previous years), while arrowtooth consumed is trending downward (Figure 88).

Factors influencing observed trends: Temporal patterns in natural mortality reflect annually varying changes in predation mortality that primarily impact age-1 fish (and to a lesser degree impact ages 2 and 3 fish in the model). Pollock are primarily consumed by older conspecifics, and pollock cannibalism accounts for 59% (on average) of total age-1 predation mortality, with the exception of the years 2006–2008 when predation by arrowtooth marginally exceeded cannibalism as the largest source of predation mortality of age-1 pollock (Figure 89). The relative proportion of age-1 pollock consumed by older pollock increased again in 2023 relative to previous years, while the relative proportion consumed by P. cod and arrowtooth declined.

Combined annual predation demand (annual ration) of pollock, P. cod, and arrowtooth flounder in 2023 was 9.26 million tons, down slightly from the 9.99 million t annual average during the warm years and large maturing cohorts of 2014–2016. Pollock represent approximately 77% of the model estimates of combined prey consumed with a long-term average of 5.73 million tons of pollock consumed annually

by all three predators in the model. From 2015–2019, individual annual rations were above average for all three predator species, driven by anomalously warm water temperatures in the Bering Sea during during those years. However, cooler temperatures in 2023 relative to the recent warm years has resulted in annual rations at or below the long-term average (Figure 90).

Implications: We find evidence of continued declines in predation mortality of age-1 pollock, P. cod, and arrowtooth flounder relative to recent high predation years (2014–2016). While warm temperatures continue to lead to high metabolic (and energetic) demand of predators, declines in total predator biomass, in particular P. cod, are contributing to an net decrease in total consumption (relative to 2016) and therefore reduced predation rates and mortality in 2021–2023. This pattern indicates continued favorable top-down conditions for juvenile groundfish survival in 2022 through predator release due to declining biomass of groundfish.

Between 1980 and 1993, relatively high natural mortality rates for pollock reflect patterns in combined annual demand for pollock prey by all three predators that was high in the mid 1980's (collectively 9.24 million t per year). The peak in predation mortality of age-1 pollock in 2016 corresponds to warmer than average conditions and higher than average energetic demand of predators combined with the maturation of the large 2010–2012 year classes of pollock and P. cod (collectively with arrowtooth 10.07 million t per year).
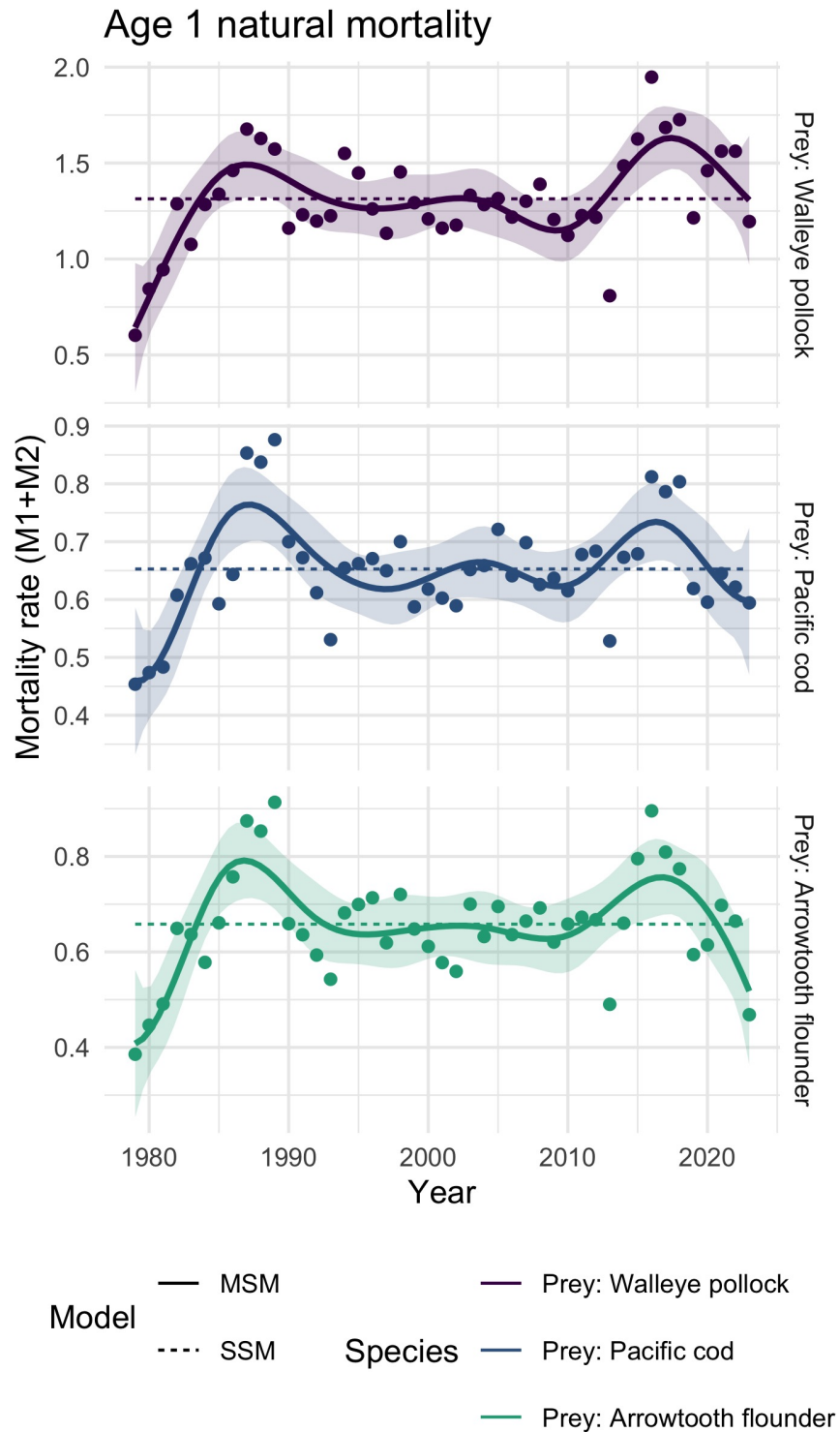
Figure 87: Annual variation in total mortality ($M1_{i1} + M2_{i1,y}$) of age-1 pollock (as prey) (a), age-1 P. cod (as prey) (b), and age-1 arrowtooth flounder (as prey) (c) from the single-species models (dashed) and the multi-species models with temperature (points and solid line). Updated from Holsman et al. (2016); more model detail can be found in Appendix 1 of the BSAI pollock stock assessment for 2023. Solid lines are a 10-y (symmetric) loess polynomial smoother indicating trends in age-1 mortality over time.
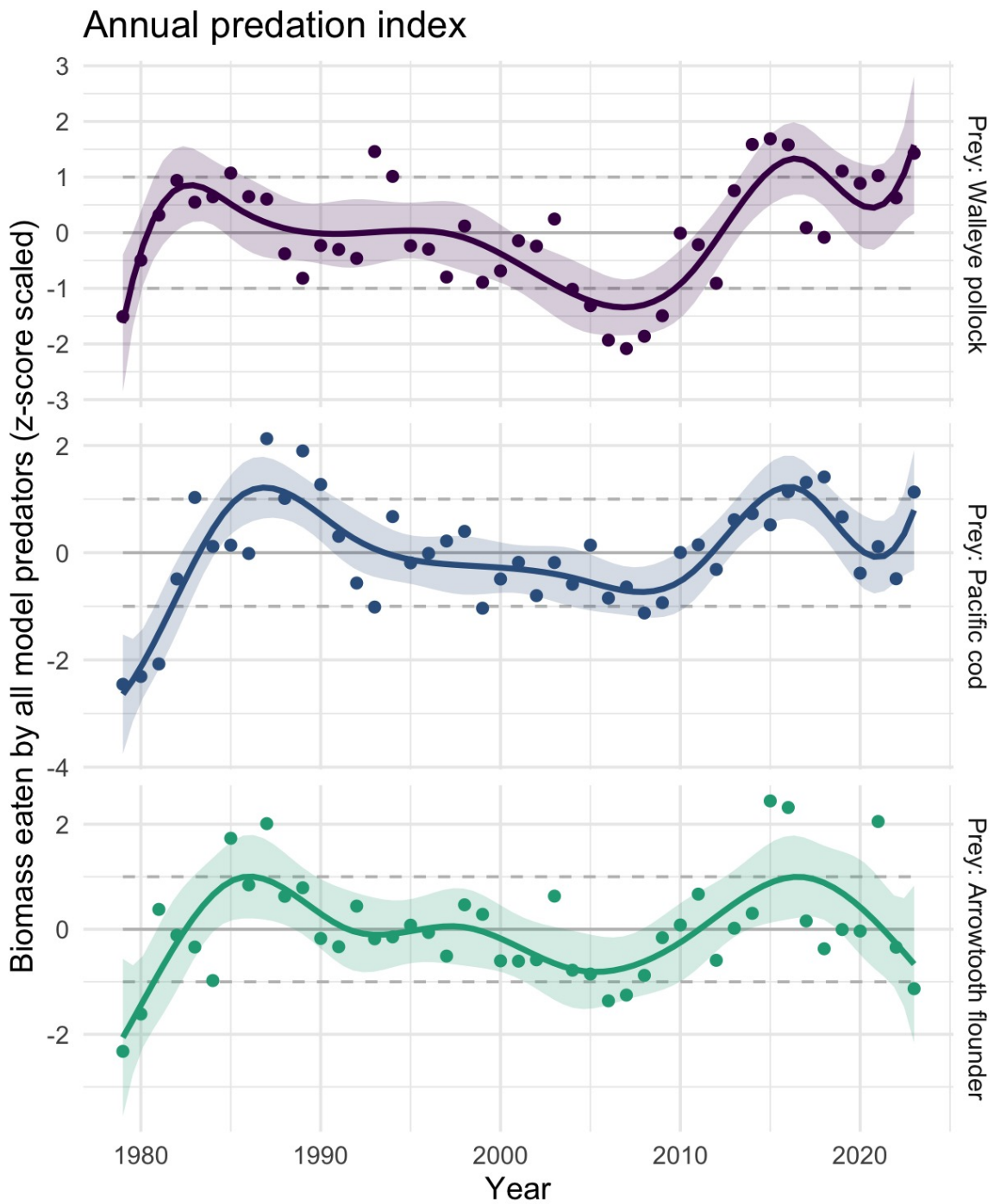
Figure 88: Multispecies estimates of prey species biomass consumed by all predators in the model (points): a) total biomass of pollock consumed by predators annually, b) total biomass of P. cod consumed by predators annually, c) total biomass of arrowtooth flounder consumed by predators annually. Gray lines indicate 1979–2023 mean estimates for each species; dashed lines represent 1 standard deviation of the mean. Solid lines are a 10-y (symmetric) loess polynomial smoother indicating trends in biomass consumed over time.
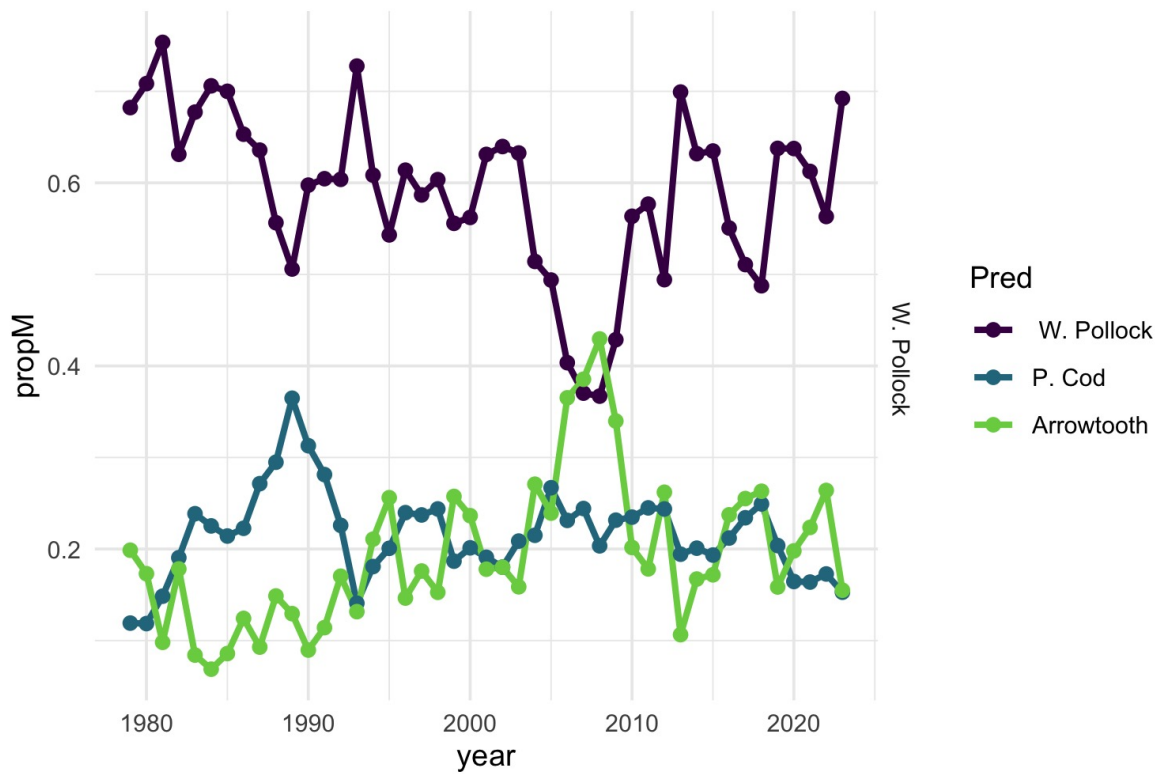
Figure 89: Proportion of total predation mortality for age-1 pollock from pollock, P. cod, and arrowtooth flounder predators across years. Updated from Holsman et al. (2016); more model detail can be found in Appendix 1 of the BSAI pollock stock assessment for 2023.
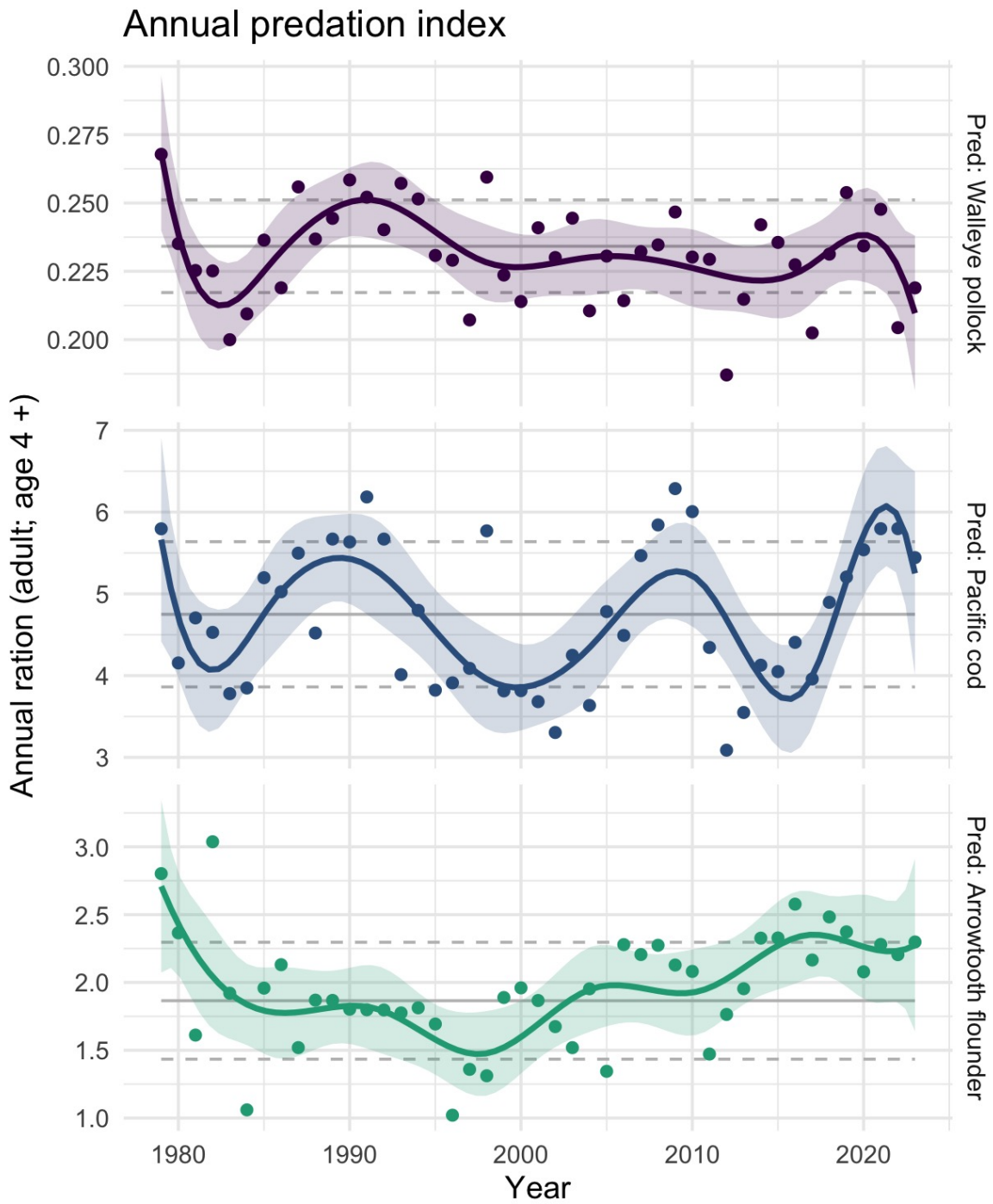
Figure 90: Multispecies estimates of annual ration (kg consumed per individual per year) for adult (age-4+) predators: a) pollock, b) P. cod, and c) arrowtooth flounder. Gray lines indicate 1979–2023 mean estimates for each species; dashed lines represent 1 standard deviation of the mean. Solid lines are a 10-y (symmetric) loess polynomial smoother indicating trends in ration over time.

Groundfish Recruitment Predictions

Temperature Change Index and the Recruitment of Bering Sea Pollock

Contributed by Ellen Yasumiishi
Auke Bay Laboratories, Alaska Fisheries Science Center, NOAA Fisheries
Contact: ellen.yasumiishi@noaa.gov
Last updated: August 2023

Description of indicator: The temperature change (TC) index is a composite index for the pre- and post-winter thermal conditions experienced by walleye pollock (*Gadus chalcogrammus*) from age-0 to age-1 in the eastern Bering Sea (Martinson et al., 2012). The TC index (year t) is calculated as the difference in the average monthly sea surface temperature in June (t+1) and August (t) (Figure 91) in an area of the southern region of the eastern Bering Sea (56.2°N to 58.1°N by 166.9°W to 161.2°W). Time series of average monthly sea surface temperatures were obtained from the NOAA Earth System Research Laboratory Physical Sciences Division website. Sea surface temperatures were based on NCEP/NCAR gridded reanalysis data (Kalnay et al., 1996, data obtained from `http://www.esrl.noaa.gov/psd/cgi-bin/data/timeseries/timeseries1.pl` (accessed August 8, 2023)). We specify Variable SST and Analysis level Monolevel Variables. Less negative values represent a cool late summer during the age-0 phase followed by a warm spring during the age-1 phase for pollock.

Status and trends: The 2022 year class TC index value is -4.74, lower than the 2021 year class TC index value of -4.36, indicating slightly worse conditions for pollock survival from age-0 and age-1 from 2022 to 2023 than from 2021 to 2022. The average expected survival is due to the smaller relative difference in sea temperature from late summer (cool) to the following spring (cool). The late summer sea surface temperature (August 9.5°C) in 2022 was 0.4°C lower than the long term average (9.9°C) and spring sea temperature (June 4.8°C) in 2023 was cooler than the long-term average of 5.3°C since 1949.

Factors causing observed trends: According to the original Oscillating Control Hypothesis (OCH), warmer spring temperatures and earlier ice retreat led to a later oceanic and pelagic phytoplankton bloom and more food in the pelagic waters at an optimal time for use by pelagic species (Hunt et al., 2002). The revised OCH indicated that age-0 pollock were more energy-rich and have higher over wintering survival to age-1 in a year with a cooler late summer (Coyle et al., 2011; Heintz et al., 2013). The 2022 year class of pollock experienced cooler late summer temperatures in 2022 during the age-0 stage and cooler spring temperatures in 2023 during the age-1 stage indicating average conditions for the overwintering survival from age-0 to age-1.

Implications: The 2022 TC index value of -4.74 was similar to the long-term average of -4.58, therefore we expect average recruitment of pollock to age-4 in 2026 from the 2022 year class (Figure 92).
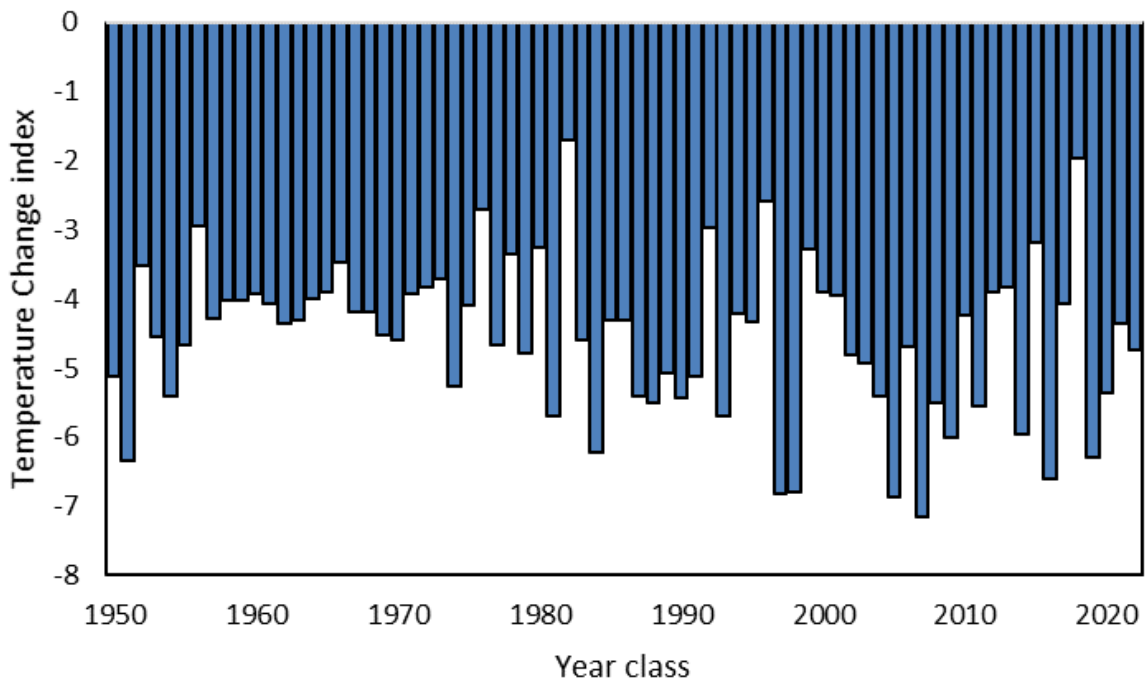
Figure 91: The Temperature Change index values for the 1950 to 2022 year classes of pollock. Values represent the differences in sea temperatures on the southeastern Bering Sea shelf experienced by the 1950–2022 year classes of pollock. Less favorable conditions (more negative values) represent a warm summer during the age-0 life stage followed by a relatively cool spring during the age-1 life stage. More favorable conditions (less negative values) represent a cool summer during the age-0 life stage followed by a relatively warm spring during the age-1 life stage.
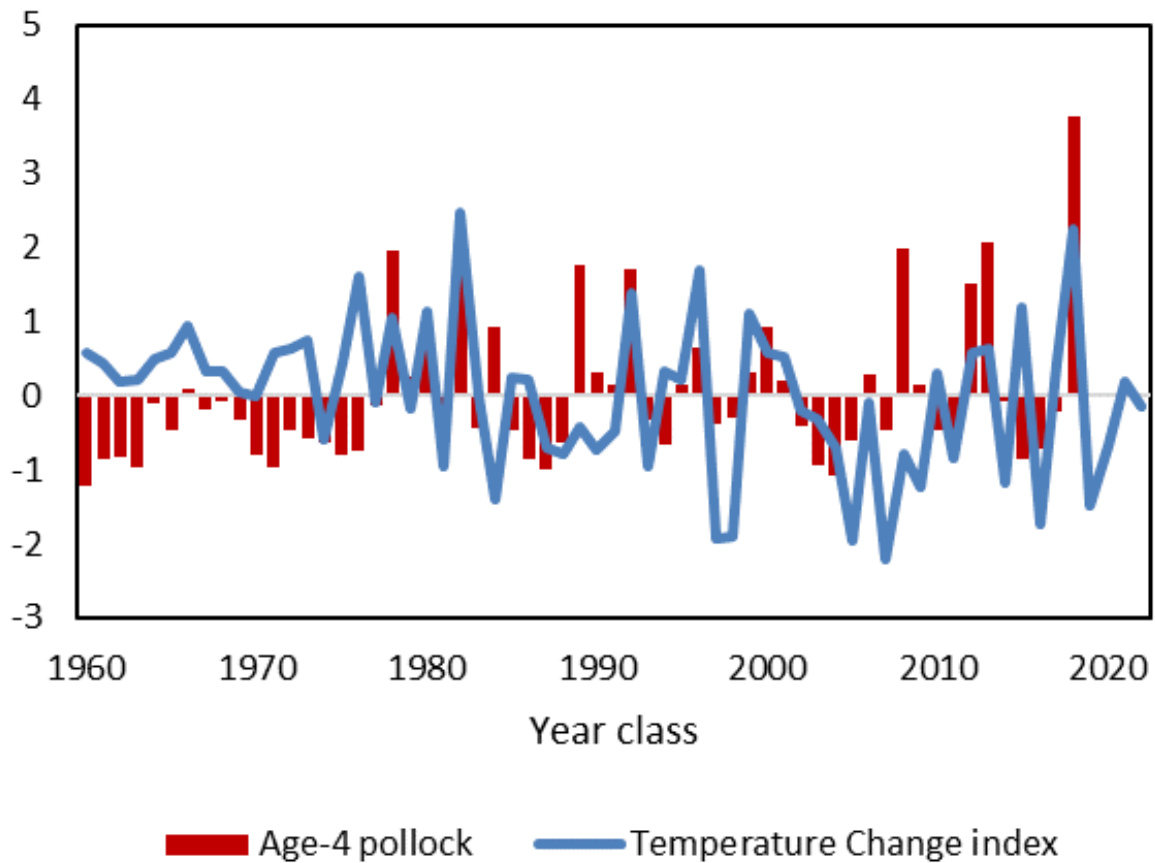
Figure 92: Normalized time series values of the temperature change index indicating conditions experienced by the 1960–2022 year classes of pollock during the summer age-0 and spring age-1 life stages. Normalized values of the estimated abundance of age-4 pollock in the eastern Bering Sea from 1964–2022 for the 1960–2018 year classes. Age-4 pollock estimates are from Table 1-24 in Ianelli et al. (2022). The TC index indicate average conditions for the 2022 year classes of pollock.

Large Copepod Abundance as an Indicator of Pollock Recruitment to Age-3 in the Southeastern Bering Sea

Contributed by Ellen Yasumiishi[1], Lisa Eisner[1], and David Kimmel[2]
[1]Auke Bay Laboratories, Alaska Fisheries Science Center, NOAA Fisheries
[2]Resource Assessment and Conservation Engineering Division, Alaska Fisheries Science Center, NOAA Fisheries
Contact: Ellen.Yasumiishi@noaa.gov
Last updated: September 2023

Description of indicator: Interannual variations in large copepod abundance during the age-0 pollock life stage were compared to age-3 pollock (*Gadus chalcogrammus*) abundance (billions of fish) for the 2002–2019 year classes on the southeastern Bering Sea shelf, south of 60°N, <200m bathymetry (Eisner et al., 2020). Estimates of age-3 pollock based on large copepod abundances collected in 2020 and 2022 are also included. The large copepod index sums the abundances of *Calanus marshallae/glacialis* (copepodite stage 3 (C3)-adult), *Neocalanus* spp. (C3-adult), and *Metridia pacifica* (C4-adult), taxa typically important in age-0 pollock diets (Coyle et al., 2011). Zooplankton samples were collected with oblique bongo tows over the water column using 60cm, 505μm mesh nets for 2002–2011, and 20cm, 153μm mesh or 60cm, 505μm nets, depending on taxa and stage for 2012–2022. Data were collected on the Bering Arctic Subarctic Integrated Survey (BASIS) fishery oceanography surveys (2002–2012, 2014–2016, 2018, 2022) and along the 70m isobath (2002–2012, 2014–2020) during mid-August to late September, for four warm years (2002–2005) followed by one average (2006), six cold (2007–2012), five warm (2014–2016, 2018, 2020), and two average years (2017 on 70m isobath, 2022 on BASIS) using methods in Eisner et al. (2014) and Kimmel et al. (2018). Zooplankton data were not available for 2013 and 2021. Age-3 pollock abundance was obtained from the stock assessment report for the 2002–2019 year classes (Ianelli et al., 2022). Two estimates of large copepod abundances from the BASIS survey data were calculated, the first using means among stations (sample-based) and the second using the means estimated from the geostatistical model, Vector Autoregressive Spatial Temporal (VAST) package version 13.0.1 (Thorson et al., 2015). We specified 500 knots, a log normal distribution for positive catch rates, and used the delta link function between probability of encounter and positive catch rate in VAST.

Status and trends: Positive significant linear relationships were found between large copepods collected during the age-0 stage of pollock (2002–2019 year classes) and stock assessment estimates of age-3 pollock three years later (2005–2022) (Figure 93). For the BASIS survey stations, the stronger relationship of age-3 pollock with the large copepod index using the VAST model compared to observed means among stations (r^2=0.29 vs r^2=0.13) appeared to be partially due to the VAST model filling in data for survey area missed in some years (e.g., 2008). The copepod index from the 70m isobath surveys explained 11% of the variation in the stock assessment estimates of pollock. Fitted means and standard errors of the age-3 pollock abundances were estimated from the linear regression model using large copepod estimates from the BASIS VAST means, BASIS sample-based means, and 70m isobath sample-based means compared to the pollock stock assessment estimates from Ianelli et al. (2022) (Figure 94). Copepod indices underestimated age-3 pollock for the 2018 year class relative to the stock assessment estimates, indicating an alternative mechanism driving the recruitment of pollock to age-3 for the 2018 year class. Copepod indices from the 70m isobath surveys during 2020 and the BASIS survey during 2022 predict below average recruitment of age-3 pollock in 2023 and 2025.

Factors influencing observed trends: Increases in sea-ice extent and duration were associated with increases in large zooplankton abundances on the shelf (Eisner et al., 2014, 2015, 2020), increases in large copepods and euphausiids in pollock diets (Coyle et al., 2011) and increases in age-0 pollock lipid content (Heintz et al., 2013). The increases in sea ice and associated ice algae and phytoplankton may provide an early food source for large crustacean zooplankton reproduction and growth (Baier and Napp, 2003; Hunt et al., 2011). These large zooplankton taxa contain high lipid concentrations (especially in cold, high ice years) which in turn increases the lipid content in their predators such as age-0 pollock and other fish that forage on these taxa. Increases in energy density (lipids) in age-0 pollock allow them to survive their first winter (a time of high mortality) and eventually recruit into the fishery. Accordingly, a strong relationship has been shown for energy density in age-0 fish and age-3 pollock abundance (Heintz et al., 2013).

Implications: Our results suggest low availability of large copepod prey for age-0 pollock during the first year of life in 2020 and 2022. These conditions may not be favorable for age-0 pollock overwinter survival and recruitment to age-3. However, in 2018 there was an increase in euphausiids in BASIS age-0 pollock diets (Andrews III et al., 2019), which may have compensated for the lack of large copepods, and enhanced overwinter survival and subsequent recruitment of the 2018 year class. Information from the 70m isobaths survey may be useful in years without a BASIS survey in the southeast Bering Sea. If the relationship between large copepods and age-3 pollock remains significant in our analysis, the index can be used to predict the recruitment of pollock three years in advance of recruiting to age-3, from zooplankton data collected three years prior. This relationship also provides further support for the revised oscillating control hypothesis that suggests as the climate warms, reductions in the extent and duration of sea ice could be detrimental large crustacean zooplankton and subsequently to the pollock fishery in the southeastern Bering Sea (Hunt et al., 2011).
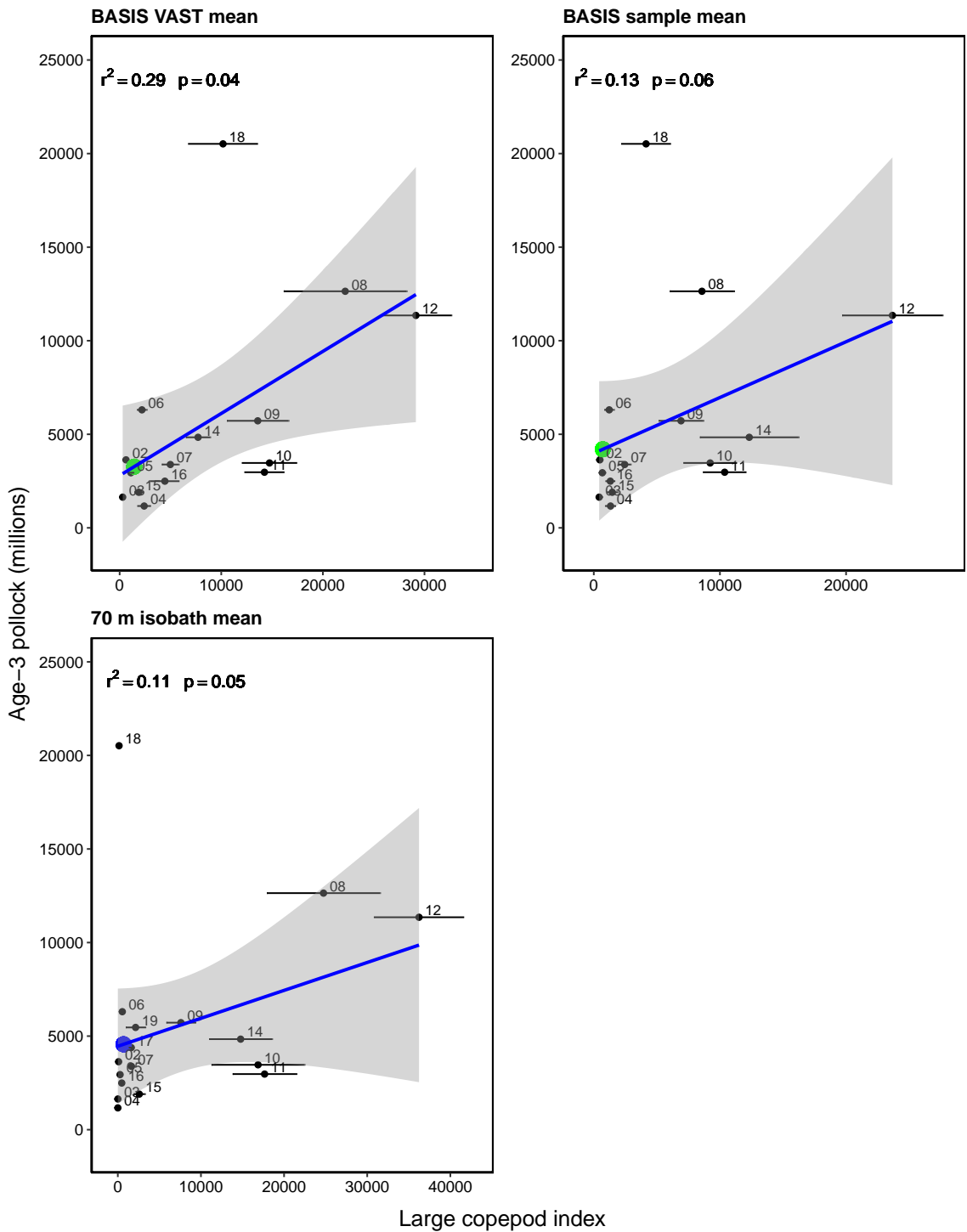
Figure 93: Linear relationships between BASIS VAST model (top left), BASIS sample-based (top right), and 70m isobath surveys (bottom) estimated mean abundance of large copepods (C+MN, sum of *Calanus marshallae/glacialis*, *Metridia pacifica*, and *Neocalanus* spp.) during the age-0 life stage of pollock, and the estimated abundance (millions) of age-3 pollock from Ianelli et al. (2022) for 2002–2019 year classes. Dots represent the predicted pollock values based on the 70m isobath large copepod index for year class 2020 (blue) and the BASIS survey large copepod index for the 2022 year class (green). No zooplankton data were available for 2013 or 2021.
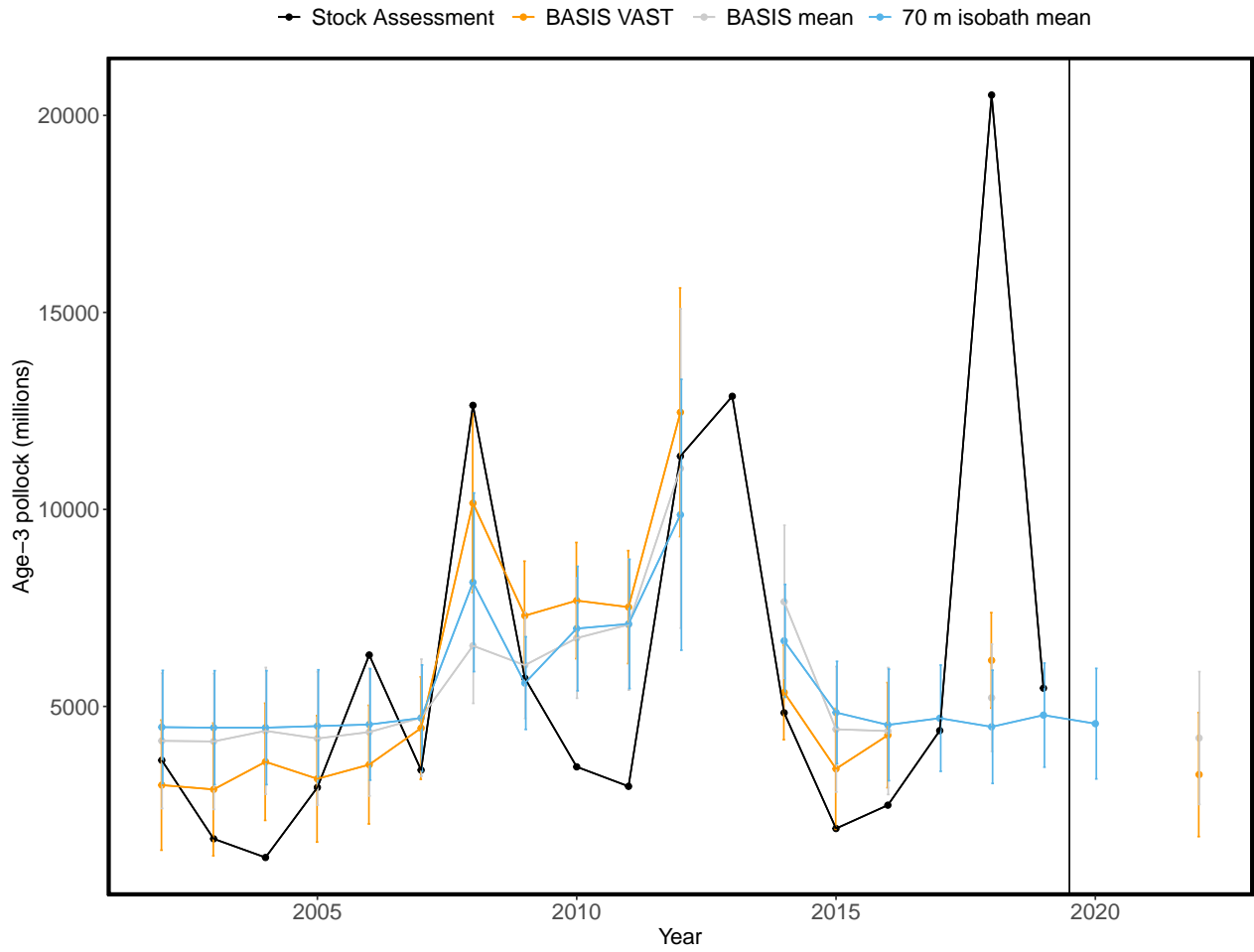
Figure 94: Fitted means and standard errors of the age-3 pollock abundance estimated from the linear regression models using BASIS VAST estimates of large copepods (orange), BASIS sample-based estimates (gray), and 70m isobath estimates (blue), and means from the pollock stock assessment estimates (black) from (Ianelli et al., 2022). Predicted estimates of age-3 pollock (recruited into fishery as age 3's in 2023 and 2025) based on large copepod mean estimates from the 70m isobath for the 2020 year class and the BASIS survey for the 2022 year class.

Benthic Communities and Non-target Fish Species

Eastern and Northern Bering Sea – Miscellaneous Species

Contributed by Thaddaeus Buser
Resource Assessment and Conservation Engineering Division, Alaska Fisheries Science Center
National Marine Fisheries Service, NOAA
Contact: thaddaeus.buser@noaa.gov
Last updated: September 2023

Description of indicator: "Miscellaneous" species fall into three groups: eelpouts (fishes of the Family Zoarcidae), poachers (fishes of the Family Agonidae), and sea stars (Class Asteroidea). The three species comprising the bulk of the eelpout group are the wattled eelpout (*Lycodes palearis*) and shortfin eelpout (*L. brevipes*) and to a lesser extent the marbled eelpout (*L. raridens*). The biomass of poachers is dominated by the sturgeon poacher (*Podothecus acipenserinus*) and to a lesser extent the sawback poacher (*Leptagonus frenatus*). The composition of sea stars is dominated by the purple-orange sea star (*Asterias amurensis*), found primarily in the inner/middle shelf, and the common mud star (*Ctenodiscus crispatus*), primarily in the outer shelf. Relative CPUE by weight (kg per hectare) was calculated and plotted for each species or species group by year for 1982–2023 for the eastern Bering Sea survey and 2010–2023 for the northern Bering Sea survey. Catch methods for the northern Bering Sea were standardized in 2010, so catches from previous years do not provide comparable data and are excluded. Relative CPUE was calculated by setting the largest biomass in the time series to a value of 1 and scaling other annual values proportionally. The standard error (±1) was weighted proportionally to the CPUE to produce a relative standard error.

Status and trends:
Eastern Bering Sea:
The 2023 relative CPUE estimate for eelpouts showed a modest increase from 2022, just above the average of the estimates over the last 10 years. For poachers, CPUE decreased from 2022, returning to levels seen in 2017, ending a multi-year upward trend (2018–2021). The 2023 poacher estimate is just below the average for the time series. The CPUE for sea stars in 2023 also broke a multi-year upward trend (2017–2021), with the 2023 estimate returning to a level last seen in 2016 (Figure 95).

Northern Bering Sea:
The relative CPUE estimates for eelpouts are much higher before 2018 than after. Whether this indicates a trend is unclear given the gaps in sampling years. For poachers, the CPUE was likewise low after 2018, but it was also low in 2010, with 2017 being an outlier of high relative CPUE. The CPUE for sea stars is remarkably consistent across the time series, especially compared with all other groups in this report (Figure 96).

Factors causing observed trends: It is difficult to identify trends, especially for the NBS given that survey has been conducted intermittently and only recently (i.e., starting in 2017) been conducted on a more regular schedule. Determining whether, for example, the low relative CPUE after 2018 in poachers (EBS and NBS) and eelpouts (NBS) represents real responses to environmental change or is an artifact of standardized survey sampling methodology (e.g., temperature dependent catchability) will require more specific research on survey trawl gear selectivity relative to interannual differences in bottom temperatures and on the life history characteristics of these epibenthic species.
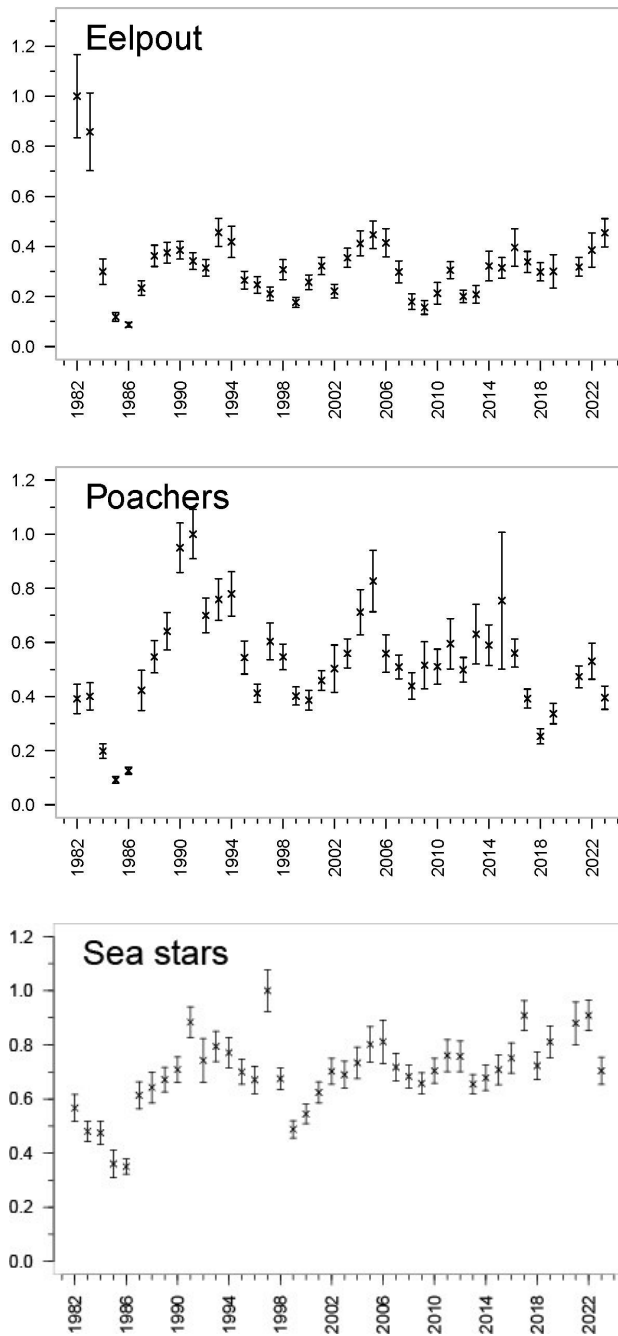
Figure 95: AFSC eastern Bering Sea shelf bottom trawl survey relative CPUE for miscellaneous fish species during the May to August time period from 1982–2023.

Implications: Eelpouts have important roles in the energy flow within benthic communities. For example, eelpouts are a common prey item of arrowtooth flounder (*Atheresthes stomias*). However, it is not known at present whether these changes in CPUE are related to changes in energy flow.
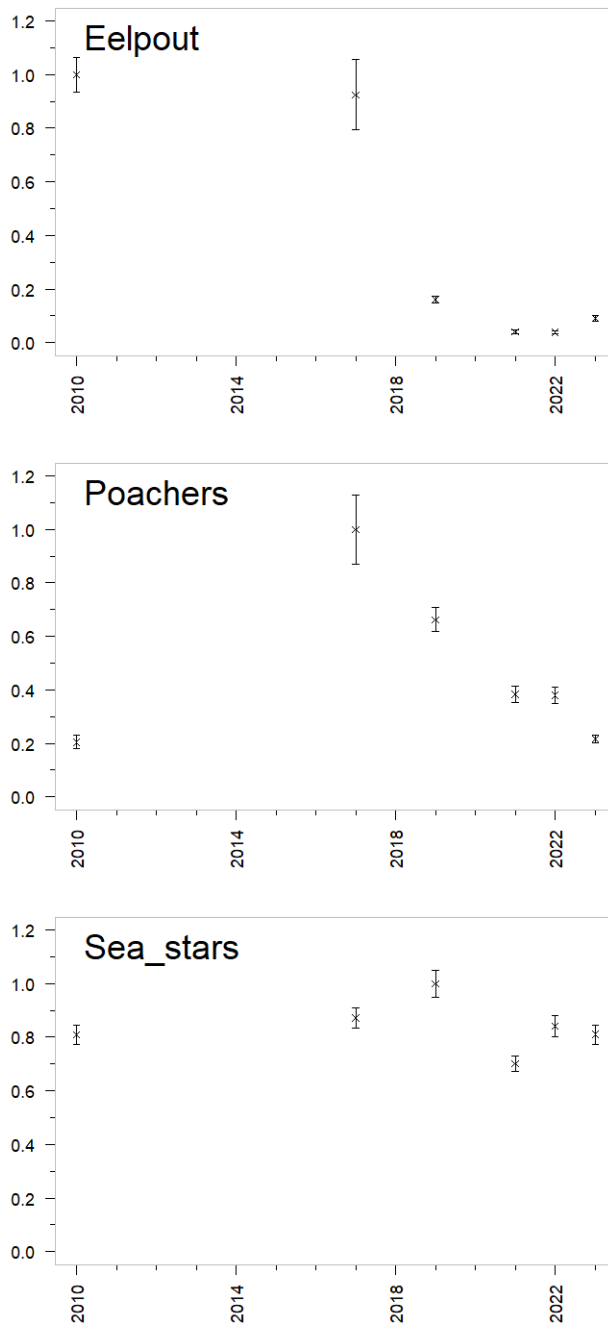
Figure 96: AFSC northern Bering Sea shelf bottom trawl survey relative CPUE for miscellaneous fish species during the July to August time period from 2010–2023.

Eastern Bering Sea Commercial Crab Stock Biomass Indices

Contributed by Jon Richar
Kodiak Laboratory, Alaska Fisheries Science Center, National Marine Fisheries Service, NOAA
Contact: jon.richar@noaa.gov
Last updated: August 2023

Description of indicator: This indicator is the commercial crab species biomass time series in the eastern Bering Sea. The eastern Bering Sea bottom trawl survey has been conducted annually since 1975 by the Resource Assessment and Conservation Engineering Division of the Alaska Fisheries Science Center. The purpose of this survey is to collect data on the distribution and abundance of crab, groundfish, and other benthic resources in the eastern Bering Sea. The data provided here include the time series of results from 1998 to the present. In 2023, 375 standard stations were sampled on the eastern Bering Sea shelf from 28 May to 3 August. The observed trends in crab biomass may be indicative of trends in either benthic production, or benthic response to environmental variability. The commercial crab biomass is also indicative of trends in exploited resources over time.

Status and trends: The historical trends of commercial crab biomass and abundance are highly variable (Figure 97). In 2023, Bristol Bay mature male red king crab biomass decreased by -23% relative to 2022 estimates, reversing a recent moderate rebound trend. Conversely, mature female red king crab biomass increased by 67%, while abundance increased by 46%, with the discrepancy being due to an increasing proportion of larger crab. Of note, this substantial increase by a hotspot station that accounted for 37% of the total mature female Bristol Bay red king crab catch. Numbers however remain near the historical low points.

The St. Matthew blue king crab adult male biomass decreased by -10% relative to 2022 estimates, continuing a declining trend decline observed since 2014. Female blue king crab biomass is not adequately sampled during this survey due to a nearshore distribution around St. Matthew Island.

Mature male Tanner biomass trends were mixed, with the eastern district seeing a 27% decrease, although this was partially offset by a 32% increase in the western district. The decrease in the eastern district mature male biomass resumes a recent declining trend which has seen biomass decline by -84% since 2014. The increase in western district mature males reverses a decline observed since 2019. Mature females increased in the western district (+18%), but declined in the eastern district (-11%).

Total snow crab biomass decreased by -16% relative to 2022, continuing an 88% decline since 2018, with this being driven by declines in mature males (-24%), immature males (-6%), legal males (-37%), mature females (-29%), immature females (-15%), and industry-preferred (-15%).

Pribilof Island crab stocks remain extremely depressed with highly variable survey biomass estimates due to trawl survey limitations related to crab habitat and the patchy crab distribution. Of note, 2023 was the first year in the history of the survey in which no mature male Pribilof blue king crab were caught, while mature females declined (-19%). As during the previous three surveys, no immature female blue king crab were caught. The Pribilof red king crab stock saw declines of -46% in both mature and legal male stocks, while mature females increased by 22%. Although catches of immature males and females were small, they improved on even smaller/nonexistent results for prior surveys.

Factors influencing observed trends: Environmental variability and exploitation affect trends in commercial crab biomass over time. Recent modeling analyses suggest that environmental variability is largely driving inter-annual variability in crab stock recruitment, although a mortality event may be occurring with snow crab, the direct driver of which is unknown.

Implications: The implications of the observed variability in crab stocks are dramatic inter-annual and inter-decadal variability in benthic predators and ephemeral (seasonal) pelagic prey resources when crab are in larval stages in the water column or as juveniles in the benthos. Although it is unclear at what life stage crab stock variability is determined, it is likely that environmental variability affecting larval survival and changes in predation affecting juvenile survival are important factors. As such, the environmental conditions affecting larval crab may also be important for larval demersal groundfish and the availability of crab as prey may be important for demersal fish distributions and survival. Disease may also be a factor, although this is speculative.
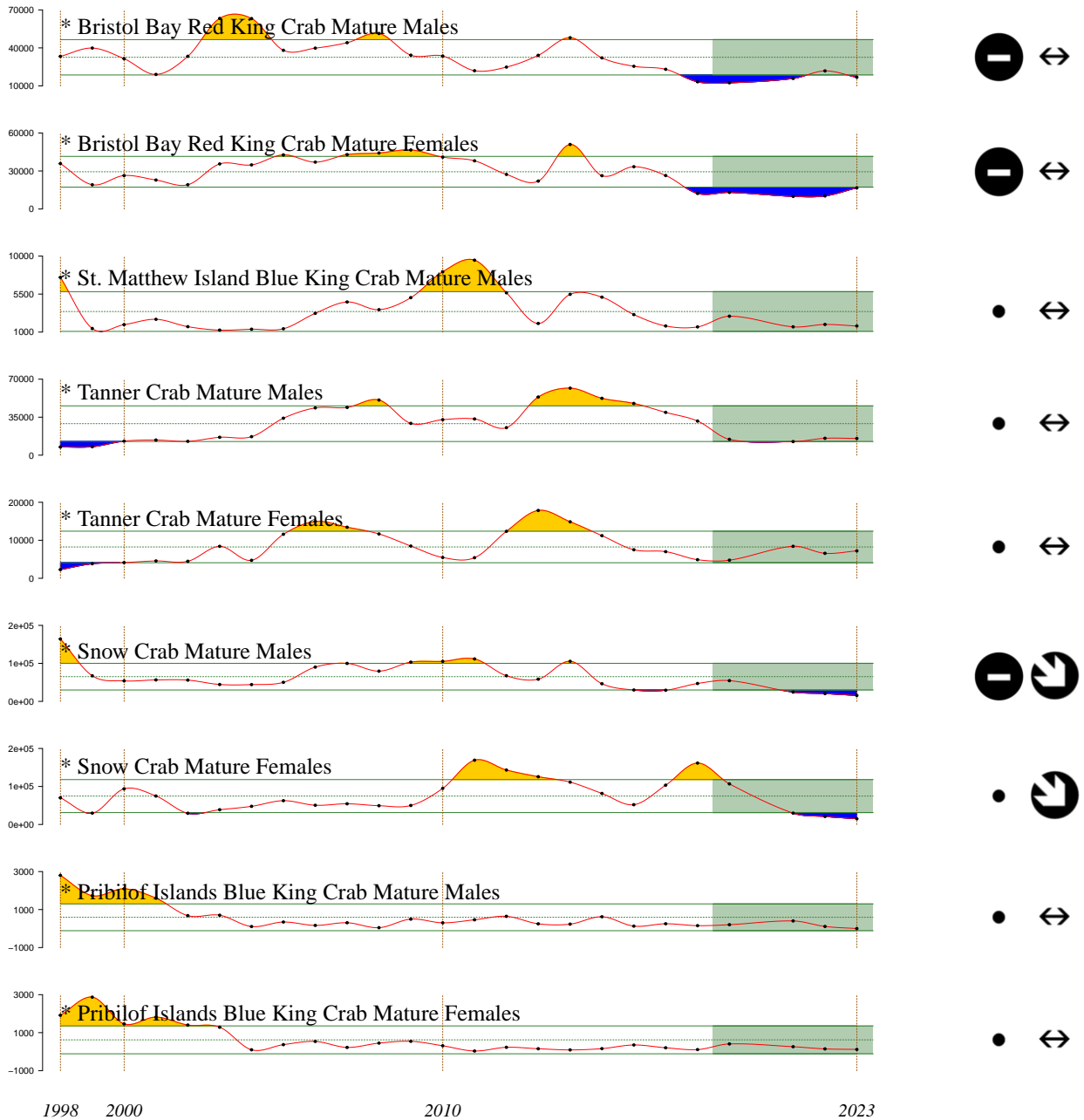
Figure 97: Biomass of commercial crab stocks caught on the NOAA eastern Bering Sea bottom trawl survey, 1998–2023.

Seabirds

Integrated Seabird Information

This integration is in response to ongoing collaborative efforts within the seabird community and contains contributions from (in alphabetical order):

Lauren Divine – Aleut Community of St. Paul Island, Ecosystem Conservation Office
Adrian Gall – ABR, Inc.—Environmental Research & Services
Sulli Gibson – Tanadgusix Corporation, St. Paul Island Tours
Timothy Jones – Coastal Observation and Seabird Survey Team [COASST], WA
Robb Kaler – U.S. Fish & Wildlife Service, Migratory Bird Management, Anchorage, AK
Aaron Lestenkof – Aleut Community of St. Paul Island, Ecosystem Conservation Office
Jackie Lindsey – Coastal Observation and Seabird Survey Team [COASST], WA
Trevor Niksik – Native Village of Savoonga
Matthew Rustand – U.S. Fish & Wildlife Service, Alaska Maritime National Wildlife Refuge, Homer, AK
Alexis Will – World Wildlife Fund, U.S. Arctic Program, University of Alaska Fairbanks

Last updated: October 2023

Summary Statement
Seabirds at the Pribilof Islands in the southeastern Bering Sea were monitored by the Alaska Maritime National Wildlife Refuge in 2023. Monitored species (common and thick billed murres, black-legged and red-legged kittiwakes, and red-faced cormorants) at the Pribilof Islands had a mixed year in terms of reproductive success. On St. George Island, reproductive success for common murres and black-legged kittiwakes was above average and was average for thick-billed murres and least auklets. On St. Paul Island, the timing of arrival of seabirds seemed average to community observers. Reproductive success was below average for common murres and black-legged kittiwakes and average for all other species monitored. Murres generally bred later and kittiwakes earlier, with murres seeming to experience nest failure later in the summer.

Colony attendance counts were average to relatively high for most species, although species that experienced recent population losses (least auklets and common murres) do not appear to be rebounding to historic numbers. Community observations at St. Paul Island indicated overall seabird numbers were above average, with a lot of red-legged kittiwake and murre eggs by the end of the season. However, no subsistence harvest of common or thick-billed murre eggs occurred on St. Paul Island in 2023 due to very low egg abundance early enough in the season to support harvest. Egging occurs early in the season to allow murres to re-lay an egg; there was a mis-match in timing between early season egging activities and later egg-laying.

On St. Lawrence Island in the northern Bering Sea, qualitative observations indicate that seabirds did well in 2023. Auklet numbers, especially crested auklets, were incredibly high at the Kitnik colony, comparable to numbers in the early 2000s, and colonies that had been essentially empty the last few years were at levels comparable to 2016.

Introduction

Seabirds are indicators of ecosystem changes in productivity, therefore population-level responses can signal shifts in prey availability that may similarly affect commercial fish populations. We synthesize information and observations from a variety of sources to provide an overview of environmental impacts to seabirds and what those indicate for ecosystem productivity as they pertain to fisheries management. We merge across information sources to derive regional summaries within the southeastern and northern Bering Sea and interpret changes in seabird dynamics with respect to understanding ecosystem productivity.

Approach

We focused on several attributes of seabirds that may serve as broader ecosystem indicators important to fisheries managers. We interpret these attributes as reflective of seabirds' life history and how they sample the ecosystem, either as fish-eating or plankton-eating species.

1. *Breeding timing* can represent conditions prior to breeding and/or phenological variation in the environment. Birds arriving to breed at an earlier date can reflect favorable winter and/or spring foraging conditions, or earlier peaks in ocean productivity.

2. *Reproductive success* can represent food availability around the colony during the breeding season, with a higher number of fledged chicks generally reflecting an increase in the local abundance of high-quality prey.

3. *Mortality* gives insight into environmental conditions and ecosystem impacts beyond breeding colonies and the breeding season.

Breeding and Reproductive Success
Southeastern Bering Sea (Pribilof Islands)
Common murres had the highest reproductive success in a decade at both of the Pribilof islands (Figures 98 and 99), albeit a small sample size. Counts of common murres on attendance plots were lower than in 2022 and remain quite low after a substantial reduction in 2015–2016. The mean hatch date was about a week later than the long-term average at both locations.

Thick-billed murres had above average reproductive success, but numbers of birds attending the colony were similar to recent years (relatively high on St. George Island/increasing in recent decades; relatively low on St. Paul Island/continued decline over recent decades). Thick-billed murres did not undergo a large population loss in 2015–2016 like common murres. The mean hatch date was about a week later than the long-term average at both locations.

Least auklets mean hatch date was 1 day earlier than the average; however, colony attendance remained very low. On St. George Island, least auklets experienced an average reproductive year but the number of nesting crevices remained low as biologists struggled to locate nests to follow. The mean count of least auklets at colony attendance plots on St. George Island was slightly lower than in 2022 and remained nearly an order of magnitude lower than the long-term mean.

Black-legged and red-legged kittiwake reproductive success was mixed in 2023 on the Pribilof Islands. On St. George Island, both species experienced above average reproductive success when compared to the long-term mean. On St. Paul Island, red-legged kittiwakes had average and black-legged kittiwakes had below average reproductive success. Timing was more than a week early for both species. Attendance was quite high, with St. Paul Island continuing to show the highest numbers of kittiwakes present since the 1970s.

Red-faced cormorants had an average year in regards to reproductive success at St. Paul Island in 2023. While monitored less intensively at St. George Island, cormorants did well, with all metrics above the long-term averages.
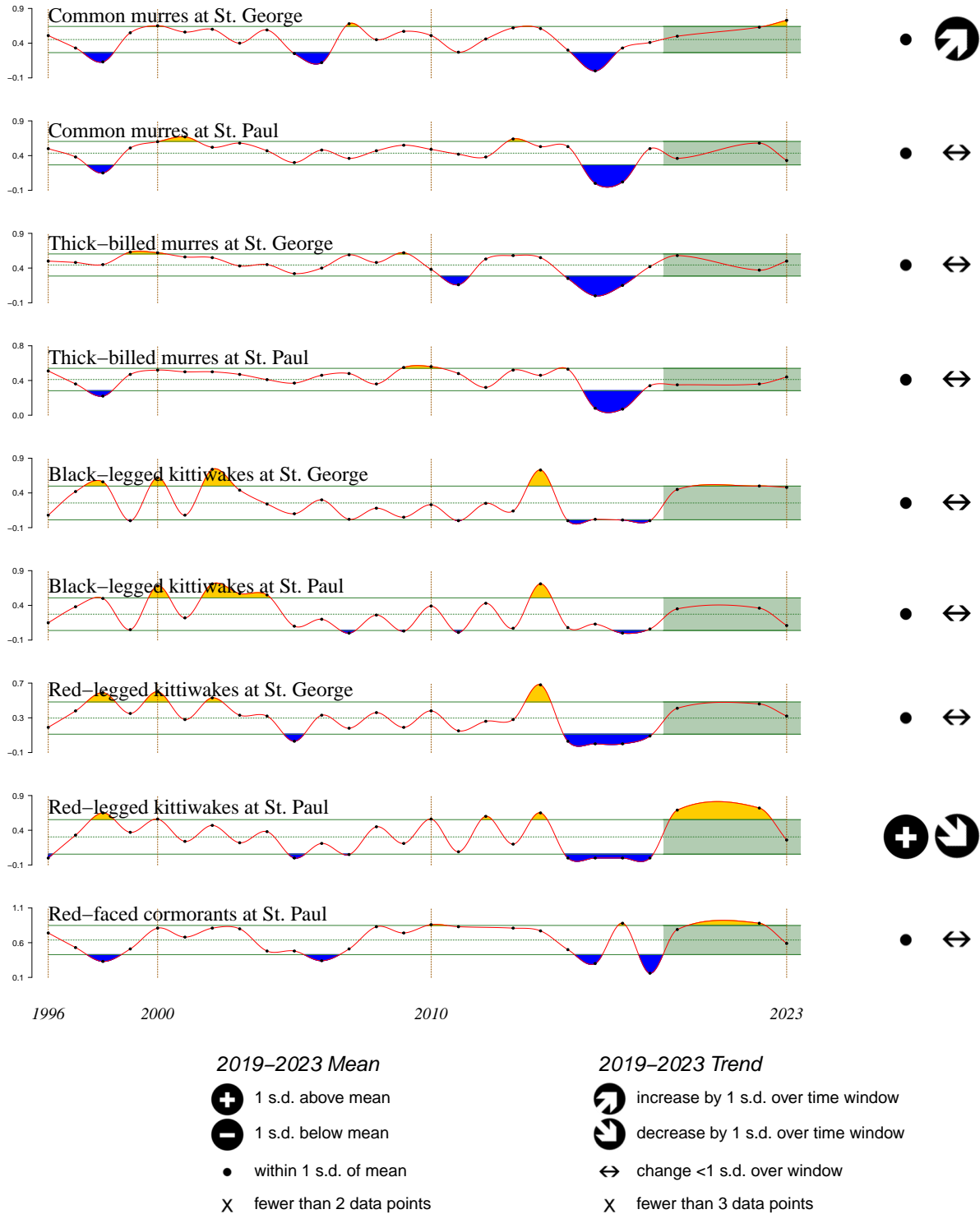
Figure 98: Reproductive success of five seabird species at St. George and St. Paul Islands between 1996–2023.

Alaska Maritime National Wildlife Refuge

2023 Seabird Report Card

Region	Annual monitoring site	Red-faced cormorants	Glaucous-winged gulls	Common murres	Thick-billed murres	Horned puffins	Tufted puffins	Red-legged kittiwakes	Black-legged kittiwakes	Northern fulmar	Fork-tailed storm-petrels	Leach's storm-petrels	Parakeet auklets	Least auklets
Chukchi Sea	Cape Lisburne													
Bering Sea	St. George	Way above		Way above	Average			Way above	Way above					Average
Bering Sea	St. Paul	Average		Below average	Average			Average	Below average					
Aleutian Islands	Buldir		Average		Below average	Average	Way above	Complete failure	Below average		Below average	Way above	Below average	Average
Aleutian Islands	Aiktak		Way above	Way above	Way above	Way above	Way above				Way above	Average		
Alaska Penin.	Chowiet	Way above		Below average	Below average	Below average	Way above		Complete failure				Average	
Gulf of Alaska	East Amatuli		Way above	Way above			Below average		Below average		Average			
Gulf of Alaska	St. Lazaria		Way above	Way above	Way above						Average	Average		

<<< Primarily fish eaters — Primarily zooplankton eaters >>>
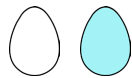
Eggs represent overall productivity relative to the long-term average.
White eggs indicate productivity derived from monitoring data;
colored eggs indicate productivity based on anecdotal observations.

Way above average!   Average   Below average   Complete failure

Figure 99: 2023 Alaska Maritime National Wildlife Refuge Seabird Report Card showing a summary of seabird productivity across monitored colonies.
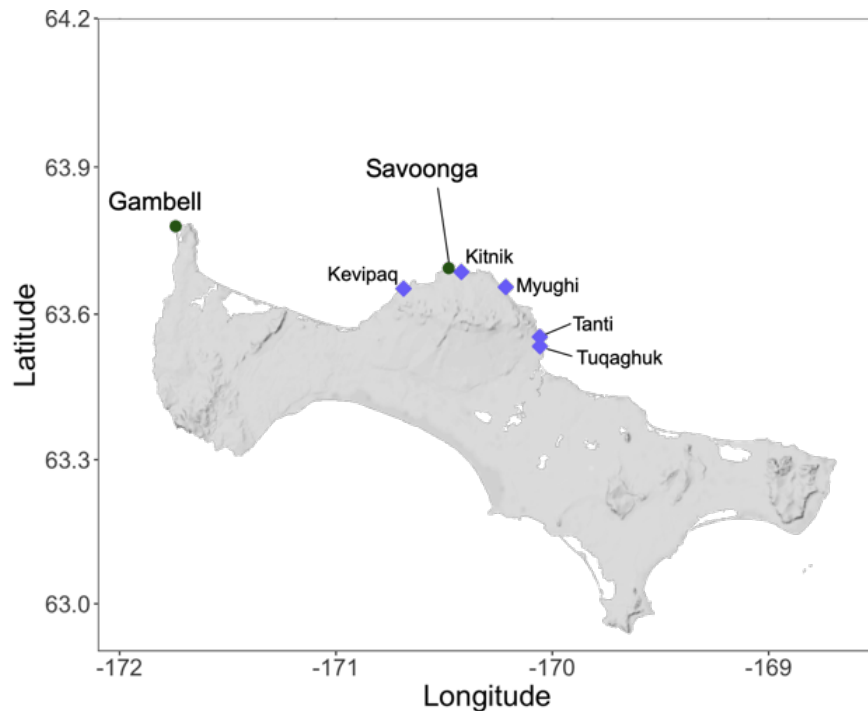
Figure 100: Map of St. Lawrence Island showing seabird colonies (purple diamonds). The communities of Gambell and Savoonga are denoted by green circles.

Northern Bering Sea (St. Lawrence Island)

In 2023 some monitoring work on St. Lawrence Island resumed, however only qualitative observations are available at this point as sample and data analysis are still pending (Figure 100). Field work began in mid-July. **Crested auklets** and **least auklets** hatched almost two weeks earlier than usual, chicks were already present on the Kitnik colony on July 16. Poor weather conditions during the summer hampered food load sampling attempts so no assessment of diet composition is available. However, food appears to have been abundant and of sufficient quality to support high colony attendance. Crested auklet numbers in particular were probably an order of magnitude higher than in recent years and comparable to numbers during field work in the early 2000s. Both auklet species were in higher attendance at colonies, using areas that had been empty in recent years.

No observations or data is currently available for **murres**.

Kittiwakes were observed in large foraging flocks close to shore in mid-July. This behavior is indicative of abundant food close to shore and has been observed in previous years when breeding success was relatively high for kittiwakes. However, no observations or data on reproductive success is currently available for kittiwakes.

General observations: There were a lot ("loads") of herring in the vicinity of Savoonga in mid-July. When out fishing, one observer noted that they encountered seven schools of herring when three was more normal.

Beached Bird Relative Abundance: Bering Sea
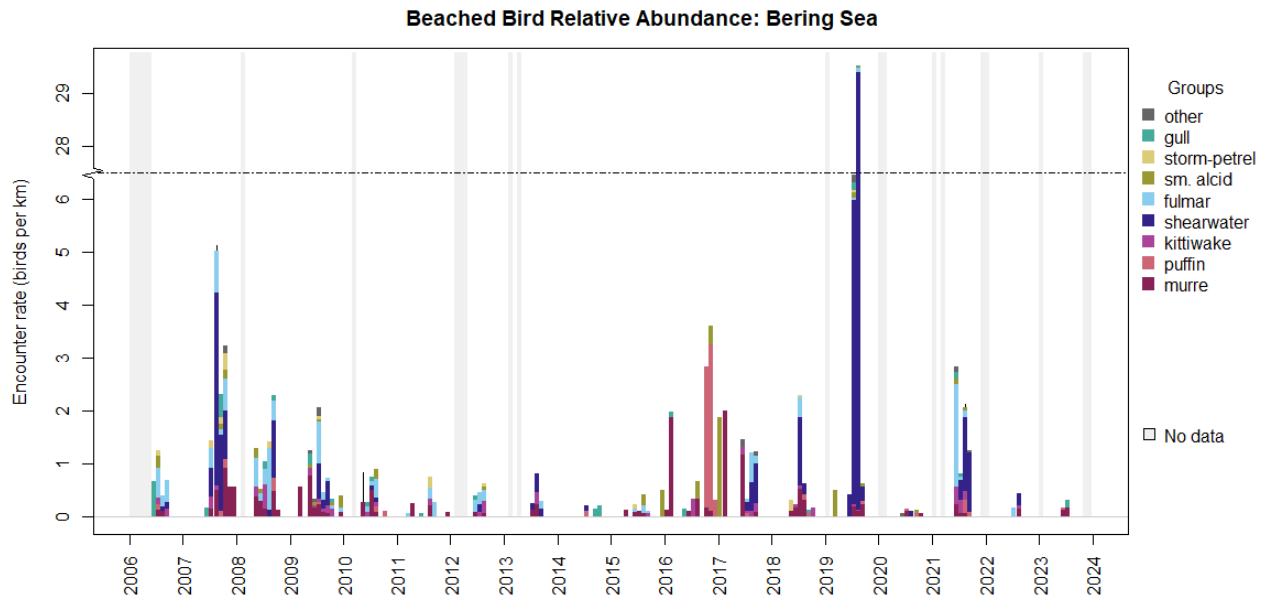
Figure 101: Month-averaged beached bird abundance, standardized per km of survey effort, for the eastern Bering Sea. Species groups (gull, storm-petrel, small alcid, fulmar, shearwater, kittiwake, puffin, murre) are depicted with different colors within each bar, with gray bars indicating months where no survey was conducted. **Note:** break in the y-axis between 6 and 28 birds/km, indicated by the dashed line, shows the magnitude of the 2019 die-off while still being able to distinguish patterns among other years. Credit: COASST.

Mortality

Eastern Bering Sea

Monitoring by the Coastal Observation and Seabird Survey Team (COASST) and regional partners provides a standardized measure of relative beached bird abundance. Surveys began in the eastern Bering Sea in 2006, and since that time over 1400 surveys have taken place across 25 beaches; in 2023, 27 surveys took place across 9 beaches, mostly concentrated on the Pribilof Islands, but sites in Bristol Bay and near Nome were also surveyed. Detailed methods for beached bird surveys can be found in Jones et al. (2019).

In 2023, surveyors reported relatively few carcasses across beaches in the Bering Sea. Encounter rates (all <1 per km) were not indicative of a die-off event. See monthly encounter rates for 2007 and 2019 in Figure 101 for examples of elevated encounter rates indicative of an unusual mortality event - typically defined as 5x the baseline rate.

In addition to monthly, effort-based surveys for beachcast seabirds, opportunistic reports of seabird mortality from beach-walkers, fishermen, and seasonal researchers are assembled by regional state, federal, tribal, and community partners each year. Species (if known), count, and location is required for each report, but standardized effort (outside of COASST and National Park Service surveys) is rarely available.

In 2023 there were relatively few opportunistic reports of additional beached bird carcasses in the eastern Bering Sea. Several reports of note concerned ~150 beached birds in early August from the Salmon River/Platinum Village on the southern side of Goodnews Bay. In mid-August ~250 beached murres were reported from the Nushagak Peninsula south of Togiak Bay in the southeastern Bering

Sea. Biologists at Togiak National Wildlife Refuge revisited both the Platinum Village area and the Nushagak area and collected samples from five murres at Platinum Village and 15 murres at Nushagak Peninsula. Fourteen of the 15 samples tested positive for Highly Pathogenic Avian Influenza (HPAI; Avian influenza Type A, bird flu virus, or H5N1) at Platinum Village, and four of five samples tested positive at the Nushagak Peninsula site. Avian influenza Type A virus does not normally infect people. Human infections with bird flu viruses are rare and most often occur after close or lengthy unprotected contact. Use best practices while harvesting birds (keep processing equipment clean, thoroughly cook meet 165°F/until juices run clear, and cook eggs). No additional opportunistic reports were received from surrounding areas, indicating these may have been isolated incidents. Overall, the relatively few opportunistic reports received, in conjunction with low encounter rates on regular beached bird surveys performed by COASST, suggests that there were no major die-off events in this region in 2023.

In 2022, reports of Highly Pathogenic Avian Influenza (HPAI) in wild seabirds and marine mammals across North America put the seabird mortality reporting community on high alert. While researchers prepared to document and collect seabirds on colonies for testing, large die-off events like those reported in the North Atlantic and European Union were not documented in Alaska. Individual reports of seabirds with HPAI from 2021–2022 (confirmed by laboratory test results) can be found through USGS[20].

Implications

Fish-eating, surface feeding seabirds include black-legged kittiwakes who feed on small schooling fish that are available at the surface (e.g., capelin, Arctic cod, juvenile pollock, and juvenile herring), making them potential indicators of processes affecting juvenile groundfish that migrate to the surface to feed. Fish-eating, diving seabirds include common murres who feed on small schooling fish (age-0 and age-1 pollock) to depths up to 90m, thus they have access to fish throughout the water column and to the ocean bottom in shallow areas. These species had mixed reproductive success at the Pribilof Islands in 2023 (average to positive on St. George Island, negative on St. Paul Island). This may indicate differences in local availability of small schooling forage fish in feeding areas utilized by seabirds of each island.

Planktivorous seabirds include least and crested auklets, which feed primarily on copepods and euphausiids. Shearwaters and thick-billed murres also consume euphausiids, along with larvae and small fish. All of these species are indicators of feeding conditions for planktivorous groundfish species, including the larvae and juveniles of fish-eating species. Other planktivorous species (e.g., auklets) had average reproductive success at the Pribilof Islands and appeared to be doing well on St. Lawrence Island where it was noted that adults were carrying food loads to provision chicks. Chick diets of crested auklets included euphausiids and least auklets were provisioning chicks with a mix of copepods, amphipods, and euphausiids.

---

[20]https://www.usgs.gov/centers/nwhc/science/distribution-highly-pathogenic-avian-influenza-north-america-20212022?utm_source=Newsletter&utm_medium=Email&utm_campaign=usgs-econews--vol-3--issue-2&utm_term=Image

Ecosystem or Community Indicators

Mean Lifespan of the Fish Community

Contributed by George A. Whitehouse[1] and Geoffrey M. Lang[2]
[1]Cooperative Institute for Climate, Ocean, and Ecosystem Studies (CICOES), University of Washington, Seattle WA
[2]Resource Ecology and Fisheries Management Division, Alaska Fisheries Science Center, National Marine Fisheries Service, NOAA
Contact: andy.whitehouse@noaa.gov
Last updated: October 2023

Description of indicator: The mean lifespan of the community is a proxy for the turnover rate of species and communities and reflects the resistance of the community to perturbations (Shin et al., 2010). Lifespan estimates of groundfish species regularly encountered during the NMFS/AFSC annual summer bottom-trawl survey of the eastern Bering Sea were retrieved from the AFSC Life History Database[21]. The groundfish community mean lifespan is weighted by biomass indices calculated from the bottom-trawl survey catch data.
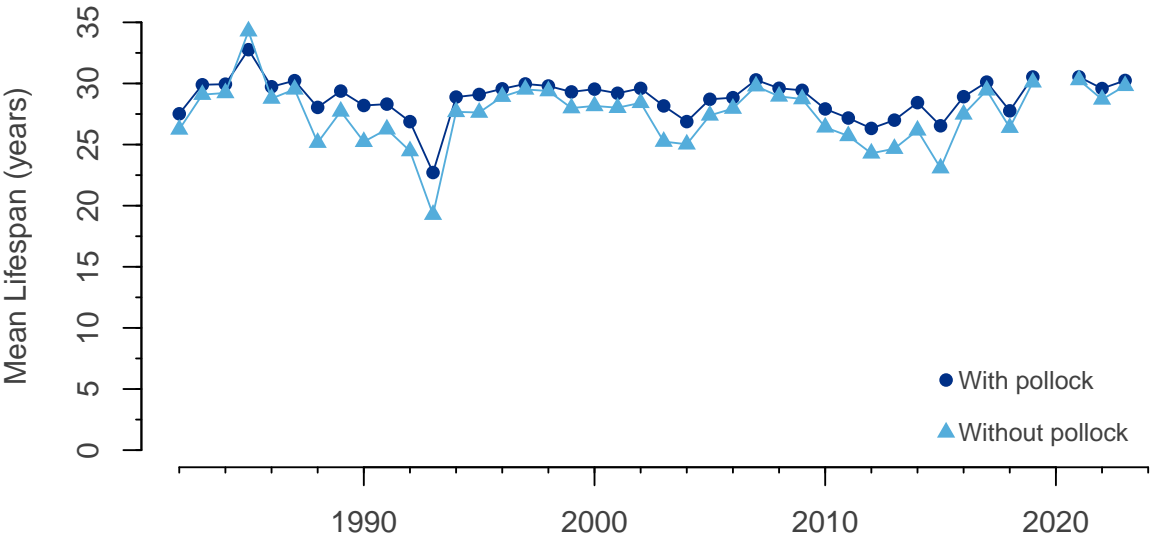
Figure 102: The mean lifespan of the eastern Bering Sea demersal fish community, weighted by biomass indices calculated from the NMFS/AFSC annual summer bottom-trawl survey. The circles are the series with pollock included and the triangles are the series without pollock included.

This indicator specifically applies to the portion of the demersal groundfish community that is efficiently sampled by the trawling gear used by NMFS during this survey at the standard survey sample stations (for survey details see Lauth et al. (2019)). Species that are infrequently encountered or not efficiently caught by the bottom-trawling gear are excluded from this indicator (e.g., sharks, grenadiers, myctophids, pelagic smelts). The survey index used here is the same as that used for foraging guild biomass indices on the report card (Figure 2).

---

[21]https://apps-afsc.fisheries.noaa.gov/refm/reem/lhweb/index.php

Walleye pollock is a biomass dominant species in the eastern Bering Sea and may drive the value of community indicators. Therefore this indicator is presented as two time series, one that includes and one that excludes walleye pollock.

Status and trends:
With pollock included: The mean lifespan of the eastern Bering Sea demersal fish community in 2023 is 30.2, up from 29.6 years in 2022, and is above the time series mean of 28.8 years (Figure 102, circles). Mean groundfish lifespan has generally been stable over the time series with only a small amount of year-to-year variation, and shows no indication of a long-term trend.

Without pollock included: The mean lifespan of the eastern Bering Sea groundfish community without walleye pollock in 2023 is 29.8, up from 28.7 years in 2022. Over the times series, the patterns and trends are similar between the two series with the values being slightly lower for the series without pollock (Figure 102, triangles). The exception to this pattern was 1985 when the mean lifespan was 32.8 with pollock included and 34.3 without pollock.

Factors influencing observed trends: Fishing can affect the mean lifespan of the groundfish community by preferentially targeting larger, older fishes, leading to decreased abundance of longer-lived species and increased abundance of shorter-lived species (Pauly et al., 1998). Interannual variation in mean lifespan can be influenced by the spatial distribution of species and the differential selectivity of species and age classes to the trawling gear used in the survey. Strong recruitment events or periods of weak recruitment could also influence the mean community lifespan by altering the relative abundance of age classes and species. For example, the low value observed in 1993 reflects a year of peak biomass index for capelin, a shorter-lived species. The peak mean lifespan for both series in 1985 was in part elevated by high biomass indices for long-lived species, such as sablefish. The lifespan of pollock is slightly higher than the mean groundfish lifespan without pollock. When pollock are removed from this indicator, there is a small decrease in value but the same overall trend is followed.

Implications: The groundfish mean lifespan has been stable over the time series of the summer bottom-trawl survey. There is no indication longer-lived species have decreased in relative abundance or are otherwise being replaced by shorter lived-species. Species that are short-lived are generally smaller and more sensitive to environmental variation than larger, longer-lived species (Winemiller, 2005). Longer-lived species help to dampen the effects of environmental variability, allowing populations to persist through periods of unfavorable conditions and to take advantage when favorable conditions return (Berkeley et al., 2004; Hsieh et al., 2006).

Mean Length of the Fish Community

Contributed by George A. Whitehouse[1] and Geoffrey M. Lang[2]
[1]Cooperative Institute for Climate, Ocean, and Ecosystem Studies (CICOES), University of Washington, Seattle WA
[2]Resource Ecology and Fisheries Management Division, Alaska Fisheries Science Center, National Marine Fisheries Service, NOAA
Contact: andy.whitehouse@noaa.gov
Last updated: October 2023

Description of indicator: The mean length of the groundfish community tracks fluctuations in the size of groundfish over time. This size-based indicator is thought to be sensitive to the effects of commercial fisheries because larger predatory fish are often targeted by fisheries and their selective removal would reduce mean size (Shin et al., 2005). This indicator is also sensitive to shifting community composition of species with different mean sizes. Fish lengths are routinely recorded during the NMFS bottom trawl survey of the eastern Bering Sea, which has occurred each year from 1982 to 2023, except in 2020. Mean lengths are calculated for groundfish species (or functional groups of multiple species; e.g., eelpouts) from the length measurements collected during the trawl survey. The mean length for the groundfish community is calculated with the species mean lengths, weighted by biomass indices (Shin et al., 2010) calculated from the bottom-trawl survey catch data.
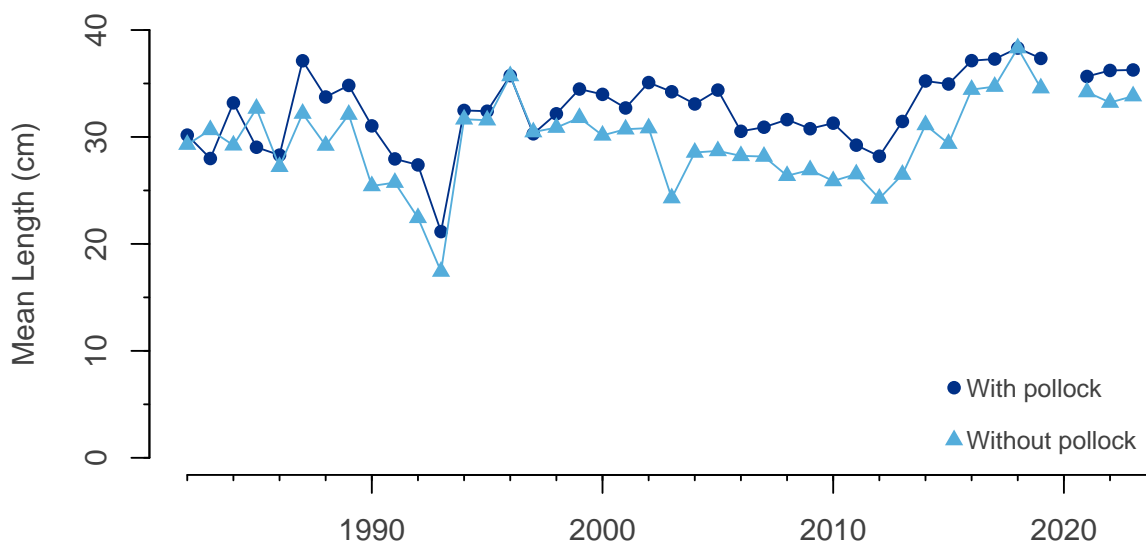
Figure 103: Mean length of the groundfish community sampled during the NMFS/AFSC annual summer bottom-trawl survey of the eastern Bering Sea (1982–2023). The groundfish community mean length is weighted by the relative biomass of the sampled species. The circles are the mean length with pollock included and the triangles are the series without pollock.

This indicator specifically applies to the portion of the demersal groundfish community that is efficiently sampled with the trawling gear used by NMFS during the summer bottom-trawl survey of the EBS at the standard survey sample stations (for survey details see Lauth et al. (2019)). Species that are infrequently encountered or not efficiently caught by the bottom-trawling gear are excluded from this indicator (e.g., sharks, grenadiers, myctophids, pelagic smelts). The survey index used here is the same as that used for foraging guild biomass indices on the report card (Figure 2).

179

Species (or functional groups) infrequently sampled for lengths (less than five times over the time series) are excluded from this indicator (e.g., capelin, eulachon, greenlings). Twenty-two species are included in this indicator. Eleven species had their lengths sampled in all 41 years of the survey time series. Another eleven species were sampled between 11 and 38 times over the time series. In years where species lengths were not sampled, we replaced with the long-term mean for that species.

Walleye pollock is a biomass dominant species in the eastern Bering Sea and may drive the value of community indicators. Therefore this indicator is presented as two time series, one that includes and one that excludes walleye pollock.

Status and trends:
With pollock included: The mean length of the eastern Bering Sea groundfish community in 2023 is 36.26 cm, nearly equal to the value of 36.22 in 2022, and remains above the long term mean of 32.6 (Figure 103, circles).

Without pollock included: The mean length of eastern Bering Sea groundfish without pollock is 33.82 cm in 2023, just up from 33.22 cm in 2022, and above the long term mean of 29.6 cm (Figure 103, triangles). This series trended upward from 2012 to 2018 then declined each survey year to 2022.

Factors influencing observed trends: This indicator is specific to the fishes that are routinely caught and sampled during the NMFS summer bottom-trawl survey. The estimated mean length can be biased if specific species-size classes are sampled more or less than others, and is sensitive to spatial variation in the size distribution of species. Changes in fisheries management or fishing effort could also affect the mean length of the groundfish community. Modifications to fishing gear, fishing effort, and targeted species could affect the mean length of the groundfish community if different size classes and species are subject to changing levels of fishing mortality. The mean length of groundfish could also be influenced by fluctuations in recruitment, where a large cohort of small forage species could reduce mean length of the community. Environmental factors could also influence fish growth and mean length by affecting the availability and quality of food or by direct temperature effects on growth rate.

Walleye pollock is a biomass dominant component of this ecosystem and year-to-year fluctuations in their mean size and biomass have a noticeable effect on this indicator. In 1993, their biomass index was above average but their mean size was the fifth lowest of the time series. Additionally, 1993 was a pronounced peak in the biomass index of capelin. This reduced the proportional contribution of other species to total groundfish biomass index, thus reducing the indicator value (i.e., mean length) in 1993. Years where this indicator attained its highest values (1987, 2016–2023) generally correspond to years of above average mean size and/or biomass index for pollock, except 2018, 2021, and 2023 where pollock mean size was above average but their biomass index was below average.

The series without pollock mirrored the overall trends in the series with pollock included, but was generally lower. This was because the mean length of pollock was generally a few cm greater than the mean length of the rest of the groundfish community. Exceptions occurred in 1983, 1985, and 2018 when the mean length of pollock was less than the mean of the rest of the groundfish community.

Implications: The mean length of the groundfish community in the eastern Bering Sea has been stable over the bottom-trawl time series (1982–2023) with some interannual variation. The collective stability of the combined biomass of relatively larger groundfish species has helped to maintain this indicator at its recent high values. Previous dips in this indicator were in part attributable to spikes in abundance of smaller forage species (e.g., capelin) as opposed to a sustained shift in community composition or reductions in species mean length.

Stability of Groundfish Biomass

Contributed by George A. Whitehouse
Cooperative Institute for Climate, Ocean, and Ecosystem Studies (CICOES), University of Washington, Seattle WA
Contact: andy.whitehouse@noaa.gov
Last updated: October 2023

Description of indicator: The stability of the groundfish community is measured with the inverse biomass coefficient of variation (CV; 1 divided by the coefficient of variation of total groundfish biomass (1/CV[B])). This indicator provides a measure of the stability of the ecosystem and its resistance to perturbations. The variability of total community biomass is thought to be sensitive to fishing and is expected to increase with increasing fishing pressure (Blanchard and Boucher, 2001). The CV is the standard deviation of the groundfish biomass index over the previous 10 years divided by the mean biomass over the same time span Shin et al. (2010). The biomass index was calculated from the catch of the NMFS/AFSC annual summer bottom-trawl survey of the eastern Bering Sea (EBS). Since 10 years of data are required to calculate this metric, the indicator values start in 1991, the tenth year in the trawl survey time series (1982–2023). This metric is presented as an inverse, so as the CV increases the value of this indicator decreases, and if the CV decreases the value of this indicator increases.
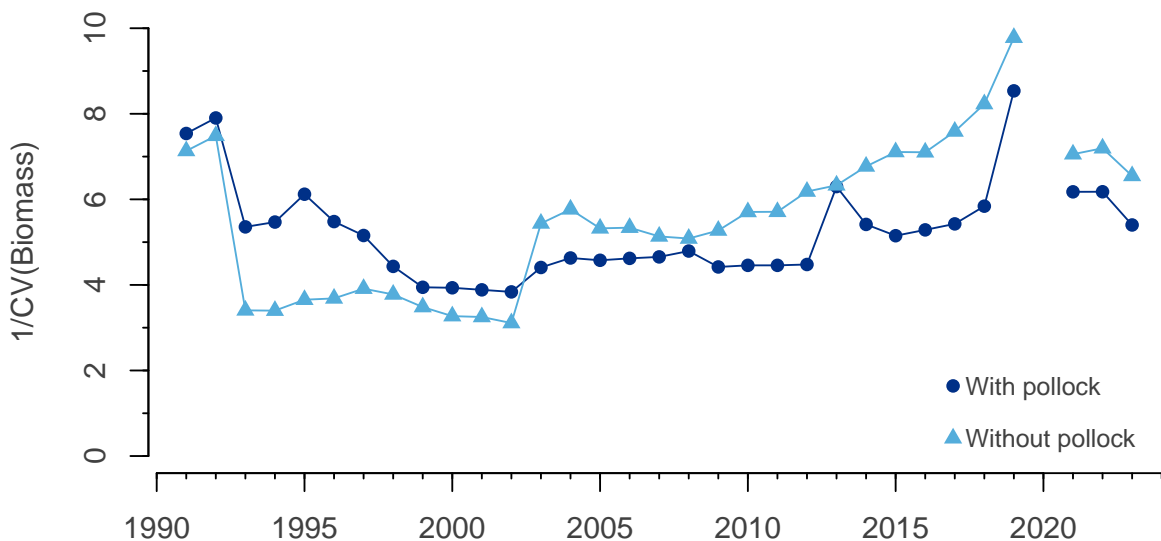
Figure 104: The stability of groundfish biomass in the eastern Bering Sea represented with the inverse biomass coefficient of variation of total groundfish biomass (1/CV[B]). The circles are the series with pollock included in the index, and the triangles are the same series but with pollock excluded.

This indicator specifically applies to the portion of the demersal groundfish community that is efficiently sampled by the trawl gear used during the annual summer bottom-trawl survey (for survey details see Lauth et al. (2019)). Species that are infrequently encountered or not efficiently caught by the bottom-trawling gear are excluded from this indicator (e.g., sharks, grenadiers, myctophids, pelagic smelts). The survey index used here is the same as that used for foraging guild biomass indices on the report card (Figure 2).

Walleye pollock is a biomass dominant species in the EBS and may drive the value of this community

indicator. Therefore this indicator is presented as two time series, one that includes and one that excludes walleye pollock.

Status and trends:
With pollock included: The state of this indicator in 2023 is 5.401, which is nearly equal to its time series mean of 5.26 (Figure 104, circles). An earlier peak of 7.90 was observed in 1992, which was followed by a steady decrease to a low of 3.84 in 2002. Since then it gradually increased to a value of 5.84 in 2018 before sharply increasing to a recent high in 2019.

Without pollock included: The groundfish stability indicator decreased from 7.19 in 2022 to 6.55 in 2023 (Figure 104, triangles). This indicator dropped sharply from 7.49 in 1992 to 3.41 in 1993, and remained below 4.0 until 2003, where the value increased to 5.44. The indicator remained relatively stable until 2010, when it began a steady upward trend to the series high value in 2019.

Factors influencing observed trends: Fishing is expected to influence this metric as fisheries can selectively target and remove larger, long-lived species affecting population age structure (Berkeley et al., 2004; Hsieh et al., 2006). Larger, longer-lived species can become less abundant and be replaced by smaller shorter-lived species (Pauly et al., 1998). Larger, longer-lived individuals help populations to endure prolonged periods of unfavorable environmental conditions and can take advantage of favorable conditions when they return (Berkeley et al., 2004). A truncated age-structure could lead to higher population variability (CV) due to increased sensitivity to environmental dynamics (Hsieh et al., 2006). Interannual variation in this metric could also be influenced by interannual variation in species abundance in the trawl survey catch, patchy spatial distribution for some species, or species distribution shifts (Stevenson and Lauth, 2019; Thorson, 2019*b*). This metric reflects the stability of the portion of the groundfish community that is represented in the catch data of the annual summer bottom-trawl survey. Both sharp increases or decreases in species index values can increase variability and reduce the indicator value.

The high values for this indicator in 2019 and at the start of the time series are indicative of stable groundfish biomass with a relatively low CV during the previous ten years. The CVs for both time series in 2019 were the lowest over their respective time series resulting in their highest indicator values. The sharp drop in total biomass in 2021, particularly for pollock, increased the CV resulting in lower indicator values in 2021. Previously, both series dropped sharply from 1992 to 1993. This was because the index for capelin in 1993 was anomalously high which increased variability and reduced the indicator value. In 2003, both series increased, which was in part due to the high capelin value in 1993 no longer being a part of the most recent 10 years.

In 2009, the series without pollock begins a steady increase towards its high value in 2019. The series with pollock has a more modest positive trend over the same span, with high values in 2013 and 2019. Pollock is a biomass dominant species in the EBS and interannual fluctuations in their biomass are sufficient to increase variability for the total groundfish community and thus, reduce the indicator value. The series without pollock is more sensitive to fluctuations of other species, such as capelin. The sharp increase in the capelin index in 1993 kept this series lower than the series with pollock included from 1993–2002.

Implications: This measure indicates that the EBS groundfish community has been generally stable over the time period examined here, particularly since 2003. While the indicator value dropped from 2022 to 2023 for both indicators (with and without pollock), both series remain above their long term means in 2023 and indicate a maintenance of community biomass stability.

Emerging Stressors

Ocean Acidification

Contributed by Darren Pilcher[1,2], Jessica Cross[3], Natalie Monacci[4], Esther Kennedy[5], Elizabeth Siddon[6], and W. Christopher Long[7]
[1]Cooperative Institute for Climate, Ocean, and Ecosystem Studies (CICOES), University of Washington, Seattle WA
[2]NOAA – Pacific Marine Environmental Laboratory [PMEL]
[3]Pacific Northwest National Laboratory
[4]Ocean Acidification Research Center, University of Alaska Fairbanks
[5]University of California, Davis
[6]NOAA Fisheries, Alaska Fisheries Science Center, Auke Bay Laboratories, Juneau, AK
[7]NOAA Fisheries, Alaska Fisheries Science Center, Kodiak Laboratory, Kodiak, AK
Contact: darren.pilcher@noaa.gov
Last updated: September 2023

Description of indicator: The oceanic uptake of anthropogenic CO_2 is decreasing ocean pH and carbonate saturation states in a process known as ocean acidification (OA). The cold, carbon rich waters of the Bering Sea are already naturally more corrosive than other regions of the global ocean, making this region more vulnerable to rapid changes in ocean chemistry. The projected areal expansion and shallowing of these waters with continued absorption of anthropogenic CO_2 from the atmosphere poses a direct threat to marine calcifiers and an indirect threat to other species through trophic interactions. These OA risks demonstrate a clear need to track and forecast the spatial extent of acidified waters in the Bering Sea.

Here, we present updated carbonate chemistry output from the Bering Sea ROMS model (Bering10K; Pilcher et al., 2019), which is updated annually and currently spans 1970–August 27, 2023. We show spatial plots for Bering Sea bottom water pH, including both the conditions in 2023 (Figure 105, left) as well as the 2023 detrended anomaly (Figure 105, right). The detrended anomaly removes the impact of ocean acidification (otherwise a slow, consistent process) and highlights the role of natural processes, which generate most of the interannual variability in the carbon system. It is calculated as the residual after removing the linear trend over the entire 1970–2023 hindcast, similar to removing the global warming trend from a long term temperature timeseries.

We focus on bottom waters and the late summer time frame because this is where we expect the most acidic waters to develop, due to the combination of ocean acidification pressures and natural seasonal biological respiration. This is also when temperatures are close to their highest and are thus most likely to have synergistic negative effect on crabs (Swiney et al., 2017). This model output is used to develop indices for both pH and the aragonite saturation state (Ω_{arag}) using threshold values of biological significance (Figures 106 and 107). The growth and survival of red king crab and tanner crab are negatively affected at pH $\leq$7.8 (Long et al., 2013), and bivalve larvae are negatively affected at Ω_{arag} <1 (Waldbusser et al., 2015). The goal of this index time series, along with the spatial anomaly plot, is to provide a quick assessment of the summer water pH and Ω_{arag} conditions compared to previous years.
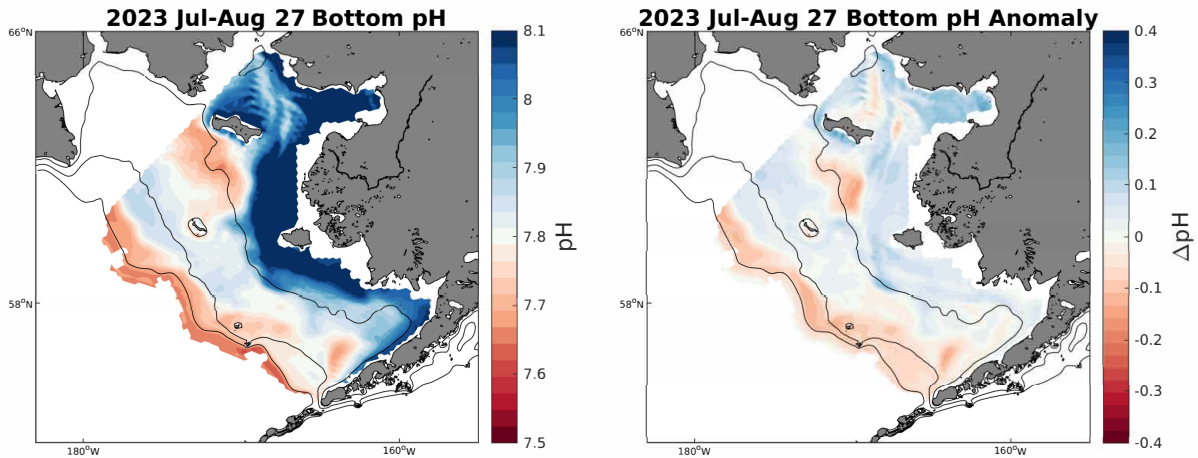
Figure 105: Model spatial maps of July-August 27 averaged bottom water pH for (left) 2023 hindcast and (right) the 2023 detrended anomaly. Contour lines denote the 50m, 100m, and 200m isobaths. Regions that are outside of the eastern Bering Sea management region are omitted. Impacts of ocean acidification on fisheries are understood to be a combination of the temporal duration, biogeochemical intensity, and spatial extent. This visualization shows both the intensity and extent of acidified conditions over the Bering Sea shelf.

Status and trends: Modeled bottom water pH and Ω_{arag} were slightly higher than the detrended shelf average baseline conditions over most of the inner and middle shelf, with pH values generally near or slightly greater than 7.8 (Figure 105, left). In general, modeled inner shelf waters had much higher pH values than normal, and were overall slightly higher than usual. An exception is the inner shelf region south of St. Lawrence Island, where modeled waters were lower in pH than normal with areas of pH <7.8. Notably, the outer shelf negative pH anomaly - a persistent anomaly in the model since 2018 - was still present, but has slightly weakened in the northwest outer shelf compared to 2022 (Figure 105, right).

Factors influencing observed trends: Modeled bottom pH and Ω_{arag} both improved this year compared to lowest to near-lowest values for the model hindcast in 2022. Most of this increase was driven by higher values throughout the inner and middle shelf, with the outer shelf still anomalously lower. However, bottom pH and Ω_{arag} values are still low relative to the entire model time frame, driven mainly by the long term decreasing trend caused by ocean acidification. We anticipate that natural variability will continue to be the dominant source of interannual variability such as that illustrated between 2022–2023, and that over decadal time frames, pH and Ω_{arag} will continue to decline with ocean acidification.

Implications: Based on the sensitivity of red king crab to pH, previous work suggests that OA may have significant negative impacts to the red king crab fishery (Seung et al., 2015; Punt et al., 2016). However, these effects are not expected to emerge at present, as other environmental variables (e.g., temperature) are better predictors of red king crab variability. Modeled pH and Ω_{arag} water conditions in Bristol Bay for 2023 are near or slightly above the detrended average conditions and the shallower inner shelf waters that serve as habitat for juvenile red king crab are relatively well buffered. Portions of the outer and middle shelf that overlap juvenile snow crab and Tanner crab habitat contain model pH values less than 7.8, although these waters are naturally relatively more acidic. A recent experimental study suggests that snow crab are resilient to these pH levels (Algayer et al., 2023), though Tanner crab juveniles can be sensitive to pH ≤ 7.8 (Long et al., 2013). At this time, there is no evidence that OA can be linked to recent declines in surveyed snow crab and red king crab populations.

Bering Sea Shelf Jul-Sep Index
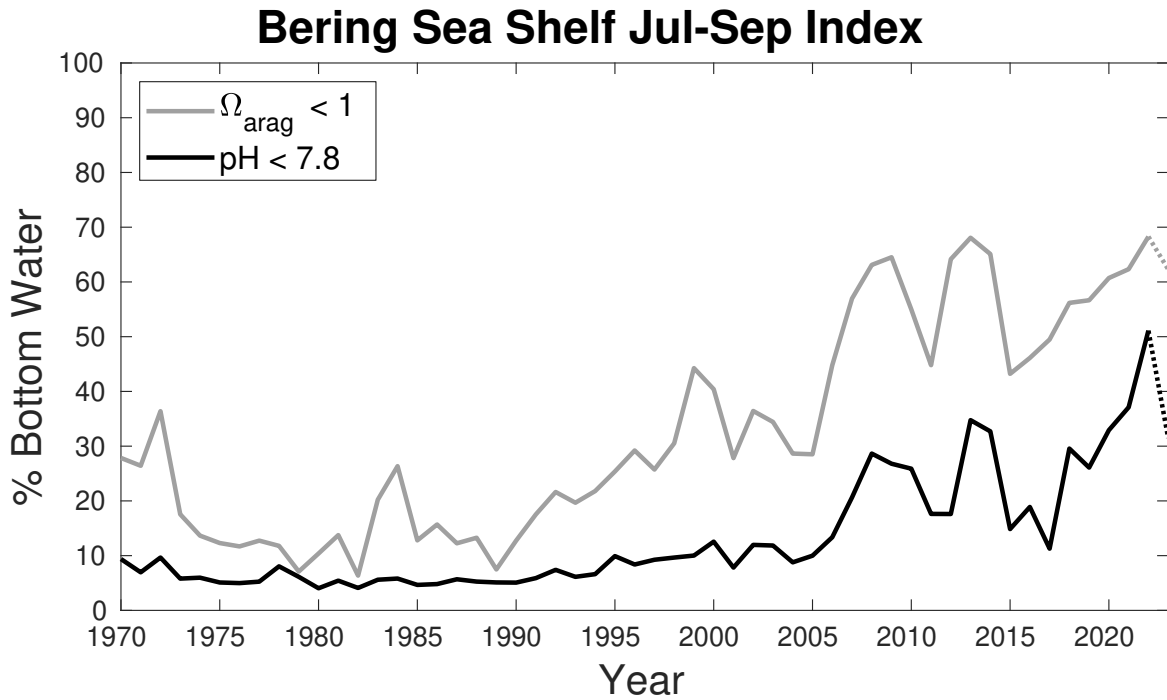
Figure 106: Model timeseries of the July-September pH index (black line) and Ω_{arag} undersaturation index (grey line). Each index is calculated as the percent of spatial area of the eastern Bering Sea region (see Figure 105) where bottom waters have a July-September average below the denoted value. The dotted portion at the end represents the incomplete 2023 value, which is run up through August 27. Impacts of ocean acidification on fisheries are understood to be a combination of the temporal duration, biogeochemical intensity, and spatial extent. This visualization shows the percent area (spatial extent) of the shelf that is exposed to potentially harmful biogeochemical conditions.
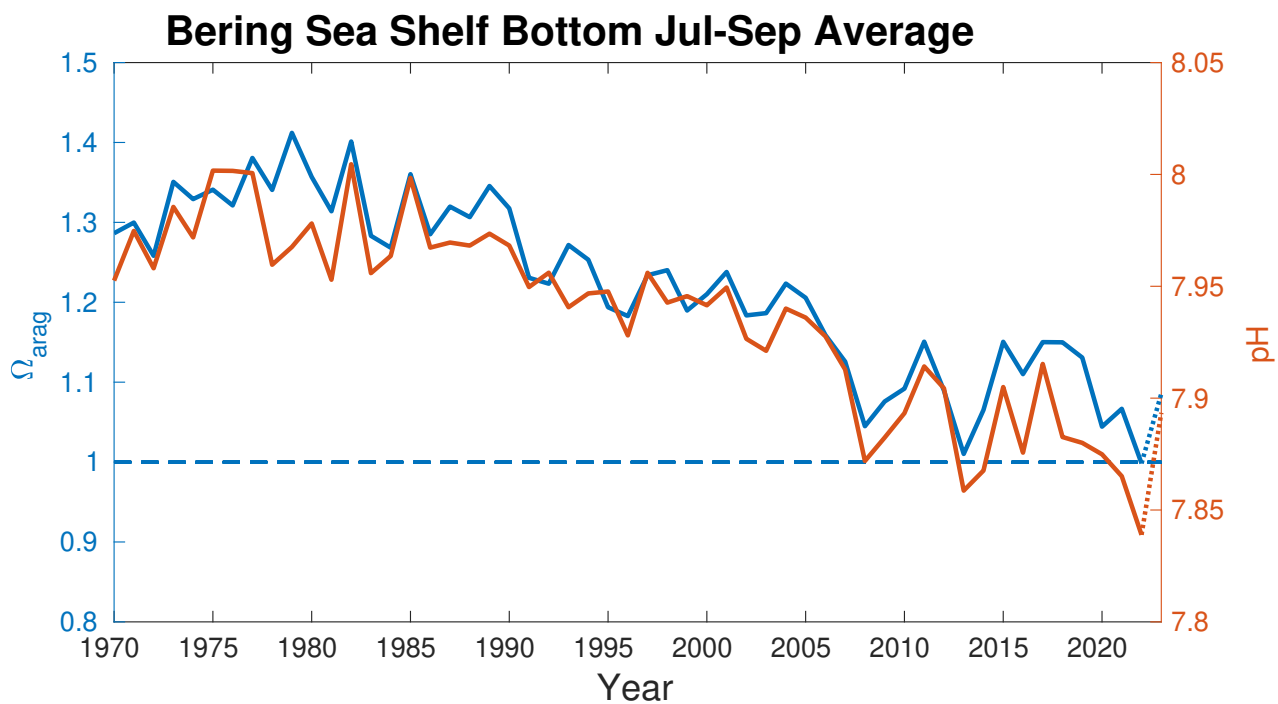
Figure 107: Model timeseries of the July-September average bottom water Ω_{arag} (left vertical axis, blue) and pH (right vertical axis, orange). The dotted portion at the end represents the incomplete 2023 value, which is run up through August 27. Impacts of ocean acidification on fisheries are understood to be a combination of the temporal duration, biogeochemical intensity, and spatial extent. Visualizing the net shelf-wide average, rather than scaling these variables spatially (see Figure 106), helps show the intensity of aggregate conditions. However, it is important to consider this figure in context with Figures 105 and 106, as a shelf-wide average may disguise some areas of resilience (e.g., cool colors, Figure 105).

Harmful Algal Blooms

Contributed by Thomas Farrugia[1], Natalie Rouse[2], Emma Pate[3], Kathleen Easley[4], and Louisa Castrodale[4]
[1] Alaska Ocean Observing System, Anchorage, AK
[2] Alaska Veterinary Pathology Services, Eagle River, AK
[3] Norton Sound Health Corporation, Nome, AK
[4] AK Department of Health and Social Services, Section of Epidemiology, Anchorage, AK
Contact: farrugia@aoos.org
Last updated: September 2023

Sampling Partners:

Alaska Ocean Observing System	NOAA WRRN-West
Alaska Sea Grant	Norton Sound Health Corporation
Alaska Veterinary Pathologists	University of Alaska Fairbanks
Aleut Community of St. Paul	USGS Alaska Science Center
Aleutian Pribilof Island Association	Woods Hole Oceanographic Institution
Knik Tribe of Alaska	

Description of indicator: Alaska's most well-known and toxic harmful algal blooms (HABs) are caused by *Alexandrium* spp. and *Pseudo-nitzschia* spp. *Alexandrium* produces saxitoxin (STX) which can cause paralytic shellfish poisoning (PSP) and has been responsible for five deaths and over 100 cases of PSP in Alaska since 1993[22]. Analyses of paralytic shellfish toxins are commonly reported as µg of toxin/100g of tissue, where the FDA regulatory limit is 80µg/100g. Toxin levels between 80µg–1000µg/100g are considered to potentially cause non-fatal symptoms, whereas levels above 1000µg/100g (∼12x regulatory limit) are considered potentially fatal.

Pseudo-nitzschia produces domoic acid which can cause amnesic shellfish poisoning and inflict permanent brain damage. *Pseudo-nitzschia* has been detected in 13 marine mammal species and has the potential to impact the health of marine mammals and birds in Alaska. No human health impacts of domoic acid (DA) have been reported in Alaska, although both acute and chronic amnesic shellfish poisoning has been reported in several states, including Washington and Oregon.

Department of Health, Section of Epidemiology (SOE) continues to partner with the Alaska Harmful Algal Bloom (AHAB) Network. Nurse consultants join monthly meetings and collaborate with stakeholders so they can be made aware of reportable illness such as PSP. In April 2022, an Epidemiology Bulletin describing cases was released[23]. More information about PSP and other shellfish poisoning can be found on the SOE website[24].

The State of Alaska tests all commercial shellfish harvests. However there is no state-run shellfish testing program for recreational and subsistence shellfish harvest. Regional programs, run by Tribal, agency, and university entities, have expanded over the past five years to provide test results to inform

---

[22] State of Alaska. Epidemiology Bulletin. 2022. Available at: http://www.epi.alaska.gov/bulletins/docs/b2022_05.pdf

[23] http://www.epi.alaska.gov/bulletins/docs/b2022_05.pdf

[24] https://health.alaska.gov/dph/Epi/id/Pages/dod/psp/default.aspx; Kathleen Easley/Louisa Castrodale, DOH Section of Epidemiology

harvesters and researchers and reduce human health risk (Figure 108). All of these entities are partners in the AHAB Network which was formed in 2017 to provide a statewide approach to HAB awareness, research, monitoring, and response in Alaska. More information on methods can be found on the Alaska HAB Network website[25].
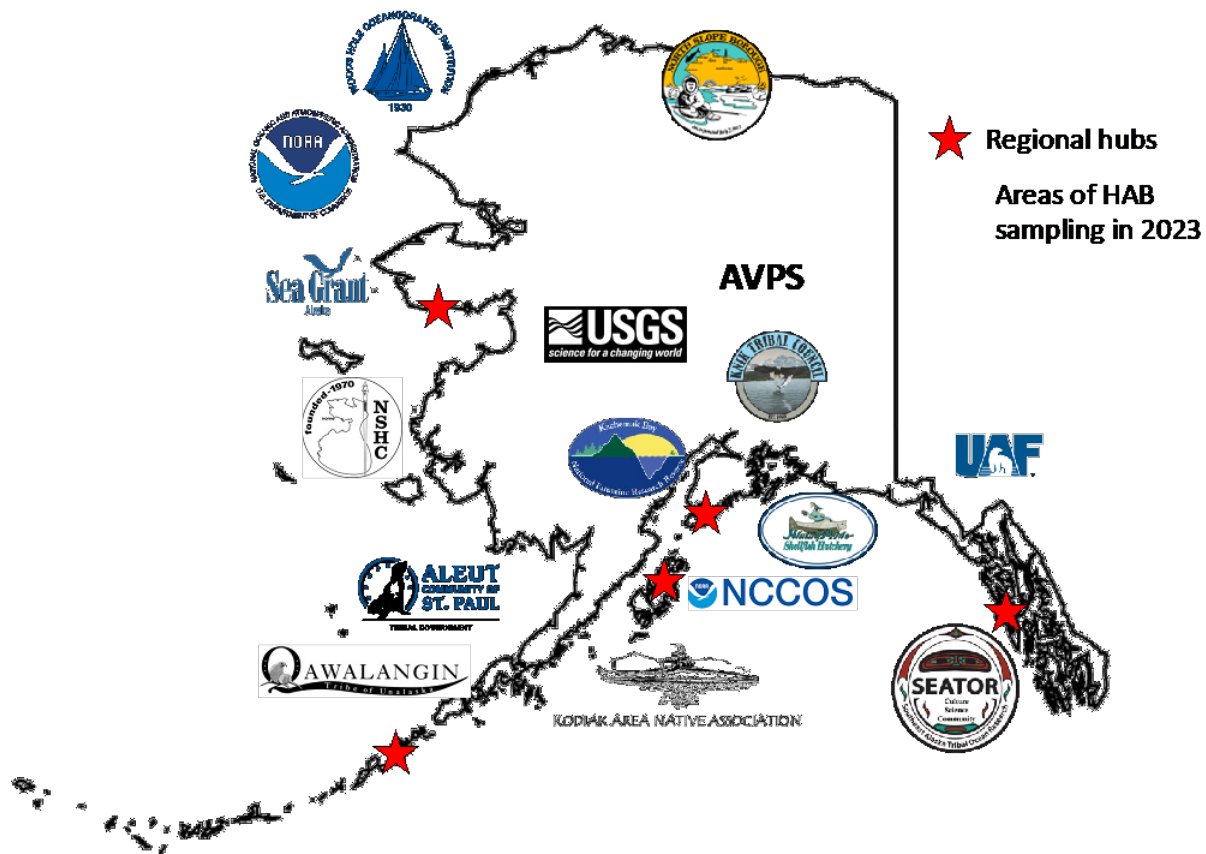
Figure 108: Map of 2023 sampling areas conducted by partners of the Alaska Harmful Algal Bloom (AHAB) Network. Opportunistic sampling of marine mammal tissue and other marine species occurs statewide and is not shown here.

Status and trends:

Alaska Region: Results from shellfish and phytoplankton monitoring showed a slight uptick in the presence of harmful algal blooms (HABs) and toxins throughout all regions of Alaska in 2023 compared to 2022, although the overall levels were still lower than in 2019–2021. Bivalve shellfish from areas that are well known for having PSP levels above the regulatory limit, including Southeast Alaska and the Aleutians, continued to have samples that tested above the regulatory limit, albeit less frequently than since 2019 and 2020. Overall, 2023 seems to have been slightly less active for blooms and toxin levels than 2019–2021, but areas continue to have HAB organisms in the water and shellfish testing well above the regulatory limit, especially between March and September. Over the last few years, the dinoflagellate *Dinophysis* has become more common and abundant in water samples and 2023 continued that trend.

---

[25]https://ahab.aoos.org

We are also seeing a geographic expansion of areas that are sampled for phytoplankton species, so the decrease in the number of HABs detected may be more related to generally cooler water temperatures, especially in the Gulf of Alaska. In the Bering Sea, HABs were monitored through the opportunistic placement of Imaging Flow Cytobots on the R/V *Sikuliaq* as it transited the Bering and Chukchi Seas on research cruises.

Alaska Veterinary Pathology Services (AVPS) and University of Alaska Anchorage spearheaded a behavioral log as part of the ECOHAB project where any unusual (and potentially HABs exposure-related) wildlife behaviors could be recorded. They also collected 27 samples for STX and DA testing at WARRN West, pending shipment this fall.

Northern Bering Sea: Norton Sound Health Corporation (NSHC) staff continue to develop the Norton Sound Tribal Harmful Algal Bloom Program (NSTHAB) along with regional partners. Water samples are being collected along with traditional seafood samples for toxin testing at all locations within the NSTHAB. In addition, water samples were collected regularly in 2023 in and near Nome, AK for microscopy to identify phytoplankton target species of *Alexandrium*, *Dinophysis*, and *Pseudo-nitzschia*. During microscopy work on samples collected in July 2023, NSHC staff detected high levels of *Dinophysis* sp. in the waters off of Cape Nome in Norton Sound. Samples were sent to NOAA and the presence of three species of *Dinophysis* was confirmed by experts using scanning electron microscopy. The *Dinophysis* species represented a major component of the phytoplankton community of the sample, leading to the determination of a bloom. *Dinophysis* is a dinoflagellate that is often found further south (British Columbia, Pacific Northwest) but is starting to be seen more commonly in Alaska waters. Under certain conditions, *Dinophysis* can produce okadaic acid, which, if consumed, can lead to Diarrhetic Shellfish Poisoning (DSP). No cases of DSP have been confirmed in Alaska to date. It is important to continue monitoring for *Dinophysis* in Alaska so that potential northward distribution shifts of this phytoplankton are recorded.

Through the ECOHAB project "Harmful algal bloom toxins in Arctic food webs", community samplers and researchers are collecting samples throughout the food web to test for HAB toxins. For more information about this project, see Lefebvre et al., p. 191.

A comprehensive summary of 2022 regional HAB monitoring efforts and results can be found here: `https://ahab.aoos.org/wp-content/uploads/2023/10/AHAB-2023-Summary-Report-final.pdf`.

Factors influencing observed trends: HABs are likely to increase in intensity and geographic distribution in Alaska waters with warming water temperatures. Observations in Southeast and Southcentral Alaska suggest *Alexandrium* blooms occur at temperatures above 10°C and salinities above 20 (Vandersea et al., 2018; Tobin et al., 2019; Harley et al., 2020). As waters warm throughout Alaska, blooms may increase in frequency and geographic extent.

Implications: HABs pose a risk to human health when present in wildlife species that people consume, including shellfish, birds, and marine mammals. Research across the state is attempting to better understand the presence and circulation of HABs in the food web. HAB toxins have been detected in stranded and harvested marine mammals from all regions of Alaska in past years (Lefebvre et al., 2016). A multi-disciplinary statewide study funded by NOAA's ECOHAB program is underway and encompasses ship-based sediments samples, water samples, zooplankton samples, krill samples, copepod samples, multiple species of fish, bivalves, and the continuation of sampling subsistence-harvested and dead, stranded marine mammals.

ECOHAB: Harmful Algal Bloom (HAB) Toxins in Arctic Food Webs

Contributed by Kathi Lefebvre[1], Donald M. Anderson[2], Gay Sheffield[3], Raphaela Stimmelmayr[4], Evangeline Fachon[2], Patrick Charapata[1], Robert Pickart[2], Emily Bowers[1], and Emma Pate[5]

[1]Environmental and Fisheries Science, Northwest Fisheries Science Center, National Marine Fisheries Service, NOAA, Seattle, WA
[2]Woods Hole Oceanographic Institution, Woods Hole, MA
[3]University of Alaska Fairbanks, Alaska Sea Grant, Nome, AK
[4]North-Slope Borough Department of Wildlife Management, Utqiagvik, AK
[5]Norton Sound Health Corporation, Nome, AK
Contact: kathi.lefebvre@noaa.gov
Last updated: September 2023

Description of indicator: *Alexandrium* and *Pseudo-nitzschia* are two common harmful algal bloom (HAB) species in Alaskan waters that produce neurotoxic compounds such as saxitoxin (STX; generated by *Alexandrium* species; causes Paralytic Shellfish Poisoning PSP) and domoic acid (DA; generated by *Pseudo-nitzschia* species; causes Amnesic Shellfish Poisoning ASP). Monitoring the presence and abundance of HAB cell (i.e., *Alexandrium* and *Pseudo-nitzschia*) densities and toxin (STX and DA) prevalence in marine food webs are useful indicators of ecosystem health and potential threats to wildlife and human health. There is clear evidence that HAB toxins are present in Arctic and Subarctic food webs (Figure 109). The risks of these toxins include human illness and death associated with seafood consumption as well as health impacts to marine wildlife at multiple trophic levels. Many commercially valuable shellfish and finfish are impacted by these toxins, as well as marine mammals, invertebrates, seabirds, and filter-feeding fishes that are harvested for subsistence purposes and consumed by Alaska's coastal communities.

Status and trends: As the climate has warmed over the past few decades, the Pacific sector of the Arctic Ocean has warmed with dramatic consequences. The quality, quantity, and duration of sea ice has decreased markedly due to earlier melting and a delayed freeze-up (Frey et al., 2014). The input of Pacific water northwards through the Bering Strait has increased, warmed, and freshened (Woodgate et al., 2012). Warmer air temperatures are peaking earlier in the season and have led to increased summer ocean warming (Pickart et al., 2013). Stronger summertime northeasterly winds have led to upwelling-favorable conditions along the western Alaskan coast (Pickart et al., 2011). Combined, these physical changes have made conditions more favorable for HAB species, particularly the dinoflagellate *Alexandrium catenella* and diatoms in the genus *Pseudo-nitzschia* (Anderson et al., 2012).

Recent studies reveal increasing toxin prevalence in food webs (Hendrix et al., 2021) and the potential for increased *Alexandrium* cyst germination in certain cyst-dense areas, such as the seafloor in the northeastern Chukchi Sea, which are directly linked to warmer ocean bottom temperatures (Anderson et al., 2021). Saxitoxin doses were estimated during an anomalously warm year (2019) in the Arctic revealing that walruses were exposed to toxin concentrations at levels known to impact human health during shellfish poisoning events, as well as rodents in controlled laboratory studies (Lefebvre et al., 2022). During October 2022, 100% of harvested bowhead whales contained low levels of saxitoxin and 40% contained low levels of domoic acid (Figure 110). This confirms a consistent trend of higher prevalence of saxitoxin than domoic acid in Arctic food webs and is observed in all regions, including the Bering Strait.
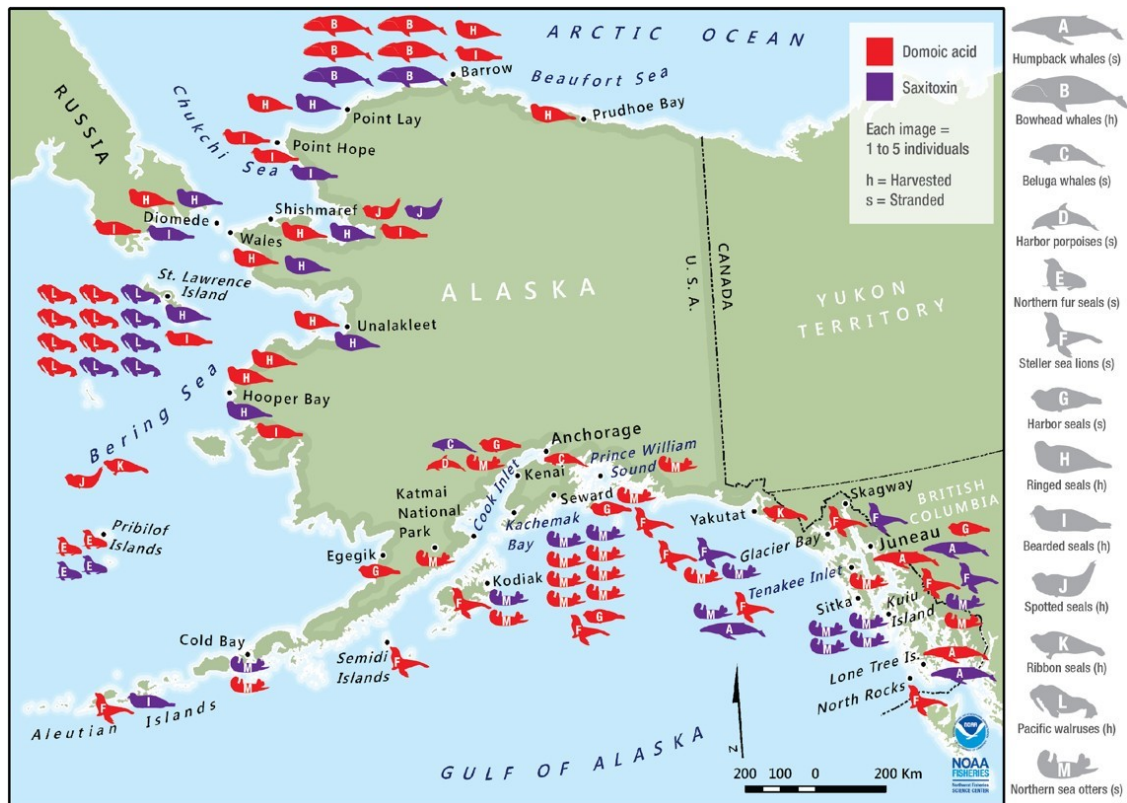
Figure 109: Algal toxins detected in stranded and harvested marine mammals confirm widespread prevalence of HABs throughout the food web in all regions of Alaska (Lefebvre et al., 2016).

In July 2023, dangerously high abundances of *Alexandrium* were identified by the imaging flow cytobot (IFCB) on board the R/V *Sikuliaq* at 47,000 cells/L. This was similar to observations reported in 2022 during the same time frame (Figure 111). As in 2022, the 2023 observation also prompted a Public Advisory on July 29, 2023. For two consecutive years, cruise-based IFCB operations documented a large and certainly dangerous *Alexandrium* bloom was moving through the Bering Strait, suggesting a regular risk to marine wildlife and ecosystem health.

Factors influencing observed trends: Increasing HAB events and toxin prevalence is linked to warming ocean temperatures throughout the water column (both surface and bottom) and increased sunlight associ- ated with the loss of sea-ice cover. Powerful storms re-suspend cysts into the water column and sustain ongoing blooms or inoculate new HAB events. Powerful storms (e.g., ex-typhoon Merbok[26]) have not been observed to date during Fall 2023 as in 2022, however, high *Alexandrium* cell counts were still observed similar to last year Figure 111).

Implications: The impacts of increased biotoxin exposure include increased risks to ecosystem, wildlife, and public health in Northern Arctic regions. As ocean temperatures continue to rise, algal growth and cyst germination rates of toxic *Alexandrium* will continue to increase. Recurrent high *Alexandrium* cell counts confirm the regular occurrence of HABs in the region that can contaminate food webs. Results indicate that HAB events are intensifying in Alaskan waters and there is a clear need to monitor HAB densities and toxin concentrations throughout the food web. Impacts also include food security concerns

---

[26]https://alaskapublic.org/2022/09/17/powerful-storm-slams-western-alaska/
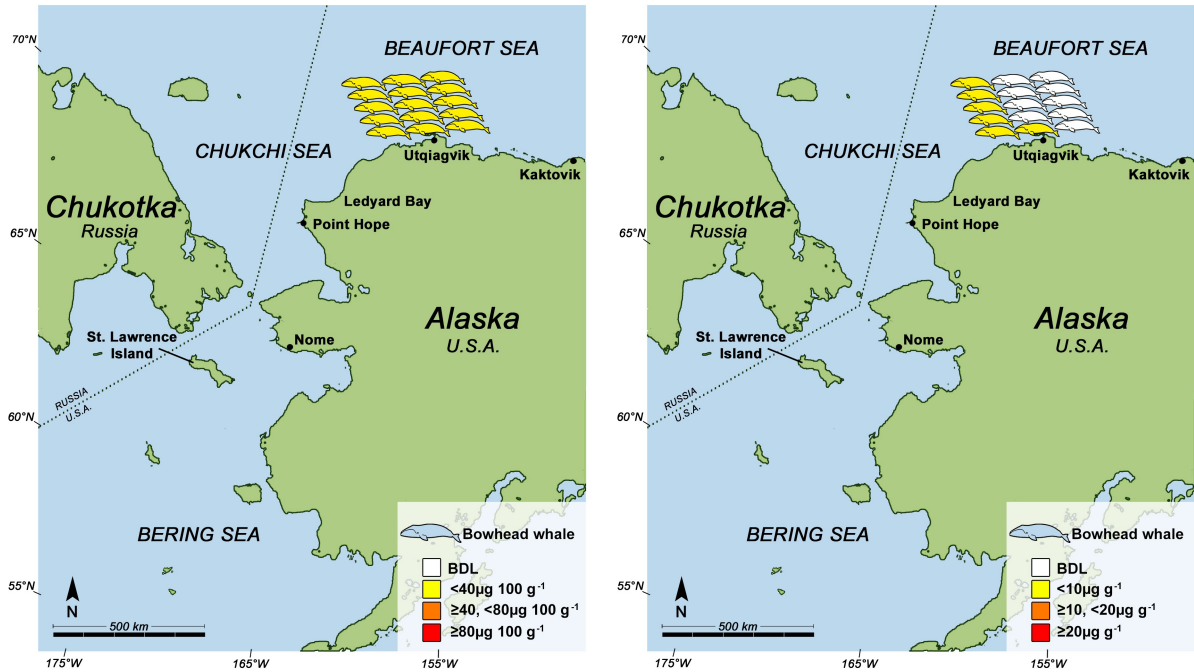
Figure 110: Low levels of harmful algal bloom toxins were detected in subsistence harvested Bowhead whales during October 2022. Left: saxitoxin in 100% of animals tested; Right: domoic acid in 40% of animals tested (unpublished data from K. Lefebvre). This trend also occurs in the Bering Strait region.
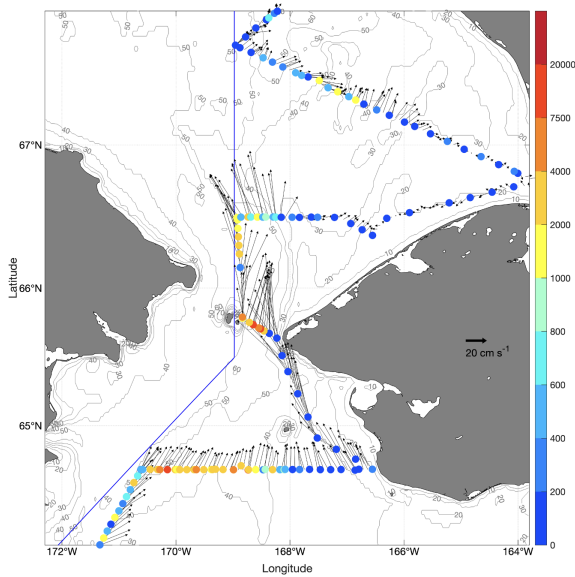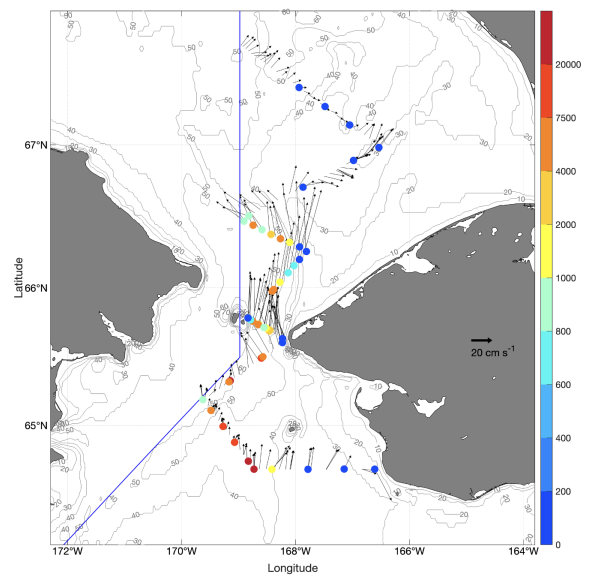
Figure 111: *Alexandrium* cell densities (cells/L) at stations (circles) sampled mid- to late- July in 2022 (right) and 2023 (left) (unpublished data from D. Anderson). Presence of high *Alexandrium* densities in both years in the Bering Sea and Bering Strait regions confirms frequent harmful algal bloom (HAB) presence in the region.

to western and northern Alaskan coastal peoples as well as conservation concerns for many species of marine resources, including several marine mammals currently listed under the Endangered Species Act (ESA). Arctic coastal community sampling efforts are being developed, but consistent funding is needed to sustain temporal and spatial monitoring coverage of HAB activity in the Alaskan ecosystem.

Future Steps:

Ongoing research projects include the continuous monitoring of *Alexandrium* and *Pseudo-nitzschia* within western and northern Alaskan waters and their biotoxins among marine trophic levels. Innovative technology such as the Imaging FlowCytobot (IFCB) allows continuous 24/7 underway sampling during extended research cruises (>1 month). The IFCB can identify *Alexandrium* and *Pseudo-nitzschia* cells and provide cell densities using machine learning based algorithms. This continues to be useful for providing real time updates on offshore bloom activity in sampled areas. Currently, models for quantifying toxin exposure risks in Arctic marine ecosystems are being developed. Thus, research cruises will continue to collect samples from organisms throughout different components of the food web (phytoplankton, zooplankton, invertebrates, fish, and marine mammals) to develop toxin trophic transfer models that will estimate biotoxin exposure to marine resources important for both commercially and/or subsistence purposes during HABs of different intensities. Data from 2019–2023 are available and various analyses relating to HAB species abundances and trophic transfer models are underway. The implementation of continuous HAB monitoring efforts such as IFCB deployments are needed to provide early warning and ensure future ecosystem and human/coastal community health.

Maintaining Diversity: Discards and Non-Target Catch

Time Trends in Groundfish Discards

Contributed by Anna Abelman
Resource Ecology and Fisheries Management Division, AFSC, NMFS, NOAA
Alaska Fisheries Information Network, Pacific States Marine Fisheries Commission
Contact: anna.abelman@noaa.gov
Last updated: September 2023

Description of indicator: Estimates of groundfish discards for 1993–2002 are sourced from NMFS Alaska Region's blend data, while estimates for 2003 and later come from the Alaska Region's Catch Accounting System. These sources, which are based on observer data in combination with industry landing and production reports, provide the best available estimates of groundfish discards in the North Pacific. Discard rates as shown in Figure 112 below are calculated as the weight of groundfish discards divided by the total (i.e., retained and discarded) catch weight for the relevant area gear-target sector. Where rates are described below for species or species groups, they represent the total discarded weight of the species/species group divided by the total catch weight of the species/species group for the relevant area-gear-target sector. These estimates include only catch of FMP-managed groundfish species within the FMP groundfish fisheries. Discards of groundfish in the halibut fishery and discards of forage fish and species managed under prohibited species catch limits, such as halibut, are not included.

Status and trends: Since 1993, discard rates of groundfish in federally-managed Alaskan groundfish fisheries have generally declined in the trawl pollock and non-pollock trawl fisheries in the eastern Bering Sea (EBS) (Figure 112). Annual discard rates in the EBS pollock trawl sector declined from 10% to about 1% in 1999 and have since remained below this level. The large increase in discard rate in 2021 is likely due to an overall decrease in total catch in NBS for pollock trawl. Rates in the non-pollock trawl sector have declined from a high of 50% in 1994 and have remained at 10% or lower since 2010. Discard rates and volumes in the fixed gear (hook-and-line and pot) sector trended upward from 2010 to 2016, reaching the highest annual discard biomass (26.7K metric tons) over the entire time series before declining from 2017 to 2021. Fixed gear discards in the northern Bering Sea trended upward from 2016 to 2018 as some vessels targeting Pacific cod moved their fishing activity northward, but these increases were offset by declines in discard biomass in the southern subregion. Through week 37 of 2023, discard biomass for non-pollock trawl and fixed sectors is trending higher relative to the 2018–2022 period, while trawl pollock gear discards are trending lower to date (Figure 113).
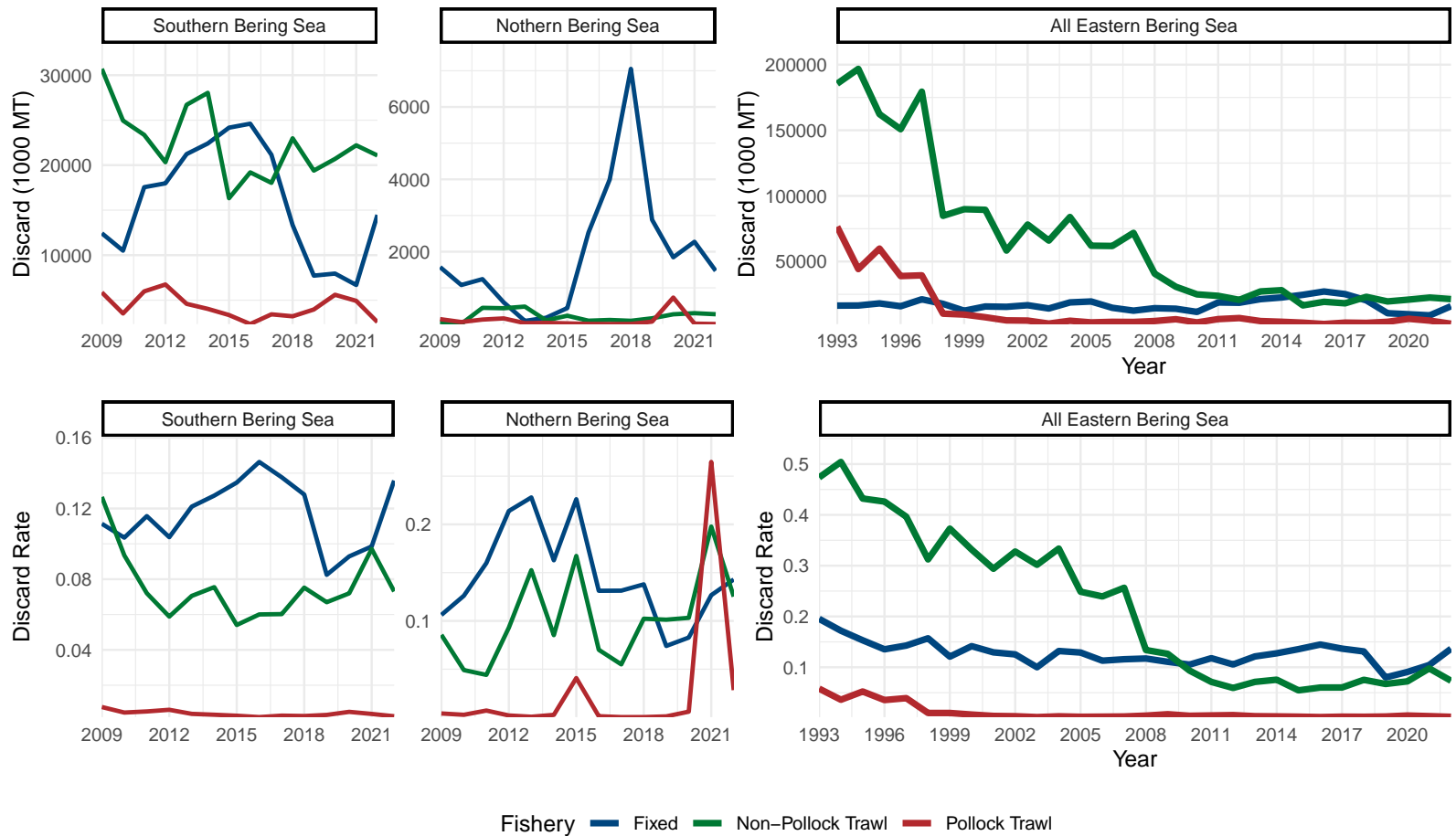
Figure 112: Total biomass and percent of total catch biomass of FMP groundfish discarded in the fixed gear, pollock trawl, and non-pollock trawl sectors for the eastern Bering Sea region, 1993–2022; and for northern (NBS) and southern (SBS) subregions, 2009–2022. Discard rates are calculated as total discard weight of FMP groundfish divided by total retained and discarded weight of FMP groundfish for the sector (includes only catch counted against federal TACs).

Factors influencing observed trends: Fishery discards may occur for economic or regulatory reasons. Economic discards include discarding of lower value and unmarketable fish, while regulatory discards are those required by regulation (e.g., upon reaching an allowable catch limit for a species). Minimizing discards is recognized as an ecological, economic, and moral imperative in various multilateral initiatives and in National Standard 9 of the Magnuson-Stevens Fishery Conservation and Management Act (Alverson et al., 1994; FAO, 1995; Karp et al., 2011). In the North Pacific groundfish fisheries, mechanisms to reduce discards include:

- Limited access privilege programs (LAPPs), which allocate catch quotas and may reduce economic discards by slowing down the pace of fishing

- In-season closure of fisheries once target or bycatch species quotas are attained

- Minimum retention and utilization standards for certain fisheries

- Maximum retainable amounts (MRAs), which allow for limited retention of species harvested incidentally in directed fisheries.
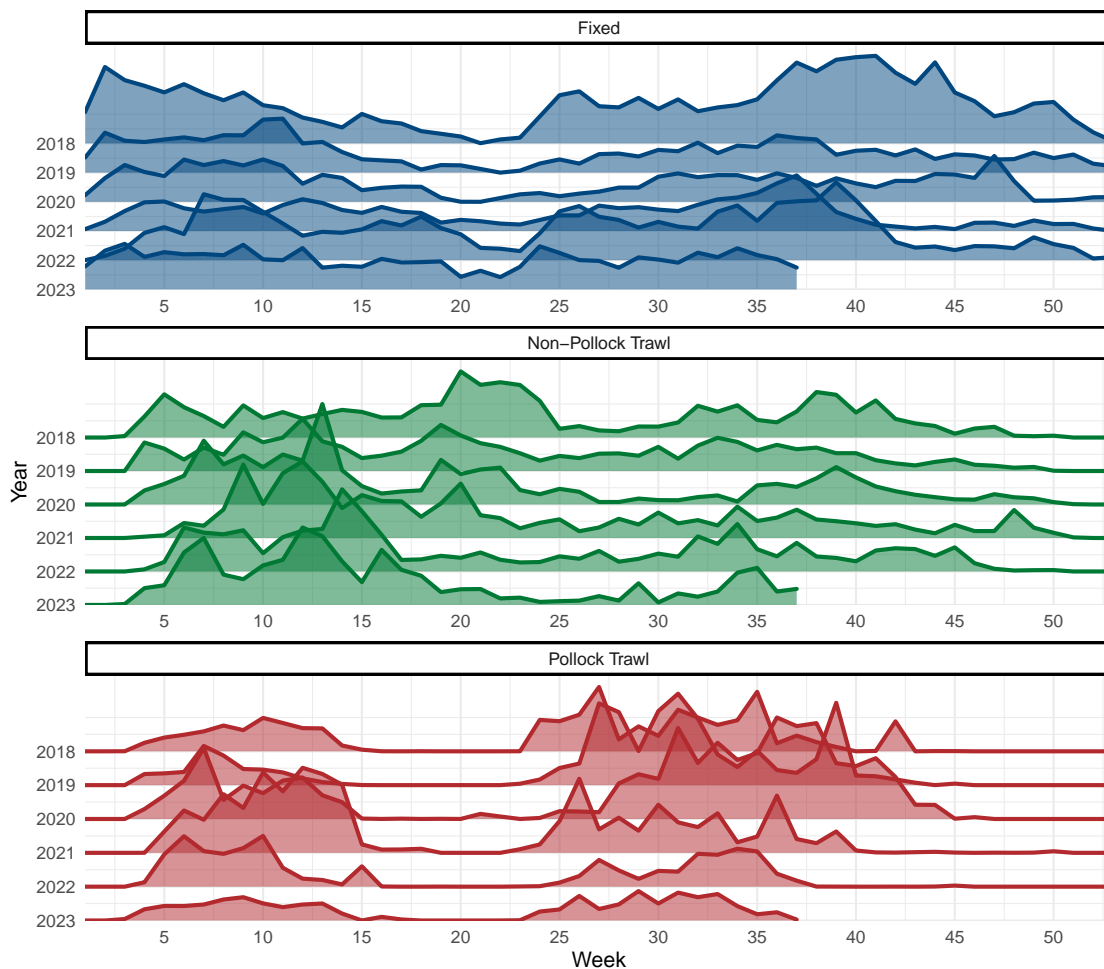
Figure 113: Total biomass of FMP groundfish discarded in the eastern Bering Sea region by sector and week, 2018–2023 (data for 2023 is shown through week 37). Plotted heights are not comparable across sectors.

Management and conservation measures aimed at reducing bycatch have contributed to an overall decline in groundfish discards since the early 1990s (NPFMC, 2016, 2017). Pollock roe stripping, wherein harvesters discard all but the highest value pollock product, was prohibited in 1991 (56 Federal Register 492). Throughout the 1990s, declines in total catch and discard of non-pollock groundfish in the pollock fishery coincided with the phasing out of bottom trawl gear in favor of pelagic gear, which allows for cleaner pollock catches (Graham et al., 2007). Full retention requirements for pollock and Pacific cod were implemented in 1998 for federally-permitted vessels fishing for groundfish (62 Federal Register 63880). Between 1997 and 1998 annual discard rates for cod fell from 13% to 1% in the non-pollock trawl sector and from 50% to 3% in the trawl pollock sector; pollock discards also declined significantly across both trawl gear sectors. In the trawl pollock fishery, discards of pollock have remained at nominal levels since passage of the American Fisheries Act, which established a sector-based LAPP and implemented more comprehensive observer requirements for the fishery in 2000. As of March 2020, the regulations 50 CFR 679.20(j) and 50 CFR 679.7(a)(5) were implemented to require operators of catcher vessels using hook-and-line, pot, or jig gear (fixed gear) to fully retain rockfish landings in the BSAI or GOA. These regulations also limit the amount of rockfish that can enter into the market with the overall purpose of limiting total catch of rockfish.

Low retention rates in the non-AFA trawl catcher processor fleet prompted Amendments 79 and 80 to the BSAI Groundfish FMP in 2008 (NPFMC, 2016). Amendment 79 established a Groundfish Retention Standard (GRS) Program with minimum retention and utilization requirements for vessels at least 125 feet LOA; industry-internal monitoring of retention rates has since replaced the program. Amendment 80 expanded the GRS program to all vessels in the fleet and established a cooperative-based LAPP with fixed allocations of certain non pollock groundfish species. In combination with the GRS program, these allocations are intended to remove the economic incentive to discard less valuable species caught incidentally in the multi-species fishery. In 2013, NMFS revised MRAs for groundfish caught in the BSAI arrowtooth flounder fishery, including an increase from 0 to 20 percent for pollock, cod, and flatfish (78 Federal Register 29248). Groundfish discard rates in the trawl flatfish fishery fell from 23% to 12% between 2007 and 2008 and have continued on a gradual decline.

Since 2003 across all EBS sectors combined, discard rates for species groups historically managed as the "other groundfish" assemblage (skate, sculpin, shark, squid, and octopus) have ranged from 65% to 80%, with skates representing the majority of discards by weight. In the fixed gear sector "other groundfish" typically account for at least 70% of total groundfish discards annually. Fluctuations in discard volumes and rates for these species may be driven by changes in market conditions and in fishing behavior within the directed fisheries in which these species are incidentally caught. For example, low octopus catch from 2007–2010 may be attributable to lower processor demand for food-grade octopus and decreases in cod pot-fishing effort stemming from declines in cod prices (Conners et al., 2016).

Implications: Fishery bycatch adds to the total human impact on biomass without providing a benefit to the Nation and as such is perceived as "contrary to responsible stewardship and sustainable utilization of marine resources" (Kelleher, 2005). Bycatch may constrain the utilization of target species and increases the uncertainty around total fishing-related mortality, making it more difficult to assess stocks, define overfishing levels, and monitor fisheries for overfishing (Alverson et al., 1994; Clucas, 1997; Karp et al., 2011). Discards of whole fish and offal have the potential to alter energy flow within ecosystems and have been observed to result in changes to habitat (e.g., oxygen depletion) and community structure (e.g., increases in scavenger populations) (Queirolo et al., 1995; Alverson et al., 1994; Catchpole et al., 2006; Zador and Fitzgerald, 2008). Monitoring discards and discard rates provides a means of assessing the efficacy of measures intended to reduce discards and increase groundfish retention and utilization.

Time Trends in Non-Target Species Catch

Contributed by George A. Whitehouse[1] and Sarah Gaichas[2]
[1]Cooperative Institute for Climate, Ocean, and Ecosystem Studies (CICOES), University of Washington, Seattle WA
[2]Ecosystem Assessment Program, Northeast Fisheries Science Center, National Marine Fisheries Service, NOAA, Woods Hole MA
Contact: andy.whitehouse@noaa.gov
Last updated: August 2023

Description of indicator: This indicator reports the catch of non-target species in groundfish fisheries in the eastern Bering Sea (EBS). Catch since 2003 has been estimated using the Alaska Region's Catch Accounting System (Cahalan et al., 2014). This sampling and estimation process does result in uncertainty in catches, which is greater when observer coverage is lower and for species encountered rarely in the catch. Since 2013, the three categories of non-target species tracked here are:

1. Scyphozoan jellyfish

2. Structural epifauna (seapens/whips, sponges, anemones, corals, tunicates)

3. Assorted invertebrates (bivalves, brittle stars, hermit crabs, miscellaneous crabs, sea stars, marine worms, snails, sea urchins, sand dollars, sea cucumbers, and other miscellaneous invertebrates).

The catch of non-target species/groups from the Bering Sea includes the reporting areas 508, 509, 512, 513, 514, 516, 517, 521, 523, 524, and 530[27].

Status and trends: The catch of jellyfish more than doubled from 2020 to 2021 (Figure 114, top). Previous high catches of jellyfish occurred in 2011, 2014, and 2018 and were each followed by a sharp decrease in jellyfish catch the following year. While the catch of jellyfish did decrease from 2021 to 2022, it did so only slightly, decreasing about 7%. Jellyfish are primarily caught in the pollock fishery.

The catch of structural epifauna trended downward from 2015 to 2020, and has remained low in 2021 and 2022 (Figure 114, middle). Benthic urochordate caught in non-pelagic trawls were the dominant component of the structural epifauna catch in 2012 and 2015–2022. In 2013 and 2014, anemones caught in the Pacific cod fishery were the dominant part of the structural epifauna catch. Sponge were the dominant component of the structural epifauna catch in 2011 and were primarily caught in non-pelagic trawls.

Sea stars comprise more than 85% of the assorted invertebrate catch in all years and are primarily caught in flatfish fisheries (Figure 114, bottom). The catch of assorted invertebrates generally trended upward from 2011 to 2015, then declined from 2015 to 2022.

Factors influencing observed trends: The catch of non-target species may change if fisheries change, if ecosystems change, or both. Because non-target species catch is unregulated and unintended, if there have been no large-scale changes in fishery management in a particular ecosystem, then large-scale

---

[27]https://www.fisheries.noaa.gov/alaska/sustainable-fisheries/alaska-fisheries-figures-maps-boundaries-regulatory-areas-and-zones

signals in the non-target catch may indicate ecosystem changes. Catch trends may be driven by changes in biomass or changes in distribution (overlap with the fishery) or both. Fluctuations in the abundance of jellyfish in the EBS are influenced by a suite of biophysical factors affecting the survival, reproduction, and growth of jellies including temperature, sea ice phenology, wind-mixing, ocean currents, and prey abundance (Brodeur et al., 2008). The lack of a clear trend in the catch of scyphozoan jellies may reflect interannual variation in jellyfish biomass and/or changes in the overlap with fisheries.
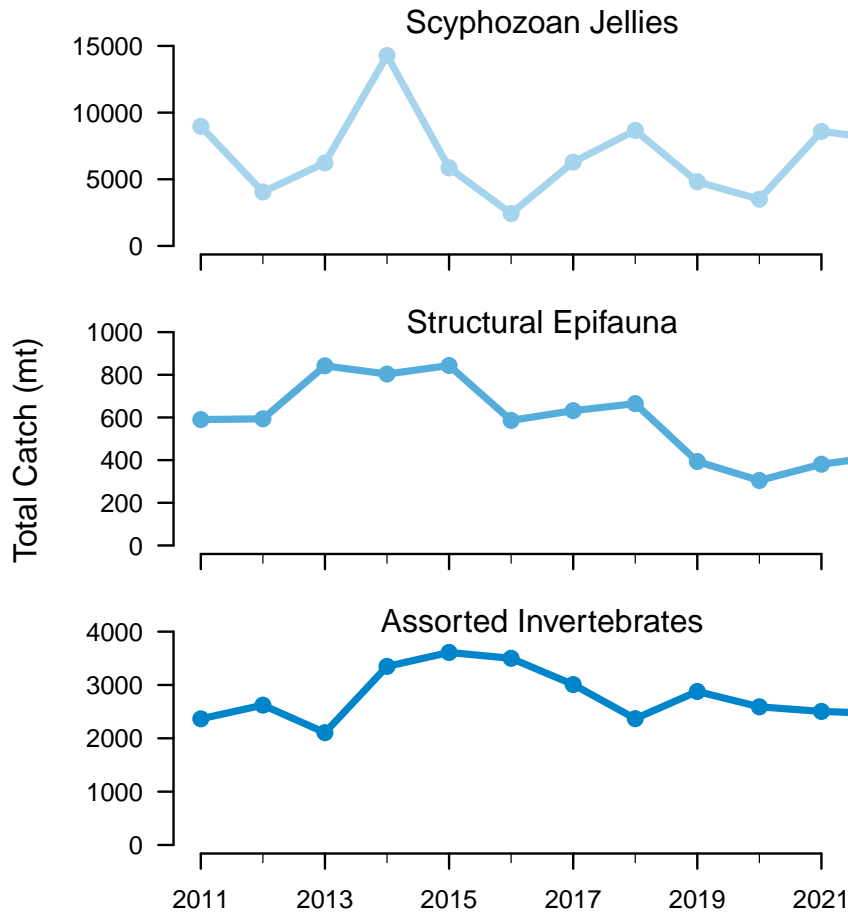
Figure 114: Total catch of non-target species (tons) in EBS groundfish fisheries (2011–2022). **Please note the different y-axis scales** between the species groups.

Implications: The catch of structural epifauna species and assorted invertebrates is very low compared with the catch of target species. Structural epifauna species may have become less available to the EBS fisheries or the fisheries avoided them more effectively. Abundant jellyfish may have a negative impact on fishes as they compete with planktivorous fishes for prey resources (Purcell and Arai, 2001), and additionally, jellyfish may prey upon the early life history stages (eggs and larvae) of fishes (Purcell and Arai, 2001; Robinson et al., 2014).

Maintaining and Restoring Fish Habitats

Area Disturbed by Trawl Fishing Gear in the Eastern Bering Sea

Contributed by Molly Zaleski[1], Scott Smeltz[2], Felipe Restrepo[2], and Mason Smith[1]
[1]Habitat Conservation Division, Alaska Regional Office, National Marine Fisheries Service, NOAA
[2]Fisheries, Aquatic Science, and Technology Laboratory, Alaska Pacific University
Contact: molly.zaleski@noaa.gov
Last updated: September 2023

Description of indicator: Fishing gear can impact habitat used by a fish species for the processes of spawning, breeding, feeding, or growth to maturity. This indicator uses output from the Fishing Effects (FE) model to estimate the area of geological and biological features disturbed over the Bering Sea domain, utilizing spatially-explicit VMS data summarized to $25km^2$ grid cells in fishable depths ($<$1000m). The time series for this indicator is available since 2003, when widespread VMS data became available, through August 2022.

Status and trends: The estimated disturbance in the northern Bering Sea was less than the southern Bering Sea, and the southern Bering Sea had the highest estimated disturbances over time for all Alaska regions (Figure 115). While the southern Bering Sea had the highest estimated percentage of habitat disturbance, the time series shows a decline in disturbance from 2003 which could represent gear modifications, shifts in gear types, and changes in effort. Figure 116 shows the location of the areas with the highest impact cumulatively from 2003 through August 2022.

Factors influencing observed trends: Trends in seafloor area disturbed can be affected by numerous variables, such as fish abundance and distribution, management actions (e.g., closed areas), changes in the structure of the fisheries due to rationalization, improved technology (e.g., increased ability to find fish, acoustics to fish near the bottom without contact), markets for fish products, and changes in vessel horsepower and fishing gear. Intensive fishing in an area can result in a change in species diversity by attracting opportunistic fish species which feed on animals that have been disturbed by fishing activity, or by reducing the suitability of habitat used by some species. It is possible that increased effort in fisheries that interact with both living and non-living bottom substrates could result in increased habitat loss/degradation due to fishing gear effects. The footprint of habitat damage varies with gear (type, weight, towing speed, depth of penetration), the physical and biological characteristics of the areas fished, recovery rates of living substrates in the areas fished, and management or economic changes that result in spatial redistribution of fishing effort.

Between 2003 and 2008, variability in area disturbed was driven largely by the seasonality of fishing in the Bering Sea, and this pattern continues to a lesser degree. In 2008, Amendment 80 was implemented, which allocated BSAI yellowfin sole, flathead sole, rock sole, Atka mackerel, and Aleutian Islands Pacific ocean perch to the head and gut trawl catcher processor sector, and allowed qualified vessels to form cooperatives. The formation of cooperatives reduced overall effort in the fleet while maintaining catch levels. In 2010, trawl sweep gear modifications were implemented on non-pelagic trawls in the Bering Sea, resulting in changes to the gear-specific contact adjustment used in the fishing effects model.

Implications: The effects of changes in fishing effort on habitat are difficult to assess, although our
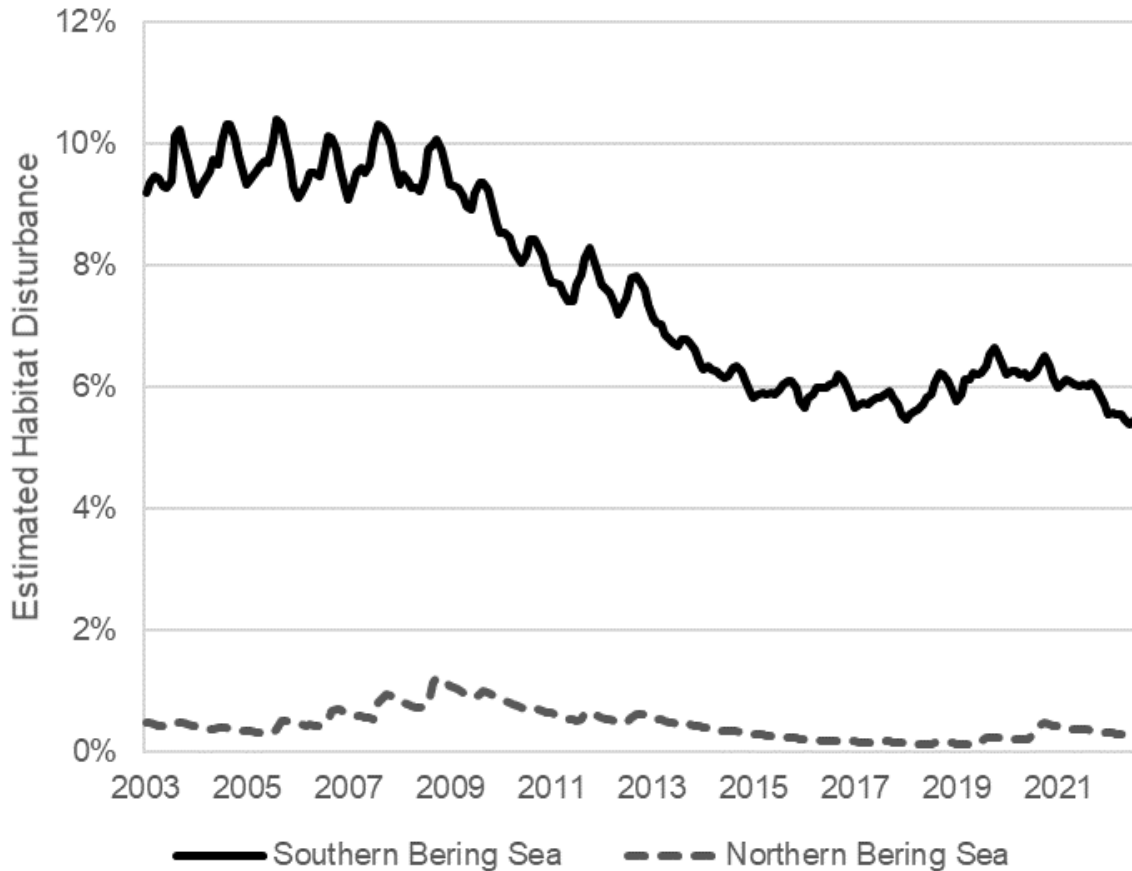
Figure 115: Estimated % habitat disturbance by bottom contact of commercial fishing gear in the southern (solid black line) and northern (dashed gray line) Bering Sea from 2003 through August 2022. The southern and northern Bering Sea regions are delineated at latitude 60°N.

ability to quantify those effects has increased greatly with the development of the Fishing Effects model as a part of the 2017 EFH 5-year Review (Simpson et al., 2017) and the updated model for the 2023 EFH 5-year Review (Zaleski et al., 2023). During the 2023 EFH 5-year Review, stock authors and experts were provided model output through December 2020 to evaluate if the estimated disturbance adversely impacted FMP species' core EFH areas. For the Bering Sea, no species were determined to have more than minimal and not temporary effects from fishing, and no stock authors elevated species for mitigation measures against fishing gear impacts to habitat (Zaleski et al., 2023).

Although the impacts of fishing across the domain are very low, it is possible that localized impacts may be occurring. The issue of local impacts is an area of active research.

No new closure areas have been added in the BSAI. For information on Habitat Conservation Areas in the eastern Bering Sea, please see: `https://www.fisheries.noaa.gov/resource/tool-app/habitat-conservation-area-maps`
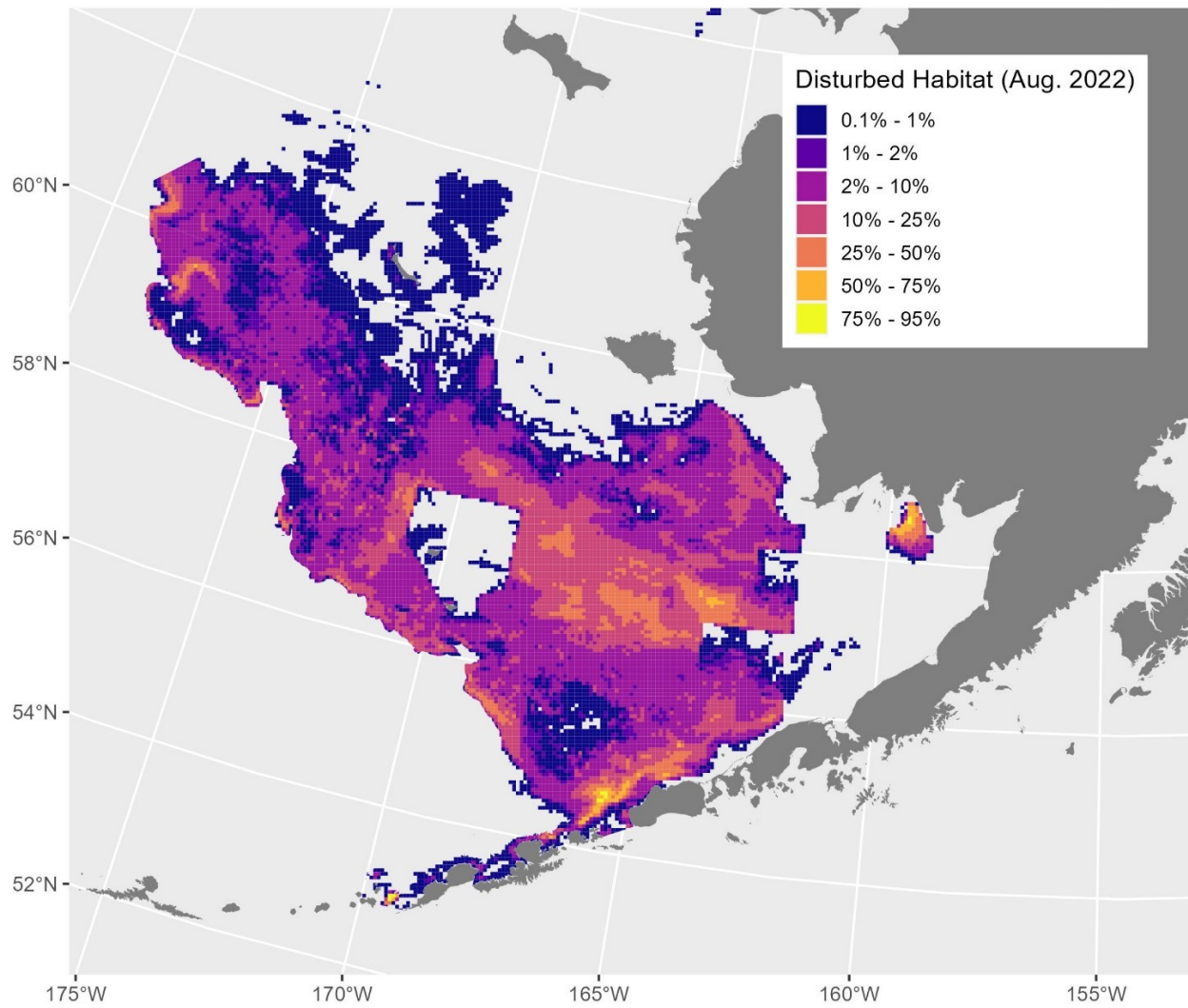
Figure 116: Map of cumulative percentage of habitat disturbed, all gears combined, from 2003 through August 2023. Note the delineation between the southern and northern Bering Sea at latitude 60°N.

Sustainability (for consumptive and non-consumptive uses)

Fish Stock Sustainability Index – Bering Sea and Aleutian Islands

Contributed by George A. Whitehouse
Cooperative Institute for Climate, Ocean, and Ecosystem Studies (CICOES), University of Washington, Seattle, WA
Contact: andy.whitehouse@noaa.gov
Last updated: August 2023

Description of indicator: The Fish Stock Sustainability Index (FSSI) is a performance measure for the sustainability of fish stocks selected for their importance to commercial and recreational fisheries[28]. The FSSI will increase as overfishing is ended and stocks rebuild to the level that provides maximum sustainable yield. The FSSI is calculated by awarding points for each stock based on the following rules:

1. Stock has known status determinations:

    (a) overfishing level is defined = 0.5

    (b) overfished biomass level is defined = 0.5

2. Fishing mortality rate is below the "overfishing" level defined for the stock = 1.0

3. Biomass is above the "overfished" level defined for the stock = 1.0

4. Biomass is at or above 80% of the biomass that produces maximum sustainable yield (B_{MSY}) = 1.0 (this point is in addition to the point awarded for being above the "overfished" level)

The maximum score for each stock is 4.

In the Alaska Region, there are 35 FSSI stocks and an overall FSSI of 140 would be achieved if every stock scored the maximum value, 4. Over time, the number of stocks included in the FSSI has changed as stocks have been added and removed from Fishery Management Plans (FMPs). To keep FSSI scores for Alaska comparable across years we report the FSSI as a percentage of the maximum possible score (i.e., 100%).

Additionally, there are 26 non-FSSI stocks in Alaska, three ecosystem component species complexes, and Pacific halibut which are managed under an international agreement. Two of the non-FSSI crab stocks are overfished but are not subject to overfishing. The Pribilof Islands blue king crab stock is in year nine of a rebuilding plan, and the Saint Matthews Island blue king crab stock is in year three of a 26-year rebuilding plan. None of the other non-FSSI stocks are known to be subject to overfishing, are overfished, or are approaching an overfished condition. For more information on non-FSSI stocks see the Status of U.S. Fisheries webpage[1].

---

[28]https://www.fisheries.noaa.gov/national/population-assessments/fishery-stock-status-updates

Status and trends: The overall Alaska FSSI generally trended upwards from 80% in 2006 to a high of 94% in 2018, then trended downward from 2018 to 2020 (Figure 117). It has remained generally flat since 2020 at 88.9% in 2023.

As of June 30, 2023, no BSAI groundfish stock or stock complex is subject to overfishing, is known to be overfished, or known to be approaching an overfished condition (Table 1). The BSAI groundfish FSSI score is 59 out of a maximum possible 64. The AI Pacific cod stock and the walleye pollock Bogoslof stock both have FSSI scores of 1.5 due to not having known overfished status or known biomass relative to their overfished levels or to B_{MSY}. All other BSAI groundfish FSSI stocks received the maximum possible score of four points.

The BSAI king and tanner crab FSSI is 17 out of a possible 20. One point was deducted for the Bristol Bay red king crab stock's biomass decreasing to below the B/B_{MSY} threshold and two points were deducted for Bering Sea snow crab becoming overfished and their biomass dropping to 23% of B_{MSY}.

The overall BSAI FSSI score is 76 out of a maximum possible score of 84 (Table 1). The BSAI FSSI trended upward from 74% in 2006 to a peak of 95.5% in 2019 but has since declined to 90.5% (Figure 118).
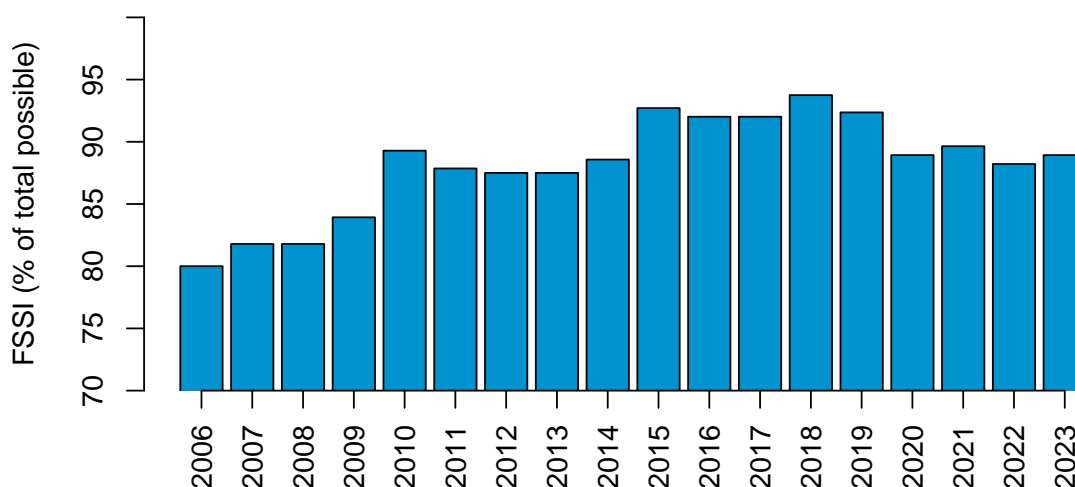
Figure 117: The trend in overall Alaska FSSI from 2006 through 2023, as a percentage of the maximum possible FSSI. The maximum possible FSSI was 140 from 2006 to 2014, 144 from 2015 to 2019, and 140 since 2020. All scores are reported through the second quarter (June) of each year, and are retrieved from the Status of U.S. Fisheries website: `https://www.fisheries.noaa.gov/national/population-assessments/fishery-stock-status-updates`.

Factors influencing observed trends: The overall trend in Alaska FSSI has been positive over much of the duration examined here (2006–2023). The recent decline in the Alaska total FSSI and in BSAI from 2021 to 2022 reflects the points lost for Bering Sea snow crab becoming overfished and their low biomass relative to B_{MSY}.

Implications: The majority of Alaska groundfish and crab fisheries appear to be sustainably managed. None of the FSSI groundfish stocks in the BSAI are subject to overfishing or known to be overfished. Only snow crab is currently overfished.
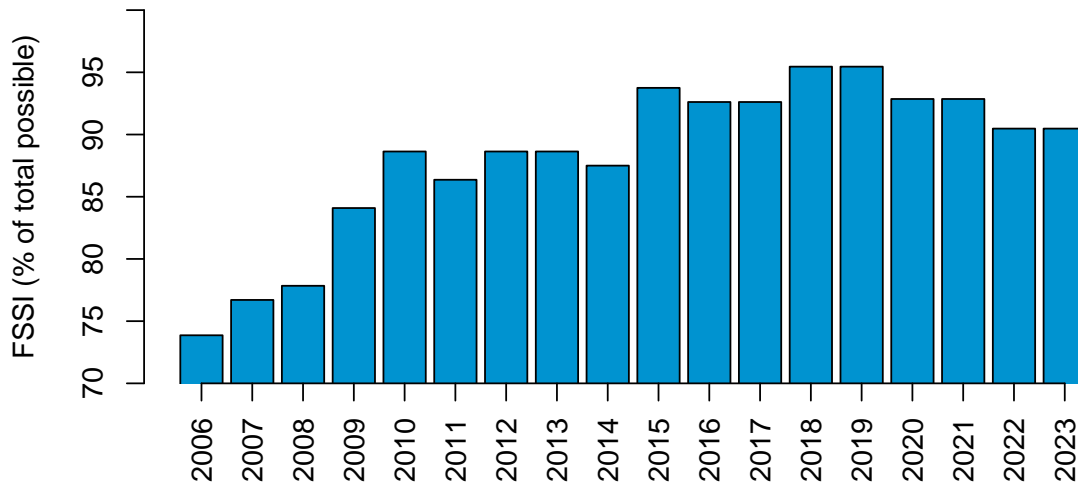
Figure 118: The trend in BSAI FSSI from 2006 through 2023 as a percentage of the maximum possible FSSI. All scores are reported through the second quarter (June) of each year, and are retrieved from the Status of U.S. Fisheries website: `https://www.fisheries.noaa.gov/national/population-assessments/fishery-stock-status-updates`.

Table 1: BSAI FSSI stocks under NPFMC jurisdiction updated through June 2023 adapted from the NOAA Fishery Stock Status Updates webpage: `https://www.fisheries.noaa.gov/national/population-assessments/fishery-stock-status-updates`. *See FSSI and Non-FSSI Stock Status Table on the Fishery Stock Status Updates webpage for definition of stocks, stock complexes, and notes on rebuilding.

Stock	Overfishing	Overfished	Approaching	Progress	B/Bmsy	FSSI Score
Golden king crab - Aleutian Islands*	No	No	No	NA	1.115/0.894	4
Red king crab - Bristol Bay	No	No	No	NA	0.58	3
Red king crab - Norton Sound	No	No	No	NA	1.27	4
Snow crab - Bering Sea*	No	Yes	No	NA	0.23	2
Southern Tanner crab - Bering Sea	No	No	No	NA	1.18	4
BSAI Alaska plaice	No	No	No	NA	1.58	4
BSAI Atka mackerel	No	No	No	NA	1.16	4
BSAI Arrowtooth flounder	No	No	No	NA	2.58	4
BSAI Kamchatka flounder	No	No	No	NA	1.5	4
BSAI Flathead sole complex*	No	No	No	NA	2.08	4
BSAI Rock sole complex*	No	No	No	NA	1.61	4
BSAI Skate complex*	No	No	No	NA	2.28	4
BSAI Greenland halibut	No	No	No	NA	1.49	4
BSAI Northern rockfish	No	No	No	NA	2.1	4
BS Pacific cod	No	No	No	NA	1.07	4
AI Pacific cod	No	Unknown	Unknown	NA	not estimated	1.5
BSAI Pacific Ocean perch	No	No	No	NA	1.60	4
Walleye pollock - Aleutian Islands	No	No	No	NA	1.31	4
Walleye pollock - Bogoslof	No	Unknown	Unknown	NA	not estimated	1.5
Walleye pollock - Eastern Bering Sea	No	No	No	NA	1.477	4
BSAI Yellowfin sole	No	No	No	NA	1.94	4

References

Aagaard, K., T. J. Weingartner, S. L. Danielson, R. A. Woodgate, G. C. Johnson, and T. E. Whitledge. 2006. Some controls on flow and salinity in Bering Strait. Geophysical Research Letters **33**.

Algayer, T., A. Mahmoud, S. Saksena, W. C. Long, K. M. Swiney, R. J. Foy, B. V. Steffel, K. E. Smith, R. B. Aronson, and G. H. Dickinson. 2023. Adult snow crab, Chionoecetes opilio, display body-wide exoskeletal resistance to the effects of long-term ocean acidification. Marine Biology **170**:63.

Alverson, D. L., M. H. Freeberg, S. A. Murawski, and J. Pope. 1994. A global assessment of fisheries bycatch and discards (Vol. 339). Food Agriculture Organization.

Anderson, D. M., T. J. Alpermann, A. D. Cembella, Y. Collos, E. Masseret, and M. Montresor. 2012. The globally distributed genus *Alexandrium*: multifaceted roles in marine ecosystems and impacts on human health. Harmful algae **14**:10–35.

Anderson, D. M., E. Fachon, R. S. Pickart, P. Lin, A. D. Fischer, M. L. Richlen, V. Uva, M. L. Brosnahan, L. McRaven, and F. Bahr. 2021. Evidence for massive and recurrent toxic blooms of *Alexandrium catenella* in the Alaskan Arctic. Proceedings of the National Academy of Sciences **118**.

Andrews III, A. G., M. Cook, E. Siddon, and A. Dimond. 2019. Prey Quality Provides a Leading Indicator of Energetic Content for Age-0 Walleye Pollock. Stock Assessment and Fishery Evaluation Report, North Pacific Fishery Management Council, 605 W 4th Ave, Suite 306, Anchorage, AK 99501.

Aydin, K., and F. Mueter. 2007. The Bering Sea - a dynamic food web perspective. Deep Sea Research Part II: Topical Studies in Oceanography **54**:2501–2525.

Baduini, C., K. Hyrenbach, K. Coyle, A. Pinchuk, V. Mendenhall, and G. Hunt. 2001. Mass mortality of short-tailed shearwaters in the southeastern Bering Sea during summer 1997. Fisheries Oceanography **10**:117–130.

Baier, C. T., and J. M. Napp. 2003. Climate-induced variability in *Calanus marshallae* populations. Journal of Plankton Research **25**:771–782.

Bailey, K. M. 1989. Interaction between the vertical distribution of juvenile walleye pollock Theragra chalcogramma in the eastern Bering Sea, and cannibalism. Mar. Ecol. Prog. Ser **53**:205–213.

Baker, M. 2023. Marine Ecosystems of the North Pacific Ocean 2009-2016: Region 14 (Northern Bering Sea), page 80 . North Pacific Marine Science Organization, Sidney, BC, Canada.

Baker, M. R., K. K. Kivva, M. N. Pisareva, J. T. Watson, and J. Selivanova. 2020. Shifts in the physical environment in the Pacific Arctic and implications for ecological timing and conditions. Deep Sea Research Part II: Topical Studies in Oceanography **177**:104802.

Balch, W., H. R. Gordon, B. Bowler, D. Drapeau, and E. Booth. 2005. Calcium carbonate measurements in the surface global ocean based on Moderate-Resolution Imaging Spectroradiometer data. Journal of Geophysical Research: Oceans **110 (C7)**.

Barbeaux, S. J., K. Holsman, and S. Zador. 2020. Marine heatwave stress test of ecosystem-based fisheries management in the Gulf of Alaska Pacific Cod Fishery. Frontiers in Marine Science **7**:703.

Batten, S. D., G. T. Ruggerone, and I. Ortiz. 2018. Pink salmon induce a trophic cascade in plankton populations in the southern Bering Sea and around the Aleutian Islands. Fisheries Oceanography **27**:548–559.

Beamish, R. J., and C. Mahnken. 2001. A critical size and period hypothesis to explain natural regulation of salmon abundance and the linkage to climate and climate change. Progress in Oceanography **49**:423–437.

Berkeley, S. A., M. A. Hixon, R. J. Larson, and M. S. Love. 2004. Fisheries sustainability via protection of age structure and spatial distribution of fish populations. Fisheries **29**:23–32.

Bi, H., H. Yu, A. I. Pinchuk, and H. R. Harvey. 2015. Interannual summer variability in euphausiid populations on the eastern Bering Sea shelf during the recent cooling event (2008–2010). Deep Sea Research Part I: Oceanographic Research Papers **95**:12–19.

Blackwell, B. G., M. L. Brown, and D. W. Willis. 2000. Relative weight (Wr) status and current use in fisheries assessment and management. Reviews in fisheries Science **8**:1–44.

Blanchard, F., and J. Boucher. 2001. Temporal variability of total biomass in harvested communities of demersal fishes. Fisheries Research **49**:283–293.

Boldt, J. 2007. Ecosystem Considerations for 2008. Stock Assessment and Fishery Evaluation Report for the Groundfish Resources of the Bering Sea/Aleutian Islands and Gulf of Alaska. North Pacific Fishery Management Council, 605 W. 4th Ave., Suite 306, Anchorage, AK 99501.

Boldt, J. L., and L. J. Haldorson. 2004. Size and condition of wild and hatchery pink salmon juveniles in Prince William Sound, Alaska. Transactions of the American Fisheries Society **133**:173–184.

Bond, N. A., M. F. Cronin, H. Freeland, and N. Mantua. 2015. Causes and impacts of the 2014 warm anomaly in the NE Pacific. Geophysical Research Letters **42**:3414–3420.

Brannian, L. K., K. A. Rowell, and F. Funk. 1993. Forecast of the Pacific herring biomass in Togiak District, Bristol Bay, 1993. Alaska Department of Fish and Game, Division of Commercial Fisheries Management and Development, Regional Information Report 2D93-42, Anchorage .

Brodeur, R., C. Mills, J. Overland, G. Walters, and J. Schumacher. 1999. Recent increase in jellyfish biomass in the Bering Sea: Possible links to climate change. Fisheries Oceanography **8**:286–306.

Brodeur, R. D., M. B. Decker, L. Ciannelli, J. E. Purcell, N. A. Bond, P. J. Stabeno, E. Acuna, and G. L. Hunt. 2008. Rise and fall of jellyfish in the eastern Bering Sea in relation to climate regime shifts. Progress in Oceanography **77**:103–111.

Brodeur, R. D., R. L. Emmett, J. P. Fisher, E. Casillas, D. J. Teel, and T. W. Miller. 2004. Juvenile salmonid distribution, growth, condition, origin, and environmental and species associations in the Northern California Current. Fishery Bulletin **102**:25–46.

Brodeur, R. D., H. Sugisaki, and G. L. Hunt. 2002. Increases in jellyfish biomass in the Bering Sea: implications for the ecosystem. Marine Ecology Progress Series **233**:89–103.

Broerse, A., T. Tyrrell, J. Young, A. Poulton, A. Merico, W. Balch, and P. Miller. 2003. The cause of bright waters in the Bering Sea in winter. Continental Shelf Research **23**:1579–1596.

Burril, S. E., V. R. von Biela, N. Hillgruber, and C. E. Zimmerman. 2018. Energy allocation and feeding ecology of juvenile chum salmon (Oncorhynchus keta) during transition from freshwater to saltwater. Polar Biology **41**:1447–1461.

Cahalan, J., J. Gasper, and J. Mondragon. 2014. Catch sampling and estimation in the Federal ground-fish fisheries off Alaska, 2015 edition. Report, U.S. Dep. Commer., NOAA Tech. Memo. NMFS-AFSC-286, 46 p.

Catchpole, T., C. Frid, and T. Gray. 2006. Resolving the discard problem - A case study of the English *Nephrops* fishery. Marine Policy **30**:821–831.

Ciannelli, L., R. Drodeur, and T. Buckley. 1998. Development and application of a bioenergetics model for juvenile walleye pollock. Journal of Fish Biology **52**:879–898.

Cieciel, K., E. V. Farley Jr, and L. B. Eisner. 2009. Jellyfish and juvenile salmon associations with oceanographic characteristics during warm and cool years in the eastern Bering Sea. North Pacific Anadromous Fish Commission Bulletin **5**:209–224.

Clucas, I. 1997. A study of the options for utilization of bycatch and discards from marine capture fisheries. FAO fisheries circular **928**:1–59.

Coachman, L. 1986. Circulation, water masses, and fluxes on the southeastern Bering Sea shelf. Continental Shelf Research **5**:23–108.

Coiley-Kenner, P., T. Krieg, M. Chythlook, and G. Jennings. 2003. Wild resource harvests and uses by residents of Manokotak, Togiak, and Twin Hills, 1999/2000. Alaska Department of Fish and Game Division of Subsistence Technical Paper **No. 275**.

Conners, M. E., K. Y. Aydin, and C. L. Conrath. 2016. Assessment of the octopus stock complex in the Bering Sea and Aleutian Islands. Report, North Pacific Fishery Management Council.

Courtney, M. B., M. D. Evans, J. F. Strøm, A. H. Rikardsen, and A. C. Seitz. 2019. Behavior and thermal environment of Chinook salmon *Oncorhynchus tshawytscha* in the North Pacific Ocean, elucidated from pop-up satellite archival tags. Environmental Biology of Fishes **102**:1039–1055.

Coyle, K. O., L. Eisner, F. J. Mueter, A. Pinchuk, M. Janout, K. Cieciel, E. Farley, and A. Andrews. 2011. Climate change in the southeastern Bering Sea: impacts on pollock stocks and implications for the Oscillating Control Hypothesis. Fisheries Oceanography **20**:139–156.

Danielson, S., O. Ahkinga, C. Ashjian, E. Basyuk, L. Cooper, L. Eisner, E. Farley, K. Iken, J. Grebmeier, and L. Juranek. 2020. Manifestation and consequences of warming and altered heat fluxes over the Bering and Chukchi Sea continental shelves. Deep Sea Research Part II: Topical Studies in Oceanography **177**:104781.

Dann, H. A. H. E. M. L. E. K. C. F., T. H., and M. B. Foster. 2023. Genetic Stock Composition of Chum Salmon Harvested in Commercial Salmon Fisheries of the South Alaska Peninsula, 2022. Report, Alaska Department of Fish and Game Divisions of Sport Fish and Commercial Fisheries, Special Publication No. 23-07, Anchorage.

DeFilippo, L. B., J. T. Thorson, C. A. O'Leary, S. Kotwicki, J. Hoff, J. N. Ianelli, V. V. Kulik, and A. E. Punt. 2023. Characterizing dominant patterns of spatiotemporal variation for a transboundary groundfish assemblage. Fisheries Oceanography .

Donnellan, M. A., S.J. 2023. Run forecasts and harvest projections for 2023 Alaska salmon fisheries and review of the 2022 season. Report, Alaska Department of Fish and Game, Special Publication No. 23-10, Anchorage, AK.

Dorn, M. W., and S. G. Zador. 2020. A risk table to address concerns external to stock assessments when developing fisheries harvest recommendations. Ecosystem Health and Sustainability **6**:1813634.

Duffy-Anderson, J. T., P. Stabeno, A. G. Andrews III, K. Cieciel, A. Deary, E. Farley, C. Fugate, C. Harpold, R. Heintz, and D. Kimmel. 2019. Responses of the northern Bering Sea and southeastern Bering Sea pelagic ecosystems following record-breaking low winter sea-ice. Geophysical Research Letters **46**:9833–9842.

Duffy-Anderson, J. T., P. J. Stabeno, E. C. Siddon, A. G. Andrews, D. W. Cooper, L. B. Eisner, E. V. Farley, C. E. Harpold, R. A. Heintz, and D. G. Kimmel. 2017. Return of warm conditions in the southeastern Bering Sea: Phytoplankton-Fish. PloS one **12**:e0178955.

Edullantes, B. 2019. ggplottimeseries: Visualisation of Decomposed Time Series with ggplot2. R package version **0.1.0**.

Eisner, L. B., J. M. Napp, K. L. Mier, A. I. Pinchuk, and A. G. Andrews III. 2014. Climate-mediated changes in zooplankton community structure for the eastern Bering Sea. Deep Sea Research Part II: Topical Studies in Oceanography **109**:157–171.

Eisner, L. B., A. I. Pinchuk, D. G. Kimmel, K. L. Mier, C. E. Harpold, and E. C. Siddon. 2018. Seasonal, interannual, and spatial patterns of community composition over the eastern Bering Sea shelf in cold years. Part I: zooplankton. ICES Journal of Marine Science **75**:72–86.

Eisner, L. B., E. C. Siddon, and W. W. Strasburger. 2015. Spatial and temporal changes in assemblage structure of zooplankton and pelagic fish in the eastern Bering Sea across varying climate conditions. Izv TINRO **181**:141–160.

Eisner, L. B., E. M. Yasumiishi, A. G. Andrews III, and C. A. O'Leary. 2020. Large copepods as leading indicators of walleye pollock recruitment in the southeastern Bering Sea: Sample-Based and spatio-temporal model (VAST) results. Fisheries Research **232**:105720.

Elison, T., P. Salomone, T. Sands, G. Buck, K. Sechrist, and D. Koster. 2018. 2017 Bristol Bay area annual management report. Report, Alaska Department of Fish and Game, Fishery Management Report No. 18-11.

Fall, J., C. Brown, N. Braem, L. Hutchinson-Scarbrough, D. Koster, T. Krieg, and A. Brenner. 2012. Subsistence harvests and uses in three Bering Sea communities, 2008: Akutan, Emmonak, and Togiak. ADFG Division of Subsistence, Technical Paper **No. 371**.

FAO. 1995. Code of Conduct for Responsible Fisheries. Food and Agriculture Organization, Rome.

Farley, E., J. Moss, and R. Beamish. 2007. A Review of the critical size, critical period hypothesis for juvenile Pacific salmon. North Pacific Anadromous Fish Commission Bulletin **4**:311–317.

Farley, E. V., A. Starovoytov, S. Naydenko, R. Heintz, M. Trudel, C. Guthrie, L. Eisner, and J. R. Guyon. 2011. Implications of a warming eastern Bering Sea for Bristol Bay sockeye salmon. ICES Journal of Marine Science **68**:1138–1146.

Ferriss, B., and S. Zador. 2022. Ecosystem Status Report 2022: Gulf of Alaska. Report, North Pacific Fishery Management Council, 1007 West Third, Suite 400, Anchorage, Alaska 99501.

Fetterer, F., K. Knowles, W. N. Meier, M. Savoie, and A. K. Windnagel. 2017. Sea Ice Index, Version 3. Regional Daily Data. Report, Boulder, Colorado USA. NSIDC: National Snow and Ice Data Center.

Frey, K. E., J. A. Maslanik, J. C. Kinney, and W. Maslowski. 2014. Recent variability in sea ice cover, age, and thickness in the Pacific Arctic region, pages 31–63 . Springer.

Froese, R. 2006. Cube law, condition factor and weight–length relationships: history, meta-analysis and recommendations. Journal of Applied Ichthyology **22**:241–253.

Funk, F., L. K. Brannian, and K. A. Rowell. 1992. Age Structured Assessment of the Togiak Herring Stock, 1978-1992, and Preliminary Forecast of Abundance for 1993. Report, Alaska Department of Fish and Game, Division of Commercial Fisheries.

Funk, F., and K. A. Rowell. 1995. Population model suggests new threshold for managing Alaska's Togiak Fishery for Pacific herring in Bristol Bay. Alaska Fishery Research Bulletin **2**:125–136.

Glover, D. M., W. J. Jenkins, and S. C. Doney. 2011. Modeling methods for marine science. Cambridge University Press.

Goethel, D., C. Rodgveller, K. Echave, S. K. Shotwell, K. Siwicke, D. Hanselman, P. Malecha, M. Cheng, M. Williams, K. Omori, and C. Lunsford. 2022. Assessment of the Sablefish Stock in Alaska. Report, North Pacific Fishery Management Council, Anchorage, AK.

Gordon, H. R., G. C. Boynton, W. M. Balch, S. B. Groom, D. S. Harbour, and T. J. Smyth. 2001. Retrieval of coccolithophore calcite concentration from SeaWiFS imagery. Geophysical Research Letters **28**:1587–1590.

Graham, C. J., T. M. Sutton, M. D. Adkison, M. V. McPhee, and P. J. Richards. 2019. Evaluation of growth, survival, and recruitment of Chinook salmon in southeast Alaska rivers. Transactions of the American Fisheries Society **148**:243–259.

Graham, N., R. S. Ferro, W. A. Karp, and P. MacMullen. 2007. Fishing practice, gear design, and the ecosystem approach—three case studies demonstrating the effect of management strategy on gear selectivity and discards. ICES Journal of Marine Science **64**:744–750.

Grüss, A., J. T. Thorson, C. C. Stawitz, J. C. Reum, S. K. Rohan, and C. L. Barnes. 2021. Synthesis of interannual variability in spatial demographic processes supports the strong influence of cold-pool extent on eastern Bering Sea walleye pollock (*Gadus chalcogrammus*). Progress in Oceanography **194**:102569.

Haberle, I., L. Bavčević, and T. Klanjscek. 2023. Fish condition as an indicator of stock status: Insights from condition index in a food-limiting environment. Fish and Fisheries .

Hare, S. R., N. J. Mantua, and R. C. Francis. 1999. Inverse production regimes: Alaska and west coast Pacific salmon. Fisheries **24**:6–14.

Harley, J. R., K. Lanphier, E. G. Kennedy, T. A. Leighfield, A. Bidlack, M. O. Gribble, and C. Whitehead. 2020. The Southeast Alaska Tribal Ocean Research (SEATOR) Partnership: Addressing Data Gaps in Harmful Algal Bloom Monitoring and Shellfish Safety in Southeast Alaska. Toxins **12**:407.

Harris, R. P., P. H. Wiebe, J. Lenz, H. R. Skjoldal, and M. Huntley. 2000. ICES Zooplankton Methodology Manual. Amsterdam, The Netherlands.

Heintz, R. A., E. C. Siddon, E. V. Farley Jr, and J. M. Napp. 2013. Correlation between recruitment and fall condition of age-0 pollock (*Theragra chalcogramma*) from the eastern Bering Sea under varying climate conditions. Deep Sea Research Part II: Topical Studies in Oceanography **94**:150–156.

Hendrix, A. M., K. A. Lefebvre, L. Quakenbush, A. Bryan, R. Stimmelmayr, G. Sheffield, G. Wisswaesser, M. L. Willis, E. K. Bowers, and P. Kendrick. 2021. Ice seals as sentinels for algal toxin presence in the Pacific Arctic and subarctic marine ecosystems. Marine Mammal Science .

Hilborn, R., T. P. Quinn, D. E. Schindler, and D. E. Rogers. 2003. Biocomplexity and fisheries sustainability. Proceedings of the National Academy of Sciences of the United States of America **100**:6564–6568.

Holsman, K. K., and K. Aydin. 2015. Comparative methods for evaluating climate change impacts on the foraging ecology of Alaskan groundfish. Marine Ecology Progress Series **521**:217–235.

Holsman, K. K., K. Aydin, J. Sullivan, T. Hurst, and G. H. Kruse. 2019. Climate effects and bottom-up controls on growth and size-at-age of Pacific halibut (*Hippoglossus stenolepis*) in Alaska (USA). Fisheries Oceanography **28**:345–358.

Holsman, K. K., J. Ianelli, K. Aydin, A. E. Punt, and E. A. Moffitt. 2016. A comparison of fisheries biological reference points estimated from temperature-specific multi-species and single-species climate-enhanced stock assessment models. Deep Sea Research Part II: Topical Studies in Oceanography **134**:360–378.

Howard, K. G., S. Garcia, J. Murphy, and T. Dann. 2019. Juvenile Chinook salmon abundance index and survey feasibility assessment in the northern Bering Sea, 2014–2016. Report, Alaska Department of Fish and Game, Fishery Data Series No. 19-04, Anchorage.

Howard, K. G., S. Garcia, J. Murphy, and T. Dann. 2020. Northeastern Bering Sea juvenile Chinook salmon survey, 2017 and Yukon River adult run forecasts, 2018–2020. Report, Alaska Department of Fish and Game, Fishery Data Series No. 20-08, Anchorage.

Howard, K. G., and V. von Biela. 2023. Adult spawners: A critical period for subarctic Chinook salmon in a changing climate. Global Change Biology **29**:1759–1773.

Hsieh, C.-H., C. S. Reiss, J. R. Hunter, J. R. Beddington, R. M. May, and G. Sugihara. 2006. Fishing elevates variability in the abundance of exploited species. Nature **443**:859–862.

Hunt, G. L., P. H. Ressler, G. A. Gibson, A. De Robertis, K. Aydin, M. F. Sigler, I. Ortiz, E. J. Lessard, B. C. Williams, and A. Pinchuk. 2016. Euphausiids in the eastern Bering Sea: A synthesis of recent studies of euphausiid production, consumption and population control. Deep Sea Research Part II: Topical Studies in Oceanography **134**:204–222.

Hunt, G. L., P. Stabeno, G. Walters, E. Sinclair, R. D. Brodeur, J. M. Napp, and N. A. Bond. 2002. Climate change and control of the southeastern Bering Sea pelagic ecosystem. Deep-Sea Research Part II-Topical Studies in Oceanography **49**:5821–5853.

212

Hunt, J., George L., K. O. Coyle, L. B. Eisner, E. V. Farley, R. A. Heintz, F. Mueter, J. M. Napp, J. E. Overland, P. H. Ressler, S. Salo, and P. J. Stabeno. 2011. Climate impacts on eastern Bering Sea foodwebs: a synthesis of new data and an assessment of the Oscillating Control Hypothesis. ICES Journal of Marine Science **68**:1230–1243.

Ianelli, J., K. K. Holsman, A. E. Punt, and K. Aydin. 2016. Multi-model inference for incorporating trophic and climate uncertainty into stock assessments. Deep Sea Research Part II: Topical Studies in Oceanography **134**:379–389.

Ianelli, J., S. Stienessen, T. Honkalehto, E. Siddon, and C. Allen-Akselrud. 2022. Assessment of the Walleye Pollock Stock in the Eastern Bering Sea. Report, North Pacific Fishery Management Council, Anchorage, AK.

Iida, T., K. Mizobata, and S.-I. Saitoh. 2012. Interannual variability of coccolithophore *Emiliania huxleyi* blooms in response to changes in water column stability in the eastern Bering Sea. Continental Shelf Research **34**:7–17.

Jones, B., P. Crane, C. Larson, and M. Cunningham. 2021. Traditional Ecological Knowledge and Harvest Assessment of Dolly Varden and Other Nonsalmon Fish Utilized by Residents of the Togiak National Wildlife Refuge. Report, Alaska Department of Fish and Game, Division of Subsistence, Technical Paper No. 482, Anchorage, AK.

Jones, T., L. M. Divine, H. Renner, S. Knowles, K. A. Lefebvre, H. K. Burgess, C. Wright, and J. K. Parrish. 2019. Unusual mortality of Tufted puffins (*Fratercula cirrhata*) in the eastern Bering Sea. PloS one **14**:e0216532.

Jurado-Molina, J., P. A. Livingston, and J. N. Ianelli. 2005. Incorporating predation interactions in a statistical catch-at-age model for a predator-prey system in the eastern Bering Sea. Canadian Journal of Fisheries and Aquatic Sciences **62**:1865–1873.

Kalnay, E., M. Kananitcu, R. Kistler, W. Collins, and D. Deaven. 1996. The NCEP/NCAR 40-year reanalysis project. Bulletin of the American Meteorological Society **77**:437–471.

Karp, W. A., L. L. Desfosse, and S. G. Brooke. 2011. US National bycatch report. Report, U.S. Dep. Commer., NOAA Tech. Memo., NMFS-F/SPO-117E, 508 p.

Kelleher, K. 2005. Discards in the world's marine fisheries: an update. Report 9251052891, Food Agriculture Org., Vol. 470.

Kimmel, D. G., L. B. Eisner, and A. I. Pinchuk. 2023. The northern Bering Sea zooplankton community response to variability in sea ice: evidence from a series of warm and cold periods. Marine Ecology Progress Series **705**:21–42.

Kimmel, D. G., L. B. Eisner, M. T. Wilson, and J. T. Duffy-Anderson. 2018. Copepod dynamics across warm and cold periods in the eastern Bering Sea: Implications for walleye pollock (*Gadus chalcogrammus*) and the Oscillating Control Hypothesis. Fisheries Oceanography **27**:143–158.

Kiorboe, T., and M. Sabatini. 1995. Scaling of fecundity, growth and development in marine planktonic copepods. Marine ecology progress series. Oldendorf **120**:285–298.

Koenker, B. L., B. J. Laurel, L. A. Copeman, and L. Ciannelli. 2018. Effects of temperature and food availability on the survival and growth of larval Arctic cod (Boreogadus saida) and walleye pollock (Gadus chalcogrammus). ICES Journal of Marine Science **75**:2386–2402.

Kotwicki, S., and R. R. Lauth. 2013. Detecting temporal trends and environmentally-driven changes in the spatial distribution of bottom fishes and crabs on the eastern Bering Sea shelf. Deep Sea Research Part II: Topical Studies in Oceanography **94**:231–243.

KRITFC. 2022. Kuskokwim River Salmon Situation Report. Report, Kuskokwim River Inter-Tribal Fish Commission. `https://static1.squarespace.com/static/5afdc3d5e74940913f78773d/t/6359792089ec3e15693c80dd/1666808118921/Salmon+Sit+Report+2022_10-03-22_FINAL.pdf`

Ladd, C., L. Eisner, S. Salo, C. Mordy, and M. Iglesias-Rodriguez. 2018. Spatial and Temporal Variability of Coccolithophore Blooms in the Eastern Bering Sea. Journal of Geophysical Research: Oceans **123**:9119–9136.

Ladd, C., and P. J. Stabeno. 2012. Stratification on the Eastern Bering Sea shelf revisited. Deep Sea Research Part II: Topical Studies in Oceanography **65**:72–83.

Laurel, B. J., M. Spencer, P. Iseri, and L. A. Copeman. 2016. Temperature-dependent growth and behavior of juvenile Arctic cod (Boreogadus saida) and co-occurring North Pacific gadids. Polar Biology **39**:1127–1135.

Lauth, R. R., E. J. Dawson, and J. Conner. 2019. Results of the 2017 eastern and northern Bering Sea continental shelf bottom trawl survey of groundfish and invertebrate fauna. Report.

Lebida, R. C., and D. C. Whitmore. 1985. Bering Sea herring aerial survey manual. Report, Alaska Department of Fish and Game, Division of Commercial Fisheries, Bristol Bay Data Report No. 85-2, Anchorage, AK.

Lefebvre, K. A., E. Fachon, E. K. Bowers, D. G. Kimmel, J. A. Snyder, R. Stimmelmayr, J. M. Grebmeier, S. Kibler, D. R. Hardison, and D. M. Anderson. 2022. Paralytic shellfish toxins in Alaskan Arctic food webs during the anomalously warm ocean conditions of 2019 and estimated toxin doses to Pacific walruses and bowhead whales. Harmful Algae **114**:102205.

Lefebvre, K. A., L. Quakenbush, E. Frame, K. B. Huntington, G. Sheffield, R. Stimmelmayr, A. Bryan, P. Kendrick, H. Ziel, and T. Goldstein. 2016. Prevalence of algal toxins in Alaskan marine mammals foraging in a changing arctic and subarctic environment. Harmful Algae **55**:13–24.

Levins, R. 1974. Discussion paper: the qualitative analysis of partially specified systems. Annals of the New York Academy of Sciences **231**:123–138.

Litzow, M. A., M. E. Hunsicker, N. A. Bond, B. J. Burke, C. J. Cunningham, J. L. Gosselin, E. L. Norton, E. J. Ward, and S. G. Zador. 2020a. The changing physical and ecological meanings of North Pacific Ocean climate indices. Proceedings of the National Academy of Sciences **117**:7665–7671.

Litzow, M. A., M. J. Malick, N. A. Bond, C. J. Cunningham, J. L. Gosselin, and E. J. Ward. 2020b. Quantifying a Novel Climate Through Changes in PDO-Climate and PDO-Salmon Relationships. Geophysical Research Letters **47**:e2020GL087972.

Livingston, P. A., K. Aydin, T. W. Buckley, G. M. Lang, M.-S. Yang, and B. S. Miller. 2017. Quantifying food web interactions in the North Pacific–a data-based approach. Environmental Biology of Fishes **100**:443–470.

Long, W. C., K. M. Swiney, C. Harris, H. N. Page, and R. J. Foy. 2013. Effects of ocean acidification on juvenile red king crab (*Paralithodes camtschaticus*) and Tanner crab (*Chionoecetes bairdi*) growth, condition, calcification, and survival. PloS one **8**:e60959.

Lovvorn, J. R., C. L. Baduini, and G. L. Hunt. 2001. Modeling underwater visual and filter feeding by planktivorous shearwaters in unusual sea conditions. Ecology **82**:2342–2356.

Mantua, N. J., S. R. Hare, Y. Zhang, J. M. Wallace, and R. C. Francis. 1997. A Pacific Interdecadal Climate Oscillation with Impacts on Salmon Production. Bulletin of the American Meteorological Society **78**:1069–1079.

Maritorena, S., O. H. F. d'Andon, A. Mangin, and D. A. Siegel. 2010. Merged satellite ocean color data products using a bio-optical model: Characteristics, benefits and issues. Remote Sensing of Environment **114**:1791–1804.

Martinson, E. C., H. H. Stokes, and D. L. Scarnecchia. 2012. Use of juvenile salmon growth and temperature change indices to predict groundfish post age-0 yr class strengths in the Gulf of Alaska and eastern Bering Sea. Fisheries Oceanography **21**:307–319.

Matson, P. G., L. Washburn, E. A. Fields, C. Gotschalk, T. M. Ladd, D. A. Siegel, Z. S. Welch, and M. D. Iglesias-Rodriguez. 2019. Formation, development, and propagation of a rare coastal coccolithophore bloom. Journal of Geophysical Research: Oceans **124**:3298–3316.

Mayzaud, P., S. Falk-Petersen, M. Noyon, A. Wold, and M. Boutoute. 2016. Lipid composition of the three co-existing *Calanus* species in the Arctic: impact of season, location and environment. Polar Biology **39**:1819–1839.

Moss, J. H., D. A. Beauchamp, A. D. Cross, K. W. Myers, E. V. Farley Jr, J. M. Murphy, and J. H. Helle. 2005. Evidence for size-selective mortality after the first summer of ocean growth by pink salmon. Transactions of the American Fisheries Society **134**:1313–1322.

Mueter, F. J., and M. A. Litzow. 2008. Sea ice retreat alters the biogeography of the Bering Sea continental shelf. Ecological Applications **18**:309–320.

Murphy, J., S. Garcia, J. Dimond, J. Moss, F. Sewall, W. Strasburger, E. Lee, T. Dann, E. Labunski, T. Zeller, A. Gray, C. Waters, D. Jallen, D. Nicolls, R. Conlon, K. Cieciel, K. Howard, B. Harris, N. Wolf, and E. Farley. 2021. Northern Bering Sea surface trawl and ecosystem survey cruise report, 2019. Report, U.S. Dep. Commer., NOAA Tech. Memo. NMFS-AFSC-423, 124 p.

Murphy, J. M., K. G. Howard, J. C. Gann, K. C. Cieciel, W. D. Templin, and C. M. Guthrie. 2017. Juvenile Chinook Salmon abundance in the northern Bering Sea: Implications for future returns and fisheries in the Yukon River. Deep-Sea Research Part II-Topical Studies in Oceanography **135**:156–167.

Napp, J. M., and G. L. Hunt. 2001. Anomalous conditions in the south-eastern Bering Sea 1997: linkages among climate, weather, ocean, and Biology. Fisheries Oceanography **10**:61–68.

NASA. 2019. NASA Goddard Space Flight Center, O.E.L., Ocean Biology Processing Group. Report, Greenbelt, MD, USA.

NPFMC. 2016. Bering Sea/Aleutian Islands Groundfish Fishery Management Plan Amendment Action Summaries. Report, North Pacific Fishery Management Council, 605 W 4th Ave Suite 306, Anchorage, Alaska 99501.

NPFMC. 2017. Fishery Management Plan for Groundfish of the Bering Sea and Aleutian Islands Management Area. Report, North Pacific Fishery Management Council, 605 W 4th Ave Suite 306, Anchorage, Alaska 99501.

Olson, M. B., and S. L. Strom. 2002. Phytoplankton growth, microzooplankton herbivory and community structure in the southeast Bering Sea: insight into the formation and temporal persistence of an *Emiliania huxleyi* bloom. Deep Sea Research Part II: Topical Studies in Oceanography **49**:5969–5990.

Ortiz, I., F. Weise, and A. Greig. 2012. Marine regions boundary data for the Bering Sea shelf and slope. UCAR/NCAR—Earth Observing Laboratory/Computing, Data, and Software Facility. Dataset. doi **10**:D6DF6P6C.

Parsons, T. R., Y. Maita, and C. M. Lalli. 1984. A manual of biological and chemical methods for seawater analysis. Publ. Pergamon Press. Oxford.

Paul, A., and J. Paul. 1999. Interannual and regional variations in body length, weight and energy content of age-0 Pacific herring from Prince William Sound, Alaska. Journal of fish biology **54**:996–1001.

Pauly, D., V. Christensen, J. Dalsgaard, R. Froese, and F. Torres. 1998. Fishing down marine food webs. Science **279**:860–863.

Perrette, M., A. Yool, G. Quartly, and E. E. Popova. 2011. Near-ubiquity of ice-edge blooms in the Arctic. Biogeosciences **8**:515–524.

Piatt, J. F., J. K. Parrish, H. M. Renner, S. K. Schoen, T. T. Jones, M. L. Arimitsu, K. J. Kuletz, B. Bodenstein, M. García-Reyes, and R. S. Duerr. 2020. Extreme mortality and reproductive failure of common murres resulting from the northeast Pacific marine heatwave of 2014-2016. PloS one **15**:e0226087.

Pickart, R., G. Moore, T. Weingartner, S. Danielson, and K. Frey. 2013. Physical Drivers of the Chukchi, Beaufort, and Northern Bering Seas. Developing a Conceptual Model of the Arctic Marine Ecosystem **2**.

Pickart, R. S., M. A. Spall, G. W. Moore, T. J. Weingartner, R. A. Woodgate, K. Aagaard, and K. Shimada. 2011. Upwelling in the Alaskan Beaufort Sea: Atmospheric forcing and local versus non-local response. Progress in Oceanography **88**:78–100.

Pilcher, D. J., D. M. Naiman, J. N. Cross, A. J. Hermann, S. A. Siedlecki, G. A. Gibson, and J. T. Mathis. 2019. Modeled effect of coastal biogeochemical processes, climate variability, and ocean acidification on aragonite saturation state in the Bering Sea. Frontiers in Marine Science **5**:508.

Pinger, C., L. Copeman, M. Stowell, B. Cormack, C. Fugate, and M. Rogers. 2022. Rapid measurement of total lipids in zooplankton using the sulfo-phospho-vanillin reaction. Analytical Methods **14**:2665–2672.

Platt, T., C. Fuentes-Yaco, and K. T. Frank. 2003. Marine ecology: spring algal bloom and larval fish survival. Nature **423**:398–399.

Punt, A. E., R. J. Foy, M. G. Dalton, W. C. Long, and K. M. Swiney. 2016. Effects of long-term exposure to ocean acidification conditions on future southern Tanner crab (*Chionoecetes bairdi*) fisheries management. ICES Journal of Marine Science **73**:849–864.

Purcell, J. E., and M. N. Arai. 2001. Interactions of pelagic cnidarians and ctenophores with fish: a review. Hydrobiologia **451**:27–44.

Queirolo, L. E., L. Fritz, P. Livingston, M. Loefflad, D. Colpo, and Y. DeReynier. 1995. Bycatch, utilization, and discards in the commercial groundfish fisheries of the Gulf of Alaska, eastern Bering Sea, and Aleutian Islands. NOAA Tech. Memo. NMFS-AFSC **58**:148.

Reum, J. C., C. R. Kelble, C. J. Harvey, R. P. Wildermuth, N. Trifonova, S. M. Lucey, P. S. McDonald, and H. Townsend. 2021. Network approaches for formalizing conceptual models in ecosystem-based management. ICES Journal of Marine Science **78**:3674–3686.

Reum, J. C., P. S. McDonald, B. E. Ferriss, D. M. Farrell, C. J. Harvey, and P. S. Levin. 2015. Qualitative network models in support of ecosystem approaches to bivalve aquaculture. ICES Journal of Marine Science **72**:2278–2288.

Richardson, A., A. Walne, A. John, T. Jonas, J. Lindley, D. Sims, D. Stevens, and M. Witt. 2006. Using continuous plankton recorder data. Progress in Oceanography **68**:27–74.

Robinson, K. L., J. J. Ruzicka, M. B. Decker, R. Brodeur, F. Hernandez, J. Quiñones, E. Acha, S. Uye, H. Mianzan, and W. Graham. 2014. Jellyfish, forage fish, and the world's major fisheries. Oceanography **27**:104–115.

Rodgveller, C. J. 2019. The utility of length, age, liver condition, and body condition for predicting maturity and fecundity of female sablefish. Fisheries Research **216**:18–28.

Rodionov, S. N., N. A. Bond, and J. E. Overland. 2007. The Aleutian Low, storm tracks, and winter climate variability in the Bering Sea. Deep Sea Research Part II: Topical Studies in Oceanography **54**:2560–2577.

Rogers, L. A., and D. E. Schindler. 2011. Scale and the detection of climatic influences on the productivity of salmon populations. Global Change Biology **17**:2546–2558.

Rohan, S., L. Barnett, and N. Charriere. 2022. Evaluating approaches to estimating mean temperatures and cold pool area from Alaska Fisheries Science Center bottom trawl surveys of the eastern Bering Sea .

Rooper, C. N., M. F. Sigler, P. Goddard, P. Malecha, R. Towler, K. Williams, R. Wilborn, and M. Zimmermann. 2016. Validation and improvement of species distribution models for structure-forming invertebrates in the eastern Bering Sea with an independent survey. Marine Ecology Progress Series **551**:117–130.

RTeam. 2023. R: A language and environment for statistical computing. R Foundation for Statistical Computing. http://www. R-project. org/., Vienna, Austria.

Ruggerone, G. T., B. A. Agler, B. M. Connors, E. V. Farley Jr, J. R. Irvine, L. I. Wilson, and E. M. Yasumiishi. 2016. Pink and sockeye salmon interactions at sea and their influence on forecast error of Bristol Bay sockeye salmon. North Pacific Anadromous Fish Commission Bulletin **6**:349–361.

Ruggerone, G. T., and J. L. Nielsen. 2004. Evidence for competitive dominance of pink salmon (*Oncorhynchus gorbuscha*) over other salmonids in the North Pacific Ocean. Reviews in Fish Biology and Fisheries **14**:371–390.

Ruggerone, G. T., A. M. Springer, G. B. van Vliet, B. Connors, J. R. Irvine, L. D. Shaul, M. R. Sloat, and W. I. Atlas. 2023. From diatoms to killer whales: impacts of pink salmon on North Pacific ecosystems. Marine Ecology Progress Series **719**:1–40.

Schindler, D. E., R. Hilborn, B. Chasco, C. P. Boatright, T. P. Quinn, L. A. Rogers, and M. S. Webster. 2010. Population diversity and the portfolio effect in an exploited species. Nature **465**:609–613.

Schindler, D. E., P. R. Leavitt, S. P. Johnson, and C. S. Brock. 2006. A 500-year context for the recent surge in sockeye salmon (*Oncorhynchus nerka*) abundance in the Alagnak River, Alaska. Canadian Journal of Fisheries and Aquatic Sciences **63**:1439–1444.

Seung, C. K., M. G. Dalton, A. E. Punt, D. Poljak, and R. Foy. 2015. Economic impacts of changes in an Alaska crab fishery from ocean acidification. Climate Change Economics **6**:1550017.

Shin, Y.-J., M.-J. Rochet, S. Jennings, J. G. Field, and H. Gislason. 2005. Using size-based indicators to evaluate the ecosystem effects of fishing. ICES Journal of marine Science **62**:384–396.

Shin, Y.-J., L. J. Shannon, A. Bundy, M. Coll, K. Aydin, N. Bez, J. L. Blanchard, M. d. F. Borges, I. Diallo, and E. Diaz. 2010. Using indicators for evaluating, comparing, and communicating the ecological status of exploited marine ecosystems. Part 2. Setting the scene. ICES Journal of Marine Science **67**:692–716.

Siddon, E. 2020. Ecosystem Status Report 2020: Eastern Bering Sea. Report, North Pacific Fishery Management Council, 1007 West Third, Suite 400, Anchorage, Alaska 99501.

Siddon, E. 2021. Ecosystem Status Report 2021: Eastern Bering Sea. Report, North Pacific Fishery Management Council, 1007 West Third, Suite 400, Anchorage, Alaska 99501.

Siddon, E. 2022. Ecosystem Status Report 2022: Eastern Bering Sea. Report, North Pacific Fishery Management Council, 1007 West Third, Suite 400, Anchorage, Alaska 99501.

Siddon, E. C., R. A. Heintz, and F. J. Mueter. 2013. Conceptual model of energy allocation in walleye pollock (*Theragra chalcogramma*) from age-0 to age-1 in the southeastern Bering Sea. Deep Sea Research Part II: Topical Studies in Oceanography **94**:140–149.

Sigler, M. F., F. J. Mueter, B. A. Bluhm, M. S. Busby, E. D. Cokelet, S. L. Danielson, A. De Robertis, L. B. Eisner, E. V. Farley, and K. Iken. 2017. Late summer zoogeography of the northern Bering and Chukchi seas. Deep Sea Research Part II: Topical Studies in Oceanography **135**:168–189.

Sigler, M. F., P. J. Stabeno, L. B. Eisner, J. M. Napp, and F. J. Mueter. 2014. Spring and fall phytoplankton blooms in a productive subarctic ecosystem, the eastern Bering Sea, during 1995–2011. Deep Sea Research Part II: Topical Studies in Oceanography **109**:71–83.

Simpson, S. C., M. P. Eagleton, J. V. Olson, G. A. Harrington, and S. R. Kelly. 2017. Essential fish habitat 5-year review: summary report, 2010 through 2015 .

Spear, A., A. G. Andrews III, J. Duffy-Anderson, T. Jarvis, D. Kimmel, and D. McKelvey. 2023. Changes in the vertical distribution of age-0 walleye pollock (Gadus chalcogrammus) during warm and cold years in the southeastern Bering Sea. Fisheries Oceanography **32**:177–195.

Spencer, P. D. 2008. Density-independent and density-dependent factors affecting temporal changes in spatial distributions of eastern Bering Sea flatfish. Fisheries Oceanography **17**:396–410.

Spencer, P. D., K. K. Holsman, S. Zador, N. A. Bond, F. J. Mueter, A. B. Hollowed, and J. N. Ianelli. 2016. Modelling spatially dependent predation mortality of eastern Bering Sea walleye pollock, and its implications for stock dynamics under future climate scenarios. ICES Journal of Marine Science **73**:1330–1342.

Springer, A. M., C. P. McRoy, and M. V. Flint. 1996. The Bering Sea Green Belt: Shelf-edge processes and ecosystem production. Fisheries Oceanography **5**:205–223.

Springer, A. M., and G. B. van Vliet. 2014. Climate change, pink salmon, and the nexus between bottom-up and top-down forcing in the subarctic Pacific Ocean and Bering Sea. Proceedings of the National Academy of Sciences **111**:E1880–E1888.

Stabeno, P., S. Danielson, D. Kachel, N. Kachel, and C. Mordy. 2016. Currents and transport on the eastern Bering Sea shelf: An integration of over 20 years of data. Deep Sea Research Part II: Topical Studies in Oceanography **134**:13–29.

Stabeno, P., J. Duffy-Anderson, L. Eisner, E. Farley, R. Heintz, and C. Mordy. 2017. Return of warm conditions in the southeastern Bering Sea: Physics to fluorescence. PloS one **12**:e0185464.

Stabeno, P. J., and S. W. Bell. 2019. Extreme conditions in the Bering Sea (2017–2018): record-breaking low sea-ice extent. Geophysical Research Letters **46**:8952–8959.

Stabeno, P. J., J. Farley, E. V., N. B. Kachel, S. Moore, C. W. Mordy, J. M. Napp, J. E. Overland, A. I. Pinchuk, and M. F. Sigler. 2012. A comparison of the physics of the northern and southern shelves of the eastern Bering Sea and some implications for the ecosystem. Deep-Sea Research Part II-Topical Studies in Oceanography **65-70**:14–30.

Stevenson, D., and G. Hoff. 2009. Species identification confidence in the eastern Bering Sea shelf survey (1982 - 2008). Report, NOAA NMFS-AFSC, 7600 Sand Point Way NE, Seattle, WA 98115, AFSC Processed Report 2009-04, 46 p.

Stevenson, D., K. Weinberg, and R. Lauth. 2016. Estimating confidence in trawl efficiency and catch quantification for the eastern Bering Sea shelf survey. Report, U.S. Dep. Commer., NOAA Tech. Memo., NMFS-AFSC-335, 51 p.

Stevenson, D. E., and R. R. Lauth. 2019. Bottom trawl surveys in the northern Bering Sea indicate recent shifts in the distribution of marine species. Polar Biology **42**:407–421.

Stockwell, D. A., T. E. Whitledge, S. I. Zeeman, K. O. Coyle, J. M. Napp, R. D. Brodeur, A. I. Pinchuk, and G. L. Hunt. 2001. Anomalous conditions in the south-eastern Bering Sea, 1997: nutrients, phytoplankton and zooplankton. Fisheries Oceanography **10**:99–116.

Stram, D. L., and J. N. Ianelli. 2015. Evaluating the efficacy of salmon bycatch measures using fishery-dependent data. ICES Journal of Marine Science **72**:1173–1180.

Suryan, R. M., M. L. Arimitsu, H. A. Coletti, R. R. Hopcroft, M. R. Lindeberg, S. J. Barbeaux, S. D. Batten, W. J. Burt, M. A. Bishop, and J. L. Bodkin. 2021. Ecosystem response persists after a prolonged marine heatwave. Scientific reports **11**:1–17.

Swiney, K. M., W. C. Long, and R. J. Foy. 2017. Decreased pH and increased temperatures affect young-of-the-year red king crab (*Paralithodes camtschaticus*). ICES Journal of Marine Science **74**:1191–1200.

Tarrant, A. M., L. B. Eisner, and D. G. Kimmel. 2021. Lipid-related gene expression and sensitivity to starvation in Calanus glacialis in the eastern Bering Sea. Marine Ecology Progress Series **674**:73–88.

Thorson, J., M. Fossheim, F. Mueter, E. Olsen, R. Lauth, R. Primicerio, B. Husson, J. Marsh, A. Dolgov, and S. Zador. 2019. Comparison of near-bottom fish densities show rapid community and population shifts in Bering and Barents Seas. Arctic Report Card .

Thorson, J. T. 2019a. Guidance for decisions using the Vector Autoregressive Spatio-Temporal (VAST) package in stock, ecosystem, habitat and climate assessments. Fisheries Research **210**:143–161.

Thorson, J. T. 2019b. Measuring the impact of oceanographic indices on species distribution shifts: The spatially varying effect of cold-pool extent in the eastern Bering Sea. Limnology and Oceanography **64**:2632–2645.

Thorson, J. T., L. Ciannelli, and M. A. Litzow. 2020. Defining indices of ecosystem variability using biological samples of fish communities: A generalization of empirical orthogonal functions. Progress in Oceanography **181**:102244.

Thorson, J. T., and K. Kristensen. 2016. Implementing a generic method for bias correction in statistical models using random effects, with spatial and population dynamics examples. Fisheries Research **175**:66–74.

Thorson, J. T., A. O. Shelton, E. J. Ward, and H. J. Skaug. 2015. Geostatistical delta-generalized linear mixed models improve precision for estimated abundance indices for West Coast groundfishes. ICES Journal of Marine Science **72**:1297–1310.

Tobin, E. D., C. L. Wallace, C. Crumpton, G. Johnson, and G. L. Eckert. 2019. Environmental drivers of paralytic shellfish toxin producing *Alexandrium catenella* blooms in a fjord system of northern Southeast Alaska. Harmful algae **88**:101659.

Tojo, N., G. H. Kruse, and F. C. Funk. 2007. Migration dynamics of Pacific herring (*Clupea pallasii*) and response to spring environmental variability in the southeastern Bering Sea. Deep Sea Research Part II: Topical Studies in Oceanography **54**:2832–2848.

Trenberth, K., and J. W. Hurrell. 1994. Decadal atmosphere-ocean variations in the Pacific. Climate Dynamics **9**:303–319.

Vandersea, M. W., S. R. Kibler, P. A. Tester, K. Holderied, D. E. Hondolero, K. Powell, S. Baird, A. Doroff, D. Dugan, and R. W. Litaker. 2018. Environmental factors influencing the distribution and abundance of *Alexandrium catenella* in Kachemak bay and lower cook inlet, Alaska. Harmful algae **77**:81–92.

Vollenweider, J. J., R. A. Heintz, L. Schaufler, and R. Bradshaw. 2011. Seasonal cycles in whole-body proximate composition and energy content of forage fish vary with water depth. Marine biology **158**:413–427.

von Biela, V. R., C. J. Sergeant, M. P. Carey, Z. Liller, C. Russell, S. Quinn-Davidson, P. S. Rand, P. A. Westley, and C. E. Zimmerman. 2022. Premature mortality observations among Alaska's Pacific Salmon during record heat and drought in 2019. Fisheries **47**:157–168.

Waga, H., H. Eicken, T. Hirawake, and Y. Fukamachi. 2021. Variability in spring phytoplankton blooms associated with ice retreat timing in the Pacific Arctic from 2003–2019. Plos one **16**:e0261418.

Waldbusser, G. G., B. Hales, C. J. Langdon, B. A. Haley, P. Schrader, E. L. Brunner, M. W. Gray, C. A. Miller, and I. Gimenez. 2015. Saturation-state sensitivity of marine bivalve larvae to ocean acidification. Nature Climate Change **5**:273–280.

Wespestad, V., and D. Gunderson. 1991. Climatic induced variation in Eastern Bering Sea herring recruitment. Report, Proceedings of the International Herring Symposium, Anchorage, AK. Alaska Sea Grant.

Wilderbuer, T., W. Stockhausen, and N. Bond. 2013. Updated analysis of flatfish recruitment response to climate variability and ocean conditions in the Eastern Bering Sea. Deep Sea Research Part II: Topical Studies in Oceanography **94**:157–164.

Wilderbuer, T. K. 2017. Eastern Bering Sea Winter Spawning Flatfish Recruitment and Wind Forcing. Stock Assessment and Fishery Evaluation Report, North Pacific Fishery Management Council, 605 W 4th Ave, Suite 306, Anchorage, AK 99501.

Wilderbuer, T. K., A. B. Hollowed, W. J. Ingraham, P. D. Spencer, M. E. Conners, N. A. Bond, and G. E. Walters. 2002. Flatfish recruitment response to decadal climatic variability and ocean conditions in the eastern Bering Sea. Progress in Oceanography **55**:235–247.

Williams, E. H., and T. J. Quinn. 2000. Pacific herring, *Clupea pallasii*, recruitment in the Bering Sea and north-east Pacific Ocean, I: relationships among different populations. Fisheries Oceanography **9**:285–299.

Winemiller, K. O. 2005. Life history strategies, population regulation, and implications for fisheries management. Canadian Journal of Fisheries and Aquatic Sciences **62**:872–885.

Woodgate, R. A., T. J. Weingartner, and R. Lindsay. 2012. Observed increases in Bering Strait oceanic fluxes from the Pacific to the Arctic from 2001 to 2011 and their impacts on the Arctic Ocean water column. Geophysical Research Letters **39**.

Wuenschel, M. J., W. D. McElroy, K. Oliveira, and R. S. McBride. 2019. Measuring fish condition: an evaluation of new and old metrics for three species with contrasting life histories. Canadian Journal of Fisheries and Aquatic Sciences **76**:886–903.

Yasumiishi, E. M., K. Cieciel, A. G. Andrews, J. Murphy, and J. A. Dimond. 2020. Climate-related changes in the biomass and distribution of small pelagic fishes in the eastern Bering Sea during late summer, 2002–2018. Deep Sea Research Part II: Topical Studies in Oceanography **181**:104907.

Zador, S. G., and S. Fitzgerald. 2008. Seabird attraction to trawler discards. Report, Alaska Fisheries Science Center, NOAA, NMFS, 7600 Sand Point Way NE, Seattle WA 98115.

Zaleski, M., T. S. Smeltz, S. Rheinsmith, J. L. Pirtle, and G. A. Harrington. 2023. 2022 Evaluation of the Fishing Effects on Essential Fish Habitat. Report, U.S. Dep. Commer., NOAA Tech. Memo. NMFS-F/AKR-29, 205 p.

Appendix

History of the ESRs

Since 1995, staff at the Alaska Fisheries Science Center have prepared a separate Ecosystem Status (formerly Considerations) Report within the annual Stock Assessment and Fishery Evaluation (SAFE) report. Each new Ecosystem Status Report provides updates and new information to supplement the original report. The original 1995 report presented a compendium of general information on the Gulf of Alaska, Bering Sea, and Aleutian Island ecosystems as well as a general discussion of ecosystem-based management. The 1996 edition provided additional information on biological features of the North Pacific, and highlighted the effects of bycatch and discards on the ecosystem. The 1997 edition provided a review of ecosystem-based management literature and ongoing ecosystem research, and provided supplemental information on seabirds and marine mammals. The 1998 edition provided information on the precautionary approach, essential fish habitat, effects of fishing gear on habitat, El Niño, local knowledge, and other ecosystem information. The 1999 edition again gave updates on new trends in ecosystem-based management, essential fish habitat, research on effects of fishing gear on seafloor habitat, marine protected areas, seabirds and marine mammals, oceanographic changes in 1997/98, and local knowledge.

In 1999, a proposal came forward to enhance the Ecosystem Status Report by including more information on indicators of ecosystem status and trends and more ecosystem-based management performance measures. The purpose of this enhancement was to accomplish several goals:

1. Track ecosystem-based management efforts and their efficacy

2. Track changes in the ecosystem that are not easily incorporated into single-species assessments

3. Bring results from ecosystem research efforts to the attention of stock assessment scientists and fishery managers

4. Provide a stronger link between ecosystem research and fishery management

5. Provide an assessment of the past, present, and future role of climate and humans in influencing ecosystem status and trends

Each year since 1999, the Ecosystem Status Reports have included some new contributions and will continue to evolve as new information becomes available. Evaluation of the meaning of observed changes should be in the context of how each indicator relates to a particular ecosystem component.

For example, particular oceanographic conditions, such as bottom temperature increases, might be favorable to some species but not for others. Evaluations should follow an analysis framework such as that provided in the draft Programmatic Groundfish Fishery Environmental Impact Statement that links indicators to particular effects on ecosystem components.

In 2002, stock assessment scientists began using indicators contained in this report to systematically assess ecosystem factors such as climate, predators, prey, and habitat that might affect a particular stock. Information regarding a particular fishery's catch, bycatch, and temporal/spatial distribution can be used to assess possible impacts of that fishery on the ecosystem. Indicators of concern can be highlighted within each assessment and can be used by the Groundfish Plan Teams and the Council to justify modification of allowable biological catch (ABC) recommendations or time/space allocations of catch.

We initiated a regional approach to the ESR in 2010 and presented a new ecosystem assessment for the eastern Bering Sea. In 2011, we followed the same approach and presented a new assessment for the Aleutian Islands based on a similar format to that of the eastern Bering Sea. In 2012, we provided a preliminary ecosystem assessment on the Arctic. Our intent was to provide an overview of general Arctic ecosystem information that may form the basis for more comprehensive future Arctic ecosystem assessments. In 2015, we presented a new Gulf of Alaska report card and assessment, which was further divided into Western and Eastern Gulf of Alaska report cards beginning in 2016. This was also the year that the previous Alaska-wide ESR was split into four separate report, one for the Gulf of Alaska, Aleutian Islands, eastern Bering Sea, and the Arctic[29].

The eastern Bering Sea and Aleutian Islands ecosystem assessments were based on additional refinements contributed by Ecosystem Synthesis Teams. For these assessments, the teams focused on a subset of broad, community-level indicators to determine the current state and likely future trends of ecosystem productivity in the EBS and ecosystem variability in the Aleutian Islands. The teams also selected indicators that reflect trends in non-fishery apex predators and maintaining a sustainable species mix in the harvest as well as changes to catch diversity and variability. Indicators for the Gulf of Alaska report card and assessment were also selected by a team of experts, via an online survey first, then refined in an in-person workshop.

Originally, contributors to the Ecosystem Status Reports were asked to provide a description of their contributed indicator, summarize the historical trends and current status of the indicator, and identify potential factors causing those trends. Beginning in 2009, contributors were also asked to describe why the indicator is important to groundfish fishery management and implications of indicator trends. In particular, contributors were asked to briefly address implications or impacts of the observed trends on the ecosystem or ecosystem components, what the trends mean and why are they important, and how the information can be used to inform groundfish management decisions. Answers to these types of questions will help provide a "heads-up" for developing management responses and research priorities. In 2018, a risk table framework was developed for individual stock assessments as a means of documenting concerns external to the stock assessment model, but relevant to setting the Acceptable Biological Catch (ABC) value for the current year. These concerns could be categorized as those reflecting the assessment model, the population dynamics of the stock, and environmental and ecosystem concerns— including those based on information from Ecosystem Status Reports. In the past, concerns used to justify an ABC below the maximum estimated by the assessment model were documented in an ad-hoc manner in the stock assessment report or in the minutes of the Groundfish Plan Teams or Scientific and

---

[29]The Arctic report is under development

Statistical Committee (SSC) reviews. With the risk table, formal consideration of concerns—including ecosystem—are documented and ranked, and the stock assessment author presents a recommendation for the maximum ABC as specified by the stock assessment model or a lower value. The recommended ABC (whether at maximum or lower) from the lead stock assessment author is subsequently reviewed and adjusted or accepted by the Groundfish Plan Team and the Scientific and Statistical Committee. Five risk tables were completed in 2018 as a test case. After review, the Council requested risk tables to be included in all full stock assessments in 2019. The SSC also requested a fourth category of concern to be added to the risk tables. The fishery performance category serves to represent any concerns related to the recommended ABC that can be inferred from commercial fisheries performance. Importantly, these concerns refer to indications of stock status, not economic performance.

In Briefs were started in 2018 for the Eastern Bering Sea, 2019 for the Gulf of Alaska, and 2020 for the Aleutian Islands. These more public-friendly succinct versions of the full ESRs are now planned to be produced in tandem with the ESRs.

In 2019, risk tables were completed for all full assessments. Ecosystem scientists collaborated with stock assessment scientists to use the Ecosystem Status Reports to help inform the ecosystem concerns in the risk tables. Some ecosystem information can also be used to inform concerns related to the population dynamics of the stock. Initially, there were 4 levels of concern from no concern to extreme. In 2023, based on a recommendation from the SSC, the levels of risk were reduced to 3, from low (no concern) to high (major/extreme). For stock assessments which include and Ecosystem and Socioeconomic Profile (ESP), the ESP is also used to inform the ecosystem risk column as well as the population dynamics and fisheries performance columns.

ESPs were initiated in 2017 (Sablefish) and ESR editors began working closely with ESP teams in 2019 (starting with GOA walleye pollock). These complimentary annual status reports inform groundfish management and alignment in research that feeds these reports increases efficiency and collaboration between ecosystem and stock assessment scientists.

This report represents much of the first three steps in Alaska's IEA: defining ecosystem goals, developing indicators, and assessing the ecosystems (Figure 119). The primary stakeholders in this case are the North Pacific Fishery Management Council. Research and development of risk analyses and management strategies is ongoing and will be referenced or included as possible.

It was requested that contributors to the Ecosystem Status Reports provide actual time series data or make them available electronically. The Ecosystem Status Reports and data for many of the time series presented within are available online at: `http://access.afsc.noaa.gov/reem/ecoweb/`. These reports and data are also available through the NOAA-wide IEA website at: `https://www.integratedecosystemassessment.noaa.gov/regions/alaska`.

Past reports and all groundfish stock assessments are available at: `https://www.fisheries.noaa.gov/alaska/population-assessments/north-pacific-groundfish-stock-assessment-and-fishery-evaluation`.

If you wish to obtain a copy of an Ecosystem Considerations Report version prior to 2000, please contact the Council office at: 1-907-271-2809.
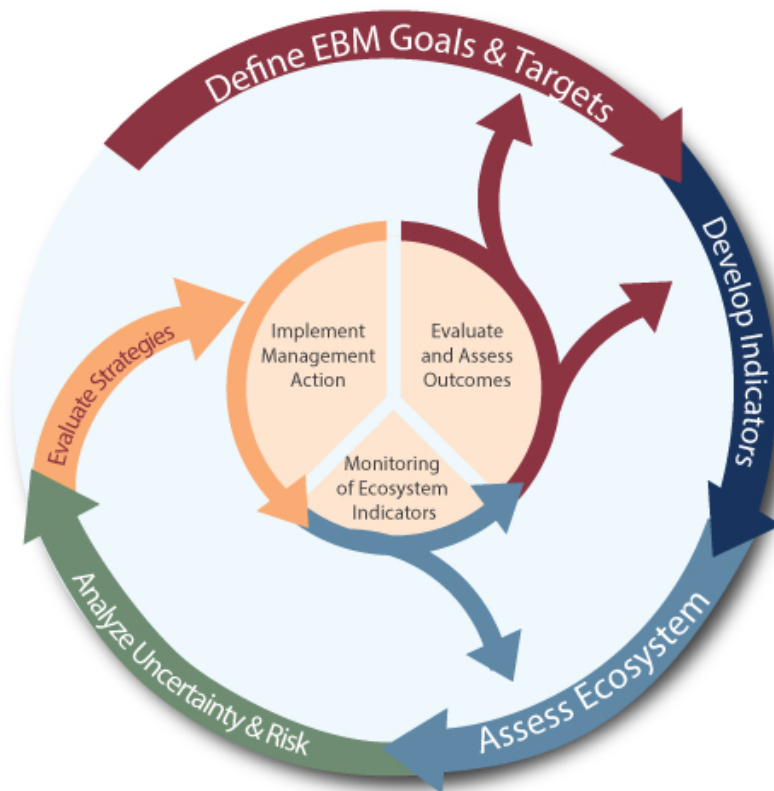
Figure 119: The IEA (integrated ecosystem assessment) process.

Responses to SSC comments from December 2022

December 2022 SSC Final Report to the NPFMC
C4 BSAI and C5 GOA Ecosystem Status Reports
The SSC received presentations from Elizabeth Siddon (NOAA-AFSC), Ivonne Ortiz (University of Washington), and Bridget Ferriss (NOAA-AFSC). Lauren Divine (Aleut Community of St. Paul Island) provided public testimony on the eastern Bering Sea (EBS) Ecosystem Status Report (ESR); there was no public testimony for the Aleutian Islands (AI) or Gulf of Alaska (GOA) ESRs. The SSC thanks the presenters for their efforts in providing excellent, clear, and well-focused summaries of information on the status of the marine ecosystems that support federally managed fisheries off Alaska. The SSC appreciated the structure of the reports and the In-Briefs and noted that the various ways of communicating the information in the reports was valuable in reaching different audiences and informing different purposes. The SSC welcomed the addition of graphics in each report demonstrating how this information is incorporated into Council processes and was pleased to hear from communities and stakeholders that they value seeing their contributions in the report and the "In Brief" products.

Thank you. We want to acknowledge the effort and thank all those involved in collecting, analyzing, interpreting, and communicating the observations included in these reports.

There were no new major environmental concerns reported from 2022, but unusual warm conditions persist in the western Aleutian Islands and conditions in the northern Bering Sea (NBS) remain of concern.

General Comments Applicable to all three ESRs
The SSC was pleased to see several instances where authors provided very long time series, which provided a context for present observations. The SSC notes that there is a need for some authors to define what is "normal" and when some aspect of the environment is considered an anomaly that is above or below "normal". When there is a reference to "long-term-mean", **the SSC requests that authors for each section be encouraged to state the period over which "normal" (the mean, or median) is calculated, and the degree of departure from the mean or median needed to identify something as an anomaly.** *It would also be helpful if authors would state the source(s) of their data and the website/url where the data can be found, if applicable.*

ESR authors and contributors paid close attention to defining time series length, defining the average or median (authors are trying to move away from using "normal"), and articulating what constitutes an anomaly. Data sources are provided, where appropriate.

The SSC recognizes that considerable thought has gone into developing a statistically sound definition of marine heat waves based on excursions above the mean temperature for a given time of the year at a given place. **The SSC suggests that it would be useful to consider that different species may react differently to a given temperature**, *regardless of location and time of year. Is there a need, and a way, to present marine heat waves in relation to the temperature sensitivities of the species of concern?*

ESR authors believe the role of the ESR is to provide whole-ecosystem context. We work closely with ESP teams as those documents are developed and produced and believe ESPs are a more appropriate report for documenting species-specific thresholds. For stock assessments that do not have ESPs, the

ESR authors will work to review species-specific reference temperatures and/or phenology (spawning, egg development, hatching timing, location, growth curves) for discussion with the stock assessment authors for risk table determinations.

The SSC understands the challenges of reporting zooplankton to species in the Rapid Assessments. That said, **the SSC suggests that additional information indicating the abundance of key copepod species that are large and lipid-rich at later stages (C4 or C5) would be valuable.**

ESR authors communicated this recommendation to AFSC zooplankton expert, David Kimmel. Below is Dr. Kimmel's response:
"We agree with the SSC that additional information on key copepod species that are lipid rich and in the C4/C5 stage would be useful. We will determine if our large copepod time-series correlates with key species, such as *Calanus glacialis*, later in the year. Identifying copepods at sea is simply not possible given the time and expertise necessary to carry out such a task across multiple ecosystem surveys."

For indicators that do not have any updated data in 2022 (e.g., groundfish surveys, Steller sea lion surveys), the SSC recommends that the authors are consistent in providing headers but omit repetition of data that was presented in the prior year without any additional updates.

The ESR editors will be consistent in not including contributions that have not been updated since the previous year's ESR. Where appropriate, we will provide headers identifying contribution that were not updated but are expected to return when new data are available. While the ESR has been largely successful in working with our collaborators to include present year data, there are still some contributions that are 1 year lagged due to data analysis requirements or the delayed availability of survey data. Sections with no updates provide the following text:
"There are no updates in this year's report. See the contribution archive for previous indicators at: https://apps-afsc.fisheries.noaa.gov/refm/reem/ecoweb/index.php."

The SSC supports further efforts to enhance the uptake of this ecosystem information into stock assessments, consistent with a nationwide push for strengthening ecosystem-based fishery management.

BSAI Ecosystem Status Reports
Eastern Bering Sea
The EBS ESR provided a thoughtful recap of conditions in the EBS during the recent warm period (2014–2021) that included the winter of 2017/2018 and 2018/2019 (summers 2018 and 2019), which were "unprecedented" in terms of low sea ice and subsequent reduced cold pool extent. During this time, the groundfish community as a whole shifted northward, primarily associated with major movements of pollock and Pacific cod from the southern shelf into the NBS and southern Chukchi Sea. During this same period, there was also a precipitous decline in snow crab abundance.

Two contributions on Noteworthy Topics were provided, one on factors affecting 2022 western Alaska Chinook salmon runs and subsistence harvest, and one reporting on development of "long-range" climate models that provide predictions out to 2100. **The excellent report on the Yukon-Kuskokwim salmon declines was notable because of the broad collaboration of individuals from federal and State of Alaska agencies, as well as from the Kuskokwim River Inter-Tribal Fish Commission, the Bering Sea Fishermen's Association, and the Ocean Conservancy. These groups cooperated in the examination of the multiplicity of factors, both within the watershed and in the ocean, that**

are likely to be contributing to the declines of these salmon runs. *The inclusion of an infographic, a map of the region and the locations of communities and villages impacted by the declines in salmon, was very helpful. The second Noteworthy Topic focused on a new model offering high resolution climate change projections for the EBS. This model provided projections of surface and bottom temperatures in the EBS out to 2100. The projections were based on two different emission scenarios, a high mitigation scenario SSP 126 and a low mitigation scenario, SSP 585. Temperature projections based on the high mitigation estimates suggested that by 2050, bottom temperatures in summer will exceed 4ºC.*

In 2022, the physical aspects of the marine environment of the EBS returned to values like those in past "average" years. *The EBS in 2021–2022 exhibited "near-normal" sea surface temperatures, with marine heat waves being infrequent and brief. Winds in winter 2022 were more northerly than the "longterm average", promoting rapid sea-ice growth in November 2021, but sea ice was thin over much of the shelf and mostly absent in the south. Sea ice extent in 2022 was greater than in 2021, but ice retreated quickly in April. The cold pool was "average" in extent when compared to other cool years. pH was relatively low over the outer and middle shelf in 2022, and near the Bering Strait, decreasing at a rate comparable to the global oceans due to ocean acidification. The impacts on the marine ecosystem from Typhoon Merbok, which occurred in mid-September 2022, are presently unknown.*

Please see the Physical Environment Synthesis section (p. 28) for a description of delayed sea ice formation in fall 2022 due, in part, to ex-Typhoon Merbok.

The biological aspects of the marine environment of the EBS were also similar to what has been seen in past "average" years. The timing of the spring bloom peak was "average" but there was a continued decrease in chlorophyll-a concentrations near the shelf break without a clear cause. There were more small copepods and fewer large copepods and euphausiids than usual in spring. The lack of large copepods in spring is likely not of concern as larval and juvenile fish will be consuming mostly small prey items during spring. However, in late summer/fall, there were fewer large copepods than usual at a time when juvenile pollock require lipid-rich prey for building energy reserves for overwintering. The SSC suggests that the contrast between spring and fall conditions in light of different prey requirements for juvenile fish in the spring and fall could perhaps be captured through an index that combines prey conditions across both seasons.

ESR authors communicated this recommendation to AFSC zooplankton expert, David Kimmel. Below is Dr. Kimmel's response:
"We agree with the SSC that finer detail on spring and fall abundances and conditions would be useful. To address this, we have further separated the Bering Sea time-series into early spring (mooring survey), late spring (larval survey), summer (age-0 survey), and early fall (mooring survey). This will help further demonstrate how these indicators change throughout the year. We have been reporting lipid content for euphausiids and large copepods (primarily *Calanus*) and do not have enough data to develop a time-series at this point, but that will be an addition to this ESR contribution in the future."

The acoustic survey of euphausiids revealed a below average abundance, though near-surface net surveys in late summer/fall showed higher numbers of euphausiids relative to the spring survey in both the southeastern Bering Sea and to past years in the northeastern Bering Sea. Jellyfish catch per unit effort (CPUE) in the bottom trawl survey was higher than the CPUE in 2021.

Given the sea-ice cover in the winter of 2021–2022, it might have been expected that the production of large, lipid-rich Calanus glacialis *would have been favored in 2022. The lack of* C. glacialis *in 2022 may be a reflection of the exceedingly low levels of sea-ice coverage in 2018, 2019, 2021, and, to a*

lesser extent, in 2022. It is important to note that a recent publication (Tarrant, A.M., Eisner, L.B., and Kimmel, D.G. 2021. Mar. Ecol. Prog. Ser. 674: 73-88; Tarrant et al., 2021) has demonstrated that the vast majority of large copepods over the eastern shelf are C. glacialis, *and not* C. marshallae. C. glacialis *grazes on ice algae in late winter/early spring to gain energy for egg production. In years with little or no sea ice over the southeastern shelf,* C. glacialis *is scarce, e.g., as in 2018.* C. marshallae *overwinters at depth off the shelf in the GOA and southward to Oregon. They feed on micro-zooplankton at depth in spring and are advected onto the shelves of Oregon, Washington and the GOA. They have been identified in the NBS and possibly are advected through the passes of the Aleutian Islands and subsequently north in the Bering Slope Current. Unless there is on-shelf advection in spring or early summer, it seems unlikely that* C. marshallae *will have large populations over the southeastern shelf when and where they would be required by age-0 pollock in the absence of* C. glacialis. *It is therefore likely that age-0 pollock will have to depend on the euphausiid* Thysanoessa raschii *as their major prey in years when sea ice fails to extend southward to the southeastern Bering Sea. However, given that there is evidence from the Barents Sea that* T. raschii *is more abundant in cold years, it is not clear how well* T. raschii *will do in a warming Bering Sea.*

ESR authors communicated this recommendation to AFSC zooplankton expert, David Kimmel. Below is Dr. Kimmel's response:
"We appreciate the interpretation of the SSC on the dynamics of 2022. A few comments: 1) We agree that the lack of ice in the preceding years likely had an impact on the *Calanus* populations observed in 2022. Lack of a large, overwintering population is likely to result in low abundances unless a series of years with significant ice cover occur. 2) We agree that the *Calanus* species on the middle shelf is likely *C. glacialis*; however, Tarrant et al. (2021) only reports results from one year and one season, thus we are reluctant to conclude this population is always *C. glacialis*. *C. marshallae* is found throughout the Bering Sea and in the Arctic, thus further refinement of the exact species composition both seasonally and interannually is necessary. To address this, the genetics group at PMEL is working towards metabarcoding and eDNA methods that can shed light on this topic. 3) Pollock do depend on *Thysanoessa raschii* and *T. inermis* during warmer years in the fall as is clear from age-0 diet data during cold and warm years and we agree that information about euphausiid population dynamics in response to interannual variability in sea-ice remains elusive."

Fish populations were near or above average biomass within the standard southern EBS bottom trawl grid in 2022 with a notable increase in pelagic foragers, in particular pollock and Pacific herring. Benthic foraging species (yellowfin sole, northern rock sole, flathead sole, and Alaska plaice) increased relative to 2021, although all but flathead sole remain below the 1982–2022 mean. Likewise, the biomass of pelagic foragers increased by 70% since 2021, a shift driven by pollock (on average 67% of pelagic fish biomass) that was up 50% from 2021. Pacific herring biomass was up 200% from 2021. The biomass of apex predators (dominated by Pacific cod and arrowtooth flounder) was up from 2021 and nearly equal to their long-term mean.

Groundfish condition in the southeastern Bering Sea declined during the recent warm stanza ending in 2021 but improved in 2022 for all species except walleye pollock, possibly reflecting improved prey availability and lower metabolic demands due to the cooling that started in 2021. Groundfish condition trends were more variable for monitored species over the northern shelf. The northward shift in the groundfish community during the recent warm stanza reached its northern maximum in 2019 before shifting south again as conditions cooled. Overall production of the groundfish community on the EBS shelf can be measured as total annual surplus production (ASP). The aggregated ASP of 14 groundfish stocks on the EBS shelf between 1978 and 2020 was highly variable, with or without pollock included,

ranging from a high of more than 1.4 million mt in 1980 to a low of less than 200,000 mt in the late 1990s. Total exploitation rates (aggregated catch/aggregated mature biomass) ranged from 6 to 13%, reflecting relatively conservative exploitation rates with the highest rates occurring early in the time series. The high reproductive success of both planktivorous and piscivorous seabirds nesting on the Pribilof Islands indicated that both large crustacean zooplankton and forage fish were sufficiently available over the shelf near the Pribilof Islands. Despite the heavy coccolithophore bloom over much of the middle and inner shelf, there were no reports of a major shearwater die-off, as has happened in the past (a small number of carcasses were reported from the Alaska Peninsula near False Pass). These positive trends are in line with those of improved groundfish condition in 2022.

The numbers of seabirds estimated to be caught incidentally in the southeastern Bering Sea fisheries in 2021 (1,892 birds) decreased from 2020 by 24% and was 52% below the 2012–2020 average. In 2021, 23 Laysan albatrosses were taken, but no black-footed or short-tailed albatrosses were bycaught. In contrast, the number of stranded northern fur seals on the Pribilof Islands increased. On St. Paul Island, 40 fur seals were entangled in fishing gear and were freed alive by the Ecosystem Conservation Office (ECO) of the Aleut Community of St. Paul Island.

For climate projections through March 2023, the National Multi-Model Ensemble shows that SST over the EBS is expected to be within ∼0.5ºC of average, indicating the short-term persistence of average thermal conditions.

Northern Bering Sea
Zooplankton in the NBS were surveyed during a late summer near-surface bongo net survey. In 2022, the abundances of both small and large copepods over the inner shelf of the NBS were lower than in recent years, whereas euphausiid abundance was higher. Lipid content of copepods in the Chirikof Basin was particularly high, suggesting that they may have been close to descending for diapause.

ESR authors communicated this comment to AFSC zooplankton expert, David Kimmel. Below is Dr. Kimmel's response: "We appreciate this comment from the SSC. One note of correction, the bongo surveys are oblique to depth and not near-surface. It is the fish trawls that are near-surface. Lipid content of copepods was indeed high and we concur that these individuals were close to entering diapause."

Similar to the most recent near-average cold-pool-extent-year in 2017, the NBS bottom trawl survey encountered moderate densities of adult walleye pollock and Pacific cod in 2022. The total CPUE of all groundfish combined increased between 2010 and 2018, and then declined to very low values in 2021 and 2022. A relative condition index calculated with the VAST model showed all species examined in 2022, including pollock 100–250 mm and >200mm in length had below-average condition, although within one standard deviation of the (short) time series mean. On St. Lawrence Island, piscivorous seabirds failed in their reproductive efforts, indicating a low availability of forage fish, which was corroborated by extremely low estimates of forage fish abundance in the NBS surface waters in 2022.

The NBS is a region where much of the annual primary production sinks to the bottom, thereby supporting a benthic food web. In 2022, the unusually low biomass of forage fish, the reproductive failure of piscivorous seabirds at St. Lawrence Island, and the poor condition in groundfish in the NBS suggest that the **NBS system may have been at or near carrying-capacity for pelagic piscivores.** *If so, this may have ramifications for juvenile salmon passing through the area.*

ESR authors agree. In several stock-specific Risk Tables in 2021 and 2022, the Ecosystem Considerations column noted concerns about ecosystem-level changes in the NBS and carring capacity (2021 Pacific cod example): "Multiple ecosystem 'red flags' occurred in the NBS this year: crab population

declines (Richar, 2021), salmon run failures in the Arctic-Yukon-Kuskokwim region (Liller, 2021), and seabird die-offs combined with low colony attendance and poor reproductive success (see Integrated Seabird Information in Siddon, 2021). In addition, results from the bottom trawl survey demonstrate a substantial drop in total CPUE in the NBS between 2019 and 2021 that reflected large decreases in all of the dominant species, including pollock (Mueter and Britt, 2021). Whether a single or suite of mechanisms can be identified to explain these coincident events, the common thread in these collapses is the marine environment in the NBS. Concerns about the food web dynamics and carrying capacity in the NBS have existed since 2018, highlighted by the gray whale Unusual Mortality Event and short-tailed shearwater mass mortality event (Siddon and Zador, 2019)."

An ongoing concern is the weak returns of Chinook, chum, and coho salmon to the Arctic/Yukon/Kuskokwim region. This is a problem of both national and international importance. The cause(s) of the decline in Chinook salmon returns is not well understood, but it is likely that climate warming in both the marine and freshwater environments and, to some extent, bycatch in EBS fisheries may be factors (see EBS ESR Noteworthy Topics).

Please see the Salmon section contribution entitled 'Factors Affecting 2023 Yukon & Kuskokwim Chum Salmon Runs and Subsistence Harvests' (p. 128).

The 2021 incidental catch of seabirds in the NBS commercial fisheries was estimated at 415 birds, a decrease of 27% from the 2020 bycatch, and below the 2012–2020 average of 621. Northern fulmars, shearwaters, and gulls were the most commonly caught. Ten Laysan albatrosses were also caught.

The SSC suggested that for species that span the EBS and NBS, indicators could be presented separately unless management is combined. Further, to help clarify some of the dynamics between these two regions, the SSC suggested that it might be valuable to see more spatial indicators incorporated (e.g., centroid/density of biomass as a 'ticker-tape' over time) that would assist in interpreting changes in abundance observed between the two regions.

ESR authors communicated this request to contributors; some contributors have provided SEBS and NBS time series (e.g., Kimmel et al. p. 90, Buser p. 70, 107, and 122) while others, such as the Report Card guilds that require catchability coefficients, did not feel they were ready to develop NBS-specific time series at this time.

Responses to Joint Groundfish Plan Team comments from September 2023

September 2023 Joint Groundfish Plan Team Report
Ecosystem Status Report (ESR) climate update
Bridget Ferris provided an overview of the Ecosystem Status Report (climate and physical information) for the EBS, AI, and GOA. This year's presentation highlighted a return to cooler, more moderate conditions across the North Pacific in 2023 after recent, multiyear extreme climate events. However, the Teams noted that the new sea surface temperature (SST) baseline of 1991–2020 versus the previous baseline of 1980–2010 includes several recent marine heat wave (MHW) events. This means that the average temperature is now warmer than previously reported and higher SST temperatures are required to constitute extreme anomalies. Cooler La Niña conditions in the North Pacific are transitioning to warming conditions with the upcoming El Niño, but climate indices are currently not aligned as would

be expected during El Niño. The authors suggested that this could be due to a time lag within the indices or that this El Niño is developing differently from those in the past. Relative to SST and sea ice extent data, the Teams suggest that a consistent baseline be used year to year to aid in comparisons, and if different baselines are used, to explicitly note them as such.

The ESR Editors agree with the challenge of interpreting data relative to different baselines. The ESRs will continue to strive for consistency and alignment in the reporting of baselines in the written report and presentations.

In 2023, EBS conditions were characterized by average SST with brief and infrequent MHWs, delayed sea ice formation, and average cold pool extent. The cold pool tongue was shifted more inshore than in recent years with the coldest bottom temperatures observed in the inner domain since 2013 and very cold water observed south of St. Matthew for the first time since 2015. Redistribution of fish and crab stocks is not expected based on the current cold pool location. AI conditions were characterized by record high SST and weakening eddy kinetic energy, resulting in reduced flow through passes. The GOA is currently experiencing the 4th consecutive year with no persistent MHW events. Brief summer MHWs in 2023 likely resulted from a lack of storms and increased stratification within the water column. New for this year, the authors presented a method for forecasting northern GOA SST based on Sitka air temperature anomaly data.

The Teams again acknowledge the immense effort of the ESR authors to collate and synthesize a broad array of environmental indices into a succinct summary that is useful for management advice. The Teams support continued presentation of the ESR to the Teams and appreciate the author's concise presentation format.

Thank you, The ESR team appreciates the opportunity to participate in the September Groundfish Plan Team meeting.

ESR CIE review
Ivonne Ortiz presented the ESR CIE review. The presentation reviewed the CIE objectives to revisit the goals and the process of the ESR. Recommendations resulting from the CIE will be addressed over the next 2–3 years. Key benefits/items identified by the reviewers were the risk tables inclusion in the stock assessments, and their discussion with stock assessment authors. The ESR team aims to improve TAC advice, strengthen and formalize risk tables, streamline and automate the report, synthesize information and use synthesis tools, and increase web presence.

The Teams requested clarification on potential refinements to the ecosystem section of the risk table based on the ESR CIE review. The ESR authors noted that different pieces of information from the ESR could inform the population dynamics section of the risk table instead of just the ecosystem section.

The ESR team hopes to work with stock assessment authors to find ways of adding value, improving efficiency, standardizing, and formalizing the inclusion of ecosystem information into risk tables. The ESR team is not proposing any specific changes to the risk table development process this year.

The Teams requested clarification on terminology used in the submitted table of CIE recommendations on the ESRs and a revised table was re-posted in response to this request.

Thank you for calling attention to the need for clarification. As noted, the ESR team provided a revised table for posting on the September Groundfish Plan Team meeting e-agenda.

The Teams encouraged the ESR authors to put ESR data on AKFIN where possible to improve acces-

sibility in the future.

The ESR team is currently in discussions with AKFIN to better integrate our process. Individual ESR contributors (including data collection programs and PIs) decide where they store their data, but the ESR team completely supports data centralization and accessibility where possible.

Responses to SSC comments from October 2023

October 2023 SSC Report
Ecosystem Status Report Preview
The SSC received presentations by Elizabeth Siddon (NOAA-AFSC), Bridget Ferriss (NOAA-AFSC), and Ivonne Ortiz (U. Washington) previewing the Ecosystem Status Reports (ESR) for the Eastern Bering Sea (EBS), the Gulf of Alaska (GOA), and the Aleutian Islands (AI), with specific attention to indicators that may be influential to consider for crab stock assessments. The SSC appreciates the effort to provide this information at the October meeting as data are still incoming and being incorporated. The SSC looks forward to the full ESR in December.

Thank you. We appreciate the opportunity to participate in your October meeting.

Generalized summaries were provided for the GOA and AI ESRs. No ecosystem concerns were identified for the GOA, and the author noted ocean temperatures remain near the long-term average with mixed pelagic feeding conditions for adult groundfish. For the AI, warming conditions persisted, characterized by high sea surface temperatures, with the winter of 2022/2023 representing one of the warmest on record since 2013. The strongest effects of this warming were present in the western and central AI. The SSC suggested information on which species are most vulnerable to these persistent conditions would be helpful for understanding ecosystem impacts.

For the EBS, specific to crab stocks, it was noted that oceanographic conditions in 2022/2023, including regional sea surface temperature trends and cold pool extent, were near the long-term averages with no red flags, suggesting good conditions for both pelagic and benthic crab. In 2023, there was a shift in timing of sea ice, with delayed sea ice growth due to slow freeze-up in Chukchi and impact of ex-typhoon Merbok. Modeled output from ROMS suggest expansion of bottom water ocean acidification (OA) conditions in 2023 (aragonite and pH). The author noted while these OA values are concerning, they were not expected to be driving crab declines as snow crab are not sensitive to declining aragonite concentrations and the nearshore habitat in Bristol Bay appears to be buffered. The SSC looks forward to seeing future work ground-truthing the modeled OA indicators.

Biological indicators showed mixed conditions for pelagic and benthic crabs. For pelagic crab, prey conditions (e.g., chlorophyll-a biomass estimates, copepod abundance, and copepod lipid content) were low in summer and fall 2023. Pelagic foragers, which are predators on pelagic crab stages, were high in 2022. For benthic crabs, indirect measurements of infaunal prey based on the 2022 benthic forager guild indicated adequate availability, but competitors and predators of benthic crabs remained high in 2022. The SSC noted that the continued high abundance of motile epifauna biomass, driven by brittle stars and other sea stars, represents a trophic 'dead-end' for energy in the benthic community and these organisms also may have direct interactions with benthic crab. It is unclear if this may represent a new community state.

Broad-scale climate patterns reflect a transition from La Niña to El Niño conditions with anticipated

warmer ocean temperatures arriving in early spring 2024. Ecological impacts of this transition remain unclear and will depend on the duration, depths, and timing of the warmer conditions. The ESR team expects to have updated forecasts of El Niño conditions for their December presentation.

Other notable observations included high bycatch of herring in the flatfish and pollock fisheries. A flatfish fishery exceeded herring PSC in 2023, the first time since 1992, and the pollock fishery was near the PSC cap. There were indications that herring were deeper and in more variable areas than in the past. This, along with predicted shifts in ice extent and phenology, highlight that the changing spatial and temporal dynamics of physical conditions may result in not only increasing or decreasing trends in biological components, but also in shifting distributions and changing biophysical interactions. The SSC discussed that even when physical conditions return to baseline, there may still be variability in the biological components, and supports the ESR authors' current efforts to develop spatio-temporal indicators of stratification and composite indices to better understand horizontal and vertical shifts in distribution that affect prey availability, species interactions, and interactions with fisheries.

Description of the Report Card Indicators

1. The North Pacific Index (NPI) winter average (Nov-Mar): The NPI index (Trenberth and Hurrell, 1994) was selected as the single most appropriate index for characterizing the climate forcing of the Bering Sea. The NPI is a measure of the strength of the Aleutian Low, specifically the area-weighted sea level pressure (SLP) for the region of 30°N to 65°N, 160°E to 140°W. Above (below) average winter (November–March) NPI values imply a weak (strong) Aleutian Low and generally calmer (stormier) conditions.

The advantage of the NPI include its systematic relationship to the primary causes of climate variability in the Northern Hemisphere, especially the El Niño-Southern Oscillation (ENSO) phenomenon, and to a lesser extent the Arctic Oscillation (AO). It may also respond to North Pacific SST and high-latitude snow and ice cover anomalies, but it is difficult to separate cause and effect.

The NPI also has some drawbacks: (1) it is relevant mostly to the atmospheric forcing in winter, (2) it relates mainly to the strength of the Aleutian Low rather than its position, which has also been shown to be important to the seasonal weather of the Bering Sea (Rodionov et al., 2007), and (3) it is more appropriate for the North Pacific basin as a whole than for a specific region (i.e., Bering Sea shelf).

Implications: For the Bering Sea, the strength of the Aleutian Low relates to wintertime temperatures, with a deeper low (negative SLP anomalies) associated with a greater preponderance of maritime air masses and hence warmer conditions.

Contact: Muyin Wang
Muyin.Wang@noaa.gov

2. Bering Sea ice extent: The Bering Sea ice year is defined as 1 August–31 July. Bering Sea ice extent data are from the National Snow and Ice Center's Sea Ice Index, version 3 (Fetterer et al., 2017), and use the Sea Ice Index definition of the Bering Sea, effectively south of the line from Cape Prince of Wales to East Cape, Russia (i.e., this index includes ice extent in both the western and eastern Bering Sea). The daily mean annual ice extent integrates the full ice season into a single value. *Implications:* Seasonal sea-ice coverage impacts, for example, the extent of the cold pool, bloom strength and timing, and bottom-up productivity.

Contact: Rick Thoman
rthoman@alaska.edu

3. Cold pool extent: Area of the cold pool in the eastern Bering Sea (EBS) shelf bottom trawl survey area (including strata 82 and 90) from 1982–2023. The cold pool is defined as the area of the southeastern Bering Sea continental shelf with bottom temperature <2°C, in square kilometers (km^2). *Implications:* The cold pool has a strong influence on the thermal stratification and influences the spatial structure of the demersal community (Spencer, 2008; Kotwicki and Lauth, 2013; Thorson et al., 2020), trophic structure of the eastern Bering Sea food web (Mueter and Litzow, 2008; Spencer et al., 2016), and demographic processes of fish populations (Grüss et al., 2021).

Contact: Sean Rohan and Lewis Barnett

Sean.Rohan@noaa.gov and Lewis.Barnett@noaa.gov

4. Proportion of open water blooms: The timing of ice retreat[30] and bloom peak was used to estimate bloom type, which differentiates between open-water blooms (i.e., ice retreat occurred ≥ 21 days prior to bloom peak) and ice-associated blooms (i.e., ice retreat occurred <21 days prior to bloom peak) for each year (Perrette et al., 2011). Timing of sea-ice retreat was determined as the date when ice coverage remained below 15% based on the 15-day running mean of the daily sea-ice fraction data. Bloom peak timing was estimated using standardized merged ocean color satellite data of 8-day satellite chlorophyll-a (chl-a, μg/L) at a 4 km-resolution from The Hermes GlobColour website[31] covering the years 1998–2023. *Implications:* Bloom type provides a metric of the bloom dynamics related to sea ice; increased ice-associated blooms tend to correlate positively with higher abundances of large zooplankton and have been suggested to favor pollock recruitment (Hunt et al., 2011).

Contact: Jens Nielsen
Jens.Nielsen@noaa.gov

5. Large copepod abundance: Large copepods (predominantly *Calanus* spp.) are quantified from 505μm mesh, 60cm bongo net samples taken during the fall (Aug/Sept) 70m isobath survey over the southern Bering Sea shelf. Detailed information on sampled taxa is provided after in-lab processing protocols have been conducted (1 year post survey). The current year value is an estimate of relative abundance derived from an at-sea Rapid Zooplankton Assessment (RZA). RZA abundance estimates may not closely match historical estimates of abundance as methods differ between laboratory processing and ship-board RZA. *Implications:* Large copepods are an important prey and trophic link between primary production and fish, marine mammals, and seabirds. The abundance of large copepods is an indicator of survival to age-3 for walleye pollock (see p. 159).

Contact: David Kimmel
David.Kimmel@noaa.gov

6. Euphausiid biomass: In the absence of direct measurements of secondary production in the eastern Bering Sea, we rely on estimates of biomass. We use an estimate of euphausiid biomass as determined by acoustic backscatter and midwater trawl data collected during biennial pollock surveys. *Implications:* Euphausiids form a key, large group of macrozooplankton that function as intermediaries in the trophic transfer from primary production to living marine resources (commercial fisheries and protected species). Understanding the mechanisms that control secondary production is an obvious goal toward building better ecosystem syntheses.

Contact: Patrick Ressler
Patrick.Ressler@noaa.gov

7. Pelagic forage fish biomass: This index represents the relative biomass of small fishes captured in the BASIS surface trawl (upper 25m) survey in the eastern Bering Sea during late summer. The aggregate biomass includes age-0 pollock, age-0 Pacific cod, herring, capelin, and all species of juvenile

---

[30]https://coastwatch.pfeg.noaa.gov/erddap/griddap/NOAA_DHW.html
[31]http://hermes.acri.fr/, Maritorena et al., 2010

salmonids. Due to changes in survey station locations and timing across years, a Vector Autoregressive Spatio-Temporal model with day of year as a catchability covariate was used. *Implications:* When this index is higher (lower), it indicates there may be more (less) food available to upper trophic predators (e.g., fish, seabirds, and mammals).

Contact: Ellen Yasumiishi
Ellen.Yasumiishi@noaa.gov

8., 9., 10., 11. Description of the fish and invertebrate guilds: We present four guilds to indicate the status and trends for fish and invertebrates in the eastern Bering Sea: motile epifauna, benthic foragers, pelagic foragers, and apex predators. Each is described in detail below. The full guild analysis involved aggregating all eastern Bering Sea species included in a food web model (Aydin and Mueter, 2007) into 18 guilds by trophic role, habitat, and physiological status (Table 2). For the four guilds included here, time trends of biomass are presented for 1982–2023. Foraging guild biomass is based on catch data from the NMFS-AFSC annual summer bottom trawl survey of the EBS shelf (<200m), modified by an Ecopath-estimated catchability coefficient that takes into account the minimum biomass required to support predator consumption (see Appendix 1 in (Boldt, 2007) for complete details). This survey index is specific to the standard bottom trawl survey area in the southeastern Bering Sea (does not include strata 82 and 90) and does not include the northern Bering Sea. The foraging guild biomass is weighted by strata area (km^2) which has resulted in a minor shift in the biomass values from reporting in previous years but the trends and patterns remain the same. Also, we no longer include species that lack time series and were previously represented by a constant biomass equal to the mid-1990s mass balance level estimated in (Aydin and Mueter, 2007).

Contact: Kerim Aydin or George A. Whitehouse
Kerim.Aydin@noaa.gov or Andy.Whitehouse@noaa.gov

Table 2: Composition of foraging guilds in the eastern Bering Sea.

Motile Epifauna	Benthic Foragers	Pelagic Foragers	Apex Predators
Eelpouts	Yellowfin sole	W. pollock	P. cod
Octopuses	Flathead sole	P. herring	Arrowtooth
Tanner crab	N. rock sole	Atka mackerel	Kamchatka fl.
King crab	Alaska plaice	Misc. fish shallow	Greenland turbot
Snow crab	Dover sole	Salmon returning	P. halibut
Sea stars	Rex sole	Capelin	Alaska skate
Brittle stars	Misc. flatfish	Eulachon	Other skates
Other echinoderms	Greenlings	Sandlance	Sablefish
Snails	Other sculpins	Other pelagic smelts	Large sculpins
Hermit crabs		Other managed forage	
Misc. crabs		Scyphozoid jellies	

8. Motile epifauna (fish and benthic invertebrates): This guild includes both commercial and non-commercial crabs, sea stars, snails, octopuses, other mobile benthic invertebrates, and eelpouts. There are ten commercial crab stocks in the current Fishery Management Plan for Bering Sea/Aleutian Islands King and Tanner Crabs; we include seven on the eastern Bering Sea shelf: two red king crab *Paralithodes camtschaticus* (Bristol Bay, Pribilof Islands), two blue king crab *P. platypus* (Pribilof

District and St. Matthew Island), one golden king crab *Lithodes aequispinus* (Pribilof Islands), and two Tanner crab stocks (southern Tanner crab *Chionoecetes bairdi* and snow crab *C. opilio*). The three dominant species comprising the eelpout group are marbled eelpout (*Lycodes raridens*), wattled eelpout (*L. palearis*), and shortfin eelpout (*L. brevipes*). The composition of seastars in shelf trawl catches is dominated by the purple-orange seastar (*Asterias amurensis*), which is found primarily in the inner/middle shelf regions, and the common mud star (*Ctenodiscus crispatus*), which is primarily an inhabitant of the outer shelf. *Implications:* Trends in the biomass of motile epifauna indicate benthic productivity and/or predation pressure, although individual species and/or taxa may reflect shorter or longer time scales of integrated impacts of bottom-up or top-down control.

9. Benthic foragers (fish only): The species which comprise the benthic foragers group are the Bering Sea shelf flatfish species, greenlings, and small sculpins. *Implications:* Trends in the biomass of benthic foragers indirectly indicate availability of infauna (i.e., prey of these species).

10. Pelagic foragers (fish and Scyphozoid jellies only): This guild includes adult and juvenile walleye pollock (*Gadus chalcogrammus*), other forage fish such as Pacific herring (*Clupea pallasi*), capelin (*Mallotus villosus*), eulachon (*Thaleichthys pacificus*), and sandlance, salmon, Atka mackerel (*Pleurogrammus monopterygius*), and scyphozoid jellies. *Implications:* Trends in the biomass of pelagic foragers largely track walleye pollock which is an important component of the Bering Sea ecosystem, both as forage and as a predator.

11. Apex predators (shelf fish only): This guild includes Pacific cod (*Gadus macrocephalus*), arrowtooth flounder, Kamchatka flounder (*Atheresthes evermanni*), Pacific halibut (*Hippoglossus stenolepis*), Greenland turbot (*Reinhardtius hippoglossoides*), sablefish (*Anoplopoma fimbria*), Alaska skate, and large sculpins. *Implications:* Trends in the biomass of apex predators indicate relative predation pressure on zooplankton and juvenile fishes within the ecosystem.

12. Multivariate seabird breeding index: This index represents the dominant trend among 17 reproductive seabird data sets from the Pribilof Islands that include diving and surface-foraging seabirds. The trend of the leading principal component (PC1) explains 51% of the variance among the data sets and represents all seabird hatch timing and the reproductive success of murres and cormorants, defined as loadings $>|0.2|$. *Implications:* Above-average index values reflect high reproductive success and/or early breeding (assumed to be mediated through food supply) and indicate better than average recruitment of year classes that seabirds feed on (e.g., age-0 pollock), or better than average supply of forage fish that commercially-fished species feed on (e.g.,capelin eaten by both seabirds and Pacific cod).

Contact: Stephani Zador
Stephani.Zador@noaa.gov

13. St. Paul Northern fur seal pup production: Pup production on St. Paul Island was chosen as an index for pinnipeds on the eastern Bering Sea shelf because the foraging ranges of females that breed on this island are largely on the shelf, as opposed to St. George Island which, to a greater extent, overlap with deep waters of the Basin and slope. Bogoslof Island females forage almost exclusively in pelagic habitats of the Basin and Bering Canyon and, as such, would not reflect foraging conditions on the shelf. *Implications:* Pup production reflects foraging conditions over the eastern Bering Sea shelf with above-average values indicating good foraging conditions.

Contact: Rod Towell
Rod.Towell@noaa.gov

Methods Description for the Report Card Plots

For each plot, the mean (green dashed line) and ± 1 standard deviation (SD; green solid lines) are shown as calculated for the entire time series. Time periods for which the time series was outside of this ± 1 SD range are shown in yellow (for high values) and blue (for low values).

The shaded green window shows the most recent 5 years prior to the date of the current report. The symbols on the right side of the graph are all calculated from data inside this 5-year moving window (maximum of 5 data points). The first symbol represents the "2019–2023 Mean" as follows: '+ or -' if the recent mean is outside of the ± 1 SD long-term range, '.' if the recent mean is within this long-term range, or 'x' if there are fewer than 2 data points in the moving window. The symbol choice does not take into account statistical significance of the difference between the recent mean and long-term range. The second symbol represents the "2019–2023 Trend" as follows: if the magnitude of the linear slope of the recent trend is greater than 1 SD/time window (a linear trend of >1 SD in 5 years), then a directional arrow is shown in the direction of the trend (up or down), if the change is <1 SD in 5 years, then a double horizontal arrow is shown, or 'x' if there are fewer than 3 data points in the moving window. Again, the statistical significance of the recent trend is not taken into account in the plotting.

The intention of the figure is to flag ecosystem features and the magnitude of fluctuations within a generalized "fisheries management" time frame (i.e., trends that, if continued linearly, would go from the mean to ± 1 SD from the mean within 5 years or less) for further consideration, rather than serving as a full statistical analysis of recent patterns.